Final Report

MARCO - POLO

Martian Transportation System

DSE Group 7

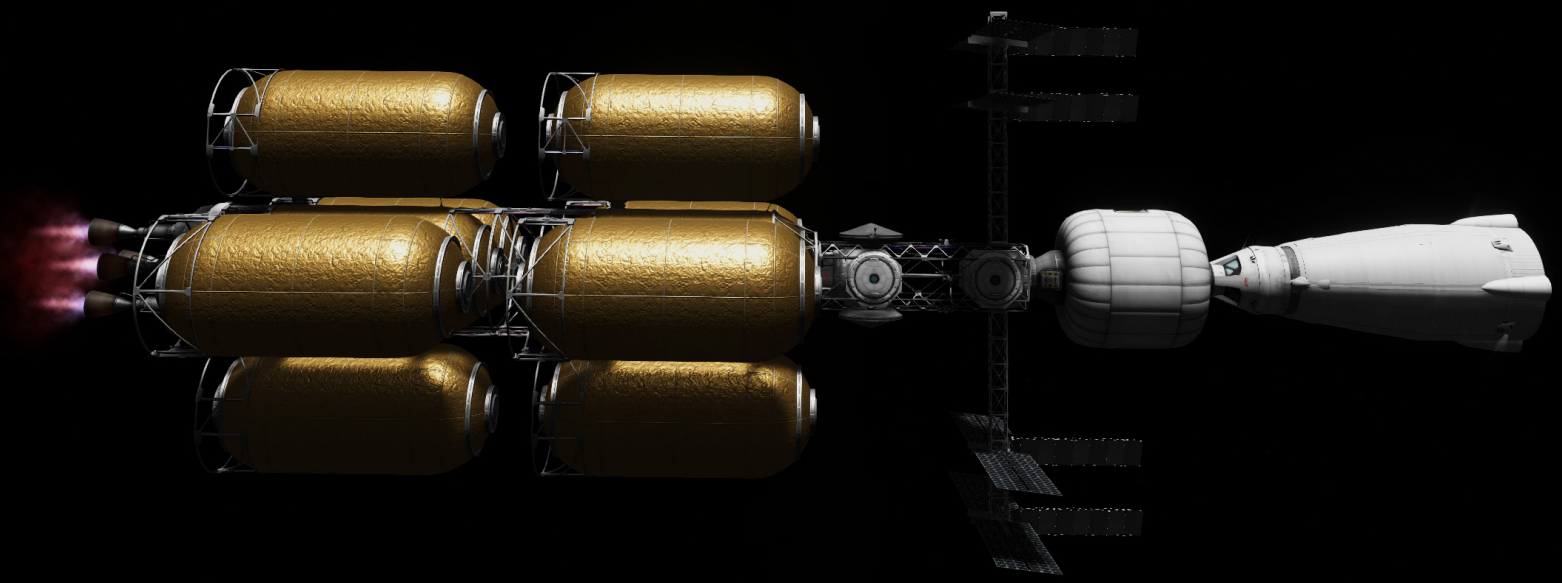

TU Delft Delft University of Technology

This page is intentionally left blank.

Final Report

MARCO - POLO

By

L. Bruun	4676645
J.R. Millán Fernández	4818334
J. Hardeveld, ook genaamd Kleuver	4786777
S.R. Kethiri	4665929
H. Köster	4652312
S.L. Kramer	4802047
Y.C.A. de Raadt	4856082
B. van Regteren	4821718
M. van Ruremonde	4439511
B. Vlyminckx	4792572

29th June 2021
TU Delft

Tutor: A. Cervone
Coaches: A. Bombelli
E. van Kampen

Version	Date	Changes
1	22-06-2021	Draft Version
2	29-06-2021	Final Version

Table of Contents

Nomenclature

Abbreviations

ADCS	Attitude Determination and Control System
ATCS	Active Thermal Control System
CMG	Control Moment Gyroscope
DM	Development
DOD	Depth of discharge
DSE	Design Synthesis Exercise
EATCS	External Active Thermal Control System
ECLSS	Environmental Control and Life Support System
EPS	Electrical Power System
ESA	European Space Agency
EVA	Extra Vehicular Activities
FBS	Functional Breakdown Structure
FFD	Functional Flow Diagram
IATCS	Internal Active Thermal Control System
IR	Inflation rate
ISS	International Space Station
ITS	Interplanetary Transportation System
LA	Launch
LEO	Low Earth Orbit
LMO	Low Mars Orbit
MAI Plan	Manufacturing, assembly and integration plan
MARCH	Martian Autarkic Research and Colonisation Habitat
MARCO	Martian Advanced Reusable Colonisation Orbiter
MD	Mission Design
MNS	Mission Needs Statement
MOI	Moment of inertia
NTP	Nuclear Thermal Propulsion
OP	Operations
PFCS	Pump Flow Control Sub-assemblies
PMAD	Power Management and Distribution
POLO	Platform for Orbital and Landing Operations
POS	Project Objective Statement
PRP	Propulsion System
PVR	Photovoltaic Radiators
RAID	Redundant Array of Inexpensive Disks
RAM	Risk After Mitigation
RBM	Risk Before Mitigation
RTG	Radioisotope Thermoelectric Generators
STR	Structure
STS	Space Transportation Segment
SWOT	Strength Weakness Opportunity Threats
TCS	Thermal Control System
TJ	Triple Junction
TLC	Telecommunication
TRL	Technology Readiness Level

List of Symbols

α	Angular acceleration
α_{man}	Angular acceleration in maneuvre
$\Delta\Psi$	Angle between velocities gravity assist
ΔV	Velocity increment
η	Efficiency
μ	Gravitational parameter
ω_{max}	Maximum angular velocity in maneuvre
ω_{SS}	Solar orientation angular velocity
ρ	Density
ρ_r	Reflectivity
σ_y	Yield Strength
τ_c	Counter-torque
τ_g	Gravitational gradient torque
τ_s	Solar torque
θ	True anomaly
θ_d	Angle allowed to be displaced by disturbance
a	Semi-major axis
c	Speed of light
c_c	Centre of mass of cylinder
c_{se}	Centre of mass of semi-ellipsoid
c_{ss}	Centre of mass of semi-sphere
c_{tank}	Centre of mass of tank
E	Energy
E	Young's Modulus
F_S	Solar force
F_T	Thruster force
h	Orbital height
h_c	Cylinder height
h_f	Height of a flat part
h_{se}	Semi-ellipsoid height
I_x	Moment of inertia in the x-axis
I_y	Moment of inertia in the y-axis
I_z	Moment of inertia in the z-axis
I_{sp}	Specific impulse
L	Length
L	Moment arm for thruster
L_m	Estimated length of MARCO
m_c	Cylinder mass
m_{prop}	Propellant mass
m_{se}	Semi-ellipsoid mass
m_{ss}	Semi-sphere mass
m_{tank}	Tank mass
MF	Margin factor
N_{burns}	Number of burns in a phase
P	Power
p	Pressure Difference
P_S	Solar pressure
R	Radius
r_c	Cylinder radius
R_E	Radius of Earth
R_M	Radius of Mars
r_p	Radius of periapsis

r_{av}	Estimated average radius of MARCO
S	Solar flux
S_r	Surface area from radiation perspective
t_b	Burn time
t_w	Waiting time before orbit maintenance burn
t_{man}	Maneuvre time
t_{phase}	Time for a phase of the trip
V_∞	Excess velocity
V_c	Cylinder volume
V_{se}	Semi-ellipsoid volume
V_{ss}	Semi-sphere volume
V_{tank}	Tank volume
w_f	Width of a flat part

1 Summary

Currently, TU Delft is performing a feasibility study for ESA about building a habitat on Mars. This study is being conducted across several faculties within TU Delft. As a part of their final bachelor thesis, 10 students from the Aerospace faculty have been given the task of designing a space transportation segment that can support the construction of a habitat on Mars and facilitate the safe transportation of crew members to and from Mars. The so called "Rhizome" habitat will be built mainly with in-situ materials on Mars and for this, several types of robots will be used, including scouting, mining and 3-D printing robots.

This report aims to explain the final design of a sustainable, reusable and easily re-configurable spacecraft that can sustain both the required materials and humans on multiple missions to Mars. It will consist of an interplanetary transportation segment called MARCO and two different types of landers called POLO cargo and POLO crew. The choice of lander depends on whether it is a crewed mission or a cargo mission. Optimising the configuration of MARCO-POLO leads to an increased payload mass and reduced cost for the project, as significantly less propellant is needed. POLO cargo was designed such that it cannot take off from Mars but will stay on the martian surface. POLO crew, however, will be able to take off from Mars and return the crew to MARCO, which will return both the crew and lander to a low Earth orbit (LEO). MARCO will function as the main transportation segment, travelling between LEO and low Mars orbit (LMO) with the landers.
The lifetime of MARCO-POLO will be 10 return trips to Mars, with the first launch being in 2028. The 10 return trips can be done in a time frame of 40 years in which the main objective of MARCO-POLO is to support the Rhizome habitat with crew and materials. The habitat has a lifetime of 20 years after it has been constructed, which means that MARCO-POLO might outlive the habitat. Should this be the case, the re-configurable nature of MARCO-POLO ensures that other missions to Mars can be supported, whether these are manned or unmanned missions.

MARCO will consist of up to 10 propellant tanks, which can be removed or added depending on the delta v requirement. Furthermore, four bi-modal engines will generate the necessary thrust and provide power when they are not in the thrust setting. During the burn times, solar arrays and batteries will provide power to MARCO-POLO. Similarly to the re-configurable nature of the propellant tanks, the habitation module will be able to be added or removed to fit the needs of the mission. As of now, the option of refuelling at the Moon is not viable and instead, refuelling will happen in LEO. However, should the cost of refuelling at the Moon drop throughout the life cycle of MARCO-POLO, this will be considered as a possibility for the later MARCO-POLO missions.
Throughout the design phase, sustainability has been in focus in the decision making and the implementation of sustainable practices has driven the design to minimise the impact on the various environments that will be encountered, while contributing to social sustainability on Earth, and still be an economically sustainable project. For the disposal of MARCO-POLO, the main consideration is not to create any space debris. However, it was also deemed unacceptable to bring back toxic nuclear waste to Earth. Therefore, once end-of-life has been reached, one part of MARCO-POLO will be disposed of in outer space. This part includes the toxic nuclear waste from the engines. The other part, however, will be brought back to Earth, where some parts will burn up in the atmosphere, and other parts will have its materials be recycled.

For future projects similar to this, where a concept needs to be developed from scratch, the trade-off made in the first phase of the project could have been performed more optimally for the concepts. The basis used for this project was that each subsystem was traded-off to see which option was the ideal. However, this can lead to a final sub-optimal concept, as some subsystems might interfere with one another. Therefore, the trade-off should rather be done on a concept basis, where the concepts drive the subsystems and not the other way around.
In the end, MARCO-POLO will be a reusable and easily re-configurable spacecraft with its modular design, and it can support both unmanned and manned missions to Mars. One of the important drivers of the final design was the approach to sustainability, which has been integrated at each step of the design process. If this project is seen through, MARCO-POLO will serve as a frontier in the upcoming interplanetary space mission section, and will be the first of its kind. With a life cycle of 10 return trips to Mars over a time frame of 40 years, it also holds the possibility of aiding future missions that still have to be developed. Once in operation, MARCO-POLO will serve as the symbol of human ingenuity, leading the way for a new generation of thoughts and ideas, and go over in history as the iconic spaceship that pushed the limit of human endeavours.

2 Introduction

Ever since humans have landed on the Moon, the next objective has been landing them on Mars as well. Now, more than fifty years later, there has not been a shortage of concept missions that intend to be the first to establish a human presence on the Red Planet. Mars is harsh and unforgiving environment, not suitable for human survival. Yet still, humans have the inherent need to go there and explore this unknown world.

The first step towards human exploration on Mars is building a habitat where people can survive without needing a heavy spacesuit. Various proposals for such a habitats have been made. One such proposal is for a habitat that is underground (excavated), and built using rovers and in-situ materials. The project described in this report is for designing the space transportation segment that will take the cargo and the crew for this habitat from Earth to Mars for several round trips. Three cargo missions will need to be conducted in order to get the habitat fully functional, after which the first humans to live in the habitat can be launched to Mars. The goal of this design is to create a fully re-usable Earth-Mars transportation segment that is able to conduct ten round trips, and transport 1000 kg of cargo, or a 5 member crew to Mars. A preliminary design has already been completed in the midterm report [8]. This report will describe the final, detailed design of the MARCO-POLO spacecraft.
The design of MARCO-POLO was an 11 week project, executed by 10 students from the Aerospace faculty at the Delft University of Technology, and it serves as the final bachelor project, also known as the Design Synthesis Exercise (DSE). It is a part of the larger feasibility study, which is called the Rhizome project, performed by TU Delft on behalf of ESA, which looks into building a habitat on Mars.

This report is structured in the following way. First, a market analysis is done in Chapter 3, to estimate the market opportunities. The sustainability approach for this design is detailed in Chapter 4. Then, the determination and management of all the risks are described in Chapter 5. Next, the project objectives and the requirements for the design are detailed in Chapter 6. A functional analysis of the design is performed in Chapter 7. Then, the astrodynamics of the missions to Mars are described in Chapter 9. The design of the propulsion subsystem is described next, in Chapter 10. The next two designs, for the electrical power system and the attitude determination and control system, are described in Chapter 12 and Chapter 13, respectively. After this, the habitat module is detailed in Chapter 16. The operations and logistics of the mission are described in Chapter 21. Afterwards, the reliability, availability, maintainability and safety (RAMS) are detailed. The production plan of the spacecraft is given in Chapter 23. Lastly, the compliance matrix and a conclusion are given in Chapter 24 and Chapter 25.

3 Market Analysis

In this chapter, a market analysis will be performed with regards to MARCO-POLO. It is crucial to be aware of the environment in the industry to be able to take advantage of potential opportunities in the market, and thus be a financially sustainable project for the foreseeable future.

This chapter will initially introduce the market demand for such a mission in Section 3.1. The stakeholders for MARCO-POLO will then be discussed in Section 3.2, followed by potential competitors in the industry in Section 3.3. Lastly, a SWOT analysis is included to clearly display the possibilities and challenges with regards to making market related decisions.

3.1 Market Demand

A critical step for the market analysis is the situation with regards to market demand. Without a demand for space missions to Mars, designing this type of mission would be useless as no investor would be wanting to jump on board. Therefore, the industry needs to be carefully analysed to design a mission that is sustainable, and interesting to potential investors.

3.1.1 Current Industry

The target industry which the project is aimed at is the space sector. This industry in itself is very broad, so the focus will be laid on space exploration and colonisation in particular. The project could be aimed at any company and/or institution which would like to shuttle cargo or crew back and forth to Mars but is not able to do it using its own means. The aim of this project is to deliver a service of a Mars transporter which private and public institutions can make use of. In recent years, talks of colonising Mars have become increasingly popular with major players like SpaceX or NASA coming up with their own plans to colonise Mars around the 2030's[1]. Morgan Stanley expects the global space industry to generate a revenue of $1.1 trillion in 2040 compared to the current $330 billion[2]. This allows for a very big growth and increase in revenue of the pioneers which are entering the business now. European investors are worried about the immature market and technology risk when they decide upon investing into New Space but are also optimistic about the fact that "eventually a few well-funded large start-ups with the capability to reinvent the entire industry will emerge as acquirers of other start-ups" [25].

If SpaceX and NASA's plan of putting humans on the Moon and Mars take flight, a demand for cargo transport will arise to support those missions. As NASA is outsourcing more and more of their missions to private companies[3], this opens up a gap for this project to jump into. Securing transport contracts from big players would fund the development of the program as well as help secure more investors in the future.

3.1.2 Future Demand

With a constant growth of people interested in space travel, and with opportunities for interplanetary colonisation and travel starting to appear, the market for a space transportation system is still in its infancy. This means that establishing a strong position in the market early on can be very beneficial, and makes it possible to become a major player in the industry, with a profitable and quickly adapting approach.

Assuming that humanity continues to further their colonisation efforts on Mars, it is reasonable to assume that a transport system to Mars is going to be required for the long term future. Humanity might have interest in harvesting resources on the martian surface, as some resources could be in greater abundance on Mars than on Earth, making harvesting and transporting them potentially cheaper than harvesting them on Earth. With some research, the system could also easily be adapted to help with regards to transporting resources from asteroids or other locations in the solar system.

Keeping in mind the human instinct for exploration, it is likely to assume that humanity would seek to explore further than Mars, to places such as the Jovian moon Europa or further into the outer solar system. This would most likely require an extensive system of transportation, in which this transport system to Mars can play a major part, guaranteeing long term longevity of such missions. With the knowledge and experience that is gained when producing

[1] https://www.businessinsider.com/elon-musk-mars-spacex-land-starship-rockets-2030-europe-2021-3?international=true&r=US&IR=T *[cited 22 April 2021]*

[2] https://knowledge.wharton.upenn.edu/article/commercial-space-economy/ *[cited 22 April 2021]*

[3] https://monroeaerospace.com/blog/nasa-says-spacex-and-boeing-outsourcing-will-save-30-billion/ *[cited 22 April 2021]*

such a system, it should easily be possible to expand and improve the system to also serve further destinations.

3.2 Stakeholders

As this project is focused on the transportation of payload to and from Mars, the major stakeholders will be the parties who are envisioning sending payload to Mars or parties benefiting from the development of the systems required to get to Mars. A brief list of major stakeholders are presented:

- **ESA** co-founded the Rhizome project to explore the potential of several technologies developed for off-Earth manufacturing. They are dependent on the project to be able to demonstrate those technologies on Mars. There are many more smaller stakeholders which will profit from the development of this project together with competitors than just the three listed.
- **TU Delft** co-founded the Rhizome project to explore the potential of several technologies developed for off-Earth manufacturing. They are dependent on the project to be able to demonstrate those technologies on Mars. Delivering good work might give TU Delft more opportunities on such projects.
- **Space Agencies or Corporations** which want to send payload to Mars will be interested in this project as it will be one of the first launches to send colonisation cargo to Mars. Being able to demonstrate that it can be done safely will be important for these third parties to continue with their missions. NASA, for example, is outsourcing more and more of their missions and payload delivery to private space companies. This will benefit this project.

3.3 Competitors

Major competition in the space industry is definitely on the rise, as humanity is seeing the potential that is available out in interplanetary space. Many companies, however, are not yet developing interplanetary missions due to the high cost and difficulty to develop and build the rocketry required to reach such destinations. Competition can be seen as a driving force, to be innovative and to bring something new to the market, or to be very cost effective being more attractive to potential stakeholders. However, competition also does come with its own risks, especially for the long run of the project, where others might use new technologies to be more efficient, thus being more attractive to customers. It is thus crucial to be aware of the competition, and their benefits and weaknesses, to formulate a good approach to compete. Two of the major competitors with respect to interplanetary transport are:

- **SpaceX** is actively working on prototyping and developing an STS using their Starship rocket, with as final goal a two stage rocket reusable rocket, with the first stage returning to Earth, and the second stage being refuelled in low Earth orbit. Their aims are a cost of $500.000 per person to Mars, with it being reduced to $200.000 on the long term. Current SpaceX plans see the first missions to Mars departing in 2024, with manned missions following in the next transfer window in 2026.
- **NASA** also has plans for an interplanetary spacecraft, namely the Mars Transit Vehicle. This design is a long term project, aiming to reach Mars orbit in 2033 using a spaceship consisting of the Orion capsule docked together with other payload carrying modules and propulsion modules. The main weakness of the NASA mission is with regards to the launch vehicle, which is suggested to be the SLS. This vehicle has an expected launch cost of $2 billion, making it economically unsustainable due to its high cost. Although competition can be healthy in certain industries, a space transportation project on such a big scale will have to be a cooperation between agencies and private companies. Therefore, the competitors will not only be competitors but might also be opportunities for cooperation.

Though these parties are strictly seen as competitors, this does not mean that cooperation is not a possibility. Due to the significant cost of such projects, it is economically viable for such companies to cooperate, as this can allow for reduced costs. Due to the resources such as staff and funding being a common limitation for such parties, joining efforts can remove or reduce the limitations, allowing for the final goal to be reached within a shorter time span.

3.4 SWOT Analysis

In Table 1, a SWOT analysis regarding the market analysis can be found. The SWOT analysis presents the strengths, weaknesses, opportunities and threats for MARCO-POLO.

Table 1: SWOT Analysis for MARCO-POLO.

	Helpful	**Harmful**
Internal	*Strengths* Project provides total coverage of trip to Mars. Re-usability to drive cost down. Knowledgeable tutors and experts available.	*Weaknesses* Not yet established in the market. Niche market, space is not for everyone.
External	*Opportunities* Lack of competition. Cooperation with ESA. New emerging markets. Interest of general public in space exploration.	*Threats* Competition have somewhat established their market position. Lack of competition can lead to lack in innovation. Feasibility study is delayed/cancelled. Reductions in budget/time allocation. Requirement changes. Stakeholders backing out. A (small) failure or setback leads to unfavourable press coverage. Public opinion on space engineering w.r.t. environmental issues.

4 Sustainability Approach

Sustainability means meeting our own needs without compromising the ability of future generations to meet their needs. In addition to natural resources, also social and economic resources are considered. Sustainability is not just environmentalism. Embedded in most definitions of sustainability one also find concerns for social equity and economic development[4]. MARCO-POLO actively incorporates these three aspects in all three phases of the project; development, manufacturing and operation. The following sections cover each of the aspects in more detail. Sustainability is not only considered as described here in this chapter, it also played an active role in the trade-off of the concepts and subsystems. Each subsystem chapter will present more specific information on how sustainability was considered, whereas this chapter covers the main ideas of making interplanetary travel sustainable based on the three core elements; environmental, social and economic sustainability.

4.1 Environmental Sustainability

For a project that revolves around colonising another planet, environmental sustainability is defined a bit differently than on Earth. During the project, at least three distinct environments can be considered and possibly a fourth one depending on the later stages of the project. There is of course the environment on Earth, then the space environment and finally the environment on Mars, and potentially the Moon if lunar refuelling becomes feasible at the later stages. This project aims at leaving the environments as close to the original state as possible. In the baseline report [9] five points were mentioned, which embraces environmental sustainability. These points are:

- **Reduction of emissions:** During the entire mission process, the total emissions of the mission are minimised. This is done by optimising the total number of flights required to get the necessary resources to Mars, and by using reusable launchers and a reusable ITS in MARCO.
- **No harm to the environment:** At no point during the mission is it acceptable that the environment undergoes any unnecessary or irreversible harm. This applies to either debris, or chemical substances on, but not limited to, the Earth, Mars and the Moon. This includes bringing nuclear waste back to Earth, which is the reason that part of MARCO-POLO will be disposed of into outer space.
- **No space debris:** In order to keep spaceflight accessible for future generations, under no circumstance may space debris be created intentionally. Any parts that go into space must be discarded by either being recycled, burning up in the atmosphere, or disposed of in outer space. With the modular nature of MARCO-POLO, it will be easy to divide the toxic material which will not go back to Earth, i.e. nuclear waste, and the material which will be recycled back on Earth.
- **Efficient mission design:** Over the course of the entire mission, a maximum efficiency with respect to production and operations is designed for. This reduces the waste of energy, resources and emissions of this project. This holds the reason for designing two different landers. The amount of propellant saved and the possibility to bring more payload with a non-reusable lander maximises the mission efficiency, more on this can be seen in Chapter 8.

[4] `https://www.mcgill.ca/sustainability/files/sustainability/what-is-sustainability.pdf` *[cited 29 June 2021]*

- **End-of-life recyclability:** In order to reduce resource usage, efforts are made to ensure that a significant amount of MARCO-POLO is to be recycled at end-of-life. Hence not all of MARCO-POLO will be disposed in outer space but a serious effort is done to bring it back to Earth to ensure it can be recycled. POLO cargo, which will stay on Mars, is designed to power the rovers and safely store the equipment needed for the Rhizome habitat. This can also be seen in Section 8.3.

4.2 Social Sustainability

Social sustainability includes "achieving a fair degree of social homogeneity" and "development that is compatible with the harmonious evolution of civil society, fostering an environment conductive to the cohabitation of culturally and socially diverse groups, while at the same time encouraging social integration, with improvements in the quality of life for all segments of the population" **europarl**. Many people may not realise what effect space travel has had on our society, but technologies originally developed for space use are now an integrated part of our lives and can be seen in broad variety of applications, ranging from medical applications to applications in sports and even to electric screwdrivers[5]. Even though the public may regard manned space flight as excessive use of resources, it is a great contributor to life on Earth and has improved life for many people all around the planet. As the public opinion on space missions can be critical in trying times, efforts need to be made to demonstrate that these manned missions continues to contribute to society in a wide range of aspects. It is thus key to keep the public opinion favourable for future developments. A few key elements are described to highlight the meaning of social sustainability:

- **Well-being:** Continuous monitoring of the individuals involved in the mission will be done. It is important to ensure that the physical and mental well-being of all members of the mission are ensured, as this can compromise the outcomes of the mission. This falls under the safety assessment as seen in Section 22.3.
- **Equality:** No discrimination of any kind with regards to gender, biological race, abilities, age, etc., should be done by the project and those involved. Equal treatment and work opportunity should be available to all those who are involved in the project. Active efforts are also made to make sure that the project group is as diverse as possible, this stimulates inclusiveness.
- **Accessibility:** Efforts will be made to make sure that any party apart of the Mars mission has access to any resources they might need to fulfil their goal.
- **Transparency:** In order to make sure that the communication with the stakeholders goes well, and gain the trust of stakeholders, there should be complete transparency with respect to the risks that might occur and the impacts these might have on the outcome of the project. This includes making a full risk register available for the main stakeholders that was identified in the Market Analysis, and also to those who might be identified at a later stage of the project. These stakeholders are continuously updated when changes occur to the risk register. The full risk register will be more extensive than the one shown in Chapter 5, and will also cover the risks identified for subsystems, which can be found in their respective chapters.
- **Job creation:** One of the major opportunities of such a large project as colonising Mars, is the creation of jobs that follows. To develop, build, test and monitor many people will be involved. It could be everything from the cleaning personal in one of the facilities to the crew that will set foot on Mars. A wide variety of jobs with root in all kinds of sectors is needed for a project like this.

Sending humans to Mars will require extensive engineering which might lead to new innovations and breakthroughs in the scientific world. At first, these innovation will not have a huge impact on society on Earth, but mainly on the colony on Mars. However, when companies find commercial applications for these sustainable innovations and breakthroughs, it will change the lives of many people. For example, long duration Mars missions will need to be able to, independently of Earth, recycle resources and waste such as food, water and oxygen. These technologies will also be applicable for certain Earth scenarios. As a matter of fact, these developments have already improved the nutrition in small villages[6]. It is expected that new technologies developed for this project will be able to improve the sustainable development of our society on Earth.

[5] https://www.nasa.gov/sites/default/files/80660main_ApolloFS.pdf *[cited 3 June 2021]]*

[6] http://youbenefit.spaceflight.esa.int/space-research-to-combat-malnutrition-in-congo/ *[cited 15 May 2021]*

4.3 Economic Sustainability

An economic sustainability plan lays-out the economic goals of the project. This plan discusses how the project funding is secured, the implications of the risk management and the general profitability of the project/mission. This plan needs to be transparent, in order to root out any financial deceit, it also needs to account for redundancies which are kept in place to facilitate the project. The three key aspects of the plan are further elaborated below and was also mentioned in the baseline report [9]:

- **Funding:** In order to have the project be sustainable, a reliable source of funding is required to afford the expensive nature of manned interplanetary missions. Reliable funding is defined as being funding which is agreed upon by parties, with respect to the amount, the timeline and with an agreement that the total sum will be transferred during the timeline. This allows for a clear overview of how much funding is received, and during which time period. It is thus crucial to keep the key stakeholders satisfied, and stay on good terms. This is done by being transparent to the stakeholders, keeping them informed clearly on progress made and involving them with major decisions that need to be made that apply to their needs.
- **Risk Management:** Managing risk is crucial to the way in which funds are allocated. Allocating funds to potentially high-risk operations might put the sustainability of the mission in jeopardy. Thus, it is crucial to clearly manage the potential risks of each mission, and to analyse these to make sure that these are clearly understood, along with their implications. A trade-off is to be made between the risks and the benefits that arise while taking these risks.
  Risk management also applies to the allocation of time of those working on the project. Having single points of failure, i.e. tasks that cannot continue when one individual is unable to continue work, puts the project into significant danger, and could cause irreversible delays. Thus, it is crucial to always have a backup available, to spread out the risk and minimise the effect of unforeseen circumstances.
- **Profitability:** Profitability insures investors stay attached to the project. Space exploration missions do not account for profit on a short term, but should be profitable on the long term. This principle applies especially, as interplanetary transport is a market that is expected to become relevant only in the relatively distant future. A plan has to be made to ensure that profit is still made after a certain period of time. Performing a market analysis is an important step in investigating the profitability of the mission and will be done in the following chapter.
  It should be noted that not all partners will look at the direct profits of this project, but they may also consider the technological advancements that can be used either directly or indirectly on Earth, and they might have an interest in becoming a key player for the use of this technology on Earth. Profitability should not only be looked as in the economic sense, technological advancements coming forth from a mission which can then be used in further missions could be seen as technological profitability. Profitability thus entails all resources gained, whether they are economical or technological or anything else. This also applies to fully publicly funded mission, where economical profits are not on the forefront of the profitability analysis.

5 Risk Management

In every engineering design project, uncertainties will arise, which can be defined as risks. These risks can have serious implications if they are not addressed properly. It is through risk management that a project successfully identifies, assesses and prioritises these risks. This is followed by a coordinated and economical application of resources to minimise or control the probability of occurrence and the impact of negative events, as well as to maximise the realisation of opportunities. These involve risks related to the project, which are discussed in this chapter, and for each subsystem, which is discussed in their respective chapters.

For the project to be successful, risk management needs to be continuously applied throughout the design process, the following steps need to be followed to successfully implement it [27]:

- **Identify:** Each new risk has to be given a unique ID and a risk is related to a certain event happening.
- **Assess:** Analysing the risks and quantifying the likelihood and impact corresponding to each risk. This gives an idea of the criticality of each risk. The values used to assess the risks and the explanation of these values can be found in Table 2.

- **Plan:** Decide on an appropriate response plan in case a risk happens.
- **Implement:** Implement the response plan for a risk.
- **Monitor/improve:** Make sure the implemented response has the desired effect on the risk. If that is not the case, the response plan should be updated.

Table 2: Scale used for assessing technical risks.

Value	Likelihood	Impact
1	Rare (<5%)	Negligible (objectives are not affected)
2	Unlikely (5-20%)	Tolerable (minimal changes to objectives, does not affect the project)
3	Possible (20-50%)	Moderate (objectives can still be met)
4	Likely (50-85%)	Substantial (objective can be met to less extent)
5	Certain (>85%)	Severe (objectives cannot be met)

The top-level risks are divided among the three phases of the project, Development (**DM**), Launch (**LA**) and Operation (**OP**). These entail the most critical risks which can derail the project. Most of these risks can be mitigated through sufficient planning and applying contingencies, but some, such as the LA01 and LA02, are beyond the control of the project as these tasks will be outsourced. The less critical risks can be found in the baseline report [9].

Table 3: Risk table including the most critical risks for each mission phase. RBM is defined as "likelihood, impact" before mitigation, RAM is "likelihood, impact" after mitigation.

ID	Risk	RBM	Mitigation	RAM
DM01	Required new technology is not yet developed prior to launch	2, 4	**Reduce** the dependencies on these technologies	2, 2
DM02	New technology exceeds the given budgets	3, 3	**Reduce** by choosing technologies further up the technical readiness scale	2, 3
DM03	Development delays	4, 4	**Reduce** with careful planning and adding margins	2, 2
LA01	Launcher fails due to a technical failure	2, 5	**Reduce** by choosing reliable launcher	1, 5
LA02	Launcher program delayed/cancelled	2, 4	**Avoid** by using a different launcher program as back-up	2, 1
LA03	Mars lander fails to launch back to Mars orbit	2, 5	**Reduce** by doing extensive analysis on Earth	1, 5
LA04	Launch causes damage to payload	3, 4	**Avoid** by designing for launch vehicle loads	1, 4
OP01	Collision with large space debris	2, 5	**Avoid** large objects	1, 5
OP02	Collision with small space debris	3, 2	**Reduce** impact of small objects by reinforcements	3, 1
OP03	Communication issues between subsystems	2, 4	**Avoid** by using the same communication protocol	1, 4
OP04	Insufficient amount of ΔV	2, 5	**Reduce** by adding a safety factor	1, 5
OP05	Connection problem between refuelling vehicle and spacecraft	3, 3	**Avoid** by using standardised and previously proven docking hardware	1, 3
OP06	Landing module is damaged upon landing	2, 5	**Reduce** by improving structural integrity	1, 5
OP07	System component failure/malfunction	2, 4	**Avoid** by implementing safety factors	1, 4
OP08	Emergency occurs on Mars	2, 5	**Reduce** with backup rations and materials	2, 3
OP09	MARCO becomes inhabitable	2, 5	**Reduce**, Separate life support systems for MARCO and POLO	2, 3

As seen in Table 3, upon applying a mitigation strategy, the risks have either become less likely or less severe. Figures 1 and 2 show the risks before and after mitigation respectively. As seen in the aforementioned figures, the top-level risks are managed sufficiently in order to reduce their impact on the project.

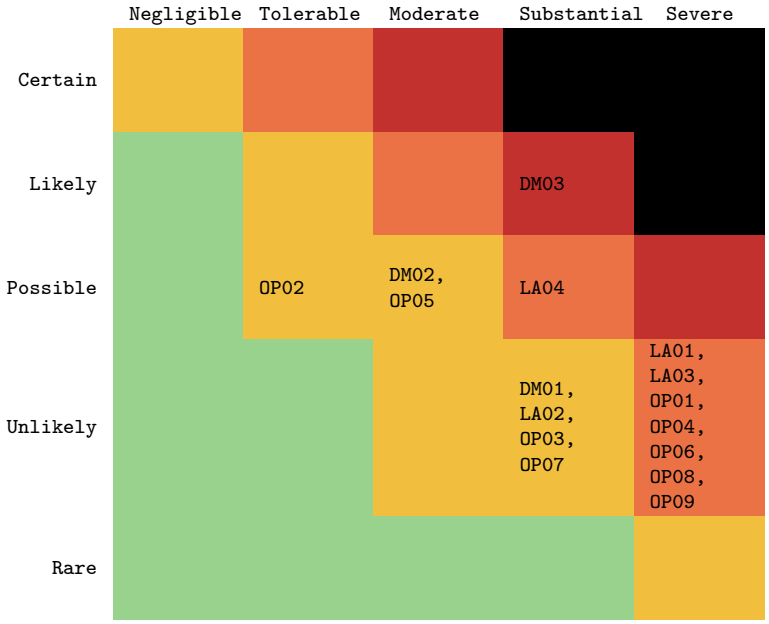

Figure 1: Risk matrix of identified top-level risks. Likelihood is listed vertically and impact is listed horizontally.

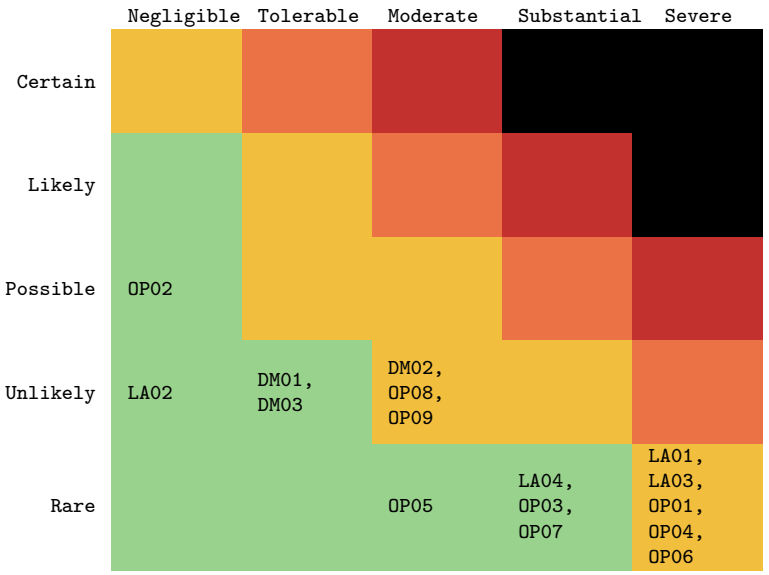

Figure 2: Risk matrix of mitigated risks. Likelihood is listed vertically and impact is listed horizontally.

6 Project Objectives and Requirements

In this chapter the project objectives and the general system/project requirements are presented. The project objective statement and the mission needs statement, which highlight the objective of the project are stated in Section 6.1. Followed by the general requirements in Section 6.2.

6.1 Project Objectives

The MARCO-POLO missions are a part of the Rhizome habitat project, which will build a habitat on Mars. For the MARCO-POLO missions, the following MNS and POS are determined:

Mission Need Statement:

To provide a system to bring all necessary human crew and materials for project Rhizome from Earth to Mars and vice-versa.

Project Objective Statement:

To design a re-usable, sustainable and easily re-configurable space transportation segment serving a martian research and colonisation habitat, with the option of (partially) refuelling at a permanent Moon station [7].

6.2 Requirements

This section only covers the general requirements for the MARCO-POLO segment and the subsequent project. The subsystem specific requirements can be found in their respective chapters. Further explanation and rationale of the general requirements can be found in the baseline [9] and midterm [8] reports. The general mission requirements are listed first, then follows the general requirements for MARCO and finally for POLO.

General Mission Requirements

User Requirements

MARCH-H-06 The whole mission shall not interfere or preclude the planning of any other missions to Mars.

MARCH-H-10 The total cost for establishing the Rhizome habitat and starting its regular operations shall not be higher than 5000 M€.

MARCH-STS-04 The maiden launch of MARCO-POLO shall be scheduled not later than 2030.

Cost

MARCH-CR-01 The launch cost shall not be higher than 25 k€ per kg of payload delivered to Mars (calculated taking into account only recurring costs, not including any development or qualification costs).

Legal

MARCH-LEG-01 The project shall adhere to the legal guidelines established by the United Nations Office for outer space affairs and outlined in *United Nations Treaties and Principles on Outer Space and Related General Assembly Resolutions.* [36]

MARCH-LEG-02 The project shall adhere to the legal guidelines working paper A/AC.105/C.2/L.315 of the United Nations General Assembly on space resource activities. [7]

Requirements for MARCO

Payload

MARCO-PAY-01 MARCO shall be able to take a payload of 150 t to Mars and back to Earth.

Crew Survival Requirements

MARCO-CWS-01 MARCO shall be able to function as an emergency home for all people in the habitat.

MARCO-CWS-02 MARCO shall be able to host no less than 5 people for 972 days in case of an emergency with the habitat.

MARCO-CWS-03 MARCO shall have redundancy for all life support systems.

MARCO-CWS-04 The crewed spacecraft sections shall have a cabin pressure of 1 atmosphere.

MARCO-CWS-05 MARCO shall store enough life support for a trip to Mars including emergency scenarios.

Scheduling

MARCO-SCH-01 MARCO shall stay in LEO for at least 100 days for each refuel function.

MARCO-SCH-02 MARCO assembly in orbit shall be completed before the year 2030.

MARCO-SCH-03 The Rhizome habitat shall be fully operational not later than 10 years after the maiden flight of MARCO-POLO.

Mission Design

MARCO-MD-03 A human crew of no less than 5 members shall be present on each crewed mission of MARCO.

MARCO-MD-04 MARCO shall deliver crew and cargo to LMO and return the crew safely to LEO.

[7] `https://www.unoosa.org/oosa/oosadoc/data/documents/2020/aac.105c.2l/aac.105c.2l.315_0.html` *[cited 18 May 2021]]*

MARCO-MD-05 MARCO shall provide a standard docking mechanism.

MARCO-MD-06 The crew on board MARCO shall be able to perform an unscheduled EVA.

MARCO-MD-07 MARCO shall provide radiation shielding such that the crew is exposed to at most 1 Sv of radiation in 10 months. [8]

MARCO-MD-08 The habitation module shall provide all necessary life support systems for the crew.

Sustainability

MARCO-SUS-01 MARCO shall be fully re-usable, for a minimum of 10 Earth-Mars return trips, with exclusion of necessary maintenance.

MARCO-SUS-02 All materials and propellants used by MARCO shall be non-toxic and not hazardous.

Safety and Reliability

MARCO-SR-01 MARCO shall have a reliability of 95 % or higher ("reliability" is intended, here, as the probability of not experiencing failures over the entire lifetime of the system).

Requirements for POLO

Payload

POLO-PAY-01 The rover system shall withstand a non-operational temperature of at least 90 K.

POLO-PAY-02 The rover system shall withstand a non-operational temperature of at most 450 K.

POLO-PAY-03 The internal operating temperature of the rover shall not be less than 250 K.

POLO-PAY-04 The internal operating temperature of the rover shall not be more than 310 K.

POLO-PAY-05 The rover shall withstand a minimum pressure of 1×10^{-11} Pa.

POLO-PAY-06 The rover shall initiate the charging sequence, if the battery charge drops below 20 %.

POLO-PAY-07 POLO shall be able to land 15 t of payload at Mars.

POLO-PAY-08 POLO shall be able to land 50 m^3 of payload at Mars.

Crew survival requirements

POLO-CWS-01 POLO crew shall be able to host no less than 5 people for 30 days.

POLO-CWS-02 POLO crew shall be able to transport no less than 5 people in case of an emergency with the habitat.

POLO-CWS-03 POLO crew shall have redundancy for all life support systems.

POLO-CWS-04 POLO crew shall have a cabin pressure between 0.75 and 1 atmosphere.

POLO-CWS-05 POLO crew shall store enough life support for a trip to land on Mars and take off from Mars, including emergency scenarios.

Scheduling

POLO-SCH-01 POLO cargo shall stay on Mars for at least 40 days for the first cycle.

Sustainability

POLO-SUS-01 All materials and propellants used by POLO shall be non-toxic and not hazardous.

[8] `https://www.nasa.gov/jpl/msl/mars-rover-curiosity-pia17601.html` *[cited 18 May 2021]*

7 Functional Analysis

In this chapter the reiterated functional breakdown structure (FBS) and functional flow diagram (FFD) for the final design of the MARCO-POLO project is presented. The first iteration of the functional analysis was already shown in the baseline report, which stated the general functions of the mission [9].

7.1 Functional Breakdown Structure

The FBS is a collection of all the functions that need to be performed during the MARCO-POLO mission. Beginning with manufacturing of the system and ending with its disposal, with a loop in the middle as MARCO-POLO is reusable. The following list, highlights the top-level functions of the project with brief explanations to each function:

F1 **Manufacture MARCO-POLO**
This function is unique for this mission. Because of the size of MARCO, the final assembly of modules has to be done in orbit. The smaller components of each modules are manufactured by various subcontractors before they are assembled into modules. These include the control module, propulsion system, habitation module, and the POLO landers (crew and cargo). This phase also includes all the necessary testing and certification of the components and the modules as a whole.

F2 **Launch and Assemble MARCO-POLO**
During this function the entire spacecraft comes together. First the command module is sent into LEO, followed by the fuel tanks, the engines and the fission reactor. Following the launch, the modules of the system are assembled in LEO, where the habitation module is added at a later stage. This function also contains the launch of both the POLO landers and their respective docking to MARCO.

F3 **Prepare MARCO-POLO**
Before MARCO-POLO takes on the long journey to Mars, MARCO is checked to see if all systems are working and possible maintenance is carried out (including orbital maintenance). Then it is refuelled, such that once the payload has been delivered by POLO, the next stop will be Mars. Refuelling will be done using several Starship launches to refuel in LEO, or in Moon orbit, when the infrastructure is set-up and the fuel cost is very similar to that on Earth. There are two types of missions, the first is a crewed mission in which case the habitation module is needed together with POLO crew. The other option is an uncrewed mission, which only consists of POLO cargo.

F4 **Transport to Mars**
Once MARCO-POLO is ready for the transfer to Mars, the course will be set to LMO and the 6-7 months transfer begin. During the transfer, the crew will be able to perform research, make minor repairs and be in contact with the ground station. Along the way to Mars, MARCO will perform a trajectory corrections if necessary.

F5 **Arrival at Mars**
When arriving at Mars, MARCO will perform orbit insertion into LMO and then POLO will un-dock from MARCO and descent to the surface. Once landed, the deployment of the cargo from the cargo hold is begun as well as the dismounting of the crew from the crew module, in case of a crewed mission. Payload and crew will then transfer to the habitat. During the first few missions where payload is brought to build MARCH, POLO cargo will be used on the surface to provide the rovers with power until the rovers can be connected to MARCH's power system.

F6 **Departure from Mars**
During the time in LMO, MARCO will function as a relay for communication with ground station on Earth. When the mission on Mars is done, MARCO-POLO will be prepared for the journey back to Earth. When it is time to leave the surface of Mars, the returning crew is secured in the cabin and the cargo is loaded into the cargo hold. POLO then launches, and performs an orbital manoeuvre to enter LMO, where it will dock to MARCO. Before returning to Earth, MARCO will be checked and once ready, MARCO-POLO will go on the journey back to Earth. In case of an uncrewed mission, POLO cargo will stay on the surface of Mars, and the ground station on Earth will prepare MARCO for its journey back to Earth.

F7 **Transport to Earth**
Transportation to Earth is similar to function F4: transport to Mars. The course is now set for the journey back to Earth, where the crew can perform research or do small repairs of the subsystems. If necessary, trajectory corrections can be performed, and the crew will be in contact with the ground station along the way.

F8 **Arrival at Earth**
After completing a successful trip, and returning back to Earth. MARCO-POLO needs to perform orbital insertion to get into LEO. MARCO-POLO will be parked in LEO and the retrieval process is initiated. In case of the cargo missions, function F3 will be initiated when the next launch window opens up. While during the crewed missions, the crew and the cargo from Mars will return to Earth in the crew capsule, after which F3 is will commence again, when the next launch window is open, unless it is the end-of-life of MARCO-POLO, in which case F9 will be initiated.

F9 **Disposal of spacecraft**
Upon completing its mission life, MARCO-POLO needs to be disposed of. Since sustainability is a high priority in this project, most of the recyclable material will be returned to Earth while the toxic non-recyclable material is sent out into outer space.

7.2 Functional Flow Diagram

This diagram displays the relation between all functions in the FBS. The arrows point at a function which occurs after the other. After function F3.3 there are two possible ways. One is an uncrewed mission and the other is for a crewed mission. It should be noted that only one of the two paths will be followed, this is indicated by the dotted arrows. Another point to note is that the manufacturing phase of all modules are done in parallel, this does not necessarily reflect real life as for example, the habitation module is not needed for the first launches. More information on the production plan and assembly phase will follow in Chapter 23.

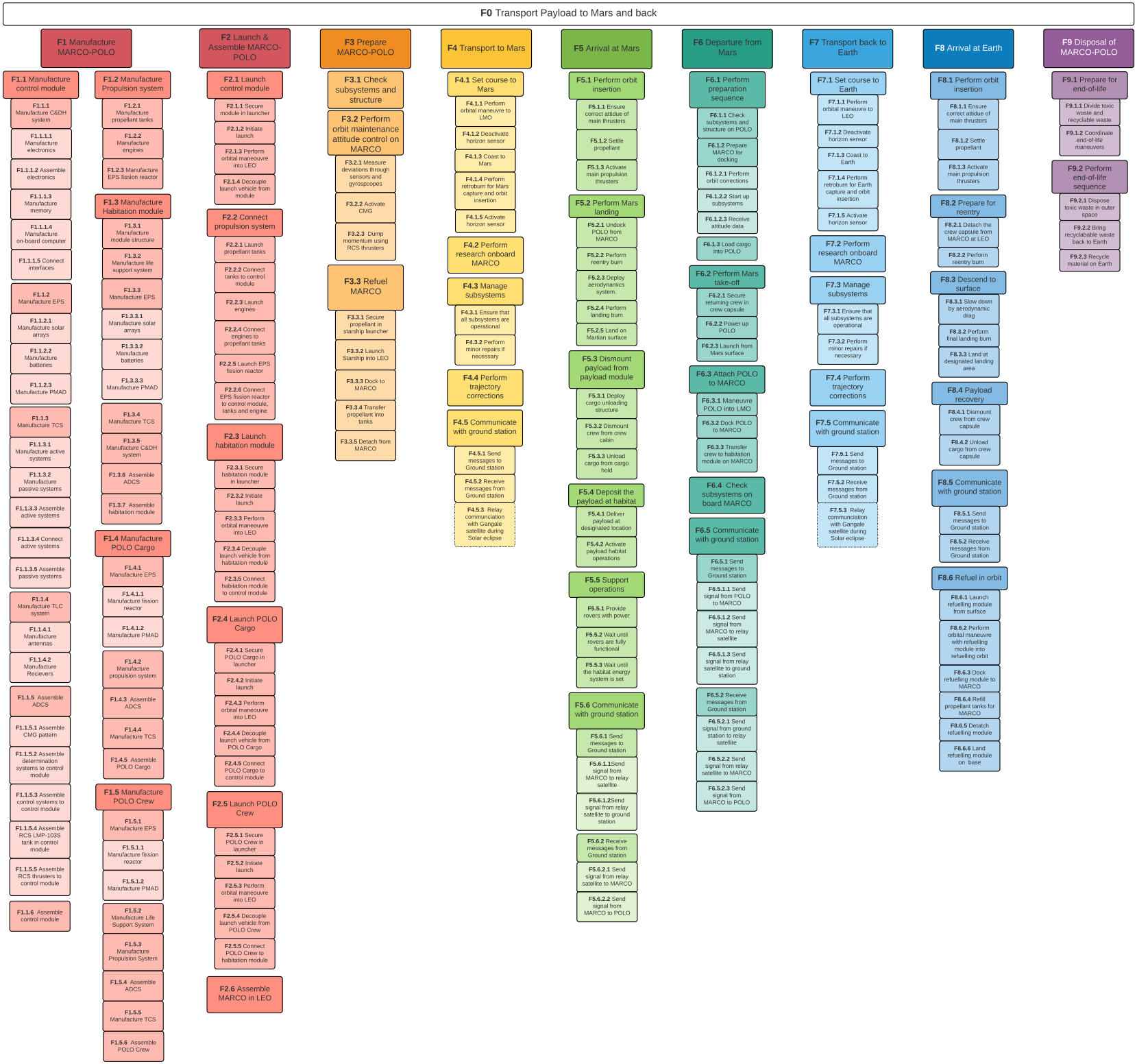
F0 Transport Payload to Mars and back
F1 Manufacture MARCO-POLO
F1.1 Manufacture control module
F1.1.1 Manufacture C&DH system
F1.1.1.1 Manufacture electronics
F1.1.1.2 Assemble electronics
F1.1.1.3 Manufacture memory
F1.1.1.4 Manufacture on-board computer
F1.1.1.5 Connect interfaces
F1.1.2 Manufacture EPS
F1.1.2.1 Manufacture solar arrays
F1.1.2.2 Manufacture batteries
F1.1.2.3 Manufacture PMAD
F1.1.3 Manufacture TCS
F1.1.3.1 Manufacture active systems
F1.1.3.2 Manufacture passive systems
F1.1.3.3 Assemble active systems
F1.1.3.4 Connect active systems
F1.1.3.5 Assemble passive systems
F1.1.4 Manufacture TLC system
F1.1.4.1 Manufacture antennas
F1.1.4.2 Manufacture Recievers
F1.1.5 Assemble ADCS
F1.1.5.1 Assemble CMG pattern
F1.1.5.2 Assemble determination systems to control module
F1.1.5.3 Assemble control systems to control module
F1.1.5.4 Assemble RCS LMP-103S tank in control module
F1.1.5.5 Assemble RCS thrusters to control module
F1.1.6 Assemble control module
F1.2 Manufacture Propulsion system
F1.2.1 Manufacture propellant tanks
F1.2.2 Manufacture engines
F1.2.3 Manufacture EPS fission reactor
F1.3 Manufacture Habitation module
F1.3.1 Manufacture module structure
F1.3.2 Manufacture life support system
F1.3.3 Manufacture EPS
F1.3.3.1 Manufacture solar arrays
F1.3.3.2 Manufacture batteries
F1.3.3.3 Manufacture PMAD
F1.3.4 Manufacture TCS
F1.3.5 Manufacture C&DH system
F1.3.6 Assemble ADCS
F1.3.7 Assemble habitation module
F1.4 Manufacture POLO Cargo
F1.4.1 Manufacture EPS
F1.4.1.1 Manufacture fission reactor
F1.4.1.2 Manufacture PMAD
F1.4.2 Manufacture propulsion system
F1.4.3 Assemble ADCS
F1.4.4 Manufacture TCS
F1.4.5 Assemble POLO Cargo
F1.5 Manufacture POLO Crew
F1.5.1 Manufacture EPS
F1.5.1.1 Manufacture fission reactor
F1.5.1.2 Manufacture PMAD
F1.5.2 Manufacture Life Support System
F1.5.3 Manufacture Propulsion System
F1.5.4 Assemble ADCS
F1.5.5 Manufacture TCS
F1.5.6 Assemble POLO Crew
F2 Launch & Assemble MARCO-POLO
F2.1 Launch control module
F2.1.1 Secure module in launcher
F2.1.2 Initiate launch
F2.1.3 Perform orbital maneouvre into LEO
F2.1.4 Decouple launch vehicle from module
F2.2 Connect propulsion system
F2.2.1 Launch propellant tanks
F2.2.2 Connect tanks to control module
F2.2.3 Launch engines
F2.2.4 Connect engines to propellant tanks
F2.2.5 Launch EPS fission reactor
F2.2.6 Connect EPS fission reactor to control module, tanks and engine
F2.3 Launch habitation module
F2.3.1 Secure habitation module in launcher
F2.3.2 Initiate launch
F2.3.3 Perform orbital maneouvre into LEO
F2.3.4 Decouple launch vehicle from habitation module
F2.3.5 Connect habitation module to control module
F2.4 Launch POLO Cargo
F2.4.1 Secure POLO Cargo in launcher
F2.4.2 Initiate launch
F2.4.3 Perform orbital maneouvre into LEO
F2.4.4 Decouple launch vehicle from POLO Cargo
F2.4.5 Connect POLO Cargo to control module
F2.5 Launch POLO Crew
F2.5.1 Secure POLO Crew in launcher
F2.5.2 Initiate launch
F2.5.3 Perform orbital maneouvre into LEO
F2.5.4 Decouple launch vehicle from POLO Crew
F2.5.5 Connect POLO Crew to habitation module
F2.6 Assemble MARCO in LEO
F3 Prepare MARCO-POLO
F3.1 Check subsystems and structure
F3.2 Perform orbit maintenance attitude control on MARCO
F3.2.1 Measure deviations through sensors and gyroscopes
F3.2.2 Activate CMG
F3.2.3 Dump momentum using RCS thrusters
F3.3 Refuel MARCO
F3.3.1 Secure propellant in starship launcher
F3.3.2 Launch Starship into LEO
F3.3.3 Dock to MARCO
F3.3.4 Transfer propellant into tanks
F3.3.5 Detach from MARCO
F4 Transport to Mars
F4.1 Set course to Mars
F4.1.1 Perform orbital maneuvre to LMO
F4.1.2 Deactivate horizon sensor
F4.1.3 Coast to Mars
F4.1.4 Perform retroburn for Mars capture and orbit insertion
F4.1.5 Activate horizon sensor
F4.2 Perform research onboard MARCO
F4.3 Manage subsystems
F4.3.1 Ensure that all subsystems are operational
F4.3.2 Perform minor repairs if necessary
F4.4 Perform trajectory corrections
F4.5 Communicate with ground station
F4.5.1 Send messages to Ground station
F4.5.2 Receive messages from Ground station
F4.5.3 Relay communciation with Gangale satellite during Solar eclipse
F5 Arrival at Mars
F5.1 Perform orbit insertion
F5.1.1 Ensure correct attidue of main thrusters
F5.1.2 Settle propellant
F5.1.3 Activate main propulsion thrusters
F5.2 Perform Mars landing
F5.2.1 Undock POLO from MARCO
F5.2.2 Perform reentry burn
F5.2.3 Deploy aerodynamics system.
F5.2.4 Perform landing burn
F5.2.5 Land on Martian surface
F5.3 Dismount payload from payload module
F5.3.1 Deploy cargo unloading structure
F5.3.2 Dismount crew from crew cabin
F5.3.3 Unload cargo from cargo hold
F5.4 Deposit the payload at habitat
F5.4.1 Deliver payload at designated location
F5.4.2 Activate payload habitat operations
F5.5 Support operations
F5.5.1 Provide rovers with power
F5.5.2 Wait until rovers are fully functional
F5.5.3 Wait until the habitat energy system is set
F5.6 Communicate with ground station
F5.6.1 Send messages to Ground station
F5.6.1.1Send signal from MARCO to relay satellite
F5.6.1.2Send signal from relay satellite to ground station
F5.6.2 Receive messages from Ground station
F5.6.2.1 Send signal from relay satellite to MARCO
F5.6.2.2 Send signal from MARCO to POLO
F6 Departure from Mars
F6.1 Perform preparation sequence
F6.1.1 Check subsystems and structure on POLO
F6.1.2 Prepare MARCO for docking
F6.1.2.1 Perform orbit corrections
F6.1.2.2 Start up subsystems
F6.1.2.3 Receive attitude data
F6.1.3 Load cargo into POLO
F6.2 Perform Mars take-off
F6.2.1 Secure returning crew in crew capsule
F6.2.2 Power up POLO
F6.2.3 Launch from Mars surface
F6.3 Attach POLO to MARCO
F6.3.1 Maneuvre POLO into LMO
F6.3.2 Dock POLO to MARCO
F6.3.3 Transfer crew to habitation module on MARCO
F6.4 Check subsystems on board MARCO
F6.5 Communicate with ground station
F6.5.1 Send messages to Ground station
F6.5.1.1 Send signal from POLO to MARCO
F6.5.1.2 Send signal from MARCO to relay satellite
F6.5.1.3 Send signal from relay satellite to ground station
F6.5.2 Receive messages from Ground station
F6.5.2.1 Send signal from ground station to relay satellite
F6.5.2.2 Send signal from relay satellite to MARCO
F6.5.2.3 Send signal from MARCO to POLO
F7 Transport back to Earth
F7.1 Set course to Earth
F7.1.1 Perform orbital maneuvre to LEO
F7.1.2 Deactivate horizon sensor
F7.1.3 Coast to Earth
F7.1.4 Perform retroburn for Earth capture and orbit insertion
F7.1.5 Activate horizon sensor
F7.2 Perform research onboard MARCO
F7.3 Manage subsystems
F7.3.1 Ensure that all subsystems are operational
F7.3.2 Perform minor repairs if necessary
F7.4 Perform trajectory corrections
F7.5 Communicate with ground station
F7.5.1 Send messages to Ground station
F7.5.2 Receive messages from Ground station
F7.5.3 Relay communciation with Gangale satellite during Solar eclipse
F8 Arrival at Earth
F8.1 Perform orbit insertion
F8.1.1 Ensure correct attidue of main thrusters
F8.1.2 Settle propellant
F8.1.3 Activate main propulsion thrusters
F8.2 Prepare for reentry
F8.2.1 Detach the crew capsule from MARCO at LEO
F8.2.2 Perform reentry burn
F8.3 Descend to surface
F8.3.1 Slow down by aerodynamic drag
F8.3.2 Perform final landing burn
F8.3.3 Land at designated landing area
F8.4 Payload recovery
F8.4.1 Dismount crew from crew capsule
F8.4.2 Unload cargo from crew capsule
F8.5 Communicate with ground station
F8.5.1 Send messages to Ground station
F8.5.2 Receive messages from Ground station
F8.6 Refuel in orbit
F8.6.1 Launch refuelling module from surface
F8.6.2 Perform orbital maneuvre with refuelling module into refuelling orbit
F8.6.3 Dock refuelling module to MARCO
F8.6.4 Refill propellant tanks for MARCO
F8.6.5 Detatch refuelling module
F8.6.6 Land refuelling module on base
F9 Disposal of MARCO-POLO
F9.1 Prepare for end-of-life
F9.1.1 Divide toxic waste and recyclable waste
F9.1.2 Coordinate end-of-life maneuvers
F9.2 Perform end-of-life sequence
F9.2.1 Dispose toxic waste in outer space
F9.2.2 Bring recyclabale waste back to Earth
F9.2.3 Recycle material on Earth

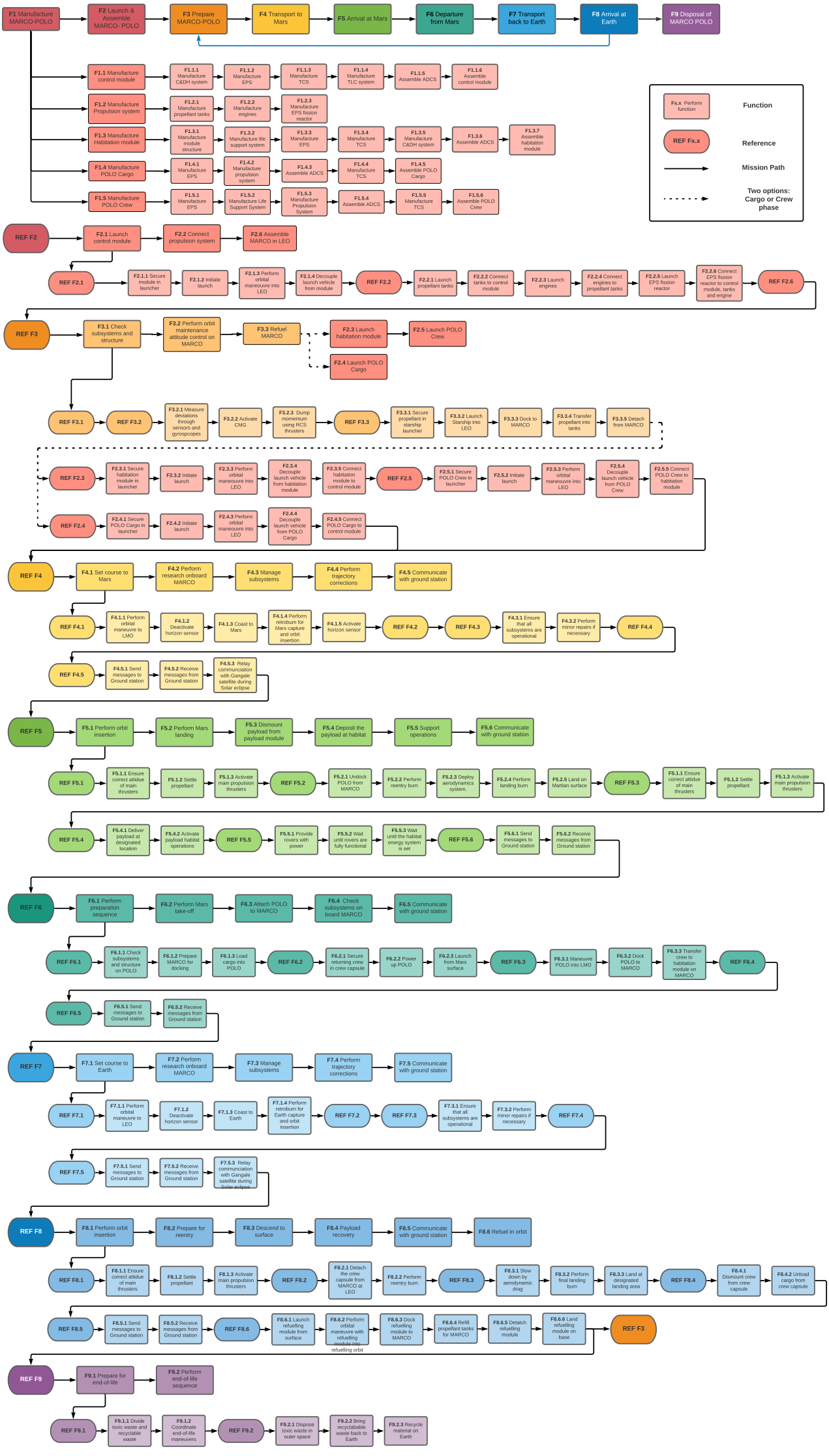
F1 Manufacture MARCO-POLO
F2 Launch & Assemble MARCO- POLO
F3 Prepare MARCO-POLO
F4 Transport to Mars
F5 Arrival at Mars
F6 Departure from Mars
F7 Transport back to Earth
F8 Arrival at Earth
F9 Disposal of MARCO POLO
F1.1 Manufacture control module
F1.1.1 Manufacture C&DH system
F1.1.2 Manufacture EPS
F1.1.3 Manufacture TCS
F1.1.4 Manufacture TLC system
F1.1.5 Assemble ADCS
F1.1.6 Assemble control module
F1.2 Manufacture Propulsion system
F1.2.1 Manufacture propellant tanks
F1.2.2 Manufacture engines
F1.2.3 Manufacture EPS fission reactor
F1.3 Manufacture Habitation module
F1.3.1 Manufacture module structure
F1.3.2 Manufacture life support system
F1.3.3 Manufacture EPS
F1.3.4 Manufacture TCS
F1.3.5 Manufacture C&DH system
F1.3.6 Assemble ADCS
F1.3.7 Assemble habitation module
F1.4 Manufacture POLO Cargo
F1.4.1 Manufacture EPS
F1.4.2 Manufacture propulsion system
F1.4.3 Assemble ADCS
F1.4.4 Manufacture TCS
F1.4.5 Assemble POLO Cargo
F1.5 Manufacture POLO Crew
F1.5.1 Manufacture EPS
F1.5.2 Manufacture Life Support System
F1.5.3 Manufacture Propulsion System
F1.5.4 Assemble ADCS
F1.5.5 Manufacture TCS
F1.5.6 Assemble POLO Crew
Fx.x Perform function
Function
REF Fx.x
Reference
Mission Path
Two options: Cargo or Crew phase
REF F2
F2.1 Launch control module
F2.2 Connect propulsion system
F2.6 Assemble MARCO in LEO
REF F2.1
F2.1.1 Secure module in launcher
F2.1.2 Initiate launch
F2.1.3 Perform orbital maneouvre into LEO
F2.1.4 Decouple launch vehicle from module
REF F2.2
F2.2.1 Launch propellant tanks
F2.2.2 Connect tanks to control module
F2.2.3 Launch engines
F2.2.4 Connect engines to propellant tanks
F2.2.5 Launch EPS fission reactor
F2.2.6 Connect EPS fission reactor to control module, tanks and engine
REF F2.6
REF F3
F3.1 Check subsystems and structure
F3.2 Perform orbit maintenance attitude control on MARCO
F3.3 Refuel MARCO
F2.3 Launch habitation module
F2.5 Launch POLO Crew
F2.4 Launch POLO Cargo
REF F3.1
REF F3.2
F3.2.1 Measure deviations through sensors and gyroscopes
F3.2.2 Activate CMG
F3.2.3 Dump momentum using RCS thrusters
REF F3.3
F3.3.1 Secure propellant in starship launcher
F3.3.2 Launch Starship into LEO
F3.3.3 Dock to MARCO
F3.3.4 Transfer propellant into tanks
F3.3.5 Detach from MARCO
REF F2.3
F2.3.1 Secure habitation module in launcher
F2.3.2 Initiate launch
F2.3.3 Perform orbital maneouvre into LEO
F2.3.4 Decouple launch vehicle from habitation module
F2.3.5 Connect habitation module to control module
REF F2.5
F2.5.1 Secure POLO Crew in launcher
F2.5.2 Initiate launch
F2.5.3 Perform orbital maneouvre into LEO
F2.5.4 Decouple launch vehicle from POLO Crew
F2.5.5 Connect POLO Crew to habitation module
REF F2.4
F2.4.1 Secure POLO Cargo in launcher
F2.4.2 Initiate launch
F2.4.3 Perform orbital maneouvre into LEO
F2.4.4 Decouple launch vehicle from POLO Cargo
F2.4.5 Connect POLO Cargo to control module
REF F4
F4.1 Set course to Mars
F4.2 Perform research onboard MARCO
F4.3 Manage subsystems
F4.4 Perform trajectory corrections
F4.5 Communicate with ground station
REF F4.1
F4.1.1 Perform orbital maneuvre to LMO
F4.1.2 Deactivate horizon sensor
F4.1.3 Coast to Mars
F4.1.4 Perform retroburn for Mars capture and orbit insertion
F4.1.5 Activate horizon sensor
REF F4.2
REF F4.3
F4.3.1 Ensure that all subsystems are operational
F4.3.2 Perform minor repairs if necessary
REF F4.4
REF F4.5
F4.5.1 Send messages to Ground station
F4.5.2 Receive messages from Ground station
F4.5.3 Relay communciation with Gangale satellite during Solar eclipse
REF F5
F5.1 Perform orbit insertion
F5.2 Perform Mars landing
F5.3 Dismount payload from payload module
F5.4 Deposit the payload at habitat
F5.5 Support operations
F5.6 Communicate with ground station
REF F5.1
F5.1.1 Ensure correct attidue of main thrusters
F5.1.2 Settle propellant
F5.1.3 Activate main propulsion thrusters
REF F5.2
F5.2.1 Undock POLO from MARCO
F5.2.2 Perform reentry burn
F5.2.3 Deploy aerodynamics system.
F5.2.4 Perform landing burn
F5.2.5 Land on Marian surface
REF F5.3
F5.1.1 Ensure correct attidue of main thrusters
F5.1.2 Settle propellant
F5.1.3 Activate main propulsion thrusters
REF F5.4
F5.4.1 Deliver payload at designated location
F5.4.2 Activate payload habitat operations
REF F5.5
F5.5.1 Provide rovers with power
F5.5.2 Wait until rovers are fully functional
F5.5.3 Wait until the habitat energy system is set
REF F5.6
F5.6.1 Send messages to Ground station
F5.6.2 Receive messages from Ground station
REF F6
F6.1 Perform preparation sequence
F6.2 Perform Mars take-off
F6.3 Attach POLO to MARCO
F6.4 Check subsystems on board MARCO
F6.5 Communicate with ground station
REF F6.1
F6.1.1 Check subsystems and structure on POLO
F6.1.2 Prepare MARCO for docking
F6.1.3 Load cargo into POLO
REF F6.2
F6.2.1 Secure returning crew in crew capsule
F6.2.2 Power up POLO
F6.2.3 Launch from Mars surface
REF F6.3
F6.3.1 Maneuvre POLO into LMO
F6.3.2 Dock POLO to MARCO
F6.3.3 Transfer crew to habitation module on MARCO
REF F6.4
REF F6.5
F6.5.1 Send messages to Ground station
F6.5.2 Receive messages from Ground station
REF F7
F7.1 Set course to Earth
F7.2 Perform research onboard MARCO
F7.3 Manage subsystems
F7.4 Perform trajectory corrections
F7.5 Communicate with ground station
REF F7.1
F7.1.1 Perform orbital maneuvre to LEO
F7.1.2 Deactivate horizon sensor
F7.1.3 Coast to Earth
F7.1.4 Perform retroburn for Earth capture and orbit insertion
REF F7.2
REF F7.3
F7.3.1 Ensure that all subsystems are operational
F7.3.2 Perform minor repairs if necessary
REF F7.4
REF F7.5
F7.5.1 Send messages to Ground station
F7.5.2 Receive messages from Ground station
F7.5.3 Relay communciation with Gangale satellite during Solar eclipse
REF F8
F8.1 Perform orbit insertion
F8.2 Prepare for reentry
F8.3 Descend to surface
F8.4 Payload recovery
F8.5 Communicate with ground station
F8.6 Refuel in orbit
REF F8.1
F8.1.1 Ensure correct attidue of main thrusters
F8.1.2 Settle propellant
F8.1.3 Activate main propulsion thrusters
REF F8.2
F8.2.1 Detach the crew capsule from MARCO at LEO
F8.2.2 Perform reentry burn
REF F8.3
F8.3.1 Slow down by aerodynamic drag
F8.3.2 Perform final landing burn
F8.3.3 Land at designated landing area
REF F8.4
F8.4.1 Dismount crew from crew capsule
F8.4.2 Unload cargo from crew capsule
REF F8.5
F8.5.1 Send messages to Ground station
F8.5.2 Receive messages from Ground station
REF F8.6
F8.6.1 Launch refuelling module from surface
F8.6.2 Perform orbital maneuvre with refuelling module into refuelling orbit
F8.6.3 Dock refuelling module to MARCO
F8.6.4 Refil propellant tanks for MARCO
F8.6.5 Detatch refuelling module
F8.6.6 Land refuelling module on base
REF F3
REF F9
F9.1 Prepare for end-of-life
F9.2 Perform end-of-life sequence
REF F9.1
F9.1.1 Divide toxic waste and recyclable waste
F9.1.2 Coordinate end-of-life maneuvers
REF F9.2
F9.2.1 Dispose toxic waste in outer space
F9.2.2 Bring recyclabable waste back to Earth
F9.2.3 Recycle material on Earth

8 Lander

The lander in this project will not be sized in the same detail as MARCO. However, it is still important to make sure that the budget estimate is correctly done. Therefore, the budget for POLO will be done first, which will ensure that the design of MARCO will be correct.

8.1 Lander Design

First, the lander design will be done. In this section, the lander will be split-up into multiple subsystems that will be designed separately, afterwards the lander budget will be presented.

8.1.1 Payload

Before sizing the lander, the required payload capacity has to be determined. The lander has to take four types of cargo to Mars: rovers, raw materials, accommodation elements and life-support. The rovers should be sent first after which the raw materials will have to arrive. Lastly, the accommodation elements and life support have to be sent in order to support the crew. The following mass and volume breakdown of the payload mostly follows from user requirements. The first breakdown is for the rovers and is given in Table 4. Since only the masses and the amount of rovers were given, the volume was obtained by looking at densities from other rovers[9].

Table 4: Rover cargo budget breakdown.

Type	**No. of Rovers**	**Mass [kg]**	**Volume [m^3]**
Scouter	400	2000	9
Driller	200	10 000	47
Excavator	200	16 000	76
Transporter	100	4000	19
Total	900	32 000	151

For the raw materials, the same mass as the rovers is estimated. The volume, however, depends on the material needed. Because the building materials will be excavated from the Martian surface, only the binder has to be taken from Earth. Studies related to 3D printing on other planets find that phosphoric acid is a good material to bind the Martian soil [76]. Therefore, the density of phosphoric acid is used, which results in a volume of 17 m^3 for the binder material.

The accommodation elements and life-support are estimated[10] to be 5000 kg and 1000 kg per person respectively. The volumes of both of these systems are 30 m^3 and 10 m^3 per person[11]. Considering that the habitat has to be able to support ten people, the total masses and volumes for all systems are shown in Table 5.

Table 5: POLO cargo budget breakdown.

Type	**Mass [kg]**	**Volume [m^3]**
Rovers	32 000	151
Binder	32 000	17
Accommodation	50 000	300
Life-Support	10 000	100
Total	124 000	568

There is room for three launches before the crew will arrive due to the available ten years in the planning (**MARCH-STS-04**, **MARCO-SCH-03**). This means that everything except for the life-support has to be taken to the Martian surface in those launches. It was deemed unsustainable to make a lander big enough to carry 38 t to Mars and be

[9] `https://mars.nasa.gov/MPF/rover/mission.html` *[cited 17 June 2021]*
[10] From a conversation with the customer. *[cited 31 May 2021]*
[11] From a conversation with the customer. *[cited 8 June 2021]*

able to return, since the mass would be too high, leading to many refuelling missions. Therefore, it was decided to make a separate lander for the cargo that is only able to land the cargo. In this way, MARCO can return without any payload mass and save propellant this way. This method is not possible for the human lander, as the crew has to be able to return to Earth. A schedule of the missions is given in Table 6.

Table 6: Budget breakdown for the POLO missions.

Launch	**Type**	**Mass [t]**	**Volume [kg m^{-3}]**
Cargo 1	Rovers	32	151
	Binder	6	3.2
	Total	38	155
	+SF	45	300
Cargo 2	Binder	13	6.9
	Accommodation	25	150
	Total	38	157
	+SF	45	300
Cargo 3	Binder	13	6.9
	Accommodation	25	150
	Total	38	157
	+SF	45	300
Crew 1	Life-Support	5	50
	Total	5	50
	+SF	6	60
Crew 2	Life-Support	5	50
	Total	5	50
	+SF	6	60

Some remarks on the budgets: firstly, the safety factor on the volume of the cargo missions is rather large because the rovers and accommodation elements can not be perfectly stacked. Therefore, a conservative number is taken in order to be sure that everything will be able to fit. The life-support is mostly food and water and that has a high packing density. Secondly, the crew missions will only take the life-support with them, as the payload mass should be as low as possible there because of the reusability requirement. The crew missions will also be able to take maintenance hardware with it on later missions.

In the end, the cargo for the crew missions will be a 16 t wet mass capsule, which includes the payload and five crew members[12]. The cargo version will have a dedicated cargo fairing with a volume of 300 m^3 and a cargo mass of 45 t.

8.1.2 Astrodynamics

Before sizing the subsystem, it is important to know how much ΔV is needed for the lander. Because the lander is split up into a cargo and crew version, two different budgets are needed. The crew lander needs both a descent and an ascent ΔV budget, while the cargo version will only need the descent budget.

For a preliminary sizing, the descent ΔV is rather hard to calculate, especially since there have been no landers that have landed in the 100 t class. However, multiple studies have been done that look at Martian descent vehicles and simulate their trajectory. From these studies, it turns out that a lander with a ballistic coefficient of 600 kg m^{-2} needs a descent ΔV of at least 700 m s^{-1} [77], [78]. Because of this rough estimate, a safety margin of 20 % is used, making the descent ΔV 840 m s^{-1}.

The ascent ΔV budget can be calculated and does not depend much on the shape and size of the vehicle. This is under the assumption that drag is negligible. Drag is often neglected for Earth launches [64], and since the Earth's

[12] `https://www.spacex.com/vehicles/dragon/` *[cited 17 June 2021]*

atmosphere is 100 times as dense as the one from Mars, it is also neglected here. The only estimate that is needed is the one for the gravity losses, which depend on the thrust to weight ratio of the lander. The formulas used for the ascent are shown in Equations 1-4 [64]. The input parameters are shown in Table 7.

$$V_{circ} = \sqrt{\frac{\mu}{r+h}} \tag{1}$$

$$V_{rad} = \sqrt{h\left(g_0 + \frac{\mu}{(r+h)^2}\right)} \tag{2}$$

$$V_{rot} = \cos(\phi)\frac{2\pi r}{t_d} \tag{3}$$

$$\Delta V = \sqrt{(V_{circ} - V_{rot})^2 + V_{rad}^2} + V_{grav} \tag{4}$$

Table 7: Input parameters for the ascent ΔV calculations.

Variable	Quantity	Unit
μ	42 828.37	$km^3\,s^{-2}$
r	3389.5	km
h	500	km
g_0	3.728	$m\,s^{-2}$
ϕ	42.109	°
t_d	88 775	s
V_{grav}	822	$m\,s^{-1}$

The outcome of the calculation is that the crew lander will need a ΔV of 4447 $m\,s^{-1}$ for the ascent phase. In Table 7, one of the inputs is V_{grav}, which is the velocity change due to gravity losses. This term was calculated with a small simulation based on timesteps that uses a gravity turn to get into orbit. Then, the total gravity loss can be obtained by summing Equation 5 for every timestep. In this equation, γ is the flight path angle and g is the gravity at the altitude of the iteration. The flight path angle was calculated using Equation 6[13]. The resulting 822 $m\,s^{-1}$ of losses is around 18% of the total ΔV budget, which fits in the expected values from literature of 14% to 19% [80].

$$dV_{grav} = g\sin(\gamma) \tag{5}$$

$$\gamma = \cos^{-1}\left(-\frac{V^2}{g(r+h)}\right) \tag{6}$$

The calculated ΔV of 4.447 $km\,s^{-1}$ also fits right in the expected 4.1 $km\,s^{-1}$ to 5.7 $km\,s^{-1}$ for an ascent vehicle to low Mars orbit [5].

8.1.3 Propulsion

The propulsion system will consist of hydrolox engines, as discussed in the midterm report [8]. Because the lander will not be designed in detail, an already existing engine is chosen, in this case the RL10A-4-2. The RL10 engine exists for over sixty years and is a reliable and efficient engine [14]. This vacuum optimised engine has a high thrust to weight ratio (61:1) and I_{sp} (451). Another advantage is that the expansion ratio is not too large at 84:1, compared to some versions that exceed 250:1, as the lander has to be able to provide thrust in an atmosphere. The characteristics are

[13] `https://wodeshu.gitee.io/orbit/text00012.html` *[cited 10 June 2021]*
[14] `https://www.rocket.com/space/liquid-engines/rl10-engine` *[cited 29 June 2021]*

shown in Table 8[15]. The values for Mars are calculated from the vacuum characteristics using Equations 7 and 8, derived from [1].

Table 8: RL10A-4-2 engine characteristics.

Variable	Quantity	Unit
T_{vac}	99.1	kN
T_{mars}	94.4	kN
$I_{sp_{vac}}$	451	s
$I_{sp_{mars}}$	430	s
A_e	0.79	m^2
P_{mars}	610	Pa

$$I_{sp_{mars}} = I_{sp_{vac}} - \frac{P_{mars} A_e}{9.81 \dot{m}} \tag{7}$$

$$T = 9.81 \dot{m} I_{sp} \tag{8}$$

Because POLO cargo only needs to land, it will only need four engines, that will make it capable of starting the landing burn with an acceleration of 1.5 times the acceleration of Mars. POLO crew, however, also needs to be able to take-off from Mars. From the gravity loss simulation, it was determined that eight engines was the best amount for this lander in terms of total mass.

8.1.4 ADCS

The lander needs to be provided with stability in order to be able to land in the correct orientation. Although an attitude control system could be used for this, after calculating the centre of mass and centre of pressure of both landers, their centre of mass lies bellow their centre of pressure, therefore making them stable (their attitude converges in the right direction).

Despite this, a displacement control system and attitude determination systems are needed. Gyroscopes and accelerometers are installed, as well as thrusters for an internal attitude determination and control. On top of this, visual aid by the use of Terrain-Relative Navigation is used. This scans the patterns directly below the lander and compares it to mapped terrain of Mars. This indicates where the lander will be making its landing.

The lander propellant mass presented in the budget for each lander is 2 t. This is calculated as a percentage of the propulsion mass, taken from literature of other lander missions [74]. Costs, volume and power are obtained using data and the same methods as presented in section 13. The visual aid camera's parameters is taken from literature, based on NASA's lander design[16].

8.1.5 Electrical Power System

Each of the two lander options has a different purpose and hence a different power requirement. In table 9, the EPS specifications for both the POLO Crew and POLO Cargo are mentioned. As stated in the midterm report [8], POLO crew generates power using a Kilopower Nuclear fission reactor[17], which can produce up to 10 kW. Using two of these reactors, the power need for POLO Crew can be met for the duration of the crewed phase, with the second one being a back-up (also used during higher loads). For the cargo specifications, the steps followed are identical to those in section 12.3.3, using the same Li-ion battery pack with the same efficiencies as that of the MARCO EPS. The battery pack is designed for a power requirement of 10 kW (based on the martian power system's output [12]) for 24 h.

[15] http://www.astronautix.com/r/rl-10a-4-2.html *[cited 29 June 2021]*

[16] https://trs.jpl.nasa.gov/bitstream/handle/2014/46727/CL%2316-2289.pdf?sequence=1 *[cited 17 June 2021]*

[17] https://www.nasa.gov/directorates/spacetech/feature/Powering_Up_NASA_Human_Reach_for_the_Red_Planet *[cited 17 June 2021]*

Table 9: EPS specifications for POLO Crew and POLO Cargo.

Lander	Parameter	Magnitude	Unit
POLO Crew	Power Generated	11.2	kW
	Mass	205.3	kg
	Volume	1.15	m^3
	Cost	32	M€
POLO Cargo	Power Required	10	kW
	Duration	24	h
	Actual Energy Stored	40.71	kW h
	Mass	176.2	kg
	Volume	0.06	m^3
	Cost	45.6	M€

8.1.6 Thermal Control

Thermal control of all equipment and crew inside POLO must be present in order to have a succesfull landing on Mars. Just like the TCS of MARCO, POLO will also make use of heat exchangers, pumps, valves, radiators and cold plates. The TCS design of POLO can be compared with the TCS of the Orion capsule. Assuming that the mass percentage of the TCS compared to the dry mass is the same as the percentage of the TCS mass of a large GEO telecommunications satellite, the TCS mass will be 5% of the total POLO mass. This is equal to 0.75 t.

For the Zero Boil Off (ZBO) system, an already researched system is used. This system will be able to provide enough cooling for the tanks to make sure that the oxygen and hydrogen do not boil-off. Since the scale for the lander will be smaller as compared to MARCO, a mass of 0.5 t is assumed [37].

8.1.7 Telecommunications

An in-depth description of the sizing of the telecommunications subsystem of POLO is given in Section 14.3, but is summarised here as well. POLO will have 2 low-gain antennas with which it will communicate with MARCO, or with relay satellites in Mars-stationary orbit. The used frequency for both these communication links is 2.25 GHz. The transmitter power needed to be able to establish these communication links is 60 W. To find the total mass- and power budget of the complete subsystem, the telecommunication subsystem of POLO was compared to that of the Mars Reconnaissance Orbiter (MRO). The total power consumption was then found to be 109 W, and the total mass of the subsystem was calculated to be 49.8 kg. The volume was determined by assuming a constant density of $0.5\,kg\,m^{-3}$ for all the components. This lead to a total volume of $0.125\,m^3$. Finally, for the cost budget, the price of the antennas and of the services of the relay satellites around Mars needed to be known. It was assumed that contact between POLO and the relay satellites was established for about 1.5 hours per day. This combined with the price per hour of the relay satellites, the total amount of days that POLO will be on Mars, and the price of the antennas, the total cost budget was estimated to be €35.3 Million. However, since this mission is such a huge undertaking, other agencies that might operate these relay satellites will probably be involved, which means the cost of using these satellites will likely reduce significantly.

8.1.8 Structures

As the lander is not designed in detail, the structure is not designed in detail. Literature teaches us that the structural mass is approximately 20% of the dry mass and that the volume is 5% of the total volume . This gives a structural mass of 2.4 t with a volume of $11.6\,m^3$ for the human lander and 2.1 t with a volume of $4.4\,m^3$ for the cargo lander.

8.1.9 C&DH

Similarly to the structure, an estimate for the mass and volume of the command and data handling system is also made based on literature. It is, however, very difficult to find accurate estimates for spacecraft similar to POLO, and thus only a very rough estimate can be made. In the ADSEE reader [5], values for small and large satellites can be found, giving values around 7% and 4% respectively. Since even the heaviest satellites are considerably smaller than POLO, it is expected that the mass fraction for POLO shall be even smaller. However, POLO does have the added complexity of needing to perform an autonomous landing. This requires additional sensors, such as cameras and barometers, to provide enough data to be able to perform such complicated manoeuvres. Taking this into account,

a mass estimate of 6% of the dry mass is made. This is quite high, due to the very large uncertainty that is present. This yields a final mass of 0.8 t.

Making a volume estimate for the C&DH is an even more difficult task. Little to no data is available from literature, as no spacecraft have similar requirements and functions as POLO. The ADSEE reader also offers little help, as it contains no statistical data either. Thus, it is assumed that a density of $1\,\mathrm{kg\,m^{-3}}$ is maintained by the C&DH system. As many components might need some space for cooling purposes, another $0.1\,\mathrm{m^3}$ is added, giving a total of $0.9\,\mathrm{m^3}$.

8.1.10 Budget Breakdown

All subsystems of the lander have now been sized, and the masses and volumes are combined in Table 10. The eventual value also includes the contingency budget for both the cargo and the crew lander. Since the sizing was preliminary, a margin of 20 % is used.

Table 10: POLO crew lander budget breakdown.

	Crew		Cargo	
System	**Mass [t]**	**Volume [m^3]**	**Mass [t]**	**Volume [m^3]**
Engines	1.3	11.1	0.67	5.7
Tanks	0.8	201	0.5	69.5
EPS	0.21	1.2	0.18	0.06
ADCS	2.0	1.6	2.0	1.6
Docking	0.27	1.0	0.27	1.0
Legs	2.0	4.0	2.0	4.0
Thermal	1.0	0.5	1.0	0.5
Telecommunications	0.1	0.13	0.1	0.13
ZBO	0.5	0.5	0.5	0.5
Structure	2.4	11.6	2.1	4.4
C&DH	0.8	0.9	0.8	0.9
Sub Total	11.3	233	9.5	88
+20%	13.6	280	11.4	106
Propellant	72.0	-	12.4	-
Payload	16.0	50	45.0	200
Total	102	156	69	306

8.1.11 Drawings

The final drawings that show the size and look of the POLO landers is given in Figure 3. Here, the orange circles represent the propellant tanks. The smaller tanks are for oxygen, and the bigger tanks are for hydrogen. The black circles are the engines. The landing legs are drawn as triangles at the bottom of the landers. The crew lander has four aerobrakes in order to slow down during descent. The cargo version has four fins that make it passively stable due to its dart-shaped nature. As this is a descent vehicle only, this does not matter and will only benefit the mission.

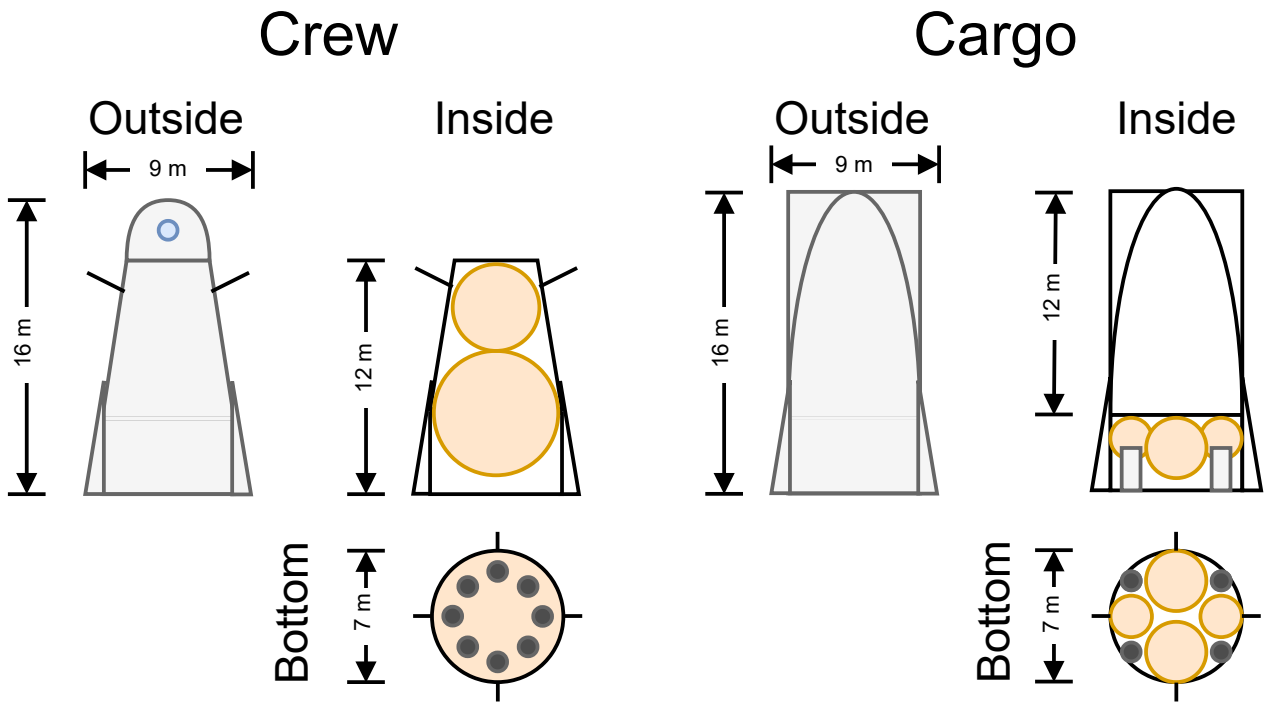

Figure 3: Schematic drawing for the POLO crew and cargo variant.

8.2 Risk Analysis

Table 11: Risk table including the most critical risks for each subsystem. RBM is defined as "likelihood, impact" before mitigation, RAM is "likelihood, impact" after mitigation.

ID	Risk	RBM	Mitigation	RAM
POLO01	Nuclear Fission reactor fails	1, 5	**Reduce** by adding redundancy with extra reactor	1, 3
POLO02	Nuclear leak due to reactor	2, 5	**Reduce** by containing the leak within POLO	2, 3
POLO03	Battery pack fails	1, 5	**Reduce** by adding redundancy	1, 3
POLO04	EPS gets damaged upon landing	3, 4	**Avoid** by designing for a soft landing (landing legs)	1, 4
POLO05	Sensors malfunction	3, 4	**Reduce** with extra sensors	3, 1
POLO06	The chosen components will drift and cause accuracy errors	4, 3	**Reduce** by adding redundancy	4, 1
POLO07	Engines do not light	2, 5	**Reduce** by adding redundancy	2, 2
POLO08	Propellant tank leak	1, 4	**Reduce** by bringing more than necessary	1, 2

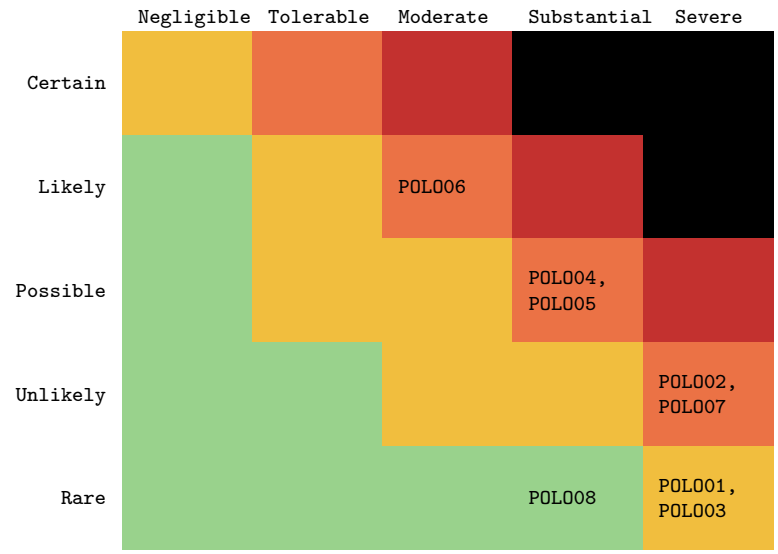

Figure 4: Risk matrix of identified subsystems risks. Likelihood is listed vertically and impact is listed horizontally.

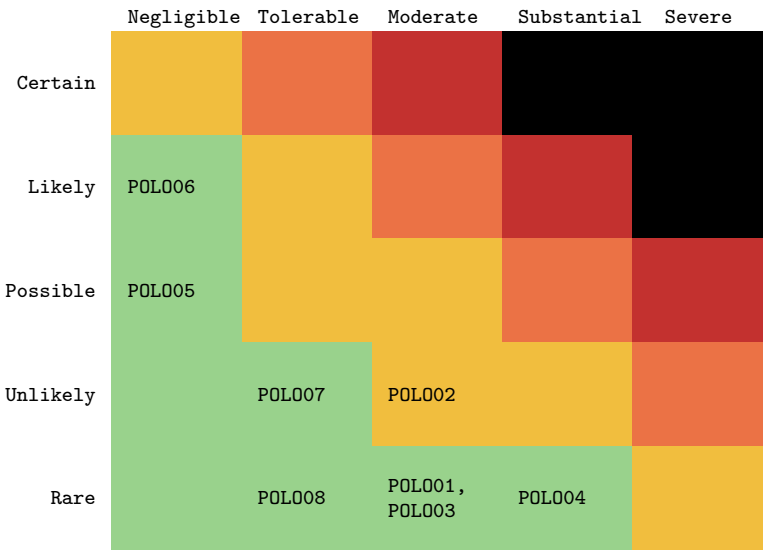

Figure 5: Risk matrix of mitigated risks. Likelihood is listed vertically and impact is listed horizontally.

8.3 Sustainability

The main consideration for designing two different landers was based on sustainability. It can seem like quite the opposite when one lander is built just to be left on another planet, but the amount of propellant saved far exceeds the impact of leaving it on Mars. The amount of propellant saved contributes to both a more environmentally and economically sustainable project. Not only did designing two landers give an opportunity for saving propellant, it also gave rise to the possibility of making one lander specific for cargo, which means that significantly more payload can be brought from Earth to Mars in one trip. This extra payload will allow for a timely completion of the Rhizome habitat within the 10-year time frame that is given.

The cargo landers that will be left on the surface of Mars, will serve multiple purposes. In the beginning, the rovers will need power before the Rhizome habitat's power system is set up. This is taken care of by the lander. Furthermore, POLO cargo will also serve as a safe storage place for equipment until the habitat is set up. This means that equipment and supplies brought up by POLO cargo will stay inside POLO cargo, safe from the harsh martian environment. As there are 13 years between the first cargo arrival and the first human arrival as seen in Table 13, the equipment will need to be protected from the martian environment for a considerable time, which POLO cargo can be used for.

8.4 Recommendations

The main focus of this report is MARCO, and not any of the landers. Therefore, for future reference, it is recommended to dedicate an entire detailed design phase for both landers to obtain the required accuracy of the design. This will allow for thorough calculations and more precise estimations of the components of the landers. As the two landers have two completely different objectives; one is to bring a large payload to the surface of Mars, the other one is to safely bring humans and a small payload to the surface of Mars and back to the surface of Earth, it is recommended to divide the two landers between two different design teams or at least into two different design phases, such that each lander is optimised for its own objective.

9 Astrodynamics

In the midterm, a preliminary analysis of the astrodynamic characteristics was done. A preliminary comparison of ΔV requirements and travel time was done, and two types of missions were looked into: conjunction and opposition, where the first has lower ΔV requirements but higher mission times, with the opposite being the case for the second.

In this section, it is decided on what the mission will look like and what the exact schedule of the missions will be. A total mission duration for MARCO is given, as well as a total, and final, ΔV budget is given. This is done by means

of porkchop plots for all the missions, which were constructed using the Python package poliastro[18]. Also generated with Python are the mappings of all the trajectories of MARCO. The requirements are also stated, and at the end of the section a compliance matrix for these requirements is given.

Finally, a summary of the total mission schedule is given, as well as the conclusion for the astrodynamic design.

9.1 Requirements

The following three requirements were further discussed in detail in the midterm report [8] where more information can be found, and only the requirement itself will be presented here.

- **M-AST-01**: The ITS shall deliver the manned missions to Mars within 350 days after launch.
- **M-AST-02**: The ITS shall perform a round trip between Earth and Mars in no more than 1050 days.
- **M-AST-03**: The trajectory taken by the ITS shall have a ΔV requirement of no more than $12\,\mathrm{km\,s^{-1}}$.

9.2 Mission design

First, a decision must be made for what type of mission will be performed: a conjunction, or opposition class mission. This of course depends on the requirements for the ΔV and the mission time. The scheduling requirement which states that the habitat must be fully functional within ten years after the maiden launch is one critical factor here, as well as the mass and the cost of the propellant.

As the total cargo mass is 114 t to get the habitat up and running and the lander can transport a maximum mass of 45 t per launch, three cargo launches are needed to get the habitat fully functional. After some calculations, it was found that this can in fact be done within ten years. As the propellant cost and mass started becoming unacceptable for ΔV requirements of more than $12\,\mathrm{km\,s^{-1}}$, it was therefore decided to use a conjunction type mission, which uses less ΔV.

Furthermore, the possibility of gravity assists was investigated. Because a conjunction class mission is used, a Venus gravity assist was eliminated as an option. A lunar gravity assist was looked into [17], [18], however this is not feasible for a reusable mission, as the Moon needs to be in a very favourable position for this to have a positive effect, while the one spacecraft that actually attempted such a manoeuvre took five months to get into the transfer orbit (it also failed, however this was not due to the manoeuvre but due to a mechanical failure). It was therefore opted not to utilise a gravity assist.

The set-up of the mission will be as follows: first, three cargo missions will be performed. These are necessary to get the habitat fully functional. Afterwards, four manned missions are planned. When these have been completed, three further missions can be performed, as MARCO is reusable for ten return trips to Mars.

For the mission schedule and ΔV, use was made of porkchop plots. The explanation for these, and the results, are given in Section 9.3.

Furthermore, the mapping of the trajectory taken by MARCO is also shown in Section 9.3. This visualises the path that MARCO takes between both planets.

9.3 Results

This subsection outlines the results of generating the porkchop plots and the necessary ΔV values. It first gives an explanation about porkchop plots in general, and how the values are obtained. Afterwards, the results of the first mission are given. The figures for the nine other missions are given in Appendix A.

9.3.1 Explanation Porkchop Plots

Porkchop plots were used to obtain the values for the ten scheduled missions: ΔV, launch and arrival date, and the mission duration. Porkchop plots are great tools for visualising the relation between launch and arrival dates and the

[18] `https://www.poliastro.space` *[cited 16 June 2021]*

required energy for this. Porkchop plots are contour plots, with launch date on the x-axis and arrival date on the y-axis. The contours show the launch characteristic energy C_3 ($km^2\,s^{-2}$), which is defined as follows:

$$C_3 = V_\infty^2 \tag{9}$$

Another contour, the blue lines, indicate the arrival excess velocity (V_∞). This is the velocity of the hyperbolic orbit at a theoretical infinite distance from the object it's orbiting, but practically the velocity of the spacecraft when leaving the sphere of influence (SOI) of the body. The dashed red lines in the plot indicate the time of flight. For every mission, the porkchop plots (to Mars and to Earth) are given, after which the mission values are shown in the tables below.

The ΔV was calculated from the characteristic energy as follows:

$$\Delta V = \sqrt{C_3 + \frac{2\mu_{planet}}{a_{LEO}}} - \sqrt{\frac{\mu_{planet}}{a_{LEO}}} \tag{10}$$

The altitude of the LEO chosen to park MARCO in is 2000 km, so a_{LEO} is this plus the radius of the Earth. Note that this has been changed from the midterm report, as this used to be 500 km. This change was made due to the fact that there will be a nuclear reactor on board, and it was found that, due to safety considerations, a Nuclear Safe Orbit (NSO) is used. These range from 1000 km to 2500 km [55]. Another consideration for this is the launcher, and its capability of launching payload to 2000 km altitude. The Starship and SLS will be used for transporting payload to LEO: these launchers have a payload capability to LEO of 90 tonnes in the case of the SLS[19], and 100+ tonnes in Starship's case for an altitude of 500 km[20]. Due to the fact that the maximum payload that has to be launched for the mission is only 69 tonnes, compared to the payload capability of these launchers, this additional altitude was not deemed an obstacle.

Because of this change in altitude, the ΔV requirements also decrease. This change aided in keeping the maximum mission ΔV under 12 $km\,s^{-1}$, even with margin, which is explained in subsection 9.5.

These plots were generated using the Python package poliastro, which takes into account eccentricity of the orbits of Earth and Mars, and the difference in inclination. The presentation of the results is as in Subsection 9.3.2, while the rest of the results are in Appendix A.

9.3.2 First Cargo Mission

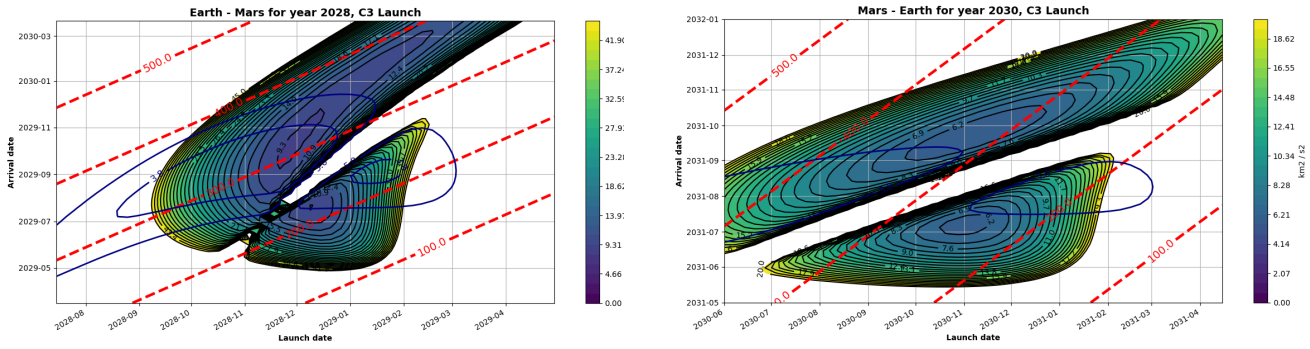

(a) Porkchop plot for the launch window in 2028

(b) Porkchop plot for the launch window in 2031

Figure 6: The porkchop plots for the first cargo mission.

[19] https://www.nasa.gov/exploration/systems/sls/to-the-moon.html *[cited 22 June 2021]*
[20] https://www.spacex.com/media/starship_users_guide_v1.pdf *[cited 22 June 2021]*

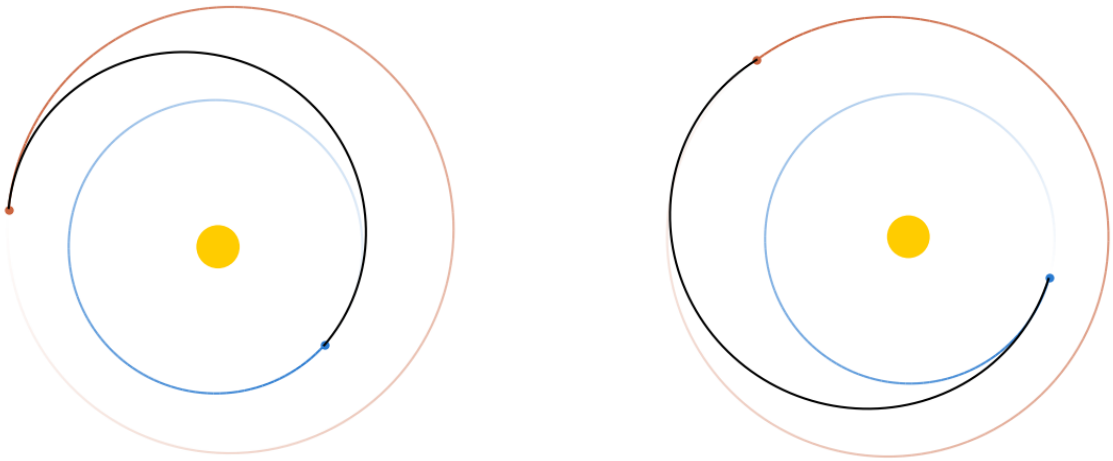

(a) Mapping of the trajectory to Mars

(b) Mapping of the trajectory to Earth

Figure 7: The trajectories of the first cargo mission.

Table 12: Mission values for the first mission.

Destination	**ΔV** [km s^{-1}]	**Launch Date**	**Arrival Date**	**Duration [days]**
Mars	5.552	22-11-2028	17-09-2029	299
Earth	5.806	30-08-2030	20-08-2031	355
Total	11.358	22-11-2028	20-08-2031	1001

9.3.3 Methodology to obtain results

This subsection aims to serve as an explanation for how the values in Table 12 were obtained.

The process of obtaining these numbers starts with the generation of the porkchop plots, using poliastro. These porkchop plots in Python come with certain arrays of values: $C_{3_{dep}}$, $C_{3_{arr}}$, $V_{\infty_{dep}}$, $V_{\infty_{arr}}$, and transfer time. The launch and arrival date are the inputs.

The minimum ΔV launch and arrival were obtained by finding the minimum sum of $C_{3_{dep}}$ and $C_{3_{arr}}$ for a combination of launch and arrival date.

The ΔV for launch and departure burns were calculated using Equation 10, by plugging in $C_{3_{dep}}$ and $C_{3_{arr}}$. The total mission ΔV were calculated by summing these values from both the trip to and from Mars. By finding the indices of these minimum ΔV launches, the launch dates, arrival dates and transfer times corresponding to these minimum ΔV values could also be found, and were then tabulated in Table 12 and in the tables in Appendix A.

9.4 Summary of Missions

Below, in Table 13, a summation of all the missions that will be conducted is given. It gives the total ΔV required over all the missions, as well as the total duration of the mission, which is 15 111 days or 41 years and 4 months for ten missions to Mars. After this, the mission is considered complete. At this time, however, it might be possible that it will still be used for further missions instead of being disposed off, but that cannot be said definitively at this time.

Table 13: Summary of all mission values.

Mission	ΔV [km s^{-1}]	Launch from Earth	Arrival at Mars	Launch from Mars	Arrival at Earth	Duration [days]
1	11.358	22-11-2028	17-09-2029	30-08-2030	13-08-2031	1001
2	11.325	20-04-2033	04-11-2033	14-05-2035	27-11-2035	951
3	11.368	14-08-2037	26-07-2038	24-07-2039	03-05-2040	993
4	10.788	18-10-2041	03-09-2042	04-08-2043	02-07-2044	988
5	11.424	09-12-2045	25-09-2046	15-01-2048	25-08-2048	990
6	11.394	25-05-2050	16-12-2050	24-06-2052	04-01-2053	955
7	10.977	07-09-2054	21-08-2055	23-07-2056	17-05-2057	993
8	10.956	07-11-2058	06-09-2059	02-08-2060	22-07-2061	988
9	11.450	04-01-2063	07-10-2063	26-02-2065	04-10-2065	1004
10	11.401	16-07-2067	06-02-2068	10-07-2069	07-04-2070	996
Total	112.165	22-11-2028	22-11-2028	22-11-2028	07-04-2070	15 111

9.5 Discussion

In the midterm report, two assumptions were made that simplified the preliminary analysis of the astrodynamics. These were that the orbits of Mars and Earth are both circular, and that the orbits are co-planar. This is not the case in the creation of the above porkchop plots, which influences the time of flight and the ΔV.

The difference in orbital inclination causes something interesting: Hohmann transfers become very energy demanding. This is due to the fact that the transfer orbit requires a large out-of-plane component, which in turn requires a significant amount of energy. This phenomenon causes a ridge to form in the middle of the porkchop plot, where no low-energy transfers are possible. If the planets are phased properly, a bridge can exist for these trajectories, although the energy requirement is still relatively high, especially compared to other parts of the plot [24].

There exist two distinct areas in porkchop plots. One corresponds to a transfer orbit with an anomaly change of less than 180°, while the other corresponds to one with more than 180°. These mission types are called type I and type II missions. Type I missions have a lower transfer time, logically. Which type has a lower ΔV depends on the relative position of the planets [24].

The difference between these two types can be seen in the mappings of the trajectories for all the missions: those with longer times of flight perform more than half an orbit around the Sun (type II), while the shorter time transfers reach Mars before going halfway around the Sun.

For the manned missions, the required ΔV was investigated for both areas of the plots, as it is beneficial for these missions to minimise the time of flight. If the ΔV was minimal for a type I transfer or if the difference was deemed acceptable, this type was chosen. The only manned mission that could follow this type I trajectory is the third mission, where this type has the lowest required ΔV. The other missions had a ΔV requirement too high for this quicker transfer.

Lastly, a small margin will have to be put on the ΔV, as a slight delay in launching from orbit might occur during the mission, which would increase the ΔV requirement. The margin was chosen to be $2\,\%$, as this provides sufficient launch opportunities for the maximum ΔV mission, adding a plan B for the date of launch. The ΔV designed for will then become $11.679\,\mathrm{km\,s^{-1}}$.

In Section 9.6, the compliance matrix for the astrodynamics requirements is shown. As can be seen, all requirements stated in Section 9.1 are fulfilled. Of course, a minimal transfer time for manned missions is ideal, so switching the scheduling around slightly could be beneficial to the crew's health, despite the fact that the scheduling of the mission would be altered. The crew would have to wait for several years for the second launch window for manned missions, as this is a type I transfer, compared to the launch window for the first manned mission, which is

9.6 Compliance requirements

Table 14: Astrodynamics Requirements Compliance.

ID	Compliance	Rationale
M-AST-01	✓	In Appendix A, it can be seen that the longest transfer time for a manned mission is 348 days. This requirement is therefore fulfilled. It could be chosen to use different launch windows for manned missions after the first cargo phase in order to reduce the maximum time of flight further, although this would alter the scheduling of the mission.
M-AST-02	✓	As can be seen in Table 13, no mission has a longer total time than this, and this requirement is therefore fulfilled.
M-AST-03	✓	As seen in Table 13 and discussed in subsection 9.5, this requirement is fulfilled as the maximum total ΔV is 11.679 km s^{-1}.

9.7 Conclusion

In this section, the astrodynamics characteristics of the MARCO-POLO missions were investigated. A ΔV budget was constructed, for which the propulsion system must be designed. The maximum required mission ΔV was calculated to be 11.450 km s^{-1}, so the propulsion system must have the capability of delivering this amount of velocity increment to MARCO.

Furthermore, the scheduling for the missions was set up, including launch and arrival dates. The duration for most missions is quite similar, ranging from 949 days to 1004 days, a difference of close to two months on a mission time of around 2.7 years. The total mission will be 15 111 days, which is more than 41 years to conduct ten Earth-Mars return trips.

This process was done using porkchop plots, which proved to be excellent tools to design a space mission architecture, nicely visualising the lowest energy trajectories for certain launch windows.

10 Propulsion

As was determined in the midterm report, nuclear thermal propulsion (NTP) was deemed to be the optimal choice for our design. In this chapter, all the aspects of this system that were considered for the are given explained. The structure is divided into two parts: the first part focuses on the engines, the second part on the propellant tanks.

10.1 Trade-off Summary

During the midterm phase of this project a trade-off was made between different engine and propellant types. The types were: Methalox, hydrolox, nuclear thermal and nuclear electric propulsion. In the end it turned out that nuclear thermal propulsion was the best method to deliver the required ΔV in a sustainable way. This is because MARCO has to be fully reusable and that makes efficiency a key part of the engine. The nuclear propulsion system will cut the propellant cost in half compared to hydrolox while still being able to deliver the same thrust levels.

There are also downsides of this propulsion system. Firstly, the technology is not yet ready for a space mission as of June 2021. A short discussion on this matter can be found in Section 10.3. Another problem is that the engine works best with hydrogen propellant. This propellant has a low density and a cryogenic storage temperature, these problems will be designed for in the propellant tank section. The last downside is the use of nuclear fuels which has some safety risks when used. Methods on how to reduce the risk are given in the risk and sustainability sections.

10.2 Requirements

MARCO-PRP-01 The propulsion system shall be able to provide a thrust range of 150 kN to 440 kN.
Rationale: This makes sure that the engine will not exceed the acceleration limit.

MARCO-PRP-02 The propulsion system shall be able to provide a total ΔV of 12 km s^{-1}.

MARCO-PRP-04 The propulsion system shall have an engine mass no greater than 25 t.

MARCO-PRP-05 The propulsion system shall provide an acceleration no greater than $2\,\mathrm{m\,s^{-2}}$.
Rationale: This makes sure that the structural components of MARCO will not fail during acceleration.

MARCO-PRP-06 The propulsion system shall be restartable for 50 uses or more.
Rationale: This accounts for ten missions with four burns with spares for corrections.

MARCO-PRP-07 The propulsion system shall have a reliability of 95 % or higher.

MARCO-PRP-08 The propulsion system shall not damage any of the structural components of the spacecraft.

MARCO-PRP-09 The propulsion system shall be able to provide thrust for 1 h per thrust period.

MARCO-PRP-10 The ITS shall be able to store 500 t of propellant.

MARCO-PRP-11 The propulsion system shall have a total thrust period per mission of 2 h.
Rationale: This is the total needed engine on time of the longest mission.

MARCO-PRP-14 The propellant tanks shall keep the hydrogen at 20 K.
Rationale: This prevents the hydrogen from boiling-off.

MARCO-PRP-15 The propellant tanks shall be able to withstand a pressure of 2 bar.
Rationale: This makes sure that the tank will not rupture under normal circumstances.

MARCO-PRP-16 The propulsion system core temperature shall not exceed 2800 K during its operations.
Rationale: This prevents a meltdown of the engine.

MARCO-PRP-17 The engines of the propulsion system shall fit in one launch of Starship and SLS
Rationale: This will make sure that the launch cost will be kept down and make assembly unnecessary.

10.3 Engine

Firstly, a distinction between different types of NTP has to be made. The different systems that were considered are:

- Pulsed nuclear thermal rocket
- Fission fragment rocket
- Liquid core
- Gas core
- Solid core

As the first launch is planned as soon as 2028, technology readiness level (TRL) played a large part in the selection of the solid core system. The TRL of solid core nuclear thermal propulsion is about 5-6, whereas the other systems are all below TRL 4 [33] [34]. Still, this technology readiness remains a point of attention. Whether NTP will be flight ready in 2028 remains to be seen, but there are strong indications of increased interest in NTP, based on NASA's budget allocation: recent investments in NTP have greatly increased the likelihood of seeing a flight capable system in 2028 [61].

10.3.1 Engine Operation

The solid core nuclear thermal engine works in the following way. Heat is generated in the nuclear core of the engine by the fission reaction of Uranium-235 isotopes. Liquid hydrogen is then pumped through the core and heated up from 20 K to the temperature of the core, which is set at 2700 K. Other research usually assumes higher core temperatures for increased specific impulse. However, as this design must have the capability of restarting at least 40 times and will have long thrust periods, it was decided to decrease the core temperature to increase system longevity. Heating of the nuclear core causes rapid expansion and increase in pressure of the hydrogen, it to be expelled through a nozzle at a high velocity. With the nuclear core temperature, the specific impulse can be calculated.

$$I_{sp} = \frac{1}{g_0}\sqrt{\frac{2\gamma}{\gamma - 1}\frac{RT}{M}} \tag{11}$$

Filling in Equation 11 with a molar mass (M) of 0.002 016 kg mol^{-1}, a specific heat ratio of 1.3 (γ), and a chamber temperature of 2700 K yields a specific impulse of 1000 s. As this is an ideal equation assuming perfectly axial flow direction, steady flow, and isentropic flow, a correction factor of 0.9 was used. This leads to a specific impulse of 900 s. This value was deemed realistic, as real-life tests have been performed that showed similar performance [35].

The thrust per engine was set to be 111 kN, as most research has been done on this class of engine, called a NERVA-derived 'Peewee' class engine. With a specific impulse of 900 s the exit velocity v_e is 8826 m s^{-1}, and the mass flow can be calculated according to Equation 12 [5]:

$$F = \dot{m} \cdot v_e \tag{12}$$

This results in a required mass flow of 12.58 kg s^{-1}. Applying a correction factor of 1.05, to account for the fact that the equation used assumes ideal conditions leads to a mass flow of 13.21 kg s^{-1}. With a density of 0.07 kg L^{-1}, this means that 189 L s^{-1} of liquid hydrogen has to be pumped through each engine. To heat one kg of hydrogen from 20 K to 2700 K, an energy of 40.2 MJ is needed. For this calculation, an average specific heat capacity of 15 kJ kg^{-1} K was used for the temperature range of 20 K to 2700 K for hydrogen [21]. Based on these calculations it was determined that for a mass flow of 13.21 kg s^{-1}, 534 MW of thermal power has to be generated inside the core.

This heat has to be generated by the fission reaction of Uranium-235. The Uranium is stored in fuel elements with channels drilled out to allow propellant to flow through and exchange heat. For most existing designs, these fuel elements are hexagonal and have a cross section length of 1.92 cm, resulting in a cross sectional area of 2.35 cm^2, and have a length of 1.32 m. Each fuel element generates around 1.2 MW of thermal power [10] [37]. Therefore, 446 fuel elements are required per engine to deliver the 534 MW of thermal power. Aside from fuel elements, the nuclear core consists of tie tubes. Tie tubes act as dual-pass heat exchangers, where hydrogen is pumped into the central supply passage at the top of the tie tube, passes down to the closed end at the bottom where it is passed through the nozzle to be able to provide cooling. The hydrogen flow then reverses, returning to the top of the tie tube in the annular return passage. The tie tube exit flow drives the turbopump. For bimodal operation, the tie tubes provide the only source of active fuel element cooling, removing decay heat from the reactor and converting it to electrical power through a Brayton cycle generator [19].

Different configurations of tie tubes with fuel elements are possible. For this design, the standard layout as given in Figure 8 is used.

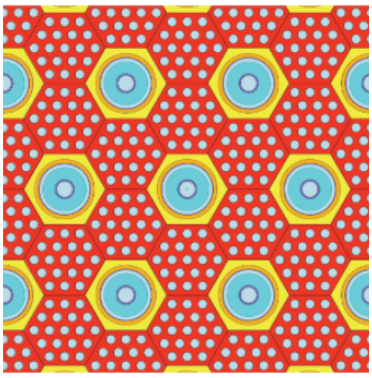

Figure 8: Layout of fuel elements and tie tubes [20].

This means that the ratio of fuel elements to tie tubes is 2:1 and thus, 223 tie tubes are required. The tie tubes have the same dimensions as the fuel elements, so the total cross sectional area of the 446 fuel elements and 223 tie tubes is 1572 cm^2. This can be approximated by a circle with a radius of 22.4 cm.

The nuclear core must be moderated in order to control the thermal output. This is done with control drums, which are placed around the nuclear core. They consist of a neutron reflector on one side and a neutron absorber on the other side. These drums can be rotated to control the number of neutrons that are reflected back into the core, speeding up or slowing down the number of fission reactions that occur therefore controlling the heat generated. These control drums have a thickness of 14.7 cm [19], leading to a total circle with a radius of 37 cm. With the

[21] https://www.engineeringtoolbox.com/hydrogen-d_976.html *[cited 7 June 2021]*

length of the fuel elements, tie tubes and control drums being 1.32 m, the volume of the core, including the control drums was calculated to be 0.57 m^3.

The nozzle exit diameter was set to be 1.87 m with an expansion ratio of 300, as this corresponds to the most standard configuration of Peewee class engines. The nozzle exit and throat areas can be calculated to be 2.75 m^2 and 0.0092 m^2, respectively. Using Equation 13, the chamber pressure can be calculated [1].

$$p_C = \frac{\dot{m}}{A^* \Gamma(\gamma)} \sqrt{\frac{R}{M} T_C} \tag{13}$$

Here, $\Gamma(\gamma)$ can be calculated according to Equation 14.

$$\Gamma(\gamma) = \sqrt{\gamma \left(\frac{1+\gamma}{2} \right)^{\frac{1+\gamma}{1-\gamma}}} \tag{14}$$

The resulting chamber pressure was calculated to be 2.3 MPa. This is lower than most values determined in other research, due to the lower core fuel temperatures assumed. This lower chamber pressure, along with the lower fuel temperature will likely improve the system's longevity and reusability.

10.3.2 Total Thrust Period

To determine the thrust period of a manoeuvre, the ΔV and the thrust level need to be known. In Chapter 9, the ΔV values of all the manoeuvres per mission are given. 4 engines producing 111 kN each are used. With the total mass at each stage of the mission known and maximum acceleration limited at 2 $m\,s^{-2}$, the thrust period of each burn can be determined. In Equation 15, a formula for determining the thrust period of a manoeuvre is given.

$$t_b = \frac{M_{initial} v_e}{T} \left(1 - e^{\frac{-\Delta V}{v_e}} \right) \tag{15}$$

Here, t_b is the thrust period or burn time, $M_{initial}$ is the total spacecraft mass at the start of the burn, T is the thrust force, and v_e is the exit velocity. For each manoeuvre, the thrust period was determined for both crewed and cargo configuration. The results can be seen in Table 42.

10.3.3 Bimodal Operation

When the engine is operating in electricity generation mode, the tie tubes are used to transport the working gas for a closed Brayton cycle generator. This working gas is a helium-xenon mixture that transports the thermal energy and drives a turbine. An added function of this system is the removal of decay heat after the propulsion system has shut down. In this design, each engine is equipped with a 25 kWe capable system, which operates at 20 % efficiency. Therefore, 125 kW of thermal power must be generated by the nuclear core, which is a factor 1000 decrease compared to propulsion mode. The excess heat is rejected through a cylindrical radiator mounted between the engine and propellant tanks. With a diameter of 8 m and required radiator area of 71 m^2, the length of this cylinder is 2.9 m. The total mass of the Brayton cycle system including heat radiator is estimated to be 1350 kg [37]. Power output can be regulated by controlling the reactivity of the core.

10.3.4 Radiation Shielding

As the propulsion system uses a nuclear core for its engines, radiation shielding will be required to protect the other subsystems and the crew from this radiation. This will add mass, but it is crucial for the proper functioning of the ITS.

The fission of Uranium-235 releases different types of radiation. The fission reaction starts by bombarding a Uranium-235 isotope with a neutron. This creates Uranium-236, which quickly dissociates into lighter elements, releasing alpha particles, neutrons, beta-radiation, and gamma radiation. The alpha particles and beta radiation are easily stopped even by thin layers of metal and pose no threat to any of the subsystems or crew. However, the neutrons and gamma radiation can penetrate much further and can be very destructive, to organisms as well as materials. Protection against these two types of radiation is investigated.

The main concern beforehand is the crew. However, as the nuclear core and crew will be separated by more than 15 m of liquid hydrogen, this concern can quickly be ignored: hydrogen is the most effective neutron radiation shield [22]. The crew will require shielding to protect from gamma radiation. This is already incorporated in the habitat structure, as the constant cosmic background radiation poses a larger threat.

One main detriment of radiation is that it can be absorbed by the propellant, causing heating and potential boiling close to the engine. This can lead to cavitation, which can in turn lead to failure of the turbopumps. However, research has shown that when accelerating at 0.5 g or higher, this risk decreases [21]. As the nuclear core thermal power and radiation output is a factor 1000 lower during electrical generation mode, the radiation shielding that will be put in place is assumed sufficient to not cause cavitation during the coast phases of the mission.

For shielding purposes, an internal and an external shield is used. The internal shield mass is included in the mass of the engine core: 2300 kg. The external shield will have to be sized separately. This external shield has a mass of up to 50% of the unshielded engine mass [22]. The upper bound was chosen, and an external shield mass of 1150 kg per engine was estimated. This would put the total shielding mass up to 4600 kg, as there are four engines.

There are two types of radiation against which the shielding must protect: neutron and gamma radiation. For neutron shielding, light materials are preferred as they are more effective for decreasing the kinetic energy of these neutrons. The two investigated materials for the neutron shield are lithium hydride and boron carbide. It was elected to use boron carbide, as there are a few downsides to using lithium hydride, despite it being lighter. These downsides are the added volume, as well as the poor thermal characteristics. Lithium hydride also displays irradiation swelling [23].

For the gamma radiation shielding, a material with a high charge density is desired, such as tungsten or lead. Gamma radiation is slowed down by contact with electrons, so a lot of electrons close together is the best configuration for this type of radiation.

The shield will have a total mass of 5000 kg (1250 kg per engine), and consist of two parts: one part made of boron carbide, and one made of tungsten or lead. The boron carbide shield would be in front, as neutron shielding can also cause secondary gamma radiation. It will be put close to the nuclear core, to cast as large of a protective 'shadow' over the vehicle as possible.

10.3.5 Thrust Vector Control and Throttling

To be able to compensate for changes in center of gravity, deal with one of the engine starting up with lag, or still provide thrust in an adequate direction during an engine-out situation, thrust vector control is an essential component for the propulsion system. In Figure 9, an overview of the engine layout is given.

In the case of one of the outside engines failing, the thrust becomes asymmetrical and a torque is generated. The magnitude of the torque depends on the thrust level of the engines, as well as the longitudinal position of the center of gravity. The aft-most center of gravity position is 32.19 m in front of the most aft part of the propellant tank, as explained in Chapter 13. The failure of one of these three engines is considered.

The two engines that are firing are symmetrical about one axis, counteracting eachother. The center of thrust of each of the engines is positioned 1.225 m away from away from the axis that they are asymmetrical about. With a center of gravity located 32.19 m away, in order to not generate a moment, the thrust force vector must point through the center of gravity. Therefore, a gimbal angle of $\tan^{-1}\left(\frac{1.225}{32.19}\right) = 2.18$ degrees is required. This will generate a force in the radial in or out direction, or the normal or anti-normal direction, which will need to be corrected for in subsequent burns.

To get a rough estimate on the required mass and power, values have been taken from a paper that researched thrust vector control for nuclear thermal propulsion [52]. In this paper, requirements were set for a gimbal range of up to 2.4° and a gimbal rate of up to $1.85\,^{\circ}\,s^{-1}$. The estimate for peak power requirement was 1000 W per engine, with an electric motor mass of 17 kg per engine. This peak power will however very rarely occur: only in the worst-case scenario. Other studies have estimated the total gimballing system mass at 50 kg to 60 kg for a 111 kN NTP engine [53] [20].

Due to certain load limits, the vehicle acceleration and therefore thrust level must be limited. The lowest thrust level that the propulsion system has to be capable of is 144 kN. With the middle engine turned off, this means that the minimal thrust per engine is 48 kN, or 43 % of the maximum thrust of the engine. This can be achieved by reducing

[22] https://hal.archives-ouvertes.fr/hal-03147500/document *[cited 15 June 2021]*

the thermal power output by rotating the control drums, as well as reducing the propellant mass flow.

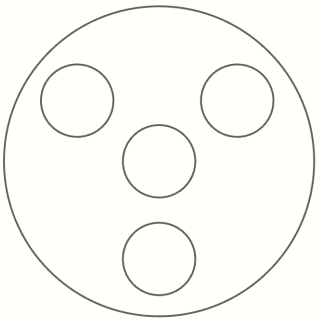

Figure 9: Schematic of the engine layout.

10.3.6 Uranium Content

Uranium-235 concentrations vary for different engines. Assuming an energy density of 1 g per megawatt-day, a continuous operation of 125 kWt for 40 years would require 1825 kg of Uranium. Assuming that each trip requires 100 minutes of full-power (512 MW per engine) operation, for a total of 10 trips, this adds another 356 kg of Uranium. This brings the total mass of Uranium to 2181 kg or 525 kg per engine. As the reactivity of the core decreases when more Uranium-235 has undergone fission, extra margins must be added to be able to maintain the desired performance. Even 545 kg cannot be incorporated into the fuel elements: the total volume of fuel elements in each engine is around 120 000 cm^3, meaning a density of Uranium of 4.5 g cm^{-3} is required. More common fissile loading of the fuel elements is around 0.5 g cm^{-3} to 1 g cm^{-3} Therefore, the fuel elements inside the engine will need to be replaced at least 4 times during the 40-year lifetime of the system. Naturally, this task cannot be performed by humans and will need to be done by robots. The specifics of this operation will need to be further researched.

10.3.7 System Budgets

Figure 15 in Section 10.5 shows a schematic overview of the propulsion system architecture. The engine uses an expander cycle to drive the turbopump. A propellant valve is opened to let liquid hydrogen into the system. At first, it passes through the tie tubes and is inserted into the nozzle to act as a coolant during engine operation. It is then passed upwards through the tie tubes again, where it heats up. This hydrogen, now turned into vapor, drives a turbine which drives the turbopump. The hydrogen is then passed through the propellant channels of the fuel elements where it is heated up further to around 2700 K, concentrated at the throat and expelled at the nozzle.

In Table 15, the engine components and their mass, as well as a total estimate for the costs are given. The nuclear core mass was determined by taking the mass of different nuclear cores, dividing them by the number of fuel elements and tie tubes that they consisted of, and multiplying that by the number of fuel elements and tie tubes in the nuclear core presented in this report. The mass of the control drums and internal shielding is incorporated in this figure. The values for engine structure, nozzle, turbomachinery and piping, internal shield, and gimballing mechanism were taken from nuclear thermal engines with similar characteristics [19][53]. An estimate for the unit cost per engine of 700 million dollars was made, based on a study performed by NASA [57]. Adding bimodal operation adds an estimated 100 million dollars per engine. This results in a total cost of 3.2 billion dollars or 2.68 billion euros for the 4 engines.

Table 15: Overview of engine components, their mass, and total cost.

Component	Mass [kg]
Nuclear core	2300
Radiation shielding	1150
Brayton cycle system	1350
Engine structure	300
Nozzle	150
Turbomachinery and piping	150
Gimballing mechanism	60
Total mass	5450
Total cost [M€]	670

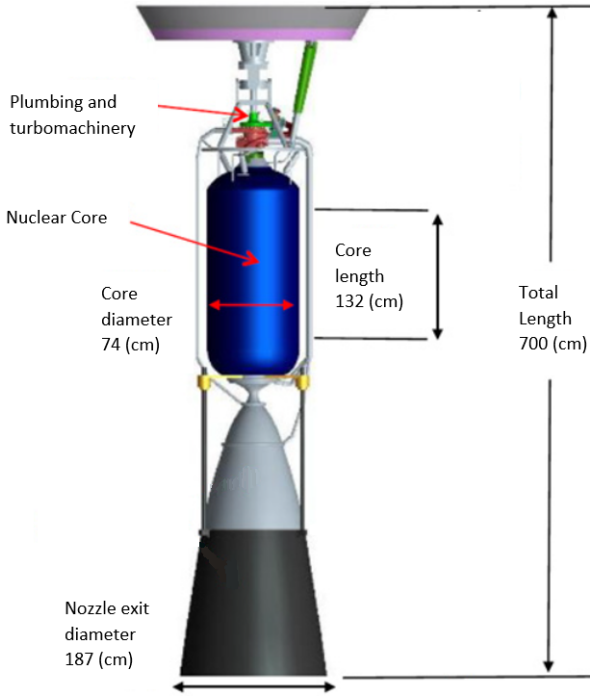

Figure 10: Overview of engine components and dimensions [56].

10.4 Propellant Storage

Because MARCO has to be fully reusable, the propellant storage solution will be the main structural component. Therefore, it is an important part of the design for MARCO. This section will go over multiple subsection of the tank design, namely the tank size, the tank structure and the cooling system.

10.4.1 Tank Size

When designing a liquid hydrogen propellant storage it is important to look at the available space inside a launch vehicle, as liquid hydrogen is volume bound instead of mass bound due to its low density of $71\,\mathrm{kg\,m^{-3}}$. This means that the 100 t payload capacity of Starship[23] will not be reached, as its maximum payload volume is $900\,\mathrm{m^3}$ which results in a propellant mass of 64 t. To get the most out of every launch the propellant tanks need to be tailored specifically to the payload fairing size, since the SLS is larger than Starship, the tank will be sized for Starship. The diameter of the Starship fairing is 8 m making this also the primary diameter of the propellant tank.

The only other dimensions that can still be sized are the bulkheads, because the tank will need to be able to store

[23] https://www.spacex.com/media/starship_users_guide_v1.pdf *[cited 14 June 2021]*

propellant under pressure a flat bulkhead was not considered. Hemispherical and elliptical bulkheads, however, are possible bulkheads. A common ratio for the elliptical bulkhead is 2:1, this means that the height of the head is only half of the radius. For this study three variants were considered, a two-sided hemispherical, a two-sided elliptical and a combination of elliptical and hemispherical. This can be seen in Figure 11. In the end the most optimal configuration in terms of volume per launch is the combination tank, this is because of its better fit at the bottom due to the flatness of the elliptical head and the roundness at the top of the hemispherical head. This configuration has a maximum volume of 704 m^3 making it able to carry 50.0 t of liquid hydrogen.

Table 16: Propellant tank size characteristics.

	Radius [m]	Length [m]	Volume [m^3]	Area [m^2]	Propellant [t]
Hemispherical	4.0	16.0	670	402	47.6
Elliptical	4.0	14.5	662	403	47.0
Combination	4.0	16.0	704	421	50.0

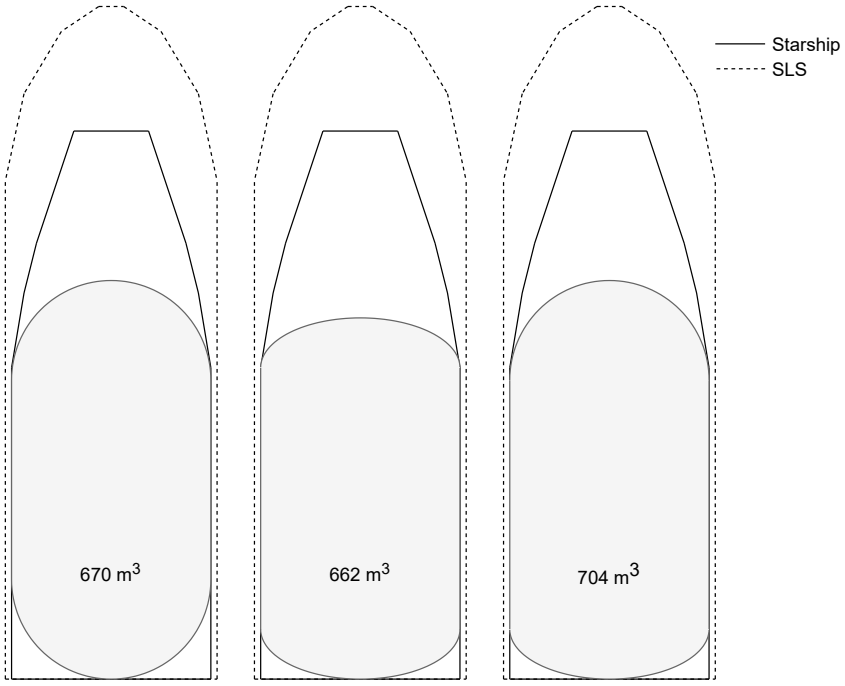

Figure 11: Comparison of the most efficient propellant tank bulkheads in Starship and SLS fairings.

10.4.2 Structure

In order to achieve the 71 kg m^{-3} density for hydrogen it has to be stored as a liquid[24] at 20 K and 2 bar, therefore it is also important for the structure to be able to hold that pressure. The skin thicknesses for the hemispherical, the longitudinal and the elliptical section can be calculated with Equation 16, 17 and 18 [69] respectively.

$$t_h = \frac{pR}{\sigma_y} \tag{16}$$

$$t_l = \frac{pR}{2\sigma_y} \tag{17}$$

[24] https://www.ilkdresden.de/en/service/research-and-development/project/hydrogen-test-area-at-ilk-dresden/ *[cited 14 June 2021]*

$$t_e(\phi) = \frac{p\sqrt{R^2\left(\cos^2\phi + 0.25\sin^2\phi\right)}}{2\sigma_y} \tag{18}$$

The radius R in these equations has been set to 4 m, however, the yield strength σ_y is not yet chosen. Aluminium, more specifically Al2915[25], is a common material for pressure tanks due to its great strength to weight ratio, but in recent years higher quality tanks are often made with titanium or composites. The latter will not be feasible for MARCO as composites are mainly used for smaller tanks with radii of less than 1 m, bigger tanks would require autoclaves that do not yet exist. Attempts have been made to make 12 m diameter tanks, but this was quickly cancelled in favour of metals, due to the high cost of the process[26]. Titanium, which is stronger than steel yet lighter, is a better competitor to aluminium. In this case Ti6Al4V[27] will be looked at. The material properties for both AL2195 and Ti6Al4V can be found in Table 17. The material properties from this table are all at 293 K, when metals are cooled they usually get stronger than this, titanium for instance has a yield strength of 1753 MPa at 4 K [63]. For the design of this tank the material properties at room temperature will be used as the tank should also survive launch loads, which will not be as cold as the operational temperature. The last variable that has to be decided on is the pressure p, this is the difference between the internal and ambient pressure of the tank. The hydrogen will be stored at 2 bar in order to be able to store it at 20 K.

Table 17: Material properties for Al2915 and Ti6Al4V.

	Density [kg m^{-3}]	Yield Stress [MPa]	Young's Modulus [GPa]
Al2195	2700	550	78
Ti6Al4V	4430	970	115

The hemispherical and longitudinal thicknesses can now be calculated, the elliptical thickness, however, is harder as it does not have a uniform thickness. The thickness depends on the location on the ellipse, the minimum and maximum thicknesses are 0.4 mm and 0.8 mm respectively. Because titanium is difficult to machine and form the thickness will be uniform throughout the ellipse, this means that the thicker 0.8 mm will be used. Producing the tank at this thickness will also be a problem, however, it has been done before with stainless steel. The Centaur upper stage uses supports to keep the tank in shape during assembly and also special welding techniques [70]. This tank is smaller than the tanks for MARCO, but due to the thicker skin in MARCO, 0.36 mm against 0.8 mm it is still exepcted to be possible. A summary of the obtained thicknesses of both Al2915 and Ti6Al4V is shown in Table 18. This table also includes the total mass of the tank skin, because titanium is 100 kg lighter than aluminium the titanium alloy will be used, as this will result in a mass saving in the order of a tonne when considering that at least ten tanks are needed.

Table 18: Propellant tank skin thicknesses for Al2915 and Ti6Al4V.

	Hemispherical [mm]	Longitudinal [mm]	Elliptical [mm]	Tank Mass [t]
Al2195	0.7	1.5	1.5	1.5
Ti6Al4V	0.4	0.8	0.8	1.4

Pressure is not the only load case for the tanks, as they are also part of the structure of MARCO. This means that compression loads also need to be considered, two failure cases will be considered: Compression and buckling. The formulas are shown in Equations 19 and 20 respectively [64].

$$F_c = 2\pi R t_l \left(\sigma_y + p\right) \tag{19}$$

$$F_b = 2\pi t_l^2 E\left(9\left(\frac{t_l}{R}\right)^{0.6} + 0.16\left(\frac{R}{L}\right)^{1.3}\left(\frac{t_l}{R}\right)^{0.3} + 0.191\left(\frac{p}{E}\right)\left(\frac{R}{t_l}\right)^2\right) \tag{20}$$

[25] https://www.constellium.com/sites/default/files/markets/airware_2195_t84_plate.pdf *[cited 14 June 2021]*
[26] https://www.teslarati.com/spacex-all-in-steel-starship-super-heavy/ *[cited 28 June 2021]*
[27] https://www.azom.com/properties.aspx?ArticleID=1547 *[cited 14 June 2021]*

An important note on the buckling equation is that it is dependent on the tank pressure, the higher the pressure the higher the buckling force. This can also be seen in Table 19, here the compression force and the buckling force at multiple pressures are given. The impact of pressure on the compression force is negligible, as the pressure is a factor thousand smaller than the yield stress of titanium. The buckling force, however, does heavily depend on the tank pressure. Considering that the force produced by the engines is 444 kN the tank will buckle at 0 bar, therefore the tank should always be under pressure. The design pressure of 2 bar is already enough to mitigate a buckling failure.

The last load case that has to be considered is the launch phase of the tanks, the tanks will launch on either Starship or SLS. The maximum accelerations of these launch vehicles are 6 g and 4 g respectively [65]. This means that in the case of Starship, using a tank mass of 1.5 t the force exerted on the tank will be 88 kN, which is lower than the force exerted on the tank when connected to the nuclear engines. It is still too much to launch the tank unpressurised, it is advised to launch the tank with 1 bar over pressure compared to the atmosphere, when in orbit this will mean that the tank will be at its design pressure of 2 bar. The tank can be either pressurised with hydrogen or inert gasses like nitrogen.

Table 19: Propellant tank compression failure forces at different pressures.

	0 bar	1 bar	2 bar
F_c [MN]	20.1	20.1	20.1
F_b [MN]	0.029	1.95	3.87

10.4.3 Thermal

In order to achieve the highest density for hydrogen it has to be stored at 20 K, at this temperature it will be in a liquid state. At this low pressure liquid state the density is 71 kg m^{-3}. The density can get higher than this, but that would require pressures well in excess of 100 bar, that would make the tank too heavy in comparison to the maximum density of around 100 kg m^{-3}. To be able to stay at this temperature a passive and active cooling method will be implemented.

Because there is no air, spray on foam insulation, or SOFI, will not be useful, as this will reduce convection by lowering the shell temperature. multi layer insulation, or MLI, however, is an effective passive method to reduce incoming sunlight by making it hard for the heat to radiate into the structure. As this will most likely not be enough to keep the hydrogen at temperature an active method consisting of a cryocooler will also be used. These coolers are not efficient and must be avoided where possible, also because the cooling capacity of the best cryocoolers is only 100 W of thermal power.

To obtain the lightest cooling option a simulation will be made that simulates the heat flow into and out of the tanks. The inputs and outputs for this model are:

Inputs:

- Solar intensity
- Earth albedo
- Engine mount conductivity
- Control module mount conductivity

Outputs:

- Cryocooler power
- Layers of MLI
- Thermal system mass

The equations that are used in this simulation are shown below [5]:

$$P_{in} = \alpha A_{in} J \tag{21}$$

$$P_{out} = \epsilon \sigma A_{out} T^4 \tag{22}$$

$$J_a = a J_s \left(\frac{R_{planet}}{R_{orbit}} \right)^2 \tag{23}$$

$$\epsilon_{eff} = \frac{1}{N(2/\epsilon - 1) + 1} \tag{24}$$

Because every tank will receive a different amount of thermal energy the layout of the tanks will be included in the model as well, a drawing is given in Figure 12. In this picture there are four different colours, each colour specifies a different tank model, this means that tank with the same colour will have the same cryocooler. With this picture a cross section slice can be made in order to calculate how much power every tank radiates to another tank, the cross section is shown in Figure 13. Here two angles are specified that show half of the power radiated to a different tank. The angles can be used in both ways. For an inter tank distance of 1 m Equations 25 and 26 can be used to calculate φ and θ respectively. The tank will not only radiate to each other via the sides, but also from the top and bottom, the area of this is the cross sectional area of the tanks. In the case of this layout the green and blue tanks will radiate to each other, as well as the red and yellow tanks.

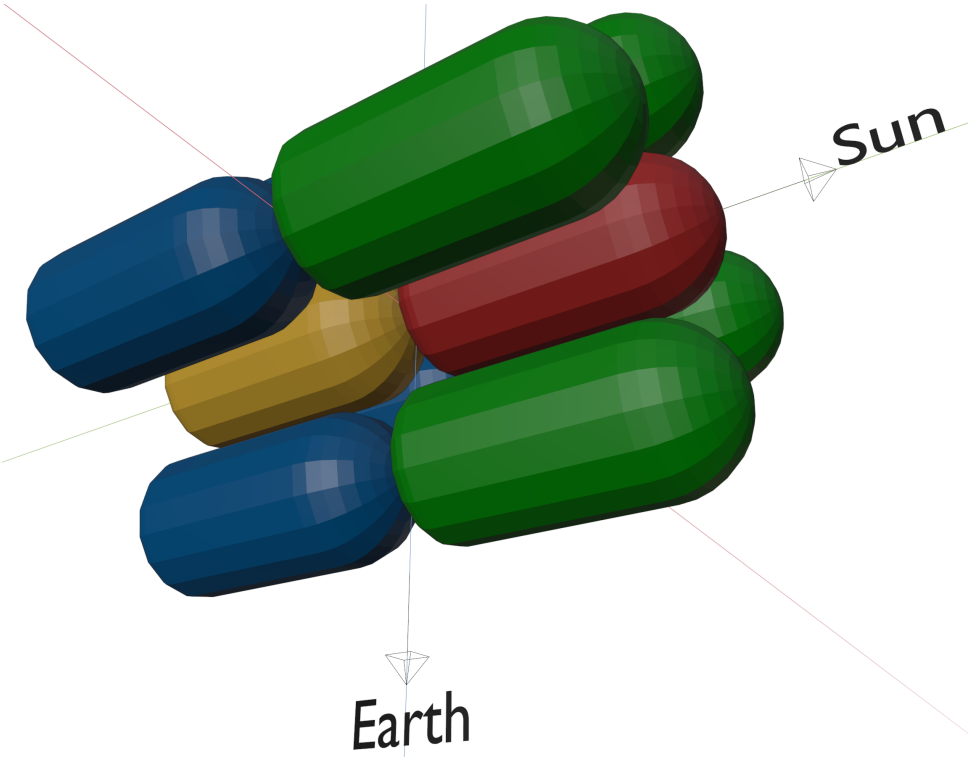

Figure 12: Tank configuration for thermal control.

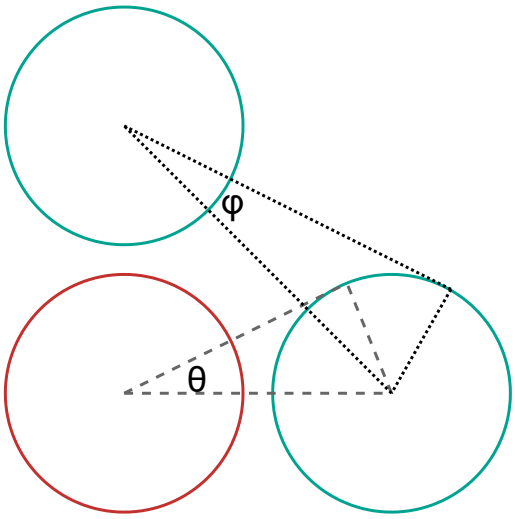

Figure 13: Thermal radiation between the propellant tanks, cross section showing the red and two green tanks.

$$\varphi = \sin^{-1}\left(\frac{R}{\sqrt{2}(2R+1)}\right) \tag{25}$$

$$\theta = \sin^{-1}\left(\frac{R}{2R+1}\right) \tag{26}$$

The tanks not only receive power from each other or from the sun, but also from the structure. The red tank will receive thermal power from the command module adaptor and the yellow tank will receive thermal power from the engine mount. The heat flux can be calculated with Equation 27. The heat flow between the tanks is considered to be negligible as the tanks will all have a temperature of around 20 K.

$$P_s = 2\pi R t_l k \frac{\Delta T}{\Delta x} \tag{27}$$

The next step is to calculate the effective radiation temperature for each of the tanks, this temperature determines how much power the neighbouring tanks will receive. Determining this temperature can be done with an iterative calculation of the input and output power for each of the tanks, this has to be done iterative because the input powers rely on the output powers of the other tanks. When the output temperature is obtained the cooling power can be calculated by subtracting the output power from the input power.

The final part of the simulation is that it should also output the mass of the thermal system. This is because the thermal system should be optimised for mass. Obtaining the mass of the MLI is done by multiplying the amount of layers with its density per layer. The cryocooler on the other hand is more complex, as the cooler needs a radiator and also mounting hardware and pipes. Relations for these components do exist, but it requires the input power of the cryocooler. The cryocooler input power can be calculated by multiplying the cooling power with 200 [67]. The relations for the mass estimates are shown in Table 20. The mass of the actual cryocooler can be estimated with Equation 28, this formula is also a function of the input power [67].

$$M_{cooler} = 0.1422 P_{in}^{0.905} \tag{28}$$

Table 20: Components sizing for the cryocooler mass [66].

Subsystem	**Specific mass [kg W^{-1}]**
Structure & Heat Transport	0.097
Radiator	0.071
Cold Plumbing & Insulation	0.025
Cables & Misc	0.032
Total	0.225

Now that the model is defined the input parameters can be set up. The cryocoolers will be sized for the worst case scenario, in the case of MARCO this will be in Earth orbit as the albedo of the Earth will be at its highest, as well as the solar radiation. The ADCS system of the spacecraft will make sure that the area of the tank pointing to the Sun will always be as small as possible. The front of the spacecraft, on the control module side, will therefore point to the sun, see Figure 12. The worst case for the Earth albedo is when it hits the spacecraft from the side, the orientation of MARCO can not always be away to the Sun and to Earth, because the solar radiation is far stronger than the Earth albedo it will prioritise pointing to the Sun. The parameters for this case are shown in Table 21.

One input parameter for the model is missing in Table 21, the amount of layers of MLI. This input parameter is used, but is different for each of the tank types as the tanks have to be optimised for mass. In principle it is possible to set the amount of layers to zero, however, this will require too much thermal power from the cryocooler and the mass of the cooling system will not be optimal. Therefore each tank has a manual amount of MLI layers chosen in order to see what the optimal amount is to get the lightest system. The results of the simulation are shown in Table 22.

Table 21: Input parameters for the propellant tank thermal simulation.

Variable	Quantity	Unit
α_{MLI}	0.08	-
ϵ_{ext}	0.66	-
ϵ_{MLI}	0.03	-
J_s	1400	$W\,m^{-2}$
σ	5.67×10^{-8}	$W\,m^{-2}\,K^{-4}$
a	0.6	-
R_{planet}	6378	km
R_{orbit}	2000	km
$k_{titanium}$	0.2	$W\,m^{-1}\,K^{-1}$
Δx	4.0	m
ΔT	250	K
ρ_{MLI}	0.047	$kg\,m^{-2}$

Table 22: Result of the cryocooler simulation per tank.

Tank	layers of MLI [#]	Cooling power [W]	cryocooler power [W]	Thermal system mass [kg]
Red	20	8.61	1721	904
Green	30	9.11	1823	1131
Blue	20	7.24	1447	447
Yellow	10	4.14	829	825

As expected the green tank has the highest thermal mass, as these tanks receive both solar radiation and Earth albedo. The red tank has the second largest thermal system as it receives solar power and also heat flow from the command module adaptor. The third biggest system is from the yellow tank, because it does not receive any solar radiation, but it does receive a large heat flow from the nuclear engine through conduction. The blue tank has the smallest system, as it only receives Earth albedo and like the other tanks also tank to tank radiation.

10.4.4 Connection Hardware

In order to connect the tanks to each other and to the rest of MARCO, docking ports and trusses will be used. The trusses will be looked into more detail in Section 11, but because they belong to the tanks itself their masses will be included in the tank budget.

There are two types of connections necessary, one being the tank to tank connection and the other is the tank to module port. Their masses are 500 kg and 327 kg respectively [68]. The tank to tank connection is heavier because a docking port alone will shear off when the spacecraft is under acceleration, therefore it also includes latches that will be attached to the front of the tanks to hold the load. The docking hardware is different for the inner and outer tank. The outer tanks will need one docking port with latch, while the inner tanks need two docking ports and four docking ports with latch. Here, the outer tanks are the green and blue tanks and the inner tanks are yellow and red.

10.4.5 Budget

The final budget of the propellant tank, including mass, volume, power and cost can be found in Table 23. Some more detail is required on some of these budgets: The skin, MLI and truss cost have been obtained by the current price per kilogram, this does not include manufacturing. The characteristics of the cooler are obtained with statistical relationships from [67]. Docking port volumes and masses come from the NASA International Docking Adaptor [68], the price is also derived from this model[28]. Lastly, it is important to note that the propellant volume of 704 m^3 per tank is not included in this material budget.

[28] `https://spaceflightnow.com/2019/08/21/eva-55/` *[cited 16 June 2021]*

Because the crew missions will need more propellant than the cargo missions, the total budget has been split up into two separate budgets. The crew total uses the multiplier given in between the brackets, as it needs the maximum amount of propellant that the propulsion system can provide. The cargo mission, however, needs six propellant tanks and will therefore fly in a two side tank configuration. This means that there will be two green and two blue tanks connected to a red and a yellow tank. In this configuration the thermal system will still receive the same amount of thermal radiation and will therefore still be able to mitigate boil-off.

After adding the budgets together, a safety factor of 5 % is added. This is the safety factor used for the final report values, therefore the safety budget is used for the final dry mass budget.

Table 23: Budget breakdown of the propellant tanks.

Tank	**System**	**Mass [t]**	**Volume [m^3]**	**Power [W]**	**Cost [k€]**
Red (x1)	Skin	1.35	0.31	0	5.4
	MLI	0.40	5.27	0	84.3
	Docking	2.65	6.00	90	111 344.6
	Truss	0.17	0.06	0	0.5
	Cooler	0.51	0.12	1721	27.8
	Total	5.08	11.8	1811	111 462.6
Green (x4)	Skin	1.35	0.31	0	5.4
	MLI	0.59	7.90	0	126.4
	Docking	0.50	1.00	15	18 557.4
	Truss	0.17	0.06	0	0.5
	Cooler	0.54	0.13	1823	29.1
	Total	3.16	9.40	1838	18 718.9
Blue (x4)	Skin	1.35	0.31	0	5.4
	MLI	0.40	5.27	0	84.3
	Docking	0.50	1.00	15	18 557.4
	Truss	0.17	0.06	0	0.5
	Cooler	0.43	0.10	1447	24.0
	Total	2.85	6.74	1462	18 671.6
Yellow (x1)	Skin	1.35	0.31	0	5.4
	MLI	0.20	2.63	0	42.1
	Docking	2.65	6.00	90	111 344.6
	Truss	0.17	0.06	0	0.5
	Cooler	0.25	0.06	829	15.0
	Total	4.62	9.06	919	111 407.7
Crew Total		33.7	85.4	15 931	372 442
+5%		35.4	89.6	16 728	391 054
Cargo Total		21.7	53.1	9331	297 651
+5%		22.8	55.7	9797	312 534

In order to get a better overview on how the propellant tanks will look a schematic can be seen in Figure 14. This is a picture of the blue propellant tank, the other tanks will look roughly similar and are therefore not shown, the big difference for the red and yellow is that they will have multiple extra docking ports on the side and at the front and back. For the others only the cryocooler size differs. The orange colour in this picture shows the MLI, the blue shows the cryocooler, red is the docking system and green is the propellant feed to the docking port.

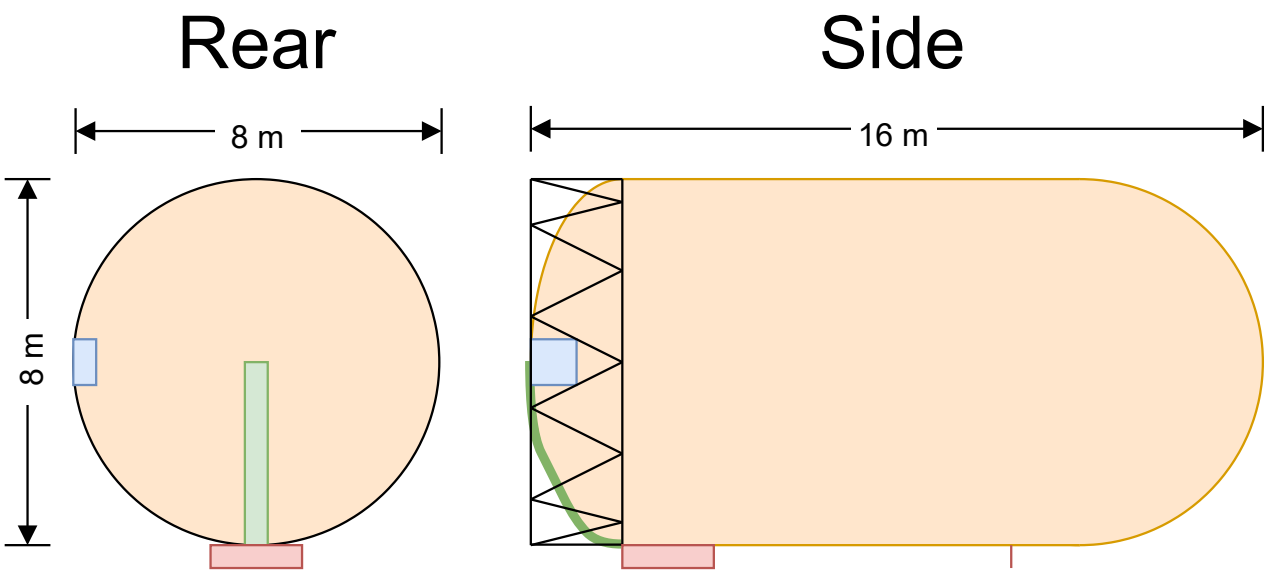

Figure 14: Schematic drawing for the blue propellant tank configuration.

10.5 System Architecture and Interfaces

In order to get a better understanding of how the different systems are related to each other some flow diagrams are made. The flow diagram for the propellant tank is shown in Figure 16. This right side of the figure shows the sensors needed to properly monitor the propellant tanks. The left side shows the hardware elements that have to be controlled by a computer.

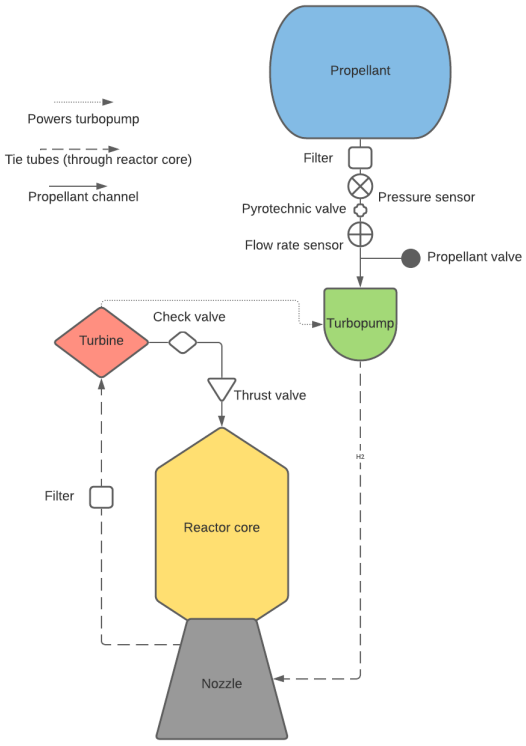

Figure 15: The propulsion system architecture.

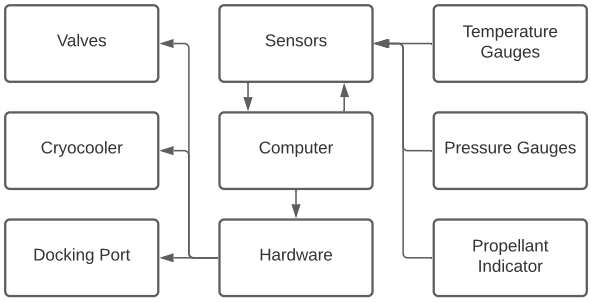

Figure 16: Hardware and software flow diagram for the propellant tank.

10.6 Risk Analysis

Table 24: Risk table including the most critical risks for each subsystem. RBM is defined as "likelihood, impact" before mitigation, RAM is "likelihood, impact" after mitigation

ID	Risk	RBM	Mitigation	RAM
PRP01	One or multiple components of the LH_2 system cause a complete failure	2, 5	**Reduce** by adding redundancy in terms of extra engines. Reduced hydrogen flow may cause overheating of the reactor, so the control drums must reduce the reactivity as quickly as possible.	1, 4
PRP02	One or more control drums fail to rotate	2, 5	**Reduce** by performing sufficient testing and inspection prior to launch	1, 4
PRP03	Reactor is not cooled sufficiently after shutdown	3, 4	**Reduce** by performing tests on worst-case scenarios for this stage of the engine operation.	1, 4
PRP04	Radiation from reactor causes cavitations in the propellant tanks, resulting in turbopump failure.	3, 5	**Reduce** by analyzing and testing the effect of radiation on hydrogen propellant	1, 5
PRP05	Gimbal mechanism fails to operate	2, 3	**Reduce** by having 4 engines, all equipped with thrust vector control to have redundancy.	2, 1
PRP06	Too much hydrogen boils-off	1, 5	**Reduce** by bringing more propellant	1, 3
PRP07	There is not enough propellant	1, 5	**Reduce** by jettisoning empty tanks to reduce required propellant	1, 3
PRP08	There is too much pressure in the tanks	2, 4	**Avoid** by venting hydrogen	2, 1
PRP09	A cryocooler fails	3, 3	**Reduce** by emptying that tank first	3, 2

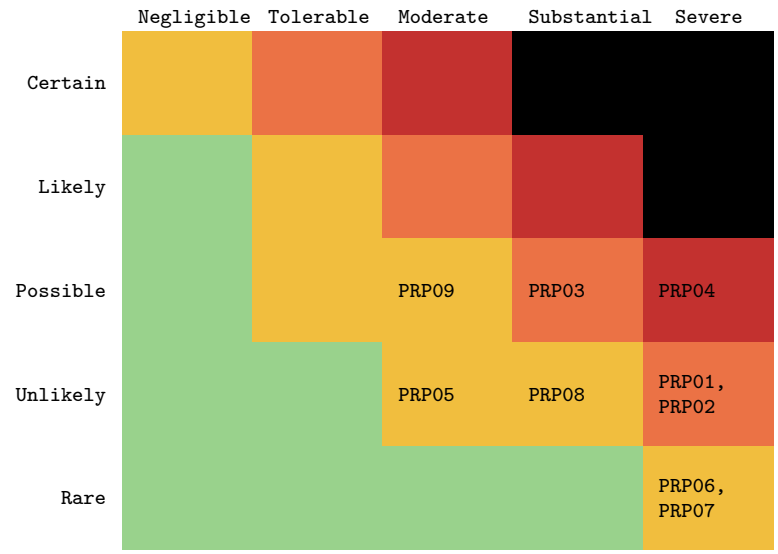

Figure 17: Risk matrix of identified subsystem risks. Likelihood is listed vertically and impact is listed horizontally.

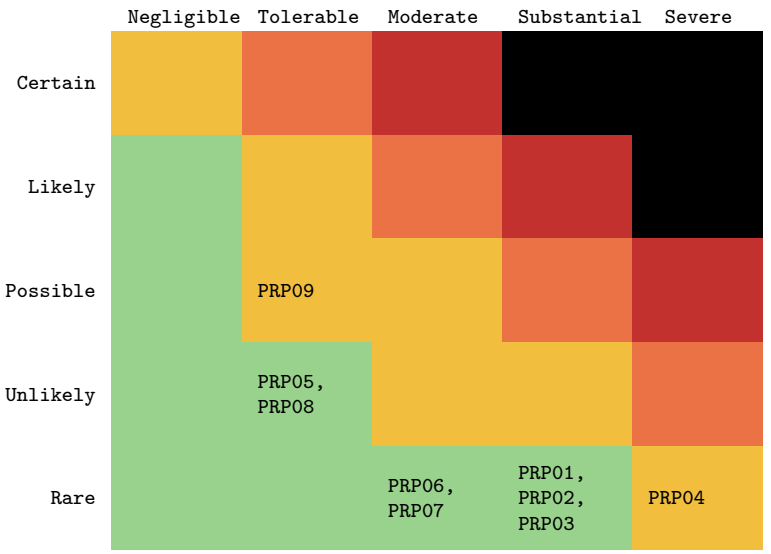

Figure 18: Risk matrix of mitigated risks. Likelihood is listed vertically and impact is listed horizontally.

10.7 Sustainability

The word 'nuclear' is one that often has negative connotations in the public view. However, nuclear thermal propulsion poses no risk to public health and safety. A first concern could be that a launch failure with the nuclear core as a payload can spread radioactive material over a large area. As the core is made out of Uranium-235, which has a half life of 700 million years, radioactive decay does not pose an issue. Only when the core is activated, which will happen in orbit, will the reactor generate radioactive material.

A valid concern is that the activated nuclear core re-enters Earth's atmosphere. To avoid this, a nuclear safe orbit has been created. These have altitudes of at least 1000 km, allowing for orbital lifetimes well over 1000 years. The orbital altitude of MARCO-POLO will be 2000 km, comfortably above the regulated minimum.

The propellant tanks are re-configurable meaning that depending on the mission requirements tanks can be removed or added. The minimum propellant mass is 100 t and the maximum is 500 t. This adaptation to the mission will make the launch cheaper, as the dry mass can be decreased, this is particularly important for the cargo missions that will only use six out of the ten tanks.

The end of life approach for propulsion can also be split up into two segments, first of all, the tanks can be brought back to Earth again in order to get recycled. The nuclear engine, however, is better not taken to Earth again as the disposal nuclear waste is still a problem here. Therefore, it is advised to take the engine segment to a grave yard orbit, or to a Sun escape trajectory.

10.8 Verification and Validation

Most verification and validation of the requirements cannot be done at this state of the project. Therefore, a table is made that shows the recommended method for further research. The overview can be found in Table 25.

Table 25: Methods for the verification and validation of the propulsion requirements.

Requirement ID	Verification and Validation Method			
	Test	Analysis	Inspection	Demonstration
MARCO-PRP-01	•			
MARCO-PRP-02		•		
MARCO-PRP-04			•	
MARCO-PRP-05		•		
MARCO-PRP-06				•
MARCO-PRP-07		•		
MARCO-PRP-08	•			
MARCO-PRP-09				•
MARCO-PRP-10			•	
MARCO-PRP-11				•
MARCO-PRP-14				•
MARCO-PRP-15	•			
MARCO-PRP-16	•			
MARCO-PRP-17			•	

10.9 Requirement Compliance and Sensitivity Analysis

For the MARCO propulsion requirements discussed in subsection 10.2, a compliance matrix is generated (as seen in Table 26) in order to establish whether or not the subsystem requirements have been met by the design. As is evident from the table, the requirements on reliability were not confirmed to be complied with. The reason for this is that figures on component or system reliability are not readily available and need to be determined through testing or thorough analysis. It is not within the scope of this report to determine these figures.

Table 26: Propulsion Requirements Compliance.

ID	Compliance	Rationale
MARCO-PRP-01	✓	Section 10.3.1
MARCO-PRP-02	✓	Section 10.3.7
MARCO-PRP-04	✓	Section 10.3.1
MARCO-PRP-05	✓	Section 10.3.1
MARCO-PRP-06	-	This has to be verified in further research.
MARCO-PRP-07	-	This has to be verified in further research.
MARCO-PRP-08	✓	Section 10.3.1
MARCO-PRP-09	✓	Section 10.3.1
MARCO-PRP-10	✓	Section 10.4.1
MARCO-PRP-11	✓	Section 10.3.2
MARCO-PRP-14	✓	Section 10.4.3
MARCO-PRP-15	✓	Section 10.4.2
MARCO-PRP-16	✓	Section 10.3.1
MARCO-PRP-17	✓	Section 19

10.10 Recommendations

For the scope of this report, only the most relevant parameters (mass, dimensions, power) were estimated. Therefore, the design presented is far from final. Considerations for future designs must go into a more detailed analysis. A general budget that was not considered for this report is the reliability of the systems, care has been taken in the

design to mitigate as many risks as possible, but these risks were not quantified.

For the engine, it must be investigated whether the system can remain operational during its 40 year scheduled lifetime. If this is not possible, it must be investigated if the system can undergo maintenance operations to extend its lifetime.

For the propellant tanks there are also still some areas that have to be looked into further. Firstly, the attachment system has not been designed in detail. Further research must find out how the propellant flow works through docking ports and also investigate if refuelling with pressure is possible. Secondly, the thermal power simulation did not include heating effects from the nuclear propulsion, due to the radiation shielding this power was assumed to be negligible, but this must be further researched. Lastly, the assembly cost for the tank itself has not been calculated, it is expected that this will form most of the cost of the tanks, but an accurate estimate was not possible to make.

11 Structures

The structures subsection is the subsection which secures every other subsystem to the spacecraft. For a few subsystems, certain structures have to be designed such that they can perform optimally. The goal is then to design a structure which is lightweight but enables the subsystem to perform its tasks.

11.1 Requirements

Requirements which have not changed with regards to the midterm report will not have their rationale listed. Those can be found in the previous report [8].

MARCO-STR-02 The structure shall provide hard points for mounting of equipment.

MARCO-STR-03 The ITS modules shall withstand longitudinal accelerations of $-20\,\mathrm{m\,s^{-2}}$ to $60\,\mathrm{m\,s^{-2}}$.

MARCO-STR-04 The ITS modules shall withstand lateral accelerations of $-20\,\mathrm{m\,s^{-2}}$ to $20\,\mathrm{m\,s^{-2}}$.

MARCO-STR-06 The structure of the ITS shall withstand normal stresses of 250 MPa.

MARCO-STR-07 The structure of the ITS shall withstand shear stresses of 200 MPa.

MARCO-STR-08 The materials of the ITS shall not yield at any stage of its life cycle.

MARCO-STR-11 The ITS structure shall have a reliability of 95 %.

MARCO-STR-12 The ITS structure shall withstand temperatures between 170 K to 420 K.

11.2 Subsystem Design and Sizing

The structures subsystem was tasked with designing a number of structures. The process for designing those structures follows a clear structure:

1. Identify external forces and moments.
2. Define dominating loading modes (e.g. bending, buckling, etc.) and initial boundary sizing conditions.
3. Use initial sizing for the dominating mode.
4. Get initial loads and stresses and determine the margin of safety to yield/failure.
5. Change parameters until every load condition is met.
6. Iterate for certain design conditions
7. Attain final design based on certain optimal conditions.

When the final dimensions of the design are obtained, a drawing can be made and the design will be complete.

A few considerations have to be made when starting to design. First, a choice of material needs to be made. This will fix most of the maximal stresses. The choice is made to use Al-7075-T7. This alloy has a high yield stress (435 MPa) which will give some leeway in the design compared to a weaker Al-7075 alloy. A safety factor of 1.2 is incorporated such that the yield strength is never reached and all mass calculations contain a 1.05 factor to account for inaccuracies.
The optimal conditions which the design is rated on are : lowest mass and performance over weight. Ultimately, the lowest mass is the most important as every single design which passes step 5 is able to handle all the loads. Extensive verification & validation has been performed to ensure that the process was completed well.
The main modes of loading which will be investigated are :

- **Bending**
  Bending for symmetric structures is governed by the following equation :

$$\sigma = \frac{Md}{I} \tag{29}$$

  where σ is the resulting bending stress around the chosen axis, M is the bending moment applied, d is the distance to the neutral axis and I is the moment of inertia about the chosen axis.

- **Buckling**
  Buckling of beams is governed by the following equation :

$$P_{buckle} = \frac{\pi^2 EI}{(KL)^2} \tag{30}$$

  where P_{buckle} is the force at which a column will buckle, E is the Young's modulus of the material used, I is the moment of inertia of the column, K is an indication of how the beam is clamped and L is the effective length of the beam. Whenever the force applied to a member is higher than the P_{buckle} and the yield stress in the same member is not exceeded, the column buckles.

- **Tension/Compression**
  The stress associated with tension and compression is governed by the following equation:

$$\sigma = \frac{F}{A} \tag{31}$$

  where σ is the resulting normal stress, F is the load creating that stress and A is the crossectional area.

- **Torsion**
  Torsion is a loading mode which can lead to failure, but in the case of the ITS it is not a predominant mode and can thus be omitted.

If in any case one of the stresses exceeds its associated yield stress, the conditions are not met for that set of parameters and a stronger designed is computed for.

11.2.1 Solar Array Support Truss

The solar array support truss is the truss which supports the solar panels and connects them to the main spacecraft body. The arrays must be large enough to be able to accommodate for the large surface needed while also maintaining structural integrity. Two solar arrays will be required to support the entirety of the panels. The main loading case here is bending due to the acceleration caused by the thrusters burning. The solar panels will be driven with drive motors to ensure that they point in the most optimal direction at all times.

For the solar array, a few boundary conditions have to be set:

- The length of the truss must be at least 15 m. This is done to be able to accommodate for the four 10.5 m x 4 msolar panels, the thermal systems with space between them and to provide sufficient clearance for any docking spacecraft on the command module.

- The truss itself is set at 1 m × 1 m. This to include enough room for cabling and mechanical contraptions.

Going through the design process mentioned above, the following truss has been designed:

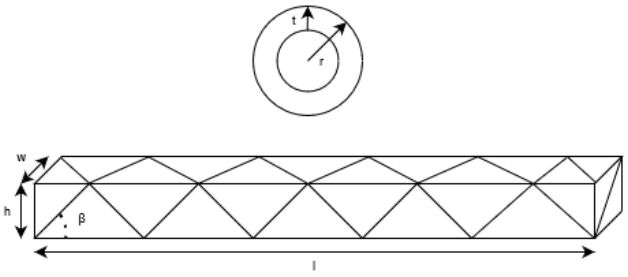

Figure 19: Drawing of solar array truss with hollow truss struts.

Table 27: Values of solar array truss.

Variable	Quantity	Unit
l	13	m
w	1	m
h	1	m
β	45	°
r	10	mm
t	1	mm
m	2364	kg

11.2.2 Tank-to-Tank Adapter

The tank-to-tank adapter enables the transmission of loads from the upper to lower ring of propellant tanks. As the bulkheads are chosen not to be load carrying, the load path has to be from skin to skin. This is done by designing an adapter which is fastened to both centre propellant tanks. The main load case present is the compression due to the acceleration and forces caused by performing manoeuvres.

For the tank-to-tank adapter, a few boundary conditions have to be set:

- The upper and lower ring of the adapter will have a radius of 4m to be flush with the propellant tanks.
- The adapter will have a height of 7 m, this leaves enough room between the lower and upper ring for a docking port which will be used for cabling and piping.

Going through the design process mentioned above, the following adapter has been designed:

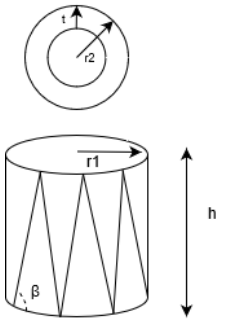

Figure 20: Drawing of tank-to-tank adapter with hollow truss struts.

Table 28: Values of tank-to-tank adapter.

Variable	Quantity	Unit
$r1$	4	m
h	7	m
β	73.3	°
$r2$	50	mm
t	5	mm
m	502	kg

11.2.3 Tank-to-Thruster Adapter

The tank-to-thruster adapter enables the connection between the thruster and lower center tank. Again, the load has to be transferred to the skin of the tank and the adapter is designed to make sure this happens. Some room is left in the adapter to accommodate a radiator which is used for thermal control for the thrusters. The main load case present is the compression due to the acceleration and forces caused by performing manoeuvres.

For the tank-to-thruster adapter, a few boundary conditions have to be set:

- The upper and lower ring of the adapter will have a radius of 4 m to be flush with the lower propellant tank and the thruster bed.
- The adapter will have a height of 3 m to be able to accommodate a conical radiator inside of it.

Going through the design process mentioned above, the following adapter has been designed:

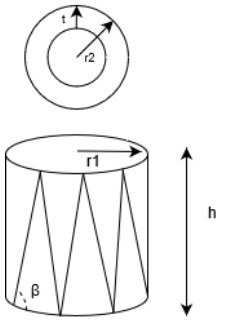

Figure 21: Drawing of tank-to-thruster adapter with hollow truss struts.

Table 29: Values of tank-to-thruster adapter.

Variable	Quantity	Unit
$r1$	4	m
h	3	m
β	35.6	°
$r2$	50	mm
t	5	mm
m	362	kg

11.2.4 Tank-to-Command Module Adapter

To be able to connect the propellant tank rings to the main body of the spacecraft, an adapter between the command module and the upper propellant tanks ring must be designed. This adapter will be different from the others as the shape of the command module having an octagonal shape. The main load case present is the compression due to the acceleration and forces caused by performing manoeuvres.

For the tank-to-command module adapter, a few boundary conditions have to be set:

- The propellant tank ring will have a 4 m radius while the command module ring will have a 2 m radius to be flush with their respective structures.
- The height of the adapter will be 5 m to be able to reach the command module while leaving room for the docking ports in between the propellant tank and the command module.

Going through the design process mentioned above, the following adapter has been designed:

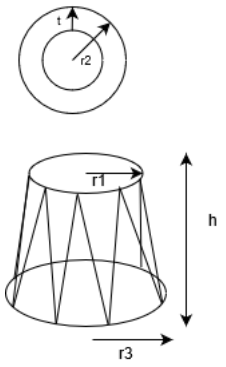

Figure 22: Drawing of tank-to-command adapter with hollow truss struts.

Table 30: Values of tank-to-command adapter.

Variable	Quantity	Unit
$r1$	2	m
h	5	m
$r3$	4	m
β	50.1	°
$r2$	50	mm
t	5	mm
m	341	kg

11.2.5 Tank Support Bed

The tank support bed enables the securing of the tanks during their launch and making sure that the loads are transferred equally along the propellant tank during launch. The main load case present is the compression due to

the acceleration and forces caused by performing manoeuvres. Ten of these adapters will be needed, one for every propellant tank. The mass and volume budgets for this adapter will be appended in the propulsion budget.

For the tank support bed, a few boundary conditions have to be set:

- The radius of the adapter is 4 m to be flush with the lower side of the propellant tank.
- The height of the adapter is 2 m.

Going through the design process mentioned above, the following adapter has been designed:

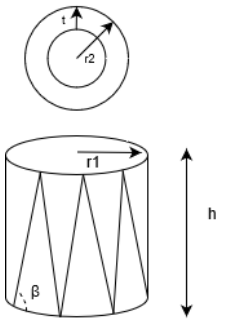

Figure 23: Drawing of tank support bed adapter with hollow truss struts.

Table 31: Values of tank support bed adapter.

Variable	Quantity	Unit
$r1$	4	m
h	2	m
β	50.1	°
$r2$	50	mm
t	5	mm
m	181	kg

Following the design of all the above mentioned structures, the following summary can be made for structures:

Table 32: Summary of structure designs.

Element	Amount	Mass [kg]	Volume [m^3]
Solar array truss	2	2364	13
Tank-to-tank adapter	1	501	352
Tank-to-thruster adapter	1	1362	151
Tank-to-command adapter	1	341	147
Total		6932	676

11.3 Risk Analysis

Table 33: Risk table including the most critical risks for each subsystem. RBM is defined as "likelihood, impact" before mitigation, RAM is "likelihood, impact" after mitigation.

ID	Risk	RBM	Mitigation	RAM
STR01	Adapter fails due to single rod failing	1, 4	**Avoid** by adding redundancy in terms of extra rods	1, 2
STR02	Buckling of individual rods	2, 3	**Avoid** by ensuring buckling load is never reached with design parameters	1, 3
STR03	Spacecraft damages solar array truss while docking, disabling the array	3, 4	**Reduced** by having the spacecraft dock with the CANADARM	1, 2
STR04	Tank-to-tank adapter fails, disconnecting upper and lower propellant tank ring	2, 5	**Reduce** by making sure the adapter is adequately over-engineered	1, 5

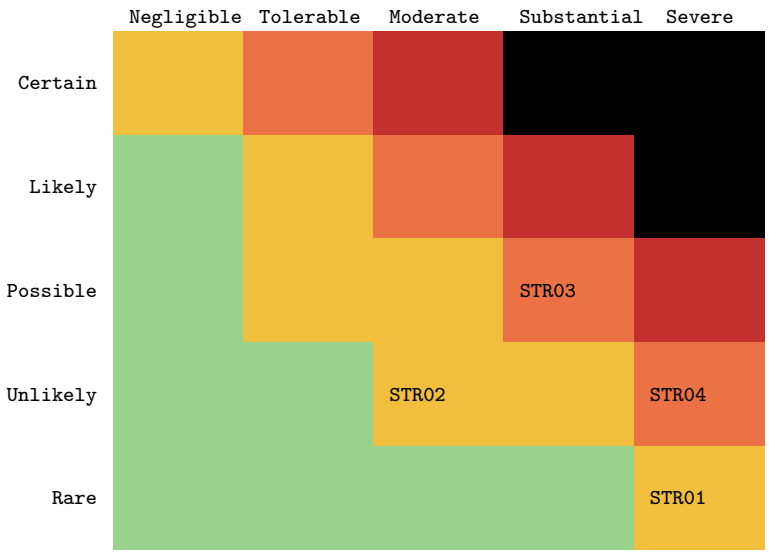

Figure 24: Risk matrix of identified subsystem risks. Likelihood is listed vertically and impact is listed horizontally.

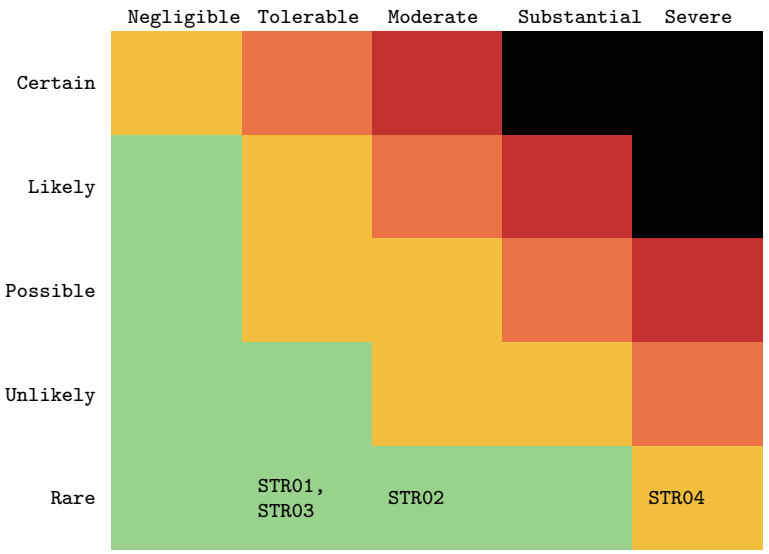

Figure 25: Risk matrix of mitigated risks. Likelihood is listed vertically and impact is listed horizontally.

11.4 Sustainability

Sustainability in the structures is achieved by the choice of materials. Aluminium is very durable and recyclable. Every designed structure can be reused in some other form or way when the ITS will reach its end-of-life. An effort is made such that the mass is kept as low as possible, which in turn reduces the amount of propellant needed which in turn enhances the sustainability. The solar array trusses also contribute to environmental sustainability by enabling the use of solar panels which again reduces the use of environmentally harmful things.

11.5 Requirement Compliance

Table 34: Structural Requirements Compliance.

ID	Compliance	Rationale
MARCO-STR-02	✓	The structures are designed such that enough space and points for mounting equipment are available.
MARCO-STR-03	✓	All elements have been designed for this condition.
MARCO-STR-04	✓	All elements have been designed for this condition.
MARCO-STR-06	✓	The yield stress of Al-7075-T7 has a value of 430 MPa.
MARCO-STR-07	✓	The shear yield stress of Al-7075-T7 has a value of 250 MPa.
MARCO-STR-08	✓	The structures are designed such that the yield stress is never reached, not even under the most demanding conditions.
MARCO-STR-11	-	Upon available data presented in this chapter, the reliability cannot yet be determined but it could be monitored by forms of Non Destructive Testing.
MARCO-STR-12	✓	Due to the properties of the material, these temperatures are well within its safety range.

11.6 Recommendations

As far as structures design goes, a more detailed design procedure could be followed. This includes FEM simulation, building scale models to do tests on. Some assumptions were made and tested after obtaining results, but some form of inaccuracy is still present which could be eliminated by performing those detailed design procedures. The current designs do not take into account load conditions which are not present in the day to day operation of the ITS but

could be taken into account to see whether they would affect the design.

12 Electrical Power System

This chapter covers the detailed design of the electrical power system (EPS) for MARCO. Based on trade-offs made in the midterm report [8], the EPS will consist of nuclear power for primary power generation, solar power for secondary generation and batteries as the energy storage solution. Taking the subsystem requirements (as seen in Section 12.2) into consideration the various components of the EPS are designed in Section 12.3. Following the final design of the EPS, a new set of risks arose, which are listed with a mitigation plan in Section 12.5, and the design's approach and consideration regarding sustainability are covered in Section 12.6. As part of verifying the subsystem's design, the compliance of the requirements is checked in Section 12.8. Wrapping up this chapter in Section 12.9 is a set of recommendations regarding the improvements of the subsystem which need to be considered, and the next steps after the design of the subsystem, which need to be implemented.

12.1 Trade-off Summary

During the first phase of the project, trade-offs of concepts and all the subsequent subsystems were performed, upon which the final design is based on. Two trade-offs were performed, one for the power generation and a second one for the energy storage solution for MARCO. The three options traded-off for EPS generation was solar power, nuclear power and fuel cells. While four options were considered for the storage solution; flywheels, regenerative fuel cells, super capacitors and batteries. The criteria which had the highest weights were the performance related ones, such as specific power, energy conversion efficiency and reliability. While maintainability, cost and technological readiness level (TRL) were used to assess the viability of the options for a space mission. The trade-offs led to the selection of two power generation possibilities; solar power and nuclear power. Fuel cells were eliminated due to their lower specific power output and their need for more frequent refuelling unlike nuclear power.
For energy storage on board MARCO, batteries were selected due their already matured implementation in the space industry (high reliability and TRL) and its high specific energy value.

For the final design of the EPS, a separate nuclear power generator has been eliminated, as a bimodal nuclear engine is being implemented to both propel MARCO and to provide power to the system as well. During the final design phase, the solar cell and array type will be decided, along with the type of battery based on the critical scenario for which the system is sized and designed for.

12.2 Requirements

The following list of requirements was generated during the first phase of the project, with their rationale being discussed in the midterm report [8].

MARCO-EPS-01 The power system shall deliver a peak power of 55 kW from 0.7 au to 1.5 au away from the sun.

MARCO-EPS-02 The power system shall deliver an average power of 48 kW from 0.7 au to 1.5 au away from the sun.

MARCO-EPS-03 The power system storage shall store 30 kW h.

MARCO-EPS-04 The power system total mass shall not exceed 8 t.

MARCO-EPS-05 The total power system shall occupy a volume of no more than 14 m^3.

MARCO-EPS-06 The primary power generation system shall be able to provide 55 kW at any given moment throughout the mission lifetime.

MARCO-EPS-07 The secondary power generation system shall be able to provide 55 kW at any given moment throughout the mission lifetime.

MARCO-EPS-08 The power system shall have a reliability of 95 %.

MARCO-EPS-09 The power system shall remain between the temperatures of 100 K to 300 K.

During the final design phase of the project a few new requirements were generated in order to completely constrain the design. The values for these requirements were derived from the subsystem design (Section 12.3).

MARCO-EPS-10 The total cost of the EPS shall not exceed 270M€.
Rationale: Discussed in Section 12.3.

MARCO-EPS-11 The PMAD shall be able to handle 55 kW.
Rationale: Discussed in Section 12.3.4.

12.3 Subsystem Design and Sizing

To size the EPS, the mission was firstly divided into phases and the average and peak power of each subsystem was found, this can be seen in Table 35 and 36, which are for the cargo and crew missions respectively. The values presented in these two tables are derived from each subsystem, and they can be found in their respective chapters. This allowed for a sizing of the EPS for the various phases. During the assembly phase, the engines will not yet be connected to the spacecraft and the solar panels together with the battery will have to provide the necessary power. Another important aspect is that the nuclear engines do not produce power when they are producing thrust (hence, they cannot provide power during burn times). This leads to another scenario that the solar panels and batteries will have to be able to deal with, this will happen in both LEO and LMO. The final scenario to be considered is in the case of an engine malfunction. If the engines malfunction, the solar arrays will have to be able to provide enough power to support the habitat and charge the battery, such that the habitat can be fully operational in LMO, even when MARCO is in the shadow of Mars.

Table 35: Power breakdown for the various subsystems in the different phases of the cargo missions. All numbers are given in kW.

Subsystem	**Phases**									
	Launch and assembly		**LEO** (2000 km)		**Earth-Mars transfer**		**LMO** (500 km)		**Mars-Earth transfer**	
	Avg.	Peak	Avg.	Peak	Avg.	Peak	Avg.	Peak	Avg.	Peak
ADCS	1.83	3.10	2.65	5.92	2.64	5.91	2.65	5.92	2.64	5.91
TLC	0.01	0.20	0.01	0.20	0.02	0.38	0.04	0.93	0.02	0.38
TCS	0.83	0.83	0.83	0.83	0.83	0.83	0.83	0.83	0.83	0.83
Propulsion	2.54	9.80	9.80	13.80	9.80	13.80	9.80	13.80	9.80	13.80
Structures	0.44	2.00	0.44	2.00	0.44	0.44	0.44	0.44	0.44	0.44
EPS	0.07	0.17	0.15	0.24	0.15	0.23	0.15	0.23	0.15	0.23
C&DH	1.00	1.00	1.00	1.00	1.00	1.00	1.00	1.00	1.00	1.00
Total	6.71	14.89	14.86	21.78	14.86	21.76	14.89	21.77	14.87	21.76

As seen in Tables 35 and 36 the total average power is the sum of the average power consumption of each subsystem, that is a part of MARCO. While the peak power consumption on the other hand is the maximum amount of power that is consumed in each phase. As seen in the aforementioned tables the total peak power is the sum of the peak powers (highlighted in orange in the tables) of ADCS, TCS, propulsion subsystem, habitation module (in Table 36 only) EPS and C&DH. Since, TCS and C&DH have the same average and peak power requirement, and the EPS power requirement is proportional to the total power consumption, the peak scenario is when both propulsion and ADCS require the most power, which is during the attitude correction procedures.
The peak power consumption of the structure is when the robotic arm is being used. It is assumed that the robotic arm will not be used when ADCS is at its peak, hence it is not included in the peak power calculation. The same goes for the TLC.

Table 36: Power breakdown for the various subsystems in the different phases of the crewed missions. Hab. mod. stands for habitation module. All numbers are given in kW.

Subsystem	Phases									
	Launch and assembly		LEO (2000 km)		Earth-Mars transfer		LMO (500 km)		Mars-Earth transfer	
	Avg.	Peak	Avg.	Peak	Avg.	Peak	Avg.	Peak	Avg.	Peak
ADCS	2.65	5.92	2.65	5.92	2.64	5.91	2.65	5.92	2.64	5.91
TLC	0.83	0.83	0.83	0.83	0.83	0.83	0.75	0.83	0.75	0.83
TCS	0.83	0.83	0.83	0.83	0.83	0.83	0.83	0.83	0.83	0.83
Propulsion	16.73	16.73	16.73	20.73	16.73	20.73	16.73	20.73	16.73	20.73
Hab. mod.	5.13	5.14	25.87	25.88	25.86	25.88	25.84	25.88	25.86	25.88
Structures	0.44	2.00	0.44	2.00	0.44	0.44	0.44	0.44	0.44	0.44
EPS	0.27	0.32	0.48	0.57	0.48	0.56	0.48	0.56	0.48	0.56
C&DH	1.00	1.00	1.00	1.00	1.00	1.00	1.00	1.00	1.00	1.00
Total	27.05	29.73	48.00	54.72	47.99	54.51	48.00	53.97	47.99	54.51

From the scenarios described above and the phases identified, the solar array and batteries have been sized for crewed mission in LMO, where the solar flux is less compared to LEO. The propulsion system is only able to provide either thrust or power and cannot provide both at the same time. Hence for the burn time for a crewed mission in LEO of 51 min plus an extra 10 min for heating/cooling, the propulsion system will not be able to produce power for 61 min. On Mars the longest burn time is orbit insertion for a crewed mission which adds up to 35 min including 10 min for heating/cooling. During these burns, the solar arrays and batteries should provide enough power for the habitat to fully function. The burn times will be shown later in Table 42.

Table 37 and 38, show some general parameters that were used to size the EPS components. The equations used to find the orbital period and eclipse time can be seen below in Equation 32 and 33.

$$T_{orbit} = 2\pi\sqrt{\frac{(h+R)^3}{\mu}} \tag{32}$$

$$T_{eclipse} = \frac{2\sin^{-1}\left(\frac{R}{h+R}\right)}{2\pi} \cdot T_{orbit} \tag{33}$$

Table 37: Planet parameters for Earth and Mars, used for sizing. Values obtained from [44] and [45].

Planet	Parameter	Symbol	Value	Unit
Earth	Radius	R_E	6378.1	km
	Gravitational parameter	μ_E	398 600	$km^3\,s^{-2}$
	Solar flux	S_E	1373	$W\,m^{-2}$
Mars	Radius	R_M	3396.2	km
	Gravitational parameter	μ_M	42 828	$km^3\,s^{-2}$
	Solar flux	S_M	610	$W\,m^{-2}$

Table 38: Orbit parameters for LEO and LMO, used for sizing. Values obtained from Equation 32 and 33.

Planet	Parameter	Symbol	Value	Unit
LEO	Orbital height	h_E	2000	km
	Orbital period	T_{LEO}	127.2	min
	Eclipse time	$T_{eclipse,LEO}$	35	min
LMO	Orbital height	h_M	500	km
	Orbital period	T_{LMO}	123.1	min
	Eclipse time	$T_{eclipse,LMO}$	41.5	min

As the EPS will be made specifically for MARCO and this mission, the cost of the EPS is evaluated using numbers from [62]. According to these numbers, the EPS will cost 32.4 k$/kg to manufacture and 64.3 k$/kg to develop. As the EPS used for MARCO is twice as big as the maximum value in the range given in [62], and that it serves as an estimate, a 20% contingency has been added. In total this brings the cost of the EPS to 253 M$. The final mass of the EPS is presented later and is 2.2 t, which was the value the cost was based on. However, this value is given in FY2010$ which means inflation needs to be taken into account. Given an average annual inflation rate (IR) of the dollar from 2010 to 2021 of 1.937%[29], the cost in FY2021$ will be:

$$FY2021\$ = FY2010\$\ (1+IR)^{No.of years} = 253 \cdot (1+0.0197)^{11} = 312M\$$$

Using a 0.82 conversion rate from US$ to € leads to a final cost of 256 M€. For the components of the EPS, the solar panel cost is known from literature and the remaining of the 256 M€ will be divided into the battery (35%), PMAD (60%) and cables (5%) to give estimates of the component cost.

12.3.1 Bimodal Nuclear Engines

As mentioned in Section 12.1, instead of using a separate radioisotope thermoelectric generator (RTG) or a nuclear reactor, a set of four bimodal engines is used as the primary energy generator. These bimodal engines will be responsible for meeting the entirety of MARCO's power requirement. Each of these engines can produce up to 25 kW of power, totalling 100 kW. Since the highest peak draw, as seen in Table 36, is 54.7 kW, three engines will be used to generate equal amounts of power, keeping the fourth engine as a redundancy. The power output for each of the engines can be altered by adjusting the control drums within the engine, which affect the reactivity of the nuclear process, hence the power output. This way it is simple to scale it down so it does not produce excessive power, however 25 kW is the maximum that one engine can provide.

The engines will not be able to provide power during the first phase of the mission as the nuclear fuel is supplied only towards the end of the phase, hence the solar arrays along with the batteries need to meet that requirement. The engines will also not be able to generate power during the burn times (4 burns per round-trip), during which time the solar array and the batteries need to supply power as well. Both these scenarios are discussed in the following sections.

12.3.2 Solar Array

In the critical scenario in LMO, where the engines fail to provide power to MARCO, the solar array and batteries need to provide 26.7 kW in order to have an operational habitation module with the necessary sub-systems operating [2]. In the aforementioned scenario, the solar array needs to provide energy to power up the habitation module during day-time and sufficiently charge the batteries, such that they can provide the required power during the eclipse periods.

The Triple Junction GaAs Ultraflex panel (TRL 8[30]) has been selected for the solar array for MARCO. Multi-junction panels are the preferred option for interplanetary and deep-space missions due to the panel's higher absorbance of broader wavelengths of light[31]. While GaAs has been picked over high-efficiency silicon as GaAs is a lighter and more efficient option. Despite the GaAs being more expensive to produce compared to other options due to its light weight, the reduction in launch cost will more than compensate for the production cost of the panel. Table 39 shows all the

[29] https://www.in2013dollars.com/us/inflation/2010?amount=1 *[cited 14 June 2021]*
[30] http://www.azurspace.com/index.php/en/products/products-space/space-solar-cells *[cited 29 June 2021]*
[31] https://www.nature.com/articles/s41598-019-40727-y *[cited 15 June 2021]*

necessary specifications for the panel, such as specific power[32], area per power[33], stowage space[34], panel efficiency[35], and cost [5].

Table 39: Triple junction GaAs Ultraflex specifications.

Parameter	Value	Unit
Specific power	150	$\mathrm{W\,kg^{-1}}$
Area per power	3.12	$\mathrm{m^2\,kW^{-1}}$
Stowage space	40	$\mathrm{kW\,m^{-3}}$
Panel efficiency	29.5	%
Cost [5]	1232	$€\mathrm{W^{-1}}$
Max. operational temp. [3]	60	°C
Min. operational temp. [3]	−160	°C
Service life	20	year
Degradation	0.5	$\%\mathrm{year^{-1}}$

In order to obtain the the required P_{SA} (with a 100 % efficiency), the day-time and night-time (eclipse) efficiencies need to be calculated. Which, as seen in Equation 34 and 35, consists of several other efficiencies, that can be found in Table 40.

$$\eta_d = \eta_{\text{power conditioning}} \cdot \eta_{\text{distribution}} \tag{34}$$

$$\eta_e = \eta_{\text{power conditioning}} \cdot \eta_{\text{charge el.}} \cdot \eta_{\text{battery}} \cdot \eta_{\text{discharge el.}} \cdot \eta_{\text{distribution}} \tag{35}$$

Table 40: Electrical Power System Efficiencies [5].

Parameter	Value [%]
Day-time Efficiency (Equation 34)	93.6
Night-time Efficiency (Equation 35)	64.9
Power Conditioning	96.5
Distribution	97
Charge	85
Battery	96
Discharge	85
Depth of Discharge	100

As seen in Table 40, a depth of discharge (DOD) of 100% is chosen. This is done to ensure an efficient cycle-life. As shown in [48], the LG-MJ1 battery that was chosen and explained in further detail in the battery section, is expected to have around 3000 cycles at a DOD of 100%. During the assembly phase of 135 days, where the batteries and solar panels function as the main power supply, the batteries will experience 1580 cycles, which is well below the 3000 life time cycles. During each mission, the batteries are expected to be discharged for maximum 10 times, when the engines do not provide power. This means that the batteries will experience less than 2000 cycles in total, which means they can be used throughout the entire mission when looking at cycle-life, and that a 100% DOD is the most efficient. In case of an emergency, the batteries will have enough cycles to be able to power the habitat for more than 100 days together with the solar arrays.

With both the day-time and night-time efficiencies known from Table 40, along with the day-time and eclipse durations

[32] https://forum.nasaspaceflight.com/index.php?action=dlattach;topic=38617.0;attach=1073291 *[cited 15 June 2021]*
[33] https://www.spectrolab.com/pv/support/Cotal_TRIPLEJUNCTION_EFF_32_2000.PDF *[cited 15 June 2021]*
[34] https://forum.nasaspaceflight.com/index.php?action=dlattach;topic=38617.0;attach=1073291 *[cited 15 June 2021]*
[35] http://www.azurspace.com/index.php/en/products/products-space/space-solar-cells *[cited 15 June 2021]*

from Table 37. The required P_{SA} with a 100 % efficiency of the solar arrays, is calculated using Equation 36 and subsequently using Equation 38, the area of the solar array is calculated taking efficiency [36] and degradation from Equation 37 [3].

$$P_{SA} \cdot t_d = \frac{P_d \cdot t_d}{\eta_d} + \frac{P_e \cdot t_e}{\eta_e} \tag{36}$$

$$L_d = (1 - \delta)^x \tag{37}$$

$$P_{sa} = S_{in} \cdot A \cdot \eta \cdot I_d \cdot L_d \cdot \cos(\Theta) \tag{38}$$

With a total required area of 334.7 m^2 (with a 5% contingency), the solar array has been sized for the critical scenario in LMO. Since the solar array and batteries also need to supply a peak power of 14.89 kW for phase 1, launch and assembly (as seen in Table 35), the solar array configuration needs to be designed for. For LEO, 32.24 kW (with 5% contingency) needs to be produced by the solar panels in order to meet the power requirement during the day and to charge the batteries for the eclipse. Using the aforementioned area of 334.7 m^2, in LEO a power of 122.65 kW would be generated which is almost quadruple the required power. Hence the solar array is divided into 8 smaller arrays, where 2 are used during phase I with an incidence angle of 34.52°. The detailed specifications for 1 of the 8 arrays are laid out in Table 41, with a 5% contingency.

Table 41: Solar Array specifications.

Parameter	**Value**	**Unit**
Power generated (at LEO with no 0° incidence) per array	15.3	kW
Mass per array	45.51	kg
Retractable mechanism (mass per array)	17.5	kg
Area per array	41.84	m^2
Volume per array	0.38	m^3
Cost per array	18.89	M€

The second purpose of the solar array is to generate sufficient power to supply MARCO, during the 4 burn periods per round-trip, when the bimodal engines do not generate any power. As stated in Section 12.3.1, the bimodal engines do not generate any power during the burn times, hence the solar array along with the batteries need to meet the requirement. Table 42, shows the burn times for both phases of the mission.

Table 42: Nuclear Engine burn times.

Phase	**Scenario**	**Location**	**Burn-time [min]**
Cargo Phase	Earth Departure Burn	LEO	25.3
	Mars Orbital Insertion	LMO	10.3
	Mars Departure Burn	LMO	6.2
	Earth Orbital Insertion	LEO	6.8
Crew Phase	Earth Departure Burn	LEO	50.8
	Mars Orbital Insertion	LMO	23.8
	Mars Departure Burn	LMO	15.9
	Earth Orbital Insertion	LEO	17.5

[36] http://www.azurspace.com/index.php/en/products/products-space/space-solar-cells *[cited 9 June 2021]*

Similar to the solar configuration design for the launch and assembly phase at the beginning of the mission, the solar array configuration is decided upon, the location of MARCO during the burn and the peak power requirement during that phase of the mission. For the burns during the cargo phase, the solar array alone was sufficient in providing power to MARCO without the help of the storage solution, with the assumption that the burn occurs when MARCO is not in a planetary eclipse and that the burns occur near LEO and LMO (used to calculate the solar flux). As seen in Table 43, the number of arrays for each burn along with their corresponding incidence angles were calculated.

Table 43: Power generation during burn-times in Cargo Phase.

Scenario	**Peak Power req. [kW]**	**Power Source**	**Array Incidence angle [°]**
Earth Departure Burn	21.78	Solar Array (2/8)	44.7
Mars Orbital Insertion	21.76	Solar Array (4/8)	37.0
Mars Departure Burn	21.77	Solar Array (4/8)	36.9
Earth Orbital Insertion	21.76	Solar Array (2/8)	44.8

Similar to the cargo phased array configurations during the engine burn, the array configurations for the crewed phase were also designed (without the need for the batteries). The number of arrays and their incidence angle for the two burns that occur near LEO, as seen in Table 44.

Table 44: Power generation during burn-times in Crew Phase.

Scenario	**Peak Power req. [kW]**	**Power Source**	**Array Incidence angle [°]**
Earth Departure Burn	54.92	Solar Array (4/8)	26.4
Earth Orbital Insertion	54.89	Solar Array (4/8)	26.5

Unlike burns that occur near LEO (Mars Orbital Insertion and Mars Departure Burn), the solar array (with an incidence angle of 0°) is unable to entirely meet the power requirement during those two burns. Hence, the batteries are employed to supply the remainder of the power for which the array can not. As seen in Table 45, the required power from the batteries and the respective energy are mentioned for the two burns near LMO.

Table 45: Required energy storage during burn-times at LMO in Crew Phase.

Scenario	**Peak Power req. [kW]**	**Req. Power from Batteries [kW]**	**Energy required [kW h]**
Mars Orbital Insertion	54.89	3.00	1.19
Mars Departure Burn	54.91	3.02	0.80

12.3.3 Battery

During the assembly phase, the batteries need to provide the necessary power at each eclipse, therefore the first step taken, was to find rechargeable batteries for the EPS. For this, several options were considered including Lithiated Nickel Cobalt Aluminum Oxide batteries (LP 33037)[37], Li-ion batteries used on ISS [46] [47] and the commercial battery LG-MJ1 which are deemed promising for future space applications [48]. In the end the LG-MJ1 was chosen for its performance and the design is based on its performance values. The main performance characteristics for each of the three battery types can be seen in Table 46.

[37] `https://www.eaglepicher.com/sites/default/files/LP%2033037%2060Ah%20Space%20Cell%20%20040319.pdf` *[cited 14 June 2021]*

Table 46: Specifications of various types of batteries.

Parameter	LP 33037	LG-MJ1	ISS Li-ion	Unit
Specific energy	0.16	0.231	0.064	$kW\,h\,kg^{-1}$
Energy density	0.393	0.653	0.0157	$kW\,h\,L^{-1}$
Energy storage	0.216	0.0121	15	$kW\,h\,h^{-1}$

As seen in Table 35 and 38 the peak power required during assembly is 15 W during an eclipse of 35 min. This is slightly higher than the other design situation in LEO, which is the moment where the engines do not provide power and the batteries should provide enough power for the habitat during eclipses. However, the critical design situation for the batteries turned out to be the case where the engines do not provide power in LMO. In this case the batteries need to provide enough power such that the habitat is fully functional during an eclipse. Based on Table 36 and 38 the power required for the habitat including ADCS and TCS is 26.7 kW and the eclipse time is 41.5 min which equals 0.69 h. This means the battery is sized to store an energy of 18.5 kW h in case of 100% efficiency. However, the batteries are not 100% efficient and the actual energy stored can be seen in Equation 39, where DOD is depth of discharge, P_{load} is the required power and η_{tot} is the total battery efficiency i.e. discharge efficiency and battery efficiency, which can be seen in Table 40 together with the DOD.

$$E_{actual} = \frac{P_{load}\, t_{eclipse}}{\eta_{tot}\, DOD} \tag{39}$$

This results in an actual energy to store in the batteries of 22.6 kW h and using the performance characteristics of the LG-MJ1 as presented in Table 46, the mass becomes 102.8 kg and the volume becomes 0.035 m^3. To these values a 5% contingency has been added and the final specifications for the batteries can be seen in Table 47.

Table 47: Energy storage system specifications for MARCO, using LG-MJ1 batteries.

Parameter	Value	Unit
Energy storage	22.6	kWh
Mass	102.8	kg
Volume	0.04	m^3
Cost	36.8	M€

12.3.4 PMAD and Cabling

There are not many current PMAD elements that can manage the 54 kW which are required for this mission. According to [49] the mass performance of PMAD's from some satellites from mid-60's to the 90's were in the range 40 $kg\,kW^{-1}$ to 183 $kg\,kW^{-1}$, this included one which had the capability of managing 100 kW. However, in the past 30 years technologies have developed significantly, and the performance has increased, so instead it was chosen to look at currently available PMAD's for sizing rather than older, outdated ones. An average of the existing PMADs were used and scaled to fit the needs of MARCO of 54 kW. The PMADs used are from Magellan Aerospace[38], AAC Clyde Space's Starbuck Mini[39] and Starbuck Micro[40], VECTRONIC Aerospace's VPCDU-1[41] and Gom space's P31U[42].

Using the average values found in Table 48, the final mass and volume of the PMAD that needs to manage the previously found maximum power output for MARCO of 54.23 kW, will be 660 kg and 0.86 m^3.

[38] https://magellan.aero/wp-content/uploads/PCU%20-%20Web%20Version%20-%20with%20data%20sheet%20paper.pdf *[cited 14 June 2021]*

[39] https://www.aac-clyde.space/assets/000/000/187/AAC_DataSheet_Starbuck-Mini_original.pdf?1614275813 *[cited 14 June 2021]*

[40] https://www.aac-clyde.space/assets/000/000/186/AAC_DataSheet_Starbuck-Micro_original.pdf?1613579830 *[cited 14 June 2021]*

[41] https://www.vectronic-aerospace.com/power-control-and-distribution/ *[cited 14 June 2021]*

[42] https://gomspace.com/UserFiles/Subsystems/datasheet/gs-ds-nanopower-p31u-29.pdf *[cited 14 June 2021]*

Table 48: Existing PMAD elements specifications.

PMAD	Mass [kg]	Power [kW]	Mass performance [kg kW^{-1}]	Volume performance [m^3 kW^{-1}]
Magellan flagship mission	25	1.5	16.7	0.018
Magellan SmallSat mission	12	0.5	24.0	0.031
Starbuck Mini	3.3	1.5	2.2	0.003
Starbuck Micro	2.45	0.12	20.4	0.033
VPCDU-1	4.14	0.54	7.7	0.008
P31U	0.1	0.05	2.0	0.003
Average	7.83	0.7	12.2	0.016

To evaluate the mass and volume of the cables used for MARCO, ISS was used as reference. It is assumed that the amount of cables will be similar to that of the ISS as the engine is placed in one end of MARCO, and the PMAD in the other. The EPS of the ISS contain 13 km of cables [50]. Looking at the NASA Parts Selection List[43], it is possible to estimate the mass and volume of the cables. Looking at the various size options for the SAE AS22759/34, which is included in the aforementioned list, and their specifics[44], an average mass of a cable of 53.87 kg km^{-1} was found together with an average cable cross section of 0.000 011 5 m^2. For 13 km of cable, this leads to a mass of 700 kg and a volume of 0.15 m^3

The values found for the PMAD and cables are all based on empirical data from other components, which may not necessarily be similar to the PMAD and cables that will be used for MARCO. Hence a 15% contingency is added to the mass and volume, and the values of the PMAD and cables can be seen in Table 49.

Table 49: PMAD and cabling specifications.

Component	Parameter	Value	Unit
Power management & distribution	Mass	767.9	kg
	Volume	1.0	m^3
	Cost	63.0	M€
Cabling	Cable length	13	km
	Mass	805.4	kg
	Volume	0.17	m^3
	Cost	5.3	M€

12.3.5 Final EPS Design

The EPS designed in this report will be designed specifically for the MARCO-POLO missions and therefore contingencies have been added to the results found in the previous sections. The final EPS will consist of the bimodal engines which can produce up to 25 kW each when they are not used for thrust. The solar array and batteries which will provide energy during the assembly phase and in case of engine failure, they will also be able to provide the necessary power to the habitat. Finally there will be a PMAD and cabling which are the largest contributor to mass in the EPS. Equation 40 shows the calculation for the total EPS mass excluding the engines, and in Table 50 the summarised values including their respective contingency can be seen.

$$M_{EPS} = M_{SA} + M_{BAT} + M_{PMD} + M_{Cable} \tag{40}$$

[43] https://nepp.nasa.gov/npsl/Wire/wire_type.htm *[cited 14 June 2021]*
[44] https://docs.rs-online.com/82ea/0900766b814ddd7f.pdf *[cited 14 June 2021]*

Table 50: Final parameters of the electrical power system of MARCO, including contingency.

Sub-system	Mass [kg]	Volume [m^3]	Cost [M€]
Solar Array (TJ GaAs Ultraflex)	503.3	3.1	151.1
Battery (LG-MJ1)	102.8	0.04	36.8
PMAD & Cabling	1573.2	1.2	68.3
Total	2179.3	4.3	256.2

12.4 System Architecture and Interfaces

The EPS consists of two power generation systems, an energy storage system and a PMAD system. The bimodal nuclear engine will serve as the primary energy system for the entirety of the round-trip, while the solar arrays will be used for the first phase (launch and assembly) and in case of an emergency only. While the batteries will provide power during the eclipse periods when the solar array is in use. Figure 26 is the system architecture for the EPS of MARCO, while a more detailed system architecture is in section 18, which show how the power reaches all sensors and subsystems of MARCO.

As seen in Figure 26, the PMAD system controls the two generation systems, transmits and delivers the power to all the subsystems and their respective components. All four systems have their own power conditioning and control system (PC&C), which interface with the PMAD system. The PMAD system consists of four main components: the switch control unit, interconnection unit, transmission unit and distribution unit. The switch control unit controls the flow of power within the EPS, inherently acting as the brain of the system. It is through the intermission unit, through which the bulk energy from the generation systems and the storage system flows through before being distributed. The distribution unit is the final unit, which delivers power to all the subsystems of MARCO. The entire system includes redundancies, which will ensure that the system functions smoothly throughout the mission duration.

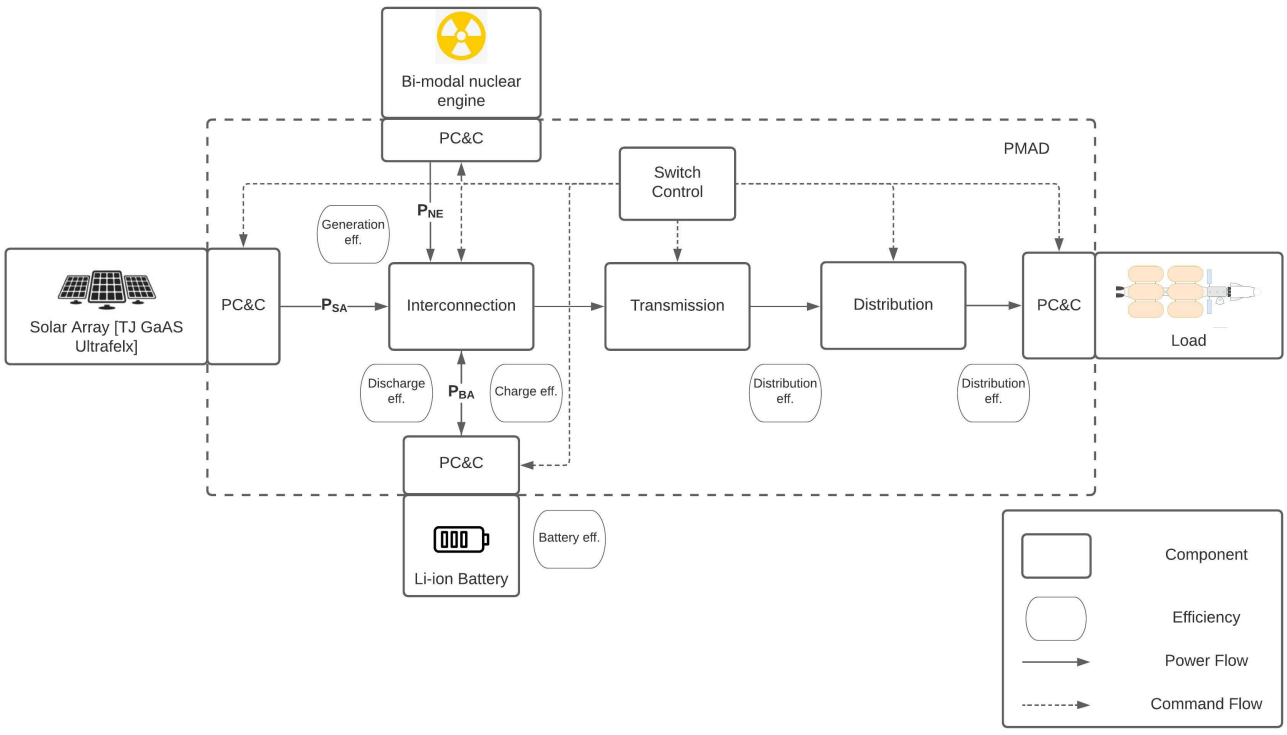

Figure 26: EPS architecture and command-flow diagram.

12.5 Risk Assessment

This section covers the major risks which are expected to occur to the EPS system during the duration of the mission. Table 51 covers the risks, their likelihood and impact (RBM) , and the mitigation strategy with the updated RAM. The likelihood and the impact are based on Table 2.

Table 51: Risk table including the most critical risks for each subsystem. RBM is defined as "likelihood, impact" before mitigation, RAM is "likelihood, impact" after mitigation.

ID	Risk	RBM	Mitigation	RAM
EPS01	Nuclear engine fails to produce power	1, 5	**Reduce** by adding redundancy in terms of the solar arrays, as discussed in section 12.3.2.	1, 2
EPS02	Radiation leak occurs	2, 3	**Avoid** by performing sufficient testing and inspection prior to launch	1, 3
EPS03	Nuclear Engine produces too much power	3, 4	**Reduced** by reducing engine output, or even shutting it down	1, 4
EPS04	Solar arrays gets damaged during launch	2, 5	**Avoid** by testing and proper packing prior to launch	1, 5
EPS05	Retractable array mechanism fails to deploy or retract	2, 3	**Avoid** by designing the structure for critical modes	2, 1
EPS06	Solar eclipse occurs during assembly phase, making the arrays produce too little power	1, 4	**Avoid** by adding a contingency to the battery sizing, as discussed in section 12.3.3	1, 1
EPS07	PMAD fails to deliver power to MARCO	2, 5	**Reduce** by implement redundancies	1, 5
EPS08	Power surge occurs	4, 3	**Avoid** by implementing surge protectors in all the components of the EPS	1, 3
EPS09	Batteries overheat	3, 2	**Avoid** by sufficiently implementing thermal control solutions	1, 2
EPS10	Wire connection loosens	3, 3	**Avoid** by testing and inspections, and **Reduce** by adding redundant wires	2, 2
EPS11	A breach occurs in the electrical insulation	3, 4	**Reduce** by using better material	2, 4

Figures 27 and 28, map the impact and likelihood of the EPS risks before and after mitigation, respectively. These figures help communicate the impact of the risk mitigation strategy and the overall improvement of the subsystem's reliability.

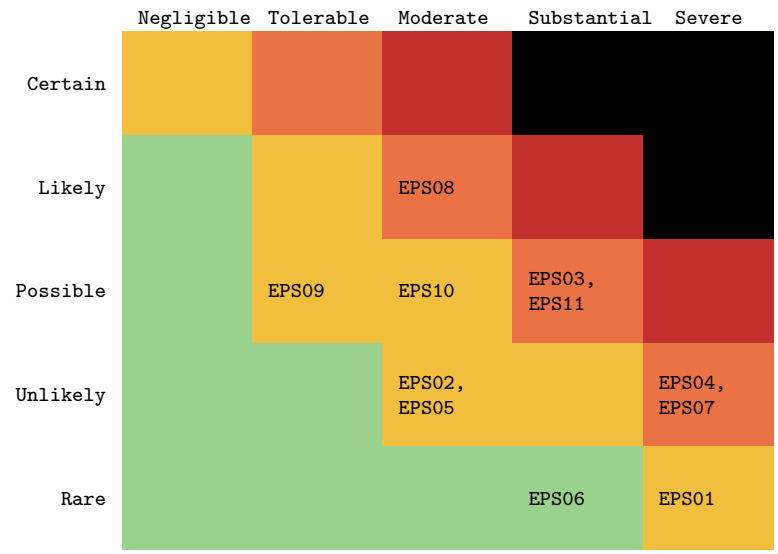

Figure 27: Risk matrix of identified Electrical Power subsystem risks. Likelihood is listed vertically and impact is listed horizontally.

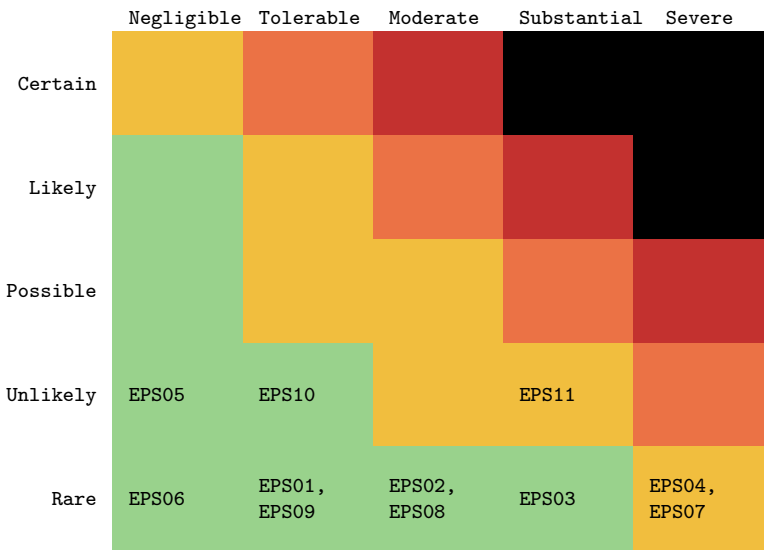

Figure 28: Risk matrix of mitigated risks. Likelihood is listed vertically and impact is listed horizontally.

12.6 Sustainability

Unlike the general sustainability approach of the project, this chapter focuses on the EPS entirely. The four main aspects considered are the design, manufacturing, operation and disposal of MARCO's EPS.

The main goal of the EPS is to provide the required amount of power to the various subsystems of MARCO as efficiently as possible. Hence, the three main components of the EPS (primary generator, secondary generator and storage) were designed for high performance and efficiency, and throughout the design process it was imperative to avoid over-designing as this is not sustainable. The use of the nuclear bi-modal engines as the primary power generator might seem unsustainable due to the use of radioactive substances and the dangerous waste it generates. But, in the case of MARCO, nuclear engines were used for propulsion as they were a more efficient option than the chemical alternatives. And with only a small modification and some extra fuel, it was possible to use the same infrastructure to generate power. Having combined thrust and power generation into one infrastructure adds to a more sustainable mission compared to using a separate nuclear power source or solely rely on solar power.

Considering the manufacturing part of the EPS, it is on a whole not the most environmentally sustainable system to manufacture as the materials used in the production of the batteries and solar arrays can be tricky to work with. This aspect is unavoidable and can only be minimised by not over-designing the system, and by implementing strict guidelines, employing experienced professionals and abiding by manufacturing regulations.

During the operations phase of the system, the EPS is highly sustainable as these systems are mostly self reliant and have a long service life. Except for the nuclear refuelling of the engines every round-trip, the system is entirely self reliant. Only half way through the mission duration (after 20 years), the solar arrays need to be replaced. Since the major components of the the EPS are housed in the control module, the disposal of the EPS will be the same as that of the module (further discussed in Section 17).

12.7 Verification and Validation

The last stage in the design process, is verifying and validating the design. The first step to verify the design is to verify the design methodology. The general equations mentioned in Section 12.3, were obtained from official TU Delft readers [5], [6], and multiple sources ensure that the equations are valid. Upon verifying the equations used for the design of the system, the specifications of the systems/components need to be verified, which is done by obtaining these specifications from manufactures of these components, as seen in Tables 39, 40, 46, and 48.

Upon verifying the equations and the inputs, the overall methodology needs to be verified, which is done by applying the same methodology on a different spacecraft altogether. For this purpose the 1998 Mars Surveyor was selected [45]. Based on the EPS data of the observation satellite, the array produces a total of 1000 W in Mars orbit, using the same GaAs panel. Assuming that the array type does not influence the generated output, and that the solar array had an incidence angle of 0°. Using the values and equations mentioned in Section 12.3.2, an area of 6.5 m^2 was calculated which is 0.9 m^2 smaller than the satellite's actual array area of 7.4 m^2 [5]. The 12% difference, can be justified because of MARCO's more efficient panel and the deviation in the value of the solar flux in Mars orbit (the value mentioned in Table 37). Other than the solar array area, all other calculations are heavily dependent on the specifications of the of the components, and since most of these specifications are of newer cutting-edge systems, and since the advertised values tend to be higher than in the actual application, these values can hence not be adequately compared to previous missions. As mentioned in Section 12.3.4, the PMAD system and the EPS cabling are estimated by extrapolating the average of several somewhat similar elements, thus creating a large margin for the design versus the actual specifications.

The second step in verifying the design, is to verify the results of the design. In order to verify the system's performance, as seen in Table 52, each EPS requirement has an accompanying method or two in order to verify the result.

[45] https://mars.nasa.gov/mars-exploration/missions/polar-lander/ *[cited 29 June 2021]*

Table 52: Methods for verifying the Electrical Power Subsystem Requirements.

Requirement ID	Verification and Validation Method			
	Test	Analysis	Inspection	Demonstration
M-EPS-01		X		
M-EPS-02		X		
M-EPS-03	X	X		
M-EPS-04			X	
M-EPS-05			X	
M-EPS-06		X		
M-EPS-07		X		
M-EPS-08	X			
M-EPS-09		X		
M-EPS-10			X	
M-EPS-11	X	X		

Validation of the system consists of three main efforts, the analysis used to show requirement compliance, ground-based validation tests conducted to reduce risk, and in-flight performance tests validation results [51]. Since, the requirement compliance is covered in Section 12.8. The remaining two sets of validation efforts encompass, numerous tests which range from modelling the system to building scaled prototypes.

12.8 Requirement Compliance and Sensitivity Analysis

For the MARCO EPS requirements discussed in Section 12.2, a compliance matrix is generated (as seen in Table 53) in order to establish whether or not the subsystem requirements have been met by the design.

Table 53: General EPS Requirements Compliance.

ID	Compliance	Rationale
MARCO-EPS-01	✓	Section 12.3
MARCO-EPS-02	✓	Section 12.3
MARCO-EPS-03	X	Table 47. The battery can store 22.6 kW h, which proved to be sufficient for the design.
MARCO-EPS-04	✓	Section 12.3.5
MARCO-EPS-05	✓	Section 12.3.5
MARCO-EPS-06	X	Section 12.3.1
MARCO-EPS-07	✓	Section 12.3.2
MARCO-EPS-08	-	Upon available data presented in this chapter, the reliability cannot yet be determined but it should be monitored during the development of the EPS.
MARCO-EPS-09	-	Section 15. This will be covered by the TCS.
MARCO-EPS-10	✓	Section 12.3
MARCO-EPS-11	✓	Section 12.3.4

Beside the aforementioned compliance matrix, a sensitivity analysis needs to be performed in order to test the rigidity of the design results. Upon the completion of the verification and validation of the design in Section 12.7, the sensitivity analysis needs to be performed, in order to ensure that the final design was the best possible design. Since, the critical scenario that was designed for, was when the bi-modal engines fail around Mars, the size of the array and batteries have been fixed. In order to verify if this was the best option, the system was instead sized for the first phase, this resulted in the system not being able to cope with the power requirement of MARCO during the critical scenario. Thus, freezing the total size of the system. The second, consideration during the design phase, was the configuration of the array (how many solar arrays would be used for each scenario), which does not have an effect on the systems performance, but even number of arrays were picked (and deployed for the various scenarios, as seen in

Table 42) in order to preserve the symmetry of the spacecraft. In the case of the battery, sizing for a complete engine failure in LMO, was critical, as it is during that scenarios eclipse period for which the battery is sized. Since, no other phase had a higher energy storage need, the sizing for the critical scenario has been selected. The only major design uncertainties arise from the sizing of the PMAD and the cabling of the system. As the PMAD is a bespoke component and its is specifically designed for a spacecraft. Since, a detailed design of the PMAD is out of the scope of this project, the size of the PMAD was extrapolated from precious spacecrafts, thus leaving a large margin of error in the component sizing, which needs to be accepted in this project. Similarly, the cabling length for the MARCO, is yet unknown and is approximated using the length of the cabling in the ISS, thus again leaving a significant margin of error.

12.9 Recommendations

This section provides recommendations on how the design could be improved and the future steps that need to be taken in order to realise the system. Firstly, the phase division in Table 35 and 36 need to be for shorter periods, and with more detail regarding the power requirement of each subsystem. Secondly, more detailed system performance analysis needs to be performed in order to get a better understanding of how the EPS copes throughout the mission. The level of precision of the component specifications need to be more thoroughly investigated, and even tested. For example, the efficiencies of the batteries and solar arrays and the degradation of the arrays. The performance of the complete system over a long time span needs to be further analysed.
With regards to safety, the feasibility of the bi-modal engines and the required precautions also need to be further studied. The solar panel's actual performance might slightly vary from what the manufacturers inform, hence the panels need to be tested before being used. In order to obtain better estimates on the cost and sizing of PMAD and cabling, it is suggested to contact the larger space agencies and benefit from their expertise and experience with larger space missions.
Furthermore, the battery performance is based on very recent research on commercial batteries for space applications, and it is recommended to test, and look into whether sizing the commercial batteries is feasible. In general commercial batteries can hold only limited capacitance and scaling it up to fit the needs of MARCO-POLO might affect the performance characteristics. Lastly, the specific configuration of the arrays need to be finalised in cooperation with the manufacturer, leading to an actual final product.

13 Attitude Determination and Control System

This chapter covers the detail design of the attitude determination and control system based on the trade-off of the midterm report [8]. All maneuvres and orbit maintenance are covered and designed for. The trade-off will be briefly described, then the requirements are given. After this, the determination system and then the control system are discussed in detail. Next, its architecture is observed, and its risks evaluated. At last, the requirements are verified and recommendations given for future research.

13.1 Trade-off Summary

During the midterm, several concepts of what type of systems would be used for the attitude determination were considered. A total of 3 trade-offs were done to determine which would make it to the final design.

The first trade-off consisted in choosing between the propellants used for the RCS thrusters. The three options were cold gas, mono-propellant and bi-propellant. Cold gas was discarded due its low efficiency. Even though it requires far less volume and complexity, for long term missions such as these, cold gas does not perform efficiently, and therefore would mean a much larger mass. Mono-propellant was chosen out of the other two due to it being simpler, and therefore more reliable, and needing only one tank, easing the sizing process.

The second trade-off was between control moment gyroscopes, and reaction/momentum wheels. Wheels tend to perform better in mass and volume, but they become extremely inefficient with spacecrafts with large mass and moments of inertia, such as MARCO. On top of this, wheels need much more de-saturation that CMGs during this large amount of time, which would increase the amount of propellant needed for RCS thrusters. CMGs were chosen as the component for internal attitude control.

The last trade-off was between horizon sensors and magnetometers for Earth orbit attitude determination. Despite magnetometers being better in mass and volume, horizon sensors are generally more precise. Horizon sensors won this final trade-off nevertheless, because of the fact that they can be also used during Mars orbit.

13.2 Requirements

MARCO-ADCS-01 The attitude determination system shall detect a change in angle of 0.5°.

MARCO-ADCS-03 The attitude control system shall provide 3-axis control.

MARCO-ADCS-04 The attitude control system shall have a total mass of no greater than 20.5 t.

MARCO-ADCS-05 The ADCS system shall have a volume of 16.2 m^3.

MARCO-ADCS-06 MARCO shall be provided with a pointing accuracy of 0.5°.

MARCO-ADCS-07 The ADCS system shall remain between the temperatures of 274 K to 309 K during its operations.

MARCO-ADCS-08 The attitude control system shall provide a minimum angular acceleration to the whole spacecraft of $3.32 \times 10^{-10} \,^\circ s^{-2}$.
Rationale: Whenever the spacecraft reaches LEO, it must accelerate to the angular speed required to operate in it ($1.99 \times 10^{-7} \,^\circ s^{-1}$*) within* 10 min.

The requirement **MARCO-ADCS-02** got replaced by **MARCO-ADCS-08** due to a mission design change. The spacecraft no longer needs to rotate at the same rate as its orbit around a planet. The value for this angular speed can be found and explained in subsubsection 13.4.3, when talking about orbit orientation.

13.3 Determination System

The determination system has the job of detecting a change in angle of 0.5° on all axis. All the device selected had an accuracy of at least this much. The tables show the amount which will be used at once on MARCO, and the total amount which will be needed throughout the entire mission lifetime. These are different due to the fact that equipment will need to be replaced in case of a failure or it reaching its end of life.

Sun sensors: Sun sensors are essential for most of the trip. They require to be oriented in as many directions as possible, in order to deal with MARCO's relative position to the Sun. of course, these will not need to be operational during eclipse times. For this, the NFSS-411 [46] sun sensors were chosen. They more than fulfil the 0.5° requirement. 12 of them were chosen to be at once in MARCO, 3 for every side covered. This is due to their short lifetime, and redundancy. The amount needed for all trips was estimated to be 24, with all of the sun sensors assumed to be replaced once.

Table 54: Technical data of the sun sensor combination.

	Amount	**Amount Mission**	**Mass [t]**	**Volume [m^3]**	**Power [kW]**	**Peak Power [kW]**	**Cost [€]**
Sun sensors	12	24	0.00063	0.0003917	0.000675	0.00234	354240

Star trackers: Star trackers are the secondary external source for attitude determination. As mentioned previously, sun sensors cannot provide data when MARCO is in an eclipse. In addition they cannot provide a 3-axis determination. Because of this, MARCO needs a star tracker, which measures determination based on stellar mapping. For this, the ST200 star tracker [47] was selected.

Table 55: Technical data of the star tracker combination.

	Amount	**Amount Mission**	**Mass [t]**	**Volume [m^3]**	**Power [kW]**	**Peak Power [kW]**	**Cost [€]**
Star trackers	4	8	0.000336	0.0002563	0.0048	0.008	1312000

Horizon sensor: Eclipses only occur during the stationary orbits around Earth or Mars. These are also the most critical phases of the trip. Because of this, it would is wise to use horizon sensors during these parts too. The

[46] http://byhead.com/index.php/Product/index/id/1 *[cited 14 June 2021]*
[47] http://byhead.com/index.php/Product/index/id/20 *[cited 14 June 2021]*

AXT25C sensor [72] was chosen for this case. The cost for the corresponding sensor could not be found, but the cost for an alternative one was obtained from the commercially available [48] and a safety margin of 2 was set. Only 2 horizon sensors are needed at once, of which only 1 of them will be operational at once. The second one is included for redundancy. They are also assumed to be replaced once, therefore needing 4 of them for the entire mission.

Table 56: Technical data of the horizon sensor combination.

	Amount	Amount Mission	Mass [t]	Volume [m^3]	Power [kW]	Peak Power [kW]	Cost [€]
Horizon sensor	2	4	0.0054	0.004764	0.017	0.017	146616

Gyroscope sensors: As the internal attitude determination device, gyroscopes were chosen, to measure any changes to angular speed and acceleration. Specifically, the ARIETIS 3-axis gyroscope system [49]. This system not only provides determination on all 3 axis, but also processes the data and is able to output a status directly to the command and data handling system. 2 of these are needed at once in the control module. 1 of them is used for redundancy. In total 6 will be used for the whole mission. Gyroscopes can drift, and therefore are assumed to be replaced not once, but twice through the entire mission.

Table 57: Technical data of the gyroscopes combination.

	Amount	Amount Mission	Mass [t]	Volume [m^3]	Power [kW]	Peak Power [kW]	Cost [€]
Gyroscopes	2	6	0.00105	0.0005139	0.00042	0.00042	61992

13.4 Control System

The control system has the job of providing MARCO with the necessary pointing accuracy, as well as handling maneuvres. The process to size the control system is much more complex and will consist of several parts.

13.4.1 Moment of Inertia

To be able to make most control calculations, the mass and moment of inertia (MOI) of the entire system must be known. The ADCS. due to being in the control module, does not change from trip to trip, so it must be designed for the worst case scenario. In this case, the worst case scenario is MARCO being on a trip with all tanks full from the beginning and all components including the habitat module.

Before dealing with the total moment of inertia, the more complex-shaped components must have their own moment of inertia determined first to be able to simplify the last calculations.

Propellant tanks: As seen before in section 10, in order to fit optimally the tanks into the launch vehicle, the shape has to be rather unusual. This is why tanks need their moment of inertia calculated individually first. Before being able to do this, the centre of mass of the tank and its mass distribution have to be determined too. Also mentioned in section 10 is the fact that there are 4 different tanks in terms of mass. Although this does change the mass and moment of inertia magnitudes, it does not change the methods to work them out, nor the ratios between the geometrical components. Each tank is composed of a cylinder central piece, a semi-sphere in one side of it, and on the other, a semi-ellipsoid. The height of the ellipsoid is half its radius.

With this knowledge, the centre of mass is found by assuming tanks have an equally and uniformly distributed mass throughout their volume, including the propellant mass and the dry mass. This way, the mass of each section of the tank can me computed in the basis of their volume. To calculate the volume of each section, Equation 41, Equation 42 and Equation 43 are used.

$$V_{se} = \frac{2}{3} \cdot \pi \cdot r_c^2 \cdot h_{se} = \frac{2}{3} \cdot \pi \cdot 4^2 \cdot 2 = 67.02\,\mathrm{m}^3 \tag{41}$$

[48] https://satcatalog.com/component/ai-ses-ir-earth-sensor/#1595033511432-eaec2f55-a5bdcbd4-9b78d9d4-03ad *[cited 16 June 2021]*

[49] https://www.innalabs.com/arietis *[cited 16 June 2021]*

$$V_{ss} = \frac{2}{3} \cdot \pi \cdot r_c^3 = \frac{2}{3} \cdot \pi \cdot 4^3 = 134.0\,\text{m}^3 \tag{42}$$

$$V_c = \pi \cdot r_c^2 \cdot h_c = \pi \cdot 4^2 \cdot 10 = 502.7\,\text{m}^3 \tag{43}$$

Once the individual volumes are computed, the total volume is calculated by $V_{tank} = V_c + V_{ss} + V_{se} = 703.7\,\text{m}^3$. Therefore, by taking the mass of a tank and the ratios in volume, the mass for each segment can be computed by $m_{se} = \frac{V_{se}}{V_{tank}} \cdot m_{tank}$, $m_{ss} = \frac{V_{ss}}{V_{tank}} \cdot m_{tank}$ and $m_c = \frac{V_c}{V_{tank}} \cdot m_{tank}$. With m_{tank} being different for every tank variation.

Table 58: All tank variation masses at maximum propellant capacity.

	Back centre tank	**Back side tanks**	**Front centre tank**	**Front side tanks**
Mass [t]	44.00	42.23	44.46	42.54

With the value for the masses, now the centre of mass has to be found. In order to do this, the centre of mass of each section has to be found. As it is taken from the tip of the semi-ellipsoid, $c_{se} = h_{se} \cdot (1 - \frac{3}{8})$, $c_{ss} = h_{se} + h_c + \frac{3}{8} \cdot r_c$ and $c_c = h_{se} + \frac{1}{2} \cdot h_c$. After this, mass moments are taken with Equation 44.

$$c_{tank} = \frac{c_{se} \cdot m_{se} + c_c \cdot m_c + c_{ss} \cdot m_{ss}}{m_{tank}} = 7.714\,\text{m} \tag{44}$$

With the centre of mass of the tank found, now the moments of inertia may be computed. It must be stated first that the moments of inertia axes were taken the same as the axes of MARCO. This means the z axis is the longitudinal axis, the x axis points in the direction of the solar array deployed and the y axis is the remaining orthogonal direction. Firstly, the individual MOI of each component must be found. This is done through Equation 45, Equation 46 and Equation 47.

$$I_{x_{se}} = I_{y_{se}} = 0.259 \cdot m_{se} \cdot r_c^2 \quad I_{z_{se}} = \frac{2}{5} \cdot m_{se} \cdot \frac{r_c^2 + h_{se}^2}{2} \tag{45}$$

$$I_{x_{ss}} = I_{y_{ss}} = 0.259 \cdot m_{ss} \cdot r_c^2 \quad I_{z_{ss}} = \frac{2}{5} \cdot m_{ss} \cdot r_c^2 \tag{46}$$

$$I_{x_c} = I_{y_c} = \frac{1}{12} \cdot m_c \cdot (3 \cdot r_c^2 + h_c^2) \quad I_{z_c} = \frac{1}{2} \cdot m_c \cdot r_c^2 \tag{47}$$

After this, to obtain the final moment of inertia, the Steiner terms were also taken into account. These simply formulate as $I_{st,seg} = m_{seg} \cdot d_{seg}$ where $d_{seg} = c_{tank} - c_{seg}$. This is applied for all components in all axes. At last, with Equation 48, the moment of inertia for a single whole tank is computed.

$$I_{tank} = I_c + I_{ss} + I_{se} + I_{st,c} + I_{st,ss} + I_{st,se} \tag{48}$$

This process is done for the 4 tank variants previously stated.

Lander: As said before, the worst case scenario is taken, therefore the heaviest lander, the crew lander is taken. The crew lander is composed of 2 shapes. A cylinder and a frustum. For the cylinder, the same equation for volume as Equation 43 is taken. In the case of a frustum, this equation is used too, only for this one, $r_c = \frac{r_{c,bottom} + r_{c,top}}{2}$, where $r_{c,bottom}$ is the larger radius and $r_{c,top}$ is the smaller radius.

To compute the centre of mass, Equation 44 is used but with the lander frustum and cylinder. As for the moment of inertia, the same approach as Equation 47 is used for both shapes, the frustum having the same average radius assumption as mentioned before.

MARCO. With all the complex shapes worked out, now the moment of inertia for the whole spacecraft can be calculated. Some other components of MARCO such as the control module and the habitat are assumed to be cylindrical and therefore make use of Equation 47. The solar arrays are assumed to be a rectangular flat surface and thus use Equation 49.

$$I_{x_{flat}} = \frac{1}{12} \cdot m_{flat} \cdot w_f^2 \quad I_{y_{flat}} = \frac{1}{12} \cdot m_{flat} \cdot (w_f^2 + h_f^2) \quad I_{z_{flat}} = \frac{1}{12} \cdot m_{flat} \cdot h_f^2 \tag{49}$$

Another notable point worth mentioning is the tank arrangement based on the different iterations made of MARCO. The first iteration, made as envisioned during the midterm report, had 10 tanks, all facing the same way and divided into two groups. Each group has a core tank and several side tanks. For the first iteration there were 4 tanks surrounding it, and for symmetry, were arranged in a cross-like manner around the core tank. Upon further sizing, the propellant increased and 12 tanks had to be included, making this pattern go from a cross to a pentagonal shape. Lastly, after decreases in subsystem mass on their individual sizing, it went back to 10 tanks. Table 59 and Table 60 show the longitudinal centre of mass from the back tip of the back tanks. The centres of mass on the x and y axis are all 0, due to symmetry.

Table 59: All centre of mass values during the main phases.

Phase	C_m [m]
Earth orbit full	32.19
Transfer to Mars	37.91
Mars orbit	32.64
Transfer to Earth	46.16
Earth orbit empty	53.61

Table 60: All centre of mass values during the refuelling phases.

Phase	C_m [m]
Refuel 1	48.74
Refuel 2	45.07
Refuel 3	42.22
Refuel 4	39.93
Refuel 5	38.06
Refuel 6	36.50
Refuel 7	35.17
Refuel 8	34.03
Refuel 9	33.05

With the centre of mass positions of each segment and their MOI, the total MOI was calculated in a similar manner to Equation 48. This whole process was all repeated several times. For a full MARCO, after the first departure burn, after the first insertion burn, after the second departure burn, after the second insertion burn, and after each refuelling session until full again. This gives a better understanding of how the moment of inertia changes throughout one trip and how it influences other parameters. As a last point, the MOI during the Mars orbit (after the first insertion burn) is assumed to not include the lander. Table 61 and Table 62 show the moments of inertia used for later calculations.

Table 61: All MOI values during the main phases.

Phase	I_x [kg m^2]	I_y [kg m^2]	I_z [kg m^2]
Earth orbit full	$2.96 \cdot 10^8$	$2.96 \cdot 10^8$	$3.21 \cdot 10^7$
Transfer to Mars	$2.23 \cdot 10^8$	$2.23 \cdot 10^8$	$1.81 \cdot 10^7$
Mars orbit	$9.10 \cdot 10^7$	$9.02 \cdot 10^7$	$1.16 \cdot 10^7$
Transfer to Earth	$1.37 \cdot 10^8$	$1.37 \cdot 10^8$	$8.32 \cdot 10^6$
Earth orbit empty	$6.66 \cdot 10^7$	$6.66 \cdot 10^7$	$3.54 \cdot 10^6$

Table 62: All MOI values during the refuelling phases.

Phase	I_x [kg m^2]	I_y [kg m^2]	I_z [kg m^2]
Refuel 1	$1.12 \cdot 10^8$	$1.12 \cdot 10^8$	$6.40 \cdot 10^6$
Refuel 2	$1.47 \cdot 10^8$	$1.48 \cdot 10^8$	$9.25 \cdot 10^6$
Refuel 3	$1.76 \cdot 10^8$	$1.76 \cdot 10^8$	$1.21 \cdot 10^7$
Refuel 4	$2.00 \cdot 10^8$	$2.01 \cdot 10^8$	$1.50 \cdot 10^7$
Refuel 5	$2.21 \cdot 10^8$	$2.21 \cdot 10^8$	$1.78 \cdot 10^7$
Refuel 6	$2.39 \cdot 10^8$	$2.40 \cdot 10^8$	$2.07 \cdot 10^7$
Refuel 7	$2.56 \cdot 10^8$	$2.56 \cdot 10^8$	$2.35 \cdot 10^7$
Refuel 8	$2.70 \cdot 10^8$	$2.70 \cdot 10^8$	$2.64 \cdot 10^7$
Refuel 9	$2.84 \cdot 10^8$	$2.84 \cdot 10^8$	$2.92 \cdot 10^7$

To verify this method, a CAD model was made, with densities set on each module according to the mass they were designed for. Figure 29 shows the model used. Some structural components such as the tank support beams and several docking ports were not included in this, but their moment of inertia can be considered negligible. The configuration as seen, is for a crew mission and at full propellant mass. The values obtained were $I_x = 2.61 \times 10^8$ kg m^2, $I_y = 2.71 \times 10^8$ kg m^2 and $I_z = 2.98 \times 10^7$ kg m^2. The values are in the correct order of magnitude

and close enough to the calculations. The small differences may be due to smaller changes to the design iterations after ADCS MOI calculations were last iterated such as the inclusion of docking ports and the engine dimensions.

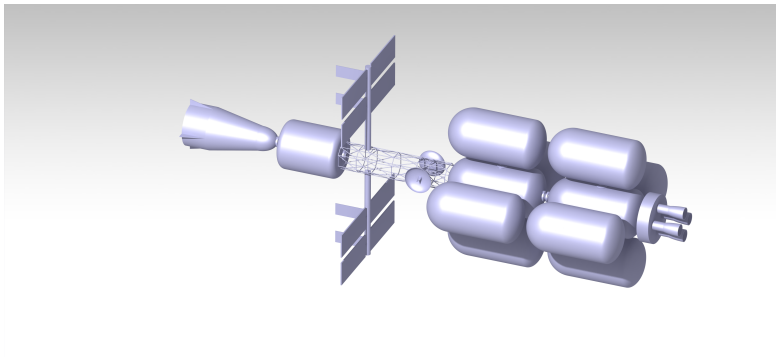

Figure 29: CAD model used for verification.

13.4.2 Disturbance Torques

Gravity gradient: This is a disturbance torque mostly present only during the stationary orbits around Earth and Mars. During the transfer orbits, it is assumed to be of negligible magnitude in comparison. The torque for the gravity gradient can be obtained by the use of Equation 50

$$\tau_g = \frac{3 \cdot \mu}{2 \cdot R_o^2} \cdot (\vec{r} \times \vec{I}\vec{r}) \tag{50}$$

The radius around the planets can be computed as $R_{o,E} = R_E + h_{o,E} = 8371$ km and $R_{o,M} = R_M + h_{o,M} = 3890$ km where h_o are the altitudes at which the orbits are in (2000 km and 500 km for Earth and Mars respectively). The vector $\vec{r}$ can be decomposed as in Equation 51.

$$\vec{r} = \begin{pmatrix} \cos(\phi) \cdot \cos(\theta) \\ \cos(\phi) \cdot \sin(\theta) \\ \sin(\phi) \end{pmatrix} \tag{51}$$

θ being the angle through the xy plane and ϕ being the present angle of inclination towards the z axis. This, of course, compared to MARCO's own inertial axis. Additionally, the moment of inertia matrix is assumed to only contain I_x, I_y and I_z, as shown in Equation 52.

$$\vec{I} = \begin{pmatrix} Ix & 0 & 0 \\ 0 & Iy & 0 \\ 0 & 0 & Iz \end{pmatrix} \tag{52}$$

The largest values for each axis are taken by varying θ and ϕ, which are treated as the disturbance torques to deal with. The values for these angles were taken for the worst case scenario on each angle each for redundancy. Table 63 shows these angles.

Table 63: Gravity gradient angles for worst case scenario.

Angle	x-Axis	y-Axis	z-Axis
$\theta[rad]$	$\frac{\pi}{2}$	0	$\frac{\pi}{4}$
$\phi[rad]$	$\frac{\pi}{4}$	$\frac{\pi}{4}$	0

Table 64 shows the torque generated by these angles.

Table 64: Disturbance torques caused by gravity gradient.

Disturbance	Earth orbit	Mars orbit
$\tau_{g_x}[Nm]$	$1.24 \cdot 10^{2}$	$3.04 \cdot 10^{-1}$
$\tau_{g_y}[Nm]$	$1.24 \cdot 10^{2}$	$3.05 \cdot 10^{-1}$
$\tau_{g_z}[Nm]$	$4.91 \cdot 10^{-2}$	$5.26 \cdot 10^{-2}$

Solar Pressure: Despite being substantially smaller for this spacecraft, solar pressure still causes attitude disturbances anyways. This means that they have to be taken into account, more so in the transfer orbits, where gravity gradient is not the main problem. To obtain the solar pressure caused by the Sun, Equation 53 must be used.

$$P_S = \frac{J_S}{c} \tag{53}$$

J_S = 1360 W m^{-2} on Earth orbit. Due to the relation $J_S \propto \frac{1}{d_S}$ where d_S is the distance from the Sun, J_S = 604.4 W m^{-2} in Mars orbit. The speed of light is taken as $c = 2.99 \times 10^8$ m s^{-1} With the solar pressure, the force exerted on MARCO can now be calculated. Due to the different shapes and materials of each component, each module/tank is calculated separately. Additionally, even though the spacecraft is supposed to face at most times towards the Sun, and thus only a force from the z axis affect it, fores from all axis of MARCO are taken too in the case of maneuvreing or unforeseen orientations. By using Equation 54, the magnitude of the force can be calculated.

$$F_S = (1 + \rho_r) \cdot S_r \cdot P_S \tag{54}$$

Reflectivity (ρ_r) has different values depending on the component. A reflectivity of 0.66 is taken for the tanks, and upper estimate of 0.6 is taken for the solar panels, and 0.5 for the rest of the modules. S_r is taken as the area which is hit by the solar radiation from the axis it comes from. For example, the fuel tanks from the x-axis would have an area of 117.7 m^2. On the other hand, from the z axis, they would only have an area of 50.3 m^2. This can calculate the forces exerted on the spacecraft, but not the torques as of now. To obtain the torques, the centre of solar pressure needs to be determined. For this, moments are taken based on the area centres of each components and the forces acting upon them. Once this is achieved, Equation 55 can be used to obtain the torque.

$$\tau_s = |C_m - C_{p,S}| \cdot F_{S_{tot}} \tag{55}$$

Of course, this changes for every phase of the trip, as the solar pressure changes and the centre of mass too. Table 65 shows the resultant torques.

Table 65: Disturbance torques caused by solar pressure.

Disturbance	Earth orbit	Transfer to Mars	Mars orbit	Transfer to Earth
$\tau_{s_x}[Nm]$	$1.46 \cdot 10^{-2}$	$2.77 \cdot 10^{-2}$	$4.03 \cdot 10^{-3}$	$8.67 \cdot 10^{-2}$
$\tau_{s_y}[Nm]$	$1.62 \cdot 10^{-2}$	$2.91 \cdot 10^{-2}$	$3.14 \cdot 10^{-3}$	$8.71 \cdot 10^{-2}$
$\tau_{s_z}[Nm]$	$8.86 \cdot 10^{-3}$	$8.86 \cdot 10^{-3}$	$3.94 \cdot 10^{-3}$	$8.86 \cdot 10^{-3}$

In addition to the torques, by creating a force on all components the spacecraft, the solar pressure also causes an overall disturbance force which creates an undesired acceleration. This must be also taken into account. Table 66 shows this.

Table 66: Disturbance forces caused by solar pressure.

Disturbance	Earth orbit	Transfer to Mars	Mars orbit	Transfer to Earth
$F_{s_x}[N]$	$6.81 \cdot 10^{-3}$	$6.81 \cdot 10^{-3}$	$3.03 \cdot 10^{-3}$	$6.81 \cdot 10^{-3}$
$F_{s_y}[N]$	$6.92 \cdot 10^{-3}$	$6.92 \cdot 10^{-3}$	$3.08 \cdot 10^{-3}$	$6.92 \cdot 10^{-3}$
$F_{s_z}[N]$	$2.15 \cdot 10^{-3}$	$2.15 \cdot 10^{-3}$	$9.57 \cdot 10^{-4}$	$2.15 \cdot 10^{-3}$

13.4.3 Maneuvres

Engine orientations: During every main engine burn to generate ΔV, MARCO must be oriented correctly. For departure burns, the spacecraft must be facing adjacent to its motion, and for arrival burns, the spacecraft must be facing opposite to its motion in order to retro-burn. Due to the variety in transfer orbits within the mission schedule, there is no specific angle for this maneuvre. Because of this, the wort case scenario has been chosen, which is a full π [rad] turn.

The time chosen to perform this maneuvre is $t_{man} = 2$ hours. This means that within those 2 hours, the thrusters must generate a steady angular acceleration towards a stable angular speed and then accelerate back to an angular speed of 0. This way, MARCO will be facing the correct orientation and not move while the burn happens. When looking at a graph of the angular speed during the maneuvres, it is composed of two straight increases and a flat line. When integrating this, the angle covered can be computed as shown in Equation 56. These maneuvres will all generate a spin around the x-axis, in order to let the solar arrays be able to rotate towards the Sun, as the actuators which spin the solar arrays act on this axis only.

$$\pi = \frac{\omega_{max} \cdot t_b}{2} + \omega_{max} \cdot (t_{man} - 2 \cdot t_b + \frac{\omega_{max} \cdot t_b}{2} \tag{56}$$

Knowing that $\omega_{max} = \alpha_{man} \cdot t_b$, the equation now can be rearranged into Equation 57.

$$(\alpha_{man}) \cdot t_b^2 - (\alpha_{man} \cdot t_{man}) \cdot t_b + (\pi) = 0 \tag{57}$$

This is a quadratic equation, and taking $A = \alpha_{man}$, $B = -\alpha_{man} \cdot t_{man}$ and $C = \pi$, it can be solved. In order to obtain α_{man}, Equation 58 is used.

$$\alpha_{man} = \frac{\tau_{man}}{I_x} = \frac{2 \cdot F_T \cdot L}{I_x} \tag{58}$$

Taking a moment arm of $L = 1.5$ m (approximate radius from first iteration of the control module) and a thrust of $F_T = 200$ N, the burn time t_b is obtained for each maneuvre. With the burn time, now the amount of propellant used can be obtained. The data provided by the HPGP manufacturers [43] gives an impulse in [Ns/kg] from which the amount of propellant mass is formulated by using Equation 59.

$$m_{prop} = \frac{2 \cdot F_T \cdot t_b}{Impulse} \tag{59}$$

This process is done for every burn. It is also important to do this after every burn too. This is because MARCO must face the sun during all orbits, and therefore will need to turn back to it after the oriented burn. Table 67 shows all the masses and burn times during these maneuvres.

Table 67: All the burn times and propellant used during the engine orientation maneuvres.

Burn	t_b [s]	m_{prop} [kg]
To Earth-Transfer burn	920.2	160.0
From Earth-Transfer burn	680.3	118.3
To Transfer-Mars burn	680.3	118.3
From Transfer-Mars burn	269.8	46.91
To Mars-Transfer burn	269.8	46.91
From Mars-Transfer burn	409.1	71.14
To Transfer-Earth burn	409.1	71.14
From Transfer-Earth burn	196.4	34.15
TOTAL	3835	666.9

As verification that these manoeuvres are done as calculated, a simulation was ran for an Earth-Transfer burn. Figure 30 shows this done; spinning πrad in two hours.

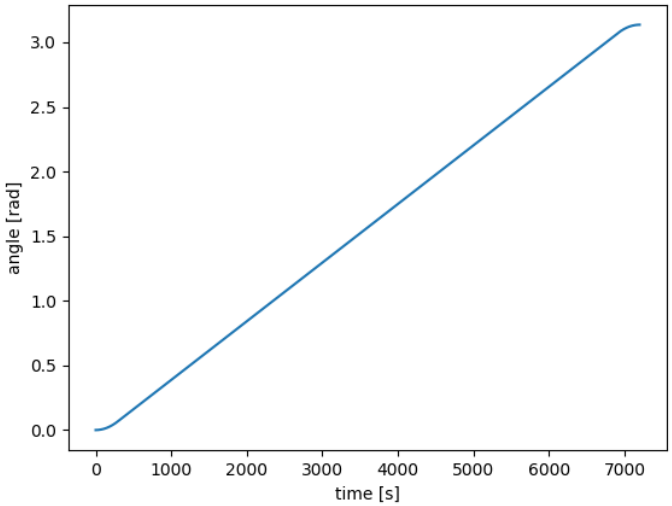

Figure 30: Engine orientation manoeuvre over 180°.

Accelerating to orbit orientation: As mentioned previously, MARCO must face the Sun at all times during every orbit. This means that its angular velocity must be Sun-synchronous. To know this, the rate of all Sun orbits must be known. When orbiting Earth and Mars, the velocity can be obtained with Equation 60.

$$\omega_{SS,E} = \frac{2 \cdot \pi}{T_{SS,E}} = 1.99 \cdot 10^{-7} \quad \omega_{SS,M} = \frac{2 \cdot \pi}{T_{SS,M}} = 1.06 \cdot 10^{-7} \tag{60}$$

Regarding transfer orbits, they vary in angle covered and time taken. Despite this, the time taken for the maneuvres does scale with the angle covered, and can be assumed that the angular speed is equal for every orbit. Similarly to Equation 60, Equation 61 obtains the sun-synchronous angular speed during transfer orbits.

$$\omega_{SS,T} = \frac{\theta_{trans}}{T_{transfer}} = \frac{3.666}{2.59 \cdot 10^{7}} = 1.41 \cdot 10^{-7} \tag{61}$$

It is assumed that after the engine orientation maneuvres, MARCO is not spinning on any axis. This means that it has to accelerate to this angular velocity from 0 rad s^{-1}. Using Equation 58, the acceleration is once more obtained. This time it is far easier to obtain the burn time with the use of Equation 62.

$$\alpha_{man} \cdot t_b = \omega_{SS} \quad t_b = \frac{\omega_{SS}}{\alpha_{man}} \tag{62}$$

To obtained the total burn time per orbit, the burn time obtained from this equation must be doubled. This is due to the fact that MARCO must decelerate to stop before the next engine orientation maneuvre.

Following the same approach as Equation 59, the amount of propellant mass can be once more obtained, and shown in Table 68

Table 68: All the burn times and propellant used during the sun-synchronous orbit orientation maneuvres.

Phase	t_b [s]	m_{prop} [kg]
Earth orbit	0.08838	0.007685
Transfer orbit to Mars	0.2100	0.01827
Mars orbit	0.06422	0.005584
Transfer orbit to Earth	0.1288	0.01120
Total	0.4914	0.04274

To verify these are the correct numbers, another simulation was done for this one too. Figure 31 shows the orbit orientation maneuvre for the transfer orbit to Mars. Unfortunately, the simulation couldn't be done of the whole orbit to show the entire angle covered, as the burn time requires very precise time intervals, and the entire orbit takes months, which proves to be a limiting factor on the device where the simulation runs. Nevertheless, when taking two points at any time after the acceleration time and formulating the gradient, an angular speed of $1.411\,45 \times 10^{-7}\,\mathrm{rad\,s^{-1}}$ is found, which is the desired one.

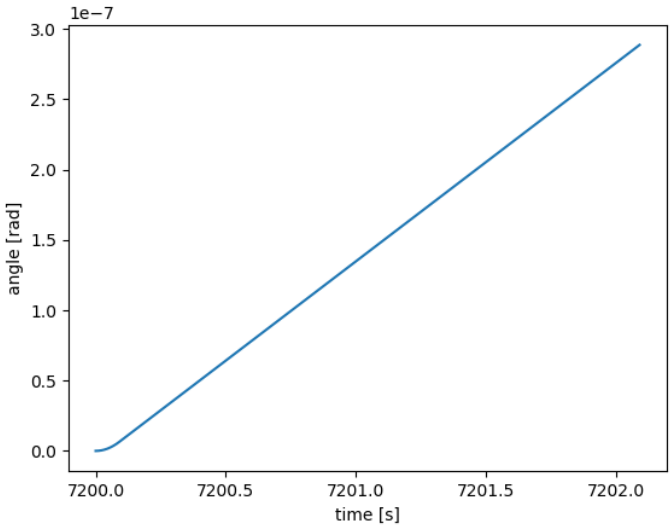

Figure 31: Beginning of transfer orbit after orientation maneuvre.

Refuelling: During refuelling, MARCO's mass, centre of mass and moment of inertia will change due to the increase in mass per tank for every refuelling phase. As there are 10 tanks, there will be similarly 10 refuelling phases during Earth orbit. It is assumed That during each phase, all tanks are equally and uniformly refuelled, therefore increasing their overall mass but not their individual and collective centre of mass. This makes calculations much easier to compute.

When the moment of inertia increases, due to the conservation of angular momentum, the angular velocity decreases. With Equation 63, the resulting angular speed can be obtained. ω_1 is treated as $\omega_{SS,E}$, previously found, as this would be the nominal speed during Earth orbit.

$$\omega_1 \cdot I_1 = \omega_2 \cdot I_2 \quad \omega_2 = \frac{\omega_1 \cdot I_1}{I_2} \tag{63}$$

Burn time to accelerate back to $\omega_{SS,E} = \omega_1$ is provided by Equation 64.

$$t_b = \frac{\omega_1 - \omega_2}{\alpha_{man}} \tag{64}$$

Of course, this maneuvre, similarly to the previous one, does not consume much propellant. Table 69 shows the total

after the 10 refuelling phases.

Table 69: Total burn time and propellant used during the refuelling maneuvres.

	t_b [s]	m_{prop} [kg]
Total	0.2635	0.04583

Orbit Maintenance: The disturbance torques seen before have to be countered and therefore the amount of burn time ad propellant used for this has to be determined. Firstly, to get the values of the counter-torques, a margin factor is set. For this mission, a margin factor of 2 is taken. With this and Equation 65, the counter-torques are calculated by using the largest torques in each phase.

$$\tau_c = (1 + MF) \cdot \tau_{max} \tag{65}$$

The values these torques have are, understandably not as high as the values needed to be generated for maneuvres. Furthermore, having to use thrusters all at all times, even if its a very low thrust, will wear out the thrusters and deplete their lifetime, or even lead to failures. For this reason, the way the thrusters act is by generating a counter torque once the disturbance torques have displaced the orientation of the spacecraft by a certain degree. The angle taken for this is the required angle mentioned in **MARCO-ADCS-01**.

First, the time taken to arrive at this angle because of disturbance torques is calculated. This can be easily found by the use of Equation 66.

$$t_w = \sqrt{\frac{2 \cdot \theta_d \cdot \tau_c}{I}} \tag{66}$$

After this, knowing that $\theta_d = 8.73 \times 10^{-3}$ rad, the maneuvre to restore MARCO to its original orientation occurs. The same method as Equation 56 and Equation 57 is used, only this time the angle which has to be covered is θ_d. Once the burn time for each of the orientation recovery burns (t_d) is known and the time for the whole maneuvre too (t_m), the number of times this has to be repeated is calculated by Equation 67.

$$N_{burns} = \frac{t_{phase}}{t_w + t_m} \tag{67}$$

At last, the total burn time can be calculated with Equation 68.

$$t_{b_{tot}} = N_{burns} \cdot t_b \tag{68}$$

With this, and the use of Equation 59 the mass of the propellant used here can also be determined. Due to the slower and less urgent nature of these maneuvres, only one thruster needs to be used at a time in this case. Because of this, these tables use half of the propellant for the same amount of burn time during the maneuvres as seen in Table 70. More fuel is used during Earth orbit, due to the fact that this is when the disturbance torques are the largest, and the MOI of MARCO is the largest too.

Table 70: Total burn time and propellant used during the orbital maintenance.

Phase	$t_{b_{tot}}$ [s]	m_{prop} [kg]
Earth orbit	2220	193.0
Transfer to Mars	301.8	26.24
Mars orbit	221.1	19.22
Transfer to Earth	185.7	16.14
Total	2928	254.6

A very similar approach was taken with regards to counteracting the solar forces acting on MARCO. This time, all the equations revolve around $F = m \cdot a$ instead of $\tau = I \cdot \alpha$. This means that force is generated instead of torque, mass is used as the spacecraft's characteristic, and acceleration instead of angular acceleration is taken. To generate a force without a torque, two thrusters of the same axis are activated, cancelling each other's torque. The displacement allowed until the maintenance maneuvre starts is assumed to be 5 m. With all this data, Table 71 shows the burn time annd propellant used for displacement maintenance.

Table 71: Total burn time and propellant used during the displacement orbital maintenance.

Phase	$t_{b_{tot}}$ [s]	m_{prop} [kg]
Earth orbit	1187	103.2
Transfer to Mars	657.7	57.19
Mars orbit	322.2	28.02
Transfer to Earth	547.7	47.63
Total	2715	236.0

Total propellant: With all of the possible usage of the thrusters covered, now a total mass for the propellant is calculated.

Table 72: Total propellant mass to be used in every trip.

Manoeuvre	m_{prop} [kg]
Engine orientation	0.6669
Orbit orientation	0.00004274
Refuelling	0.00004586
Orbit Maintenance 1	0.2546
Orbit Maintenance 2	0.2360
Total	1.158

By applying the density of the propellant being used (LMP-103s), 1.24 t m^{-3}, the volume comes down to 0.9339 m^3. The cost for synthesising the fuel is 1200 \$$kg^{-1}$, resulting in a cost of 11206800 €. Each refuel is estimated to cost 480000 \$ and therefore a total cost of 3936000 € is needed for this. Additionally, the cost for the waste disposal while synthesising is 65 \$$kg^{-1}$, making it for the whole mission 752700 €. Table 73 shows this data more clearly.

Table 73: Technical data for the LMP-103s propellant.

	Mass [t]	**Volume [m^3]**	**Cost [€]**
LMP-103s propellant	1.158	0.9339	15595500

One last piece of information to consider is the technical aspects of the HPGP thrusters too and how they are sized. The price per thruster was estimate by using the price trend on the lower thrust thrusters and scaling it up [43]. Their lifetime is not large and therefore, they need to be replaced on every trip.

Table 74: Technical data from the HPGP 200 N thrusters.

	Amount	**Amount Mission**	**Mass [t]**	**Volume [m^3]**	**Power [kW]**	**Peak Power [kW]**	**Cost [€]**
HPGP thrusters	12	120	0.0684	0.01293	1.8	3	3936000

13.4.4 Control Moment Gyroscopes

When having to size control moment gyroscopes, this had to be done by taking literature values from the ISS. The ISS operates in LEO, which coincidentally is also the phase which requires the most attitude control in this mission. This means that by designing with the ISS in mind, the CMGs are being designed for the worst case scenario. Taken from sources [54], the ISS uses 4 control moment gyros which generate a torque of 259 N m each. By taking the

largest moment of inertia of the ISS from sources [59] (when in step 108, 3R - after rendezvous) and making a ratio with a fully fuelled MARCO, MARCO possesses a maximum moment of inertia 1.62 times larger than the ISS. It is assumed therefore that the control moment gyroscopes needed for MARCO must generate torque 1.62 times larger than the ISS, leaving it at 412 N m each.

The largest CMGs commercially available found are the CMG 75-75 S [60], which generate a torque of 75 N m. The amount of torque required is 5.56 times higher. Knowing that $\tau \propto I \cdot \alpha$, and assuming that α is unchanged, the moment of inertia of the newly sized CMG must be 5.56 times higher. When taking the dimensions of these CMGs, it is apparent their radius is 0.5 m and their mass is 69 kg. Knowing that $I \propto m \cdot r^2$, the radius of the CMGs was changed a factor of 1.536 to reach a moment of inertia 5.56 times higher. The average and peak powers are assumed to increase linearly by 5.56. In the end, 4 of these need to be included within MARCO. The results of this is shown in Table 75. The cost shown is taken from a literature estimate [75], as both the costs for CMG 75-75 S and the ISS CMGs could not be found.

Table 75: Technical data from the control moment gyroscopes.

	Mass [t]	**Volume [m^3]**	**Average power [kW]**	**Maximum power [kW]**	**Cost [€]**
CMG	0.6512	1.179	0.8132	2.857	1100000

The control moment gyroscopes are arranged in a similar pattern to that of the ISS, simulating a pyramid configuration [75], and therefore creating redundancy in the case of a failed or drifting gyroscope.

13.5 System Architecture and Interfaces

Before presenting the system architecture, a layout of the thruster system is shown in Figure 32. This is a simple diagram of how it works. The pressurised LMP-103s propellant tank feeds directly into the thrusters through a valve system. These valves are latch valves. Latch valves open and close upon an electrical signal. They will remain open or closed until the next signal is sent. This allows the system to not only control which thruster is fed with fuel, but also the amount of time fed. Additionally, by including two latching valves for every individual thruster, reliability is increased, as, in the case one of these valves breaks while shut, another one can close the propellant feed. The pressure transducer is in charge of monitoring the pressure of the system and the tank.

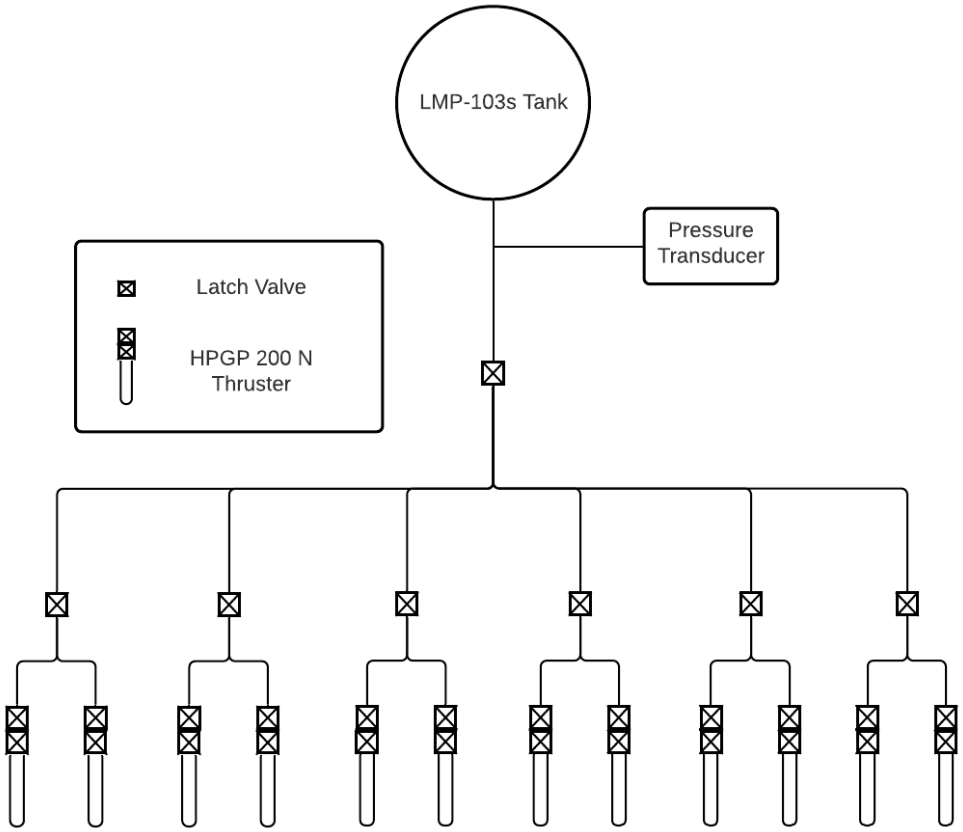

Figure 32: Architecture of the RCS thruster system.

The system architecture for ADCS shown in Figure 33 shows the interaction the control system and determination system have with each other.The control and data handling device receives signals from all determination devices. Some like the star tracker already posses a processing unit which converts all the signals it receives into data. Others like the sun sensor just output signals, which will have to be processed by the C&DH system. Regardless, the C&DH system, once it has processed the attitude status of the spacecraft, it will both send it to the telecommunications system to send the status of MARCO's attitude and then send signals to power management. Power management will then activate or de-activate the control system actuators. When there is a malfunction or a change int he mission's orbit from the ground station, the C&DH systems informs each of the detectors which depend on it in order to change configuration.

The final parameters for the entire system can be observed in Table 76. They were summed up from both the control and determinations sections.

Table 76: Final parameters of the ADCS.

	Mass [t]	**Volume [m^3]**	**Average power [kW]**	**Maximum power [kW]**	**Cost [M€]**
Grand total	1.885	2.132	2.64	5.88	22.81

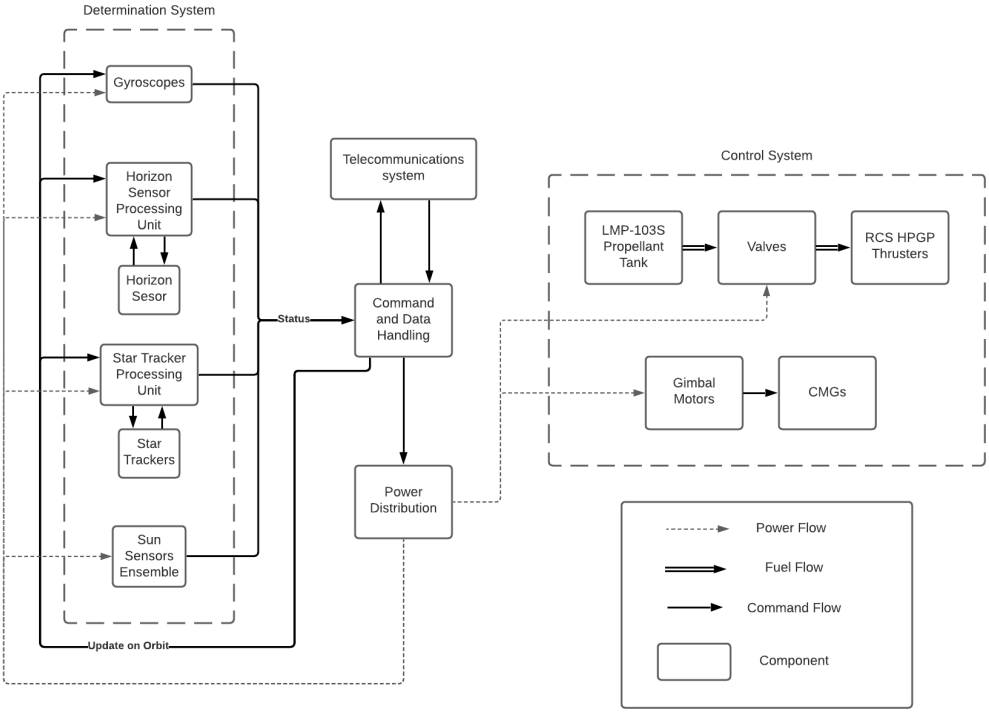

Figure 33: Architecture of the ADCS system.

13.6 Risk Assessment

This section covers the major risks which are expected to occur to the ADCS system during the duration of the mission. Table 77 covers the risks, their likelihood and impact (RBM) , and the mitigation strategy with the updated RAM.

Table 77: Risk table including the most critical risks for each subsystem. RBM is defined as "likelihood, impact" before mitigation, RAM is "likelihood, impact" after mitigation.

ID	Risk	RBM	Mitigation	RAM
ADCS01	Thruster does not turn on	2, 5	**Reduce** by using extra thrusters	2, 2
ADCS02	Thruster does not turn off	3, 5	**Avoid** by designing with additional valves	1, 5
ADCS03	Thrusters do not provide sufficient pointing accuracy	2, 4	**Reduce** by designing for required accuracy	1, 4
ADCS04	Sensors malfunction	3, 4	**Reduce** with extra sensors	3, 1
ADCS05	The chosen components will drift and cause accuracy errors	4, 3	**Reduce** by adding redundancy	4, 1

Figures 34 and 35, map the impact and likelihood of the ADCS risks before and after mitigation, respectively. These figures help communicate the impact of the risk mitigation strategy and the overall improvement of the subsystem's reliability.

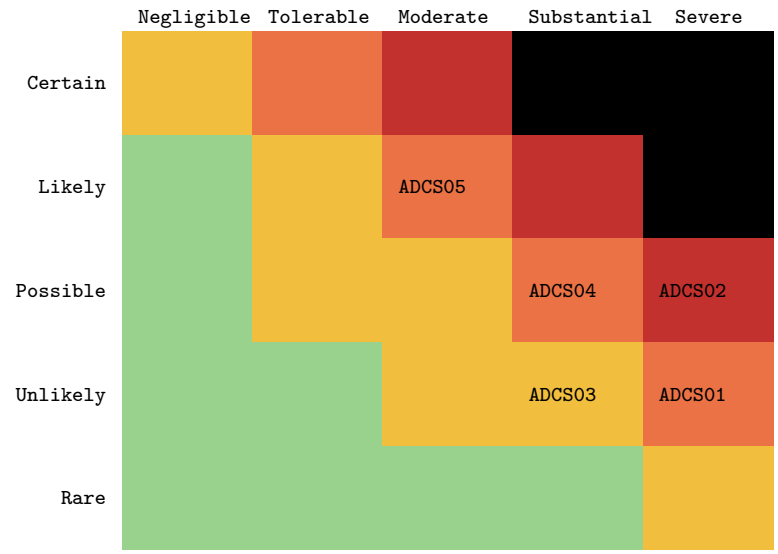

Figure 34: Risk matrix of identified ADCS risks. Likelihood is listed vertically and impact is listed horizontally.

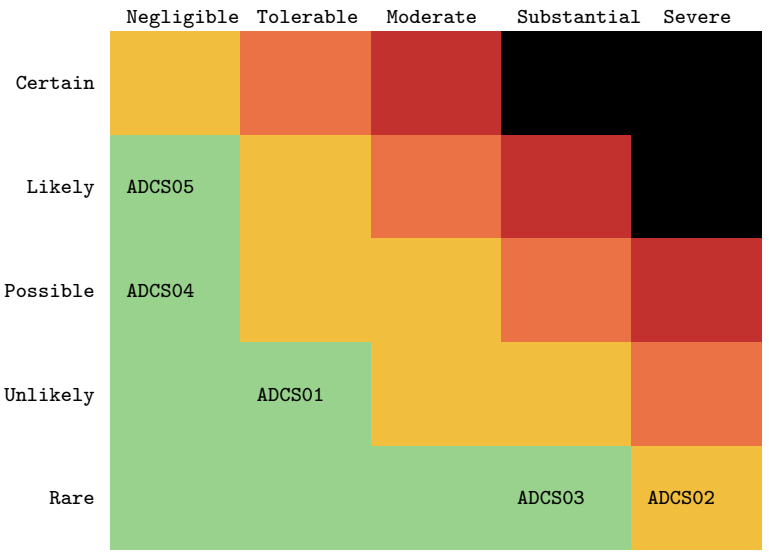

Figure 35: Risk matrix of mitigated risks. Likelihood is listed vertically and impact is listed horizontally.

13.7 Sustainability

Forming part of the control module, the sustainability in terms of disposal of this subsystem depends mostly on the disposal of the system. Despite this, there is a very notable point to bring up. The fuel used for the RCS thrusters is LMP-103s mono-propellant.

As an alternative to hydrazine, which is close to being banned, LMP-103s is a non-toxic mono-propellant developed for space missions. Taken from the source [43], this propellant lacks all the dangers which hydrazine has, such as toxicity, being a cancer hazard, corrosiveness, having flammable vapours and being an environmental hazard. Its exhaust gases are far less dangerous, as well as being more tolerant to radiation and more stable. Adding on to this, LMP-103s performs better in many areas too. Its temperature range is wider, it is more dense, and therefore requires less volume for storage, as well as providing more impulse.

At the moment, LMP-103s is more expensive than hydrazine, as it is harder to develop, but the more it is tested and the more it is synthesised, the cheaper it will get to manufacture. When making LMP-103s, there is almost no waste, which is all non-toxic and hazardous, unlike hydrazine's large amounts of toxic waste. On top of this, it can be transported by conventional means, greatly reducing the costs of it. Greatly reducing the costs too, is the fact that the refuelling procedure is far cheaper than that of hydrazine. Lastly, LMP-103s is able to use much of the hydrazine equipment, greatly reducing the development costs.

This choice of propellant is very important for sustainability. It reduces all hazards, both environmental and to the crew and everyone involved, as well as not having as many complications or costs for future missions due to the versatility and easy usage. As a last point, the more the HPGP thrusters for this propellant are tested, the more they can be easily manufactured in bulk, therefore reducing further costs for future missions.

13.8 Requirement Compliance and Sensitivity Analysis

Table 78: Requirement compliance table for ADCS.

ID	Compliance	Rationale
MARCO-ADCS-01	✓	As shown in subsubsection 13.4.3, this was what was designed for.
MARCO-ADCS-03	✓	As shown in subsubsection 13.4.2 and subsubsection 13.4.3, this was what was designed for.
MARCO-ADCS-04	✓	As shown in subsection 13.5, the total mass ended up being far smaller, as no fast maneuvres were needed.
MARCO-ADCS-05	✓	As shown in subsection 13.5, the total volume ended up begin far smaller for the same reason as **MARCO-ADCS-04**, even if the CMGs were bigger than expected.
MARCO-ADCS-06	✓	As seen in subsection 13.3, the angle to be maintained for orbit maintenance was 0.5°.
MARCO-ADCS-07	✓	The thrusters will provide a larger acceleration than this.

As a sensitivity analysis, it is safe to say that a change in parameters while scarcely change the requirement compliance. The mass and volume of the subsystem is far bellow the required values, and even a complete change of configuration to the tank arrangement (and therefor moment of inertia) does not make it surpass it. As an example, the system was designed for 12 tank configuration with significantly higher moment of inertia, which only increased its mass by 1 t. As for **MARCO-ADCS-07**, using a similar approach as shown above Figure 31, the acceleration obtained was found to be $1.5625 \times 10^{-6}\,\mathrm{rad\,s^{-2}}$, a value far exceeding those needs.

13.9 Recommendations

As a recommendation for future development, it is important to look more in depth into control moment gyroscopes and how they work. When arranged in pattern, each CMG has a gimbal angle in which it functions to store angular momentum. In order to generate a torque, the gimbal angle must be changed. When arranged, there are several gimbal angle combinations in which no angular momentum will be stored anymore, and therefore no torque can be generated. Because of this, using CMGs to generate torque will lead to this, which is called a singularity vector. To be able to get the CMGs out of this singularity, the RCS thrusters would need to generate a counter-toque that acts as a disturbance torque. Despite the fact that the system was designed to have redundancy to CMGs, redundancy could still be implemented by simply applying a safety margin to the amount of propellant needed to take the CMGs out of the singularity points.

14 Telecommunications

In this chapter, the design of the telecommunication subsystem will be outlined. First, a summary of the trade-offs for this subsystem will be presented. This is followed by the list of requirements. Then, the actual design of the subsystem will be discussed. Afterwards, the system architecture and interfaces with the other subsystems will be discussed, after which a section on the risk analysis follows. Then, sustainability will be briefly discussed, followed by the requirement compliance matrix and a small sensitivity analysis. The chapter is then concluded with some recommendations.

14.1 Trade-off Summary

In the midterm phase of the project, four trade-offs were made for the telecommunications subsystem. Firstly, it was decided that radio frequency technology was going to be used instead of optical communications. The main reasons are the low TRL for optical, and the fact that almost no infrastructure is available for optical communications. Secondly, the types of antennas for MARCO were decided upon. MARCO will have four antennas in total; two high-gain and two low-gain antennas. The high-gain antennas will be the main means of communication, and the low-gain antennas will be used as back-up. Having 2 antennas of each type enables MARCO to receive and send signals at the same time. The third trade-off was made to decide how many ground stations on Earth and how many relay satellites in LEO will be used. It was decided that 3 ground stations will be used, each at longitudes of 120° apart from each other. No relay satellites in LEO are then needed because the three ground stations already provide

full coverage. Finally, a trade-off was needed to determine if relay satellites outside of LEO were needed. It was decided that 2 Gangale relays are needed to eliminate the loss of communication with spacecraft around Mars during solar conjunction. Additionally, some type of relay satellite(s) around Mars are needed, since having only MARCO act as a relay for POLO when it is landed on Mars will not be enough to meet **MARCO-TLC-02**.

14.2 Requirements

The following list of requirements was generated during the first phase of the project, with their rationale being discussed in the midterm report [8].

MARCO-TLC-02 The communication between the ITS and a ground-station on Earth shall be interrupted no more than 45 minutes at a time.

MARCO-TLC-03 The telecommunication system shall have a signal to noise ratio of at least 15 dB when communicating between Mars orbit and Earth.

MARCO-TLC-04 The telecommunication system shall have a bandwidth of at most 200 MHz.

MARCO-TLC-05 The telecommunication system mass shall not exceed 300 kg.

MARCO-TLC-06 The telecommunication system volume shall not exceed 30 m^3.

MARCO-TLC-07 The telecommunication system shall have a payload data rate of 5 Mbps.

MARCO-TLC-08 The telecommunication system shall have a command data rate of 100 kbps.

MARCO-TLC-09 The telecommunication system shall remain between the temperatures of 75 K to 350 K during operations.

MARCO-TLC-11 The telecommunication system shall consume no more than 1 kW of power.

14.3 Telecommunications Design and Sizing

In this section, the design methodology of the telecommunications subsystem is discussed in detail. Firstly, the configuration of the relay satellites will be discussed. This is followed by the analysis of the link budgets, and finally, the outcome of the design is presented.

14.3.1 Configuration of Relay Satellites

In Section 14.1, it is mentioned that relay satellites around Mars are needed to provide a low enough down time of the communication between the lander and the ground operations on Earth. Since sending humans to Mars is such an important mission and such a huge undertaking, we can assume that a small constellation of relay satellites around Mars will be available. The most conventional way to set up this constellation would be to have 3 relay satellites in Mars-stationary orbits, also called Areostationary orbit, at longitudes of 120° apart. This way, almost every part of Mars can be covered, except for locations near the poles, and therefore, future crewed Mars mission that will visit different locations on Mars, can also make use of this constellation. However, if one of these three satellites fails, there would be no way to retain full coverage of the surface of Mars. In addition, since the habitat will be located at 42.1° north of the equator, having 3 relay satellites in Areostationary orbit results worst case in an elevation of about 11°. This elevation was obtained by calculating the distances between the lander, the centre of Mars, and the relay satellite, and then using the cosine rule to calculate the elevation angle. The relay satellite was assumed to be located over a point on the surface of Mars 60° east from the longitude of the landing site, which is the worst case scenario when considering 3 relay satellites. The obtained 11° can be sufficient, but is rather low. Therefore, it was decided to have a constellation of 4 relay satellites in Areostationary orbit, each 90° longitudinally apart. This greatly increases the redundancy of the system, since if one of these satellites fails, the other 3 could reposition themselves slightly to retain full coverage of the martian surface. Additionally, the worst case elevation angle for the lander is significantly increased to about 21°.

Now that it is clear what relay satellites will be used, it is possible to determine all the different communication links between the different spacecraft and ground stations. These communication links can be found in Table 79. For each communication link, there must be communication possible in both directions. Communication with POLO is only needed when it is performing its landing on or take-off from Mars, or when it is landed on Mars. In all other

scenarios, POLO is docked with MARCO, so then all (if any) communications with POLO are performed through MARCO.

The frequencies used for these links can also be found in the table below. As can be seen, frequencies of up to 32 GHz (i.e. Ka band) are used. Although this frequency range is not yet commonly used at the moment, multiple sources, including NASA, state that this frequency will become very common in the near future [31][50]. In addition, the Kepler spacecraft, which is currently operational, already uses a parabolic antenna that operates at frequencies in the Ka band as its primary means of sending its gathered scientific data [30]. Therefore, we can safely conclude that MARCO can use its two parabolic high-gain antennas to send signals in the K- or Ka band.

POLO will have two low-gain antennas that will operate in the X band. This is also already proven to work, since Perseverance also uses a low-gain antenna to send signals in the X band[51]. In addition, MARCO has 2 back-up low-gain antennas in case both of the high-gain antennas fail. These will also operate at frequencies in the X band. These antennas are also not meant to be able to meet the same requirements as the high-gain antennas, especially when considering bit rates, since these are just meant as a last resort when no other means of communication is available anymore.

Table 79: All possible communication links between the different spacecraft and ground stations.

Transmitter/ Receiver	**Receiver/ Transmitter**	**Frequency Range**	**Used Frequency [GHz]**
Earth ground stations	MARCO	Ka band	32
Earth ground stations	Mars relay satellites	Ka band	32
Earth ground stations	Gangale relay satellites	Ka band	32
Mars relay satellites	MARCO	K band	25
Mars relay satellites	POLO	X band	7
Mars relay satellites	Gangale relay satellites	K band	25
MARCO	POLO	X band	7
MARCO	Gangale relay satellites	K band	25

14.3.2 Link Budget

The most important part of the sizing of the telecommunications subsystem was setting up all the different link budgets, since this determines if an adequate signal to noise ratio (SNR) can be achieved, so that the signal is intelligible. This had to be done for each communication link presented in Table 79. In order to calculate the SNR, we first need to calculate the power received by the receiving antenna, and the noise power of the signal.

The power received can be obtained by taking into account each loss and gain of the power of the signal. Gains can be obtained by increasing the transmitter power or by shaping the antenna such that the signal is sent in a specific direction, rather than in all directions. In the case of a parabolic antenna, the gain can be calculated using Equation 69 [40].

$$G = \frac{\pi^2 \cdot D^2 \cdot \eta}{\lambda^2} \tag{69}$$

In this equation, G is the obtained gain, D is the diameter of the antenna, λ is the wavelength, and η is the efficiency of the antenna, which will be taken equal to 0.8, as this is the efficiency that can be achieved nowadays [39]. The gain of both the transmitting and receiving antenna needs to be taken into account when calculating the link budget. The wavelength is determined by the selected frequency of the signal, since they are related to each other by Equation 70.

$$\lambda = \frac{c}{f} \tag{70}$$

Here, c is the speed of light, and f is the frequency of the signal. The frequency used for a certain communication link can be found in Table 79.

[50] https://mars.nasa.gov/mro/mission/communications/commkaband/ *[cited 26 June 2021]*
[51] https://mars.nasa.gov/mars2020/spacecraft/rover/communications/ *[cited 28 June 2021]*

The main loss is caused by the signal spreading out when travelling through free space, which is referred to as the free space path loss, or shortly, the space loss. Equation 71 describes how to calculate the space loss [40].

$$L_S = \left(\frac{\lambda}{4\pi r}\right)^2 \tag{71}$$

Here, λ is the wavelength of the transmitted signal, and r is the distance between the transmitting and receiving antenna. Other losses include atmospheric losses, and losses due to the imperfect efficiencies of the cabling or other devices in the telecommunication subsystem [40].

Each of the above mentioned variables where converted to decibels by using Equation 72.

$$X_{dB} = 10 \cdot \log(X) \tag{72}$$

After converting each variable to decibels, the total power received can be calculated by adding up the transmitted power with each gain and loss, as can be seen in Equation 73.

$$P_R = P_T + L_T + G_T + L_S + L_A + G_R + L_R \tag{73}$$

In this equation, each variable is in decibels. Furthermore, the subscript R is used for the receiving antenna, and subscript T for the transmitting antenna. P stands for power, G for gain, L_S stands for the space loss, and otherwise, L stands for the losses in the telecommunication subsystems due to the imperfect efficiencies.

The noise power mainly depends on the thermal environment of the antennas, and on the selected bandwidth. The values of the antenna temperatures are taken from literature [41]. After obtaining the noise temperatures, the noise power can be easily calculated using Equation 74.

$$P_N = kTB \tag{74}$$

Here, k is the Boltzmann's constant, which is equal to $1.380 \times 10^{-23}\,\mathrm{J\,K^{-1}}$, T is the noise temperature, and B is the bandwidth. The noise power was then also converted to decibels. Finally, the SNR can be straightforwardly calculated by taking the sum of the received power and the noise power. To comply with the requirements, an SNR of at least 15 dB has to be attained. On top of this, a design margin of 3 dB was applied.

The bit rate that the communication link can achieve is also an important parameter. It can be calculated using the Shannon–Hartley theorem, which can be found in Equation 75.

$$C = B \log_2(1 + SNR) \tag{75}$$

In this equation, C is the data rate in bit/s, B is the bandwidth, and the SNR is unit-less, and not in decibels. The Shannon–Hartley theorem only gives the upper theoretical limit of the bit rate that can be achieved. However, with current coding technologies such as turbo-codes, bit rates that are close to this limit can be achieved [32]. Therefore, an efficiency of 90% was assumed when calculating the bit rate.

The parameters that can be changed, and therefore control the design, are the transmitter power, the bandwidth, and the size (and thus the gain) of the antennas. However, these parameters are of course limited by the requirements. For MARCO, **MARCO-TLC-06** limits the diameter of its two antennas to 4.5 m. This meant that a transmitter power of 330 W and a bandwidth of 1.1 MHz were needed to achieve the required SNR and bit rate.

All the above equations were put in a spreadsheet and were manually verified. Afterwards, they were copied to set up each individual link budget. Some link budgets were also completely calculated by hand, to check if nothing went wrong when copying the equations. These two checks were deemed sufficient for verifying the design process of the telecommunications subsystem.

14.3.3 Design Outcome

Setting up all the different link budgets mentioned in Table 79 resulted in obtaining the diameter and transmitter power of the antennas on each spacecraft. An overview of this can be found in Table 80, and the complete link budget tables are displayed in Appendix B. The values for the ground stations on Earth were taken from literature [42], as well as the diameter of the antennas of the relay satellites [29], since they will not be designed by us. This resulted in the relay satellites being over-designed for this mission. However, this can still be beneficial, because when the habitat will be permanently crewed, higher data rates will likely be required by the habitat.

In Appendix B, two link budgets are not included, namely the one between the Mars stationary satellites and MARCO, and the one between MARCO and POLO. The first of these was not considered, since the distance between them when communication might be established (i.e. when MARCO is in LMO) will be not more than 20 000 km. And since they both have high-gain antennas to communicate with each other and can achieve a high output power, this link will be easily established when needed. The link budget between MARCO and POLO is not considered, because MARCO has the same size of antennas as the Mars stationary relay satellites, it has a lower orbit altitude, and it can achieve the same output power as when the Mars relays are communicating with POLO. Therefore, it can be concluded that this link will also be adequate.

Table 80: Overview of the antennas used on each spacecraft and their size and transmitter power.

Spacecraft/ Ground station	**Number and Type of Antennas**	**Diameter of Antenna (if applicable) [m]**	**Transmitter Power [W]**
MARCO	2 High-gain 2 Low-gain	4.5 -	330
POLO	2 Low-gain	-	60
Earth ground stations (3)	1 High-gain	34	20000
Mars relay satellites (4)	2 High-gain	4.5	1000
Gangale relay satellites (2)	2 High-gain	7.0	750

Having obtained the transmitter power and the diameter of the antennas, a detailed calculation of the mass-, power-, volume- and cost budget for MARCO and POLO can be performed. First of all, the mass budget is calculated. This was done by comparing MARCO and POLO to the Mars Reconnaissance Orbiter (MRO) [38], as can be seen in Table 81. Some of the parts used on MRO were scaled up relative to the power increase between MRO and MARCO. For example, the transmitter power of MARCO is three times as high as for MRO, so the amplifier of MARCO that has to provide this power, is also three times as heavy as the amplifier for MRO. The same holds for POLO, but here, the amplifier has a lower mass since the transmitter power of POLO is smaller compared to MRO. The mass of the high-gain antennas of MARCO were also scaled, but this time relative to the reflective area of the antenna. The mass of the gimbals for MARCO is also double the mass for MRO, since MARCO has two high-gain antennas, each with their own gimbal system, whereas MRO only has one high-gain antenna. Other parts have the same mass for both MRO and MARCO. For example, the transponder has the same mass for MRO and MARCO, since both transponders have to handle a similar data rate [38].

Table 81: Breakdown of the mass budget of MARCO and POLO in comparison with the Mars Reconnaissance Orbiter [38].

Component	**MRO [kg]**	**MARCO [kg]**	**POLO [kg]**
Transponder	6.4	6.4	6.4
Travelling-wave tube amplifiers	12.1	39.9	7.26
Total assembly of all antennas	22.6	91.3	3.30
High-gain antenna	*19.1*	*43.0 (2x)*	*0*
2 Low-gain antennas	*0.8*	*2.6*	*0.60*
Miscellaneous hardware	*2.7*	*2.7*	*2.7*
HGA gimbals and drive motors	45	90	9
Waveguides and coax	8.3	8.3	8.3
USOs (2)	1.7	1.7	1.7
UHF subsystem	11.5	11.5	11.5
Total	**107.6**	**261.6**	**49.8**

To calculate the total power needed for the complete telecommunication subsystem, a similar method as for the mass budget was applied. This lead to a total power consumption of 998 W for MARCO and 109 W for POLO.

The volume budget consists out of two parts: The high-gain antennas, and every other component of the telecommunications subsystem. The volume of the antennas was calculated with the assumption that the antennas have the shape of a cylinder, with the height being a fifth of the diameter. For the other components, a density of 0.5 $kg\,m^{-3}$ was assumed [5], and the volume was then calculated based on this density and the mass of the components. This resulted in a total volume for the telecommunications subsystem for MARCO of 29.06 m^3, of which 28.63 m^3 is used by the two high-gain antennas. For POLO, the total volume came out to be 0.125 m^3.

To calculate the cost, it was necessary to know for how long the relay satellites and ground stations are going to be used, since they are very expensive to use. **MARCO-TLC-02** limits the down-time of communication with the spacecraft to 45 minutes at a time. However, a very short status update each 45 minutes would already suffice. Therefore, it was assumed that each day, on average 1 hour of communication with MARCO is established. For POLO, this will be 1.5 hours, since landing on/taking off from Mars and performing operations on the Martian surface is considered more critical. For MARCO, mainly the ground stations on Earth will be used to establish communication, whereas for POLO, the Mars relay satellites are the primary means of communicating with MARCO or with ground operations on Earth. In addition, approximately 5.5% of the time, no direct communication between Earth and Mars is possible due to Solar conjunction, and therefore the Gangale relay satellites have to be used as well [29].

To then calculate the total cost, the price per hour of using the relay satellites or ground station was multiplied by the amount of hours that they will be used. The total mission time will be around 42 years, and POLO will be approximately 4341 days on Mars. The price per hour was obtained through communication with an external expert on the topic[52]. On top of that, the cost of the antennas itself was also added, to get the complete cost of the telecommunication subsystem over its life span. The overview of the different costs can be found in Table 82.

Table 82: Breakdown of the cost budget of MARCO and POLO. Prices are in M €.

		Unit cost	**Amount**	**Price per hour**	**Amount of hours**	**Subtotal**
MARCO	High-gain antennas	4	2	0	0	8
	Low-gain antennas	0.5	2	0	0	1
	Deep Space Network link	1	1	0.002	15330	31.66
	Gangale relays	0	0	0.005	882	4.41
POLO	Low-gain antennas	0.5	2	0	0	1
	Mars relays	0	0	0.005	6511.5	32.5575
					Total (+5% margin)	**82.6**

This cost might seem high for just the telecommunication subsystem. However, since sending humans to Mars is such a huge undertaking, other agencies that might operate the relay satellites will probably be involved in this mission as well. Therefore, the cost of using these relay satellites will likely reduce significantly.

To summarise, Table 83 displays all the budgets for MARCO and POLO separately. All the values presented in this table have a 5% design margin included.

Table 83: Summary of the mass-, power-, volume- and cost budget of MARCO and POLO.

Spacecraft	**Mass** [kg]	**Power** [W]	**Volume** [m^3]	**Cost** [M €]
MARCO	261.6	998	29.06	47.3
POLO	49.8	109	0.125	35.3

14.4 System Architecture and Interfaces

The system architecture of the telecommunications subsystem is fairly straightforward. If a message has to be sent from MARCO, C&DH will first send this data to the transponder. The transponder then encodes this digital data

[52] From a conversation with Stefano Speretta [07/06/2021]

into a radio frequency signal. Afterwards, this signal will go through the amplifier, which significantly increases the power of the signal. Finally, the signal is sent by the one of the antennas. The gimbal of the antenna ensures the signal is sent in the correct direction.
When receiving data, everything happens in reverse order. The radio signal is firstly received by an antenna, after which it is amplified so it can be understood more easily. Then, the transponder decodes the signal into a digital signal, and this data is finally sent to C&DH.
To further clarify the architecture, a schematic drawing of it was made, which can be found in Figure 36.

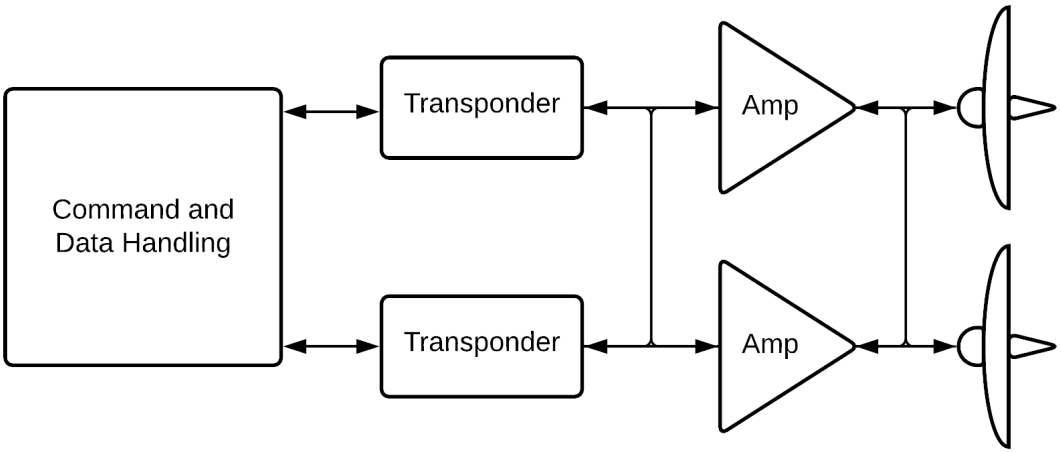

Figure 36: Simple drawing of the architecture of the telecommunication subsystem.

The transponders and amplifiers are components that have a relatively high failure rate. Therefore, there will be numerous redundant components. However, only one of the redundant components will work at a time when sending/receiving a signal. The others will only be used when the first component fails.
The above displayed architecture is only for the two high-gain antennas of MARCO. However, the architecture for the low-gain antennas is exactly the same, apart from the antennas themselves of course.

Both high-gain antennas will be mounted on one gimbal each, such that they can point in the correct direction when sending or receiving a signal. Both these antenna-gimbal set-ups are then mounted on the outside of the control module. A schematic drawing of this can be found in Figure 40.

The interfaces with the other subsystems of MARCO are not very complicated either. First of all, electrical power from EPS is needed in order to power all the components of this subsystem. Secondly, C&DH must provide all the messages that need to be sent to the transponder of the telecommunication subsystem, so that it can translate these digital messages into signals that can be sent by the antennas. Similarly, all the incoming signals will be decoded and converted to digital signals by the transponder, which will then send these messages back to C&DH. Furthermore, the attitude of the spacecraft must be provided by ADCS, so that the gimbals of the antennas know in what direction they need to point the antennas. Thermal control also needs to make sure the antennas and components stay within their required temperature range, and finally, the structures subsystem needs to make sure the antennas are properly connected to the control module.

14.5 Risk Analysis

Table 84 gives an overview of the most critical risks of the telecommunications subsystem. The mitigation strategy is also presented in this table. Most of the risks are mitigated by adding redundancy, or by taking advantage of the fact that having 2 high-gain antennas and 2 low-gain antennas as back-up has a very high redundancy by itself.

Table 84: Risk table including the most critical risks for the telecommunication subsystem. RBM is defined as "likelihood, impact" before mitigation, RAM is "likelihood, impact" after mitigation.

ID	Risk	RBM	Mitigation	RAM
TLC01	Gimbal fails	2, 5	**Reduce** by adding redundancy or **Accept** and use other antenna	1, 5
TLC02	Transponder fails	4, 4	**Reduce** by having redundant transponders	4, 1
TLC03	Amplifier fails	3, 4	**Reduce** by having redundant amplifiers	3, 1
TLC04	Structural failure of antenna	1, 5	**Accept** and use other antenna	1, 5

14.6 Sustainability

Since the telecommunications subsystem is very small compared to the overall spacecraft, the impact of its parts on the overall sustainability of MARCO can be considered negligible. The relay satellites that are used by MARCO, on the other hand, do have a large impact on sustainability. However, these satellites will not only be used just for this mission. Numerous other missions to Mars can benefit from these relay satellites as well. This enables these future missions to reduce the size of their telecommunication subsystem, which can have a positive effect on sustainability in the long run. This concept can be clarified further by using an analogy: the satellites that are currently operating in Mars orbit each have their own telecommunication subsystem capable of communicating with Earth, which can be compared with everyone having their own car. But the relay satellites can act as public transport: they are able to handle communication links from multiple satellites around Mars. Public transport is of course more sustainable than everyone having their own car, which justifies the deployment and use of these relay satellites.

14.7 Requirement Compliance and Sensitivity Analysis

In Table 85, it is checked if each requirement is met, with a corresponding rationale. As can be seen, each requirement is met, so the design can be considered verified.

Table 85: Requirement compliance table for the telecommunications subsystem.

ID	Compliance	Rationale
MARCO-TLC-02	✓	As discussed in Subsection 14.3.3, there will be at least a small status update every 45 minutes.
MARCO-TLC-03	✓	As discussed in Subsection 14.3.2, this was what was designed for.
MARCO-TLC-04	✓	None of the link budgets have a bandwidth of more than 20 MHz.
MARCO-TLC-05	✓	As shown in Subsection 14.3.3, the total mass does not exceed the requirement.
MARCO-TLC-06	✓	As shown in Subsection 14.3.3, the total volume does not exceed the requirement.
MARCO-TLC-07	✓	As discussed in Subsection 14.3.2, this was what was designed for.
MARCO-TLC-08	✓	As discussed in Subsection 14.3.2, this was what was designed for.
MARCO-TLC-09	✓	Thermal control has the capability of achieving this.
MARCO-TLC-11	✓	As shown in Subsection 14.3.3, the total power needed does not exceed the requirement.

When talking about sensitivity analysis, MARCO still has some margin in the mass budget, but almost no margin for the power- and volume budget. However, of all the link budgets, the one from MARCO to Earth when MARCO is in Mars orbit, was the most critical one. So, if the data rate needs to be increased, for example, MARCO could still use the Mars- or Gangale relay satellites to meet the new data rate requirement. This will increase the cost, but as discussed earlier, the cost of the relay satellites will probably decrease significantly.

14.8 Recommendations

In Section 14.1, it is mentioned that radio frequency is used instead of optical telecommunications, because optical does not have a good TRL right now. If, however, the TRL increases significantly in the coming years, optical communication might become the better option. This would only be the case when all the relay satellites are able to support optical communications as well, which might also further increase the cost. In any case, it could be beneficial to investigate further in optical communications.

15 Thermal Control System

While operating the MARCO-POLO, monitoring and maintaining the temperatures of all equipment is necessary to achieve acceptable performance and durability of the equipment. The ambient air temperature inside the habitat must also be maintained in a range of 291 K and 300 K in order to give sufficient comfort for the crew. The thermal control system maintains the temperature on the inside and outside of the spacecraft. The thermal control system can be divided into two sections: the active thermal control system and the passive thermal control system. First, the active thermal control system will be discussed. Second, the passive thermal control system will be elaborated. Finally, the thermal control system of the propulsion subsystem will be covered.

15.1 Trade-off Summary

In the Thermal Control trade-off, the conclusion was made that MARCO-POLO will use a combination of an active thermal control system and a passive thermal control system. Components such as radiators, heaters, pumps and paint will be used for the Thermal Control design, since these components are best suited to meet the requirements for the system.

15.2 Requirements

The following list of requirements was generated during the first phase of the project, with their rationale being discussed in the midterm report [8].

MARCO-TCS-01 The thermal control system shall keep the energy storage system within operating temperatures (between 100 K to 300 K).

MARCO-TCS-02 The thermal control system shall keep the sections where humans are between 291 K to 300 K.

MARCO-TCS-03 The thermal control system shall keep the sections where material and equipment are between 90 K to 450 K.

MARCO-TCS-04 The mass of the thermal control system shall not exceed 10 t.

MARCO-TCS-05 The thermal control system shall keep all subsystem components at their operating temperature range.

MARCO-TCS-06 The thermal control system shall have a volume no greater than 40 m^3.

15.3 Active Thermal Control System

The Active Thermal Control System (ATCS) pumps a fluid in a closed-loop circuit such that it can perform three functions: heat collection, heat transportation and heat rejection [11]. The ATCS can be further divided into subsystems as shown in Figure 37. The ATCS consists of the Internal Active Thermal Control System (IATCS) and the External Active Thermal Control System (EATCS).

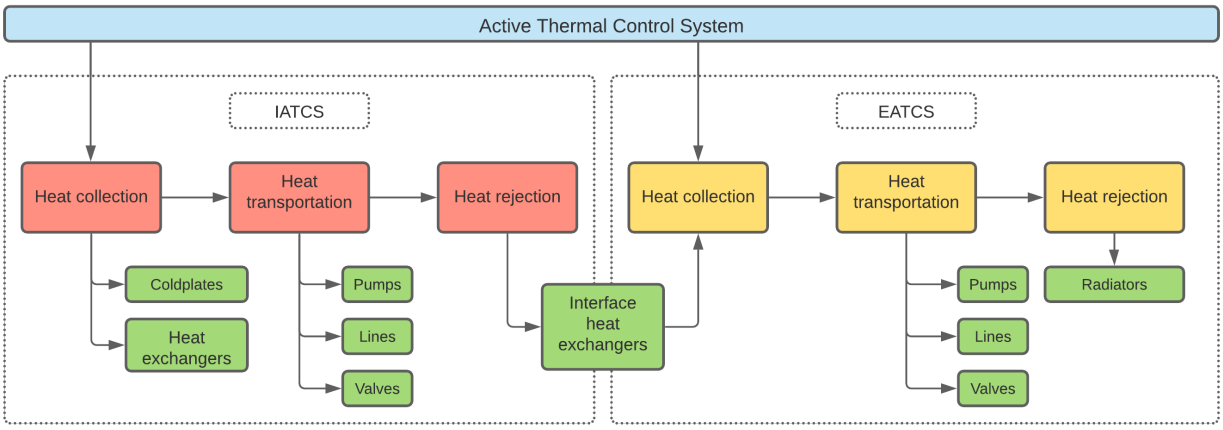

Figure 37: Design architecture of the ATCS.

The IATCS uses water as a heat transportation liquid and is only used inside the habitat where water will not freeze and is safe to use considering the health of the crew. The IATCS is a closed loop system inside the habitat such that it can provide constant coolant supply to equipment and the overall habitat. Two separate loops are used, a Low Temperature Loop (LTL) and a Moderate Temperature Loop (MTL). Due to this, the heat loads can be divided into two loops which also simplifies heat load management. Additionally, two loops provide redundancy in case one loop fails.

The EATCS uses ammonia coolant, cold plates, Pump Flow Control Sub-assemblies (PFCS) and radiators. The excess heat is removed through cold plates and heat exchangers. Both are cooled by ammonia loops which transport the heat to the outside of MARCO. Then, the ammonia flows through the radiators located on the outside of MARCO, where the ammonia releases the heat by radiation to space. This cools down the ammonia such that it can enter the inside of MARCO again and restart this process. Ammonia is used since it has an extremely low freezing point of -77 °C. The ammonia is pumped through the system by the PFCS which acts as the heart of the system.

Radiators are used to radiate the excess heat into deep space. The area of the radiators have been calculated using a numerical integration method and the following formula:

$$(J_s + J_{a_{earth}} + J_{a_{mars}})\alpha A_a + (J_{IR_{earth}} + J_{IR_{mars}})\varepsilon_{IR} A_a + P_{dissipated} = \varepsilon_{IR}\sigma A_e T^4_{MARCO} + \varepsilon_{IR_{rad}}\sigma A_{e_{rad}} T^4_{rad} \quad (76)$$

The albedo flux of Earth will be very close to zero when MARCO is near Mars, and the albedo flux of Mars will be negligible near Earth. The same goes for the IR-flux of Earth and Mars. The habitat and the control module will have a maximum wall temperature of 313 K due to solar radiation and IR-radiation of Earth and Mars. This temperature will occur when MARCO is in LEO and in full sunlight. The coldest temperature will occur when MARCO is in LMO and is not receiving any solar flux. This temperature will be equal to 176 K. Since the pressurised control module and habitat are insulated very well, the heat flux during the eclipse will not be significant to influence the temperature of those module. With Equation 76, the radiating area of the radiators can be calculated.

The dissipated power is assumed to be 20% of the total power minus the power of the propulsion cooler, since this was already taken into account for the propulsion design. The temperature of the radiators is assumed to be equal to the maximum allowable temperature of the ammonia in the pipes, which is equal to 292 K [11]. A radiator radiating area was found to be 71 m^2. The actual area of the radiator is half the radiating area, therefore the actual radiator area is equal to 35.5 m^2. After adding safety factors and taking the individual panel size into account, an radiator area of 40 m^2 was established. A thickness of 5 cm was assumed such that the volume equals 2 m^3.

Table 86: Input parameters for the ATCS.

Variable	Quantity	Unit
α_{hab}	0.38	-
$\alpha_{control}$	0.38	-
α_{truss}	0.4	-
α_{array}	0.91	-
ϵ_{hab}	0.3	-
$\epsilon_{control}$	0.5	-
ϵ_{truss}	0.3	-
ϵ_{array}	0.81	-
J_s	1400	$W\,m^{-2}$
σ	5.67×10^{-8}	$W\,m^{-2}\,K^{-4}$
T_{rad}	291.8	K
T_{MARCO}	313	K

MARCO uses four radiator arms to limit the total length of one radiator arm. One radiator arm has an length of 5 m and a width of 2 m. Additionally, using four radiator arms adds more redundancy to the TCS. Besides radiators, the TCS uses three PFCS, six cold plates and three heat exchangers which will allow for accurate temperature control of MARCO. Piping will run through the control module and the habitat from the cold plates to the heat exchangers where the water from the internal loops releases its heat to the external ammonia loops. Then the coolant runs over the truss past the solar arrays into the radiators where the ammonia radiates its heat into space. With this configuration, the internal temperature of the habitat and the control module will range between 294 K and 295 K and all subsystems and components will not exceed their maximum temperature.

Table 87: Budget table for the TCS.

TCS Budget	Mass [kg]	Volume [m^3]	Power [W]
Radiator (x2)	566	2	
PFCS[11] (x3)	1061.4	6.09	825
Cold Plates[11] (x6)	296.4		
Tubing	200		
Liquid coolant[11]	236	0.29	
Heat exchangers[11] (x3)	124	0.21	
Total	2360	8.59	825

15.4 Passive Thermal Control System

The Passive Thermal Control System mainly exists of paint coatings on the exterior of MARCO-POLO. The control module will have white paint on the exterior and the Bigelow B330 standard color is also white such that both structures have a relatively low absorption coefficient which reduces the high temperatures close to Earth. Additionally, quality insulation is used in both the control module and in the habitat such that the emissivity coefficient is really small. This ensures that the vital modules do not lose significant amounts of heat due to radiation.

The color black on the exterior of MARCO is also a consideration. This will increase the absorptivity of MARCO such that the temperature inside MARCO will increase. Near Mars, this is desired. However, near Earth, this means that the radiator area must increase which will increase the total mass of the TCS. Therefore, white paint is used for the exterior.

15.5 Risk Assessment

This section covers the major risks which are expected to occur to the TCS during the duration of the mission. Table 88 covers the risks, their likelihood and impact (RBM) , and the mitigation strategy with the updated RAM.

Table 88: The risks for the TCS. RBM is defined as "likelihood, impact" before mitigation, RAM is "likelihood, impact" after mitigation.

ID	Risk	RBM	Mitigation	RAM
TCS01	Radiators do not extend	2, 5	**Avoid** by testing the radiators extending mechanism and **Reduce** by using multiple radiators	1,3
TCS02	Pump does not work properly	2, 3	**Avoid** by performing sufficient testing and inspection prior to launch	1, 3
TCS03	Leak in one of the loops	2, 4	**Reduced** by reducing the pressure inside the pipes or even shutting down that specific loop	1, 4
TCS04	External paint does not cover full exterior or gets ripped off by radiation or debris	3, 3	**Reduce** by inspecting the full spacecraft for any inconsistencies and applying a thick layer of paint	2, 3
TCS05	Orienting the radiators does not function	2, 3	**Avoid** by designing the structure for critical modes	1, 3
TCS06	Heat exchangers fail	2, 4	**Avoid** by extensive testing and **Reduce** by adding redundancy to the system with extra heat exchangers	1, 2
TCS07	Valves do not operate correctly	2, 4	**Avoid** by using highly reliable valves	1, 3

Figures 38 and 39, map the impact and likelihood of the TCS risks before and after mitigation, respectively. These figures help communicate the impact of the risk mitigation strategy and the overall improvement of the subsystem's reliability.

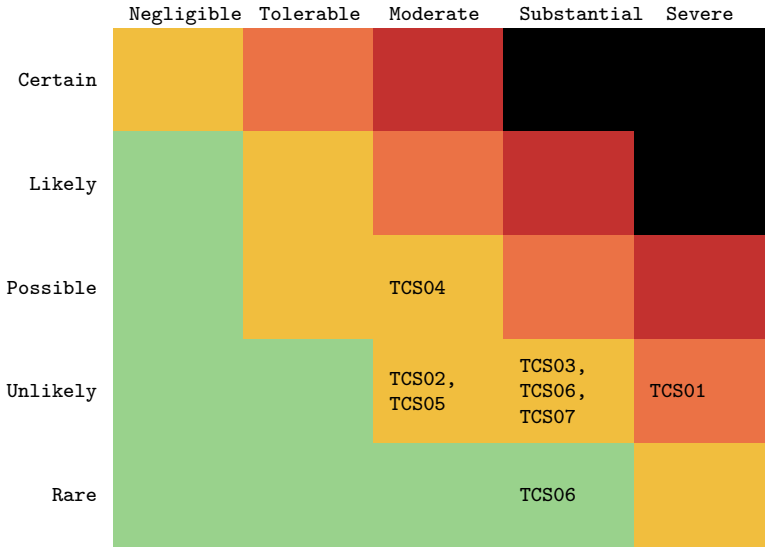

Figure 38: Risk matrix of identified Thermal Control subsystem risks. Likelihood is listed vertically and impact is listed horizontally.

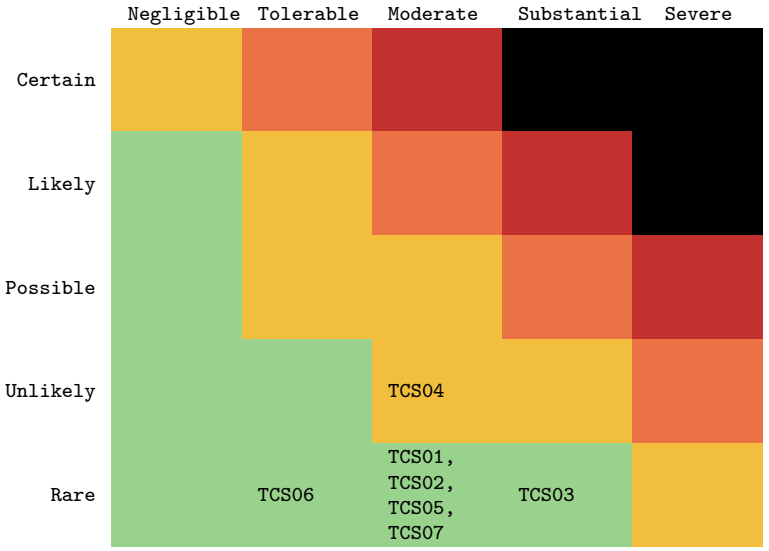

Figure 39: Risk matrix of mitigated risks. Likelihood is listed vertically and impact is listed horizontally.

15.6 Sustainability

With every design choice, the impact on the sustainability of the TCS was considered. Particularly for the TCS, it is desired to waste the least amount of heat where possible. To do this, high quality insulation is present on the inside of the modules such that temperature regulation becomes more efficient. In contrary, it is also desired to get rid of

excess heat as efficient as possible. This has to do with the PFCS efficiency and how much power is required for the pumps. Therefore, highly reliable and efficient pumps have been selected.

In terms of social sustainability, the fluid loops inside the modules contain water as coolant such that the health of the crew is at no risk. On the outside, ammonia is used. However this should be no hazard for the crew. Also, temperature fluctuation is a risk for the crew and payload. Therefore, the TCS provides great temperature regulation inside MARCO.

15.7 Requirement Compliance and Sensitivity Analysis

It is of great paramount that the requirements of the TCS are met. Therefore, the requirement compliance must be discussed. This is done via the compliance matrix shown in Table 89.

Table 89: General requirements compliance.

ID	Compliance	Rationale
MARCO-TCS-01	✓	As explained in Section 15.3, the extreme temperatures will fluctuate between 176 K and 313 K, meeting this requirement
MARCO-TCS-02	✓	From Section 15.3, this requirement is met
MARCO-TCS-03	✓	Same reasoning as MARCO-TCS-01
MARCO-TCS-04	✓	Shown in Table 87, the total mass of the TCS does not exceed 10 tonnes
MARCO-TCS-05	✓	All components will not reach there maximum temperature stated in Section 15.3
MARCO-TCS-06	✓	Shown in Table 87, the total volume of the TCS does not exceed 40 m^3

In case of a change in parameters, the TCS design will need to change as well. The main part that will change is the radiator area, however, this is easily scalable while considering the loads on the truss. Depending on the amount of sub-components which need cooling inside MARCO, more cold plates might be needed which will increase the total weight of the TCS.

15.8 Recommendations

In the future, for further research or design of the TCS system for a interplanetary spacecraft, new TCS technologies might be more reliable or effective instead of the relatively heavy and big radiators. Mainly because this design has mostly the ISS as reference. New technologies such as flexible radiators or origami radiators are being research right now. Only the TRL is too low to even consider it for this interplanetary transportation segment. But maybe in the future, new technologies could take over and make the TCS more efficient and light weight. For a future, more detailed design, the layout of all pipes, cold plates, pumps and valves should be made such that a high detailed mass can be acquired.

16 Habitation Module

This report will not go in depth with the design of the habitation module of MARCO, rather the habitation module will be chosen from existing habitation modules. The five modules that were considered are all based on Gateway habitat concepts and the numbers are taken from [71]. Table 90 shows the main criteria on which the decision of habitat were taken. At first a trade-off was made, which showed that three modules scored exactly the same and that two were performing below the standard. The main focus was the mass of the module and the habitable and stowage volume. On these parameters the Boeing/Lockheed Martin module as well as the Northrop Grumman performed worse than the others, especially regarding total mass, and they were ruled out. With three similarly performing modules, it was decided to score them 1-3 in each category and the one to score best would then be chosen. It turned out to be the Bigelow habitation module that had the best score, and therefore it was chosen as the module to support the crewed missions.

Table 90: Key characteristics of habitation modules that can be used for MARCO.

Habitation Module	**Power consumption** [kW]	**Total volume** [m^3]	**Habitable volume** [m^3]	**Stowage volume** [m^3]	**Total mass** [kg]
NASA MIG	26.64	317	84.81	99.13	55 550
Bigelow BA330	26.7	330	101.52	99.18	58 018
Sierra Nevada	26.82	324	87.3	100.72	60 927
Boeing/Lockheed Martin	27.18	384	90.28	123.82	76 722
Northrop Grumman	27.15	348	48.03	123.8	81 394

The Bigelow BA330 habitation module has all the necessary sub-systems, such as power, propulsion, avionics, thermal etc. for the system to function independently and autonomously, whilst supporting up to 6 crew members on interplanetary missions [71]. Table 91 gives a mass breakdown on subsystem level with supplies for 5 crew members on a 1200 days mission, and Table 92 mentions the specifications of the module.

Table 91: Mass breakdown into subsystem level of the Bigelow habitation module based on [71].

Mass breakdown [kg]	
Structures	10 992
Propulsion bus	1875
Power	1207
Avionics	1621
Thermal	1911
ECLSS	4393
Crew systems	3254
EVA	1116
Research	764
Robotics	943
Inert mass	
Stowed provisions	16 200
Consumables	19 150
Non-propellant fluids	83
Propellant	300
In-space stage adapter	1304
Total mass in orbit	65 113

Table 92: Parameter specifications for the Bigelow habitation module based on [71].

Parameter	**Value**	**Unit**
Habitation length	13.70	m
Habitation diameter	6.70	m
Habitable volume	101.52	m^3
Stowage volume	99.18	m^3
Power usage	26.70	kW
Keep alive power (uncrewed)	5.96	kW
Operating pressure	101.3	kPa
Solar array area	243.41	m^2
Thermal radiator area	100.51	m^2
Production cost [73]	125	M$

For the purpose of integrating the BA330 habitation module to MARCO, certain alterations have to be made to the habitation module. Instead of using the separate command module which is provided with the habitat, the habitation module will dock to the control module of MARCO. Certain functions will be taken over by the control module of MARCO, thus making them redundant on the habitation module. The propulsion bus, power system, avionics system, thermal system, EVA and the robotics will all be removed from the habitation module as each of these systems is present in MARCO's control module. Hence Table 93, shows the mass breakdown of the BA330 habitation module for its application to MARCO. It is assumed that radiation shielding is included in the structural mass.

Table 93: MARCO habitation module mass-breakdown.

Mass breakdown [kg]	
Structures	10 992
ECLSS	4393
Crew systems	3254
Research	764
Inert mass	
Stowed provisions	16 200
Consumables	19 150
Non-propellant fluids	83
Propellant	300
In-space stage adapter	1304
Total mass in orbit	56 440

The Bigelow habitat has an expected lifespan of 20 years [73], which means that it has to be replaced at some point during the crewed mission, if these are to continue after 20 years. This does not change much for the project but is something that should be considered and worked out in more detail closer to the crewed missions and the end-of-life of the habitat. In case the habitation module needs to be replaced, this can easily be done in LEO between two missions.

17 Command module

This chapter discusses the design of the command module of MARCO. The command module is the heart of MARCO, containing almost all the crucial subsystems on or within it. This chapter will discuss the design of the command module, including a discussion of some of the systems that are added to the module. In subsection 17.2 a description and explanation of the systems present on MARCO is given. This is followed by the design and sizing of the command module structure in subsection 17.3. In subsection 17.4 a careful analysis of all the possible risks related to the command module is performed. The sustainability of the command module is covered in subsection 17.5. Lastly in subsection 17.7 recommendations for further design are given.

17.1 Requirements

MARCO-TCS-01 The command module shall be able to dock to the tanks, habitat, lander and refuelling system simultaneously
Rationale: The command module functions as the central point of MARCO, connecting all parts together

MARCO-TCS-02 The command module shall house the EPS systems
Rationale: The command module houses the important systems that are always present

MARCO-TCS-03 The command module shall house the ADCS systems
Rationale: The command module houses the important systems that are always present

MARCO-TCS-04 The command module shall house the command and data handling systems
Rationale: The command module houses the important systems that are always present

MARCO-TCS-05 The command module shall be able to pump fuel from a refuelling tank to the main tanks and the lander
Rationale: The command module is the attachment point for all vehicles involved in refuelling

MARCO-TCS-06 The command module shall allow for EVA missions to be performed
Rationale: EVA missions are used to perform repairs to MARCO

MARCO-TCS-07 The command module structure shall be able to carry the load imposed by the engines.
Rationale: The command module structure is the load carrying component between the tanks and payload modules

MARCO-TCS-08 The command module shall be able to carry the load imposed by the ADCS systems
Rationale: The ADCS system is present on the command module, and needs to be able to perform the requires manoeuvres

MARCO-TCS-09 The command module structure shall not yield at any stage of its life cycle
Rationale: Yielding means irreversible damage, which would require significant repairs

MARCO-TCS-10 The command module shall provide attachment points for the solar array truss, the Canadarm2 and the communication systems
Rationale: The mentioned systems need to be correctly attached to the command module

17.2 On board systems

As mentioned, the command module contains the vast majority of the subsystems present on MARCO.These include:

- Telecommunications
- Solar arrays
- Electrical storage
- Thermal control
- Attitude determination and control
- Command and data handling
- Refuelling systems
- EVA Hatch
- Canadarm2
- Multiple docking ports

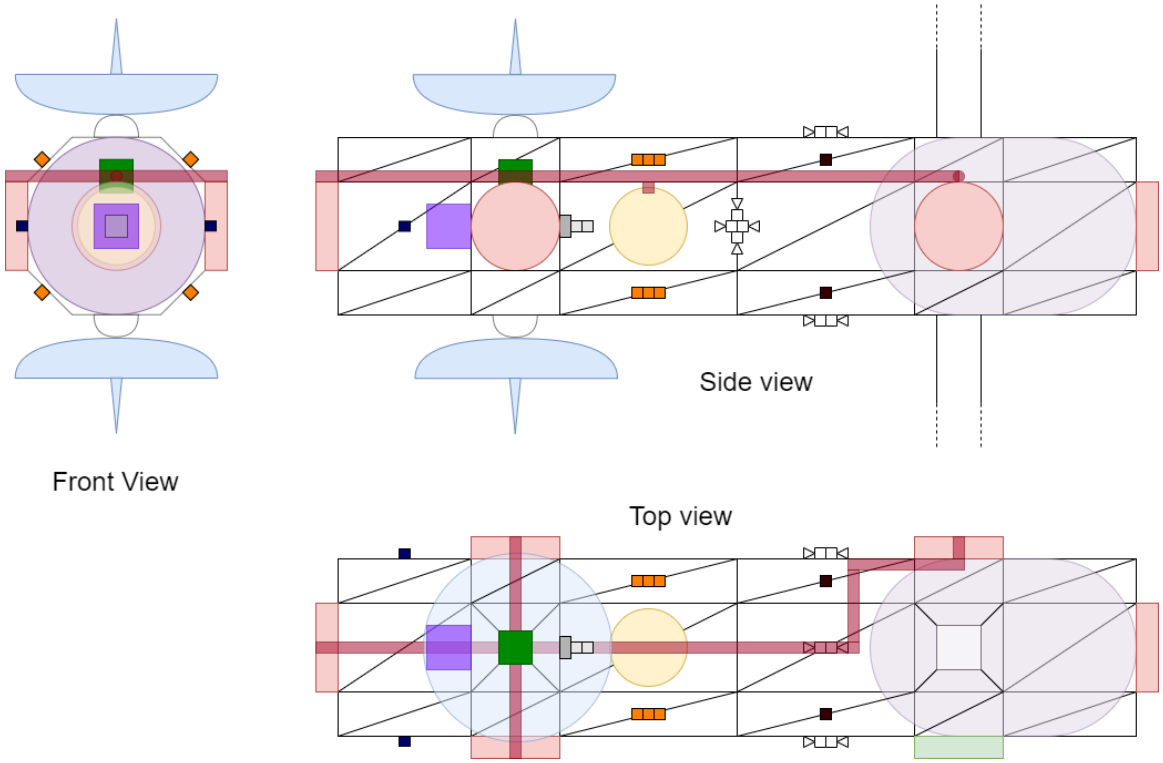

Figure 40: Simple drawing of the command module and its components.

Table 94: Colour coding of the diagram.

Colour	Component	Colour	Component
Red	Docking Port	Orange	Solar sensor
Green	EVA Hatch	Dark grey	CMG
Blue	Telecom dish	White square + triangle	RCS Thruster
Purple	Pressurised component	Dark blue	Horizon sensor
Dark green	Fuel pump	Black	Star tracker
Dark red	Fuel pipe	Dark purple	EPS system + Batteries

A simple drawing showing some of these subsystems can be seen in Figure 40. Please note that the solar and thermal array is not drawn entirely, but can still be seen on the right. A legend for the colors is also given in Table 94. Please note that the ADCS components are not drawn to scale, but are merely present to indicate an approximate location.

Of these systems, those that do not have their own dedicated section, will be discussed here.

17.2.1 Docking Ports

The system contains a total of 5 docking ports. Two of these are placed at both ends of the module, connecting to the fuel tanks and habitat at either end. There are then another two docking ports placed on the side closer to the tanks, which are used for refuelling. A more detailed explanation of the refuelling can be found in subsubsection 17.2.3

The final docking port is placed on the side of the habitat, and connects to the pressurised component of the module. This can allow for emergency evacuations of the habitat, if its other docking port no longer functions. It is also able to take over the refuelling functions of the two previously mentioned docking parts in case of failure.

For the three docking ports on the side, a keep out zone is also specified. This is in the shape of a circle with a given diameter centred in the middle of the docking port. These are based on the largest expected attachment plus 2 m. For the two docking ports closer to the tanks, this keep out zone diameter is set at 10 m. For the docking port connecting to the pressurised model, this is also set at 10 m, as this port needs to be able to function as a replacement in case of failure.

Additionally, the Canadarm2, solar and thermal panel truss, and telecom dish also need to be attached to the command module. For the truss structure and telecommunication antennas, a single fixed connection is required. The Canadarm2 however requires multiple attachment points, to be able to manoeuvre along the length of the command module. Two attachment points are placed on either side of the command module, which should allow the Canadarm2 to access all parts of the command module. A total of 300 kg is assumed to be required for this, which gives 360 kg after application of a 1.2 safety factor.

17.2.2 Command and Data Handling

The command and data handling system is the brain of the spacecraft, having to process the data that comes in from the many different sensors across the spacecraft. Since C&DH was not one of our main systems to design, only a very preliminary weight estimate was done.

Firstly, it can be noted that there are not much data that needs to be processed. Though the craft is very large, there are no scientific instruments that are running that would require processing of their data. This reduces the required processing power and data storage and keeps the mass low. Due to the large spacecraft size however, a significant amount of cables are required. With the command module being 19 m long, and the maximum total length of MARCO reaching 76 m, cables need to run to both extremes. The effect of this can be minimised somewhat by placing smaller computers near crucial systems such as the engines, which will lead to less cables being required. These cables and/or extra flight computers will push the mass of the system up however.

Keeping these ideas in mind, a mass estimate is then made based on information from the ADSEE Reader and a paper by T.P. Polsgrove et al [79]. From the ADSEE reader it is given that for planetary spacecraft the C&DH takes up around 5% of the total spacecraft dry mass. Assuming here that the habitat is not part of the dry mass, since the spacecraft used in the source are also unmanned, this would give a subsystem mass of around 3.3 t. It should be noted however, that the majority, if not all, planetary craft are significantly smaller than MARCO. This means that these estimates should be taken somewhat lightly, as C&DH size does not scale linearly with total dry mass.

Therefore, a look is also taken at the other source [79], which contains a detailed list of masses for every subsystem for a similar mars mission. For C&DH a mass of 900 kg is found, with an additional 360 kg for backup systems and spare parts, totalling out to 1260 kg. It should be noted that this craft is somewhat smaller however, so the expected system mass is predicted to be somewhat higher.

From these two sources, we get a broad range of values ranging from 1.3 t to 3.3 t. An intuitive guess would be taking the average at 2.3 t, as the lower bound estimate is predicted to be too low, and the upper bound estimate is predicted to be too high. Thus, after applying a 1.2 safety factor, the C&DH mass is set at 2.8 t.

17.2.3 Refuelling Systems

In order to perform the refuelling that is required for both MARCO and POLO, an integrated refuelling system is added to the command module. The two docking ports closer to the propellant tanks, on the side of the module function as main attachment points for refuelling. One of these will be used as a connection point for a full propellant tank, which is brought to MARCO. It has a diameter of 8 m, and will be connected to the docking port with aid of the Canadarm. The opposite docking port will then be connected to POLO, which will also be manoeuvred to the command module with the help of the Canadarm.

There are three pipes that need to be connected to a refuelling ship, one for liquid hydrogen, one for liquid oxygen, and one for the ADCS propellant. These pipes are placed next to the docking ports, and will make contact once the docking has been successfully completed. These will then be attached and connecting firmly to each other using a system of pins and hooks, that lock the pipes together, similarly to how the docking ports function.

The liquid hydrogen pipes will connect to a central pump, which can pump the propellant to any of the other attached crafts. For liquid oxygen this is similar, however it does not require a pipe to the main tanks of MARCO as this does not need oxygen. The ADCS propellant will be pumped directly into the storage tank, that is also present in the command module. The ACDS propellant can then be pumped to the same docking ports as the other liquids, as POLO also requires refuelling of its ADCS propellant. A detailed estimate into the mass of this system is not performed, but a mass of 300 kg is taken as a preliminary estimate. This is based on the RRM system, which is weighted at 250 kg, to which 50 kg of plumbing is added to transport the fuel. [53]

17.2.4 Canadarm2

Another very useful system on board of the command module is the Canadarm2. This is a robotic arm, used for construction and maintenance of MARCO, and will also be used for berthing of the capsule, lander, and refuelling vehicles. Having the Canadarm available does add weight, but allows for more precise margins when connecting systems, and removes the need for ADCS systems on board of separate components, who otherwise would need to use thrusters to position themselves accordingly.

17.2.5 EVA system

The pressurised part of the command module also functions as an EVA hatch. When it is docked to the habitat, the small pressurised chamber will function as an airlock, allowing for pressurisation and depressurisation. The hatch is placed on the bottom, as can be identified in Figure 40 by the green square. The pressurised chamber is a simple sphere, with a radius of 2 m. The shape is extended somewhat near the docking ports, to allow for a smooth connection. The required systems for EVA are also present in the command module, however they have not been extensively sized. The mass is estimated based on data from the paper by Polsgrove et al [79], which puts EVA support and crew systems together at around 2.75 t. Applying a safety factor of 1.2, gives a mass for the EVA system of MARCO of 3.3 t.

17.3 Module Design

The main design of the command module is concerning the structural component. It needs to carry the load from the propulsion module onto all the systems attached and further along MARCO. Since the ADCS thrusters are also positioned on the command module, a sideways force caused by these thrusters must also be carried by the module. This means that the truss needs to be able to handle compressive, buckling bending, and shear loads.

The shape of the cross sectional area structure was chosen to be an octagon, with sides of 2 and 1.4 for the straight and diagonal edges respectively, as is seen in Figure 41. This would closely follow the shape of the internal pressurised

[53] $https://nexis.gsfc.nasa.gov/robotic_refueling_mission.html$

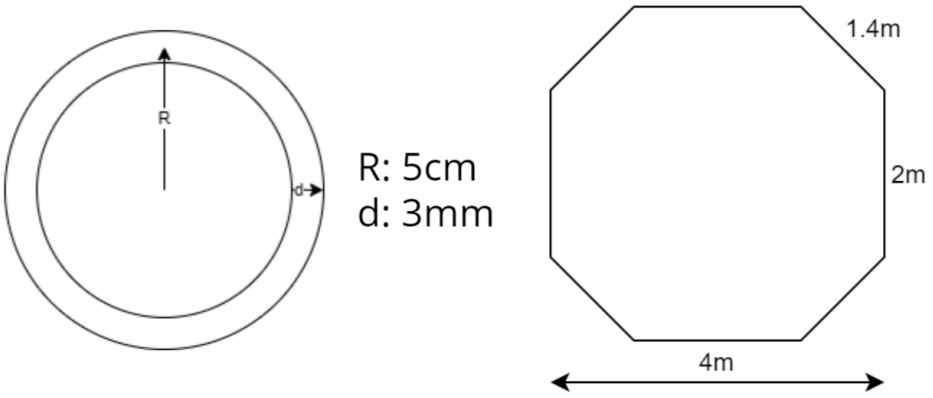

Figure 41: Command module beam structure.

component, while still being an easy shape to attach docking ports or other structures to. In the longitudinal direction, a standard shape with rectangles was chosen, with beams across the diagonals to reinforce the structure. These are not expected to carry any of the load, however should still be able to sustain the structure if failure occurs of one of the main longitudinal beams, as they do have the same thickness and are considered when designing. This could be considered an overdesigned structure, however failure of this structure would instantly lead to a failed mission. Since loss of life is not acceptable, this small increase in weight is deemed acceptable. The beams that make up the truss structure are simple hollow cylinders, with a diameter of 10 cm and a thickness of 3 mm as can be seen in Figure 41.

The material chosen for the command module structure is the same as for the other structural components, namely aluminium 7075-T7. It has a high maximum yield stress of 435 MPa, a Young's modulus of 70 GPa and a density of 3000 kg/m^3, making it a lightweight and strong material.

The total load that is transferred through the truss is defined by the maximum acceleration, and mass of the command module and the structures above it. Since the acceleration of MARCO is limited at 2 m/s^2, and the maximum mass above the command module is equal to 181.2 t, this gives a maximum force of 364 kN.

17.3.1 Compressive Loads

The compressive loads are straightforward to work out. Using $\sigma = \frac{F}{A}$, we can then work out that the required area is 0.000 836 m^2 or 8.36 cm^2. Applying a safety factor of 1.2, we get a minimum total area of 10.00 cm^2. Since the structure is an octagon, this means that every individual beam only needs to have a surface area of just over 1.25 cm^2. This is not likely to be a killer requirement, as the required area per beam is quite small. With the aforementioned size of the beams, a total area of 38 cm^2 is reached, far exceeding this requirement.

17.3.2 Buckling Loads

The buckling loads in a structure are governed by Equation 77. With all ends fixed, a K of 0.5 is achieved, to which for design purposes a 1.3 safety factor is applied. Initially, between the two docking ports the longest segment of the structure was present, at approximately 8.3 m, though this was changed later. By adding another structural octagon in between these two, the segment was split up in two. Though this does have a slight increase in mass, it leads to a nearly fourfold increase of the buckling strength of individual beams, allowing for a significant reduction in thickness and thereby mass. Thus the maximum length of an individual beam becomes 4.5 m. The moment of inertia for a hollow cylinder as used, is given by $0.25 \cdot \pi \cdot (r_2^4 - r_1^4)$

$$P_{buckle} = \frac{\pi^2 \cdot E_{Young's} \cdot I}{(K \cdot L)^2} \tag{77}$$

Using all these numbers, this gives a buckling load of 47.6 kN for each of the 8 truss segments, allowing them to carry a total load of 381 kN. Just slightly over the maximum load of 364 kN, making the size of the beam well designed.

17.3.3 Shear and Bending Loads

Due to the relatively low force of the thrusters compared to the main engine, shear and buckling loads are negligible when designing the command module. The maximum force of the ADCS thrusters is only 200 N compared to the 364 kN force of the main engine.

17.3.4 Mass breakdown

Taking all components of the command module into account, a final mass breakdown can be made. Note that this also contains the mass of the C&DH subsystem, which might be considered separate in other sources. This can be seen in Table 95.

Table 95: Command module mass breakdown.

Component	**Mass** [kg]
Structure	590
Pressurised component	160
Attachment points	360
EVA Systems	3300
Refuelling systems	360
Docking ports	1650
Canadarm2	1800
C&DH	2800
Subtotal	11 010
Total	11 570

These values are then summed, after which a safety factor of 1.05 is applied to give a final design mass of 11 420 kg.

17.4 Risk Assessment

The command module contains the majority of the important subsystems, and it is thus crucial that any risks related to the structure are carefully analysed.

Table 96: Risk table including the most critical risks for the command module. RBM is defined as "likelihood, impact" before mitigation, RAM is "likelihood, impact" after mitigation.

ID	**Risk**	**RBM**	**Mitigation**	**RAM**
COMD01	Refuelling docking port fails	2, 4	**Reduce** by adding additional docking port	2, 2
COMD02	Refuelling pump fails	2, 4	**Reduce** by having a secondary one **Reduce** by making it easy to replace	2, 2
COMD03	Failure of main structure	2, 5	**Accept** by having redundancy in structure	1, 2
COMD04	On board flight computer fails due to bit flip	3, 5	**Reduce** use backup computer while computer reboots	3, 1
COMD05	On board flight computer fails entirely	2, 5	**Reduce** use backup computer and repair/replace once possible	2, 2
COMD06	Canadarm2 fails	2, 3	**Reduce** by performing repairs **Accept** and replace the Canadarm2	2, 1
COMD07	EVA system fails	2, 5	**Avoid** by performing careful maintenance and inspections	1, 5

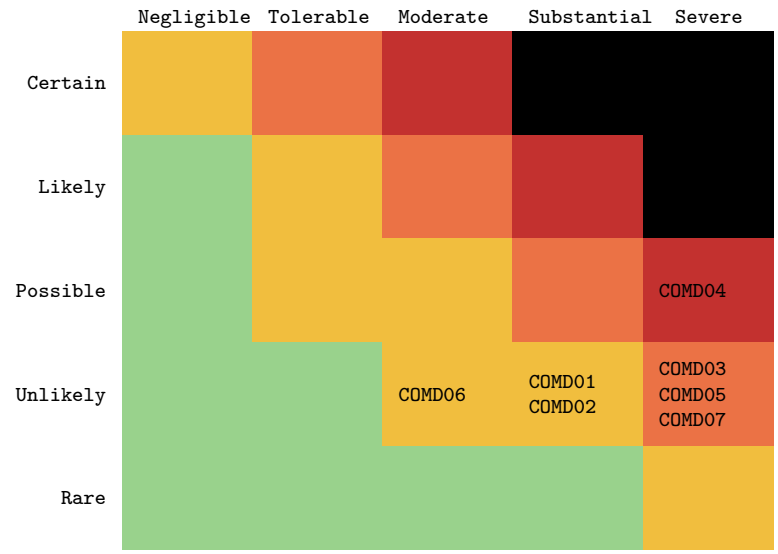

Figure 42: Risk matrix of identified command module risks. Likelihood is listed vertically and impact is listed horizontally.

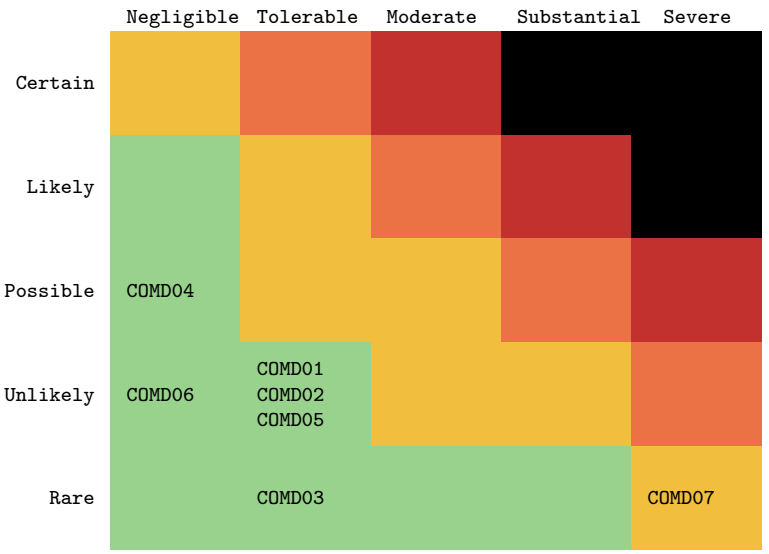

Figure 43: Risk matrix of mitigated risks. Likelihood is listed vertically and impact is listed horizontally.

17.5 Sustainability

The command module is a crucial part of the spacecraft, however it does not have much impact on the sustainability of MARCO. Since the majority of components on the command module are expected to be used throughout the entire duration of MARCO, the main focus for sustainability lies on the end of life. Due to the size, it could be taken back down to earth using Starship, however this is most likely not the optimal approach, as this would require a lot of propellant burned. A different idea is to disassemble some components, and reuse these on different spacecraft, such as using the EVA tank, Canadarm2 or on board computer. Reusing the structural outside seems very impractical, and would either have to be deorbited, or brought down to earth.

17.6 Requirement Compliance

Table 97: Command module requirements compliance.

ID	Compliance	Rationale
MARCO-TCS-01	✓	Sufficient docking ports are present on the command module.
MARCO-TCS-02	✓	The command module has been designed for this condition.
MARCO-TCS-03	✓	The command module has been designed for this condition.
MARCO-TCS-04	✓	The command module has been designed for this condition.
MARCO-TCS-05	✓	The command module contains fuel pipes and a fuel pump.
MARCO-TCS-06	✓	The command module contains the required EVA systems
MARCO-TCS-07	✓	The command module can withstand the calculated load.
MARCO-TCS-08	✓	The low loads imposed by the ADCS systems can easily be withstood.
MARCO-TCS-09	✓	The command module structure has been designed with the yield stress as a maximum stress.
MARCO-TCS-10	✓	The command module contains sufficient attachment points.

17.7 Recommendations

This preliminary estimate has given a good indication of the mass and sizing of the systems on board of the command module. However for some systems, a very basic estimation has been done, which can be significantly improved upon. For C&DH, the EVA systems and refuelling systems a more detailed analysis can be performed to reduce uncertainty, and to most likely bring down the mass of the structure. Additionally it could be possible to bring down the mass

of the structure somewhat by more accurately designing and taking into account the load bearing properties of the diagonal beams. However the mass of the structures being only 400 kg it is not likely that this will have a significant impact.

18 System Architecture

A system architecture is the conceptual model that defines the structure, behaviour, and the interactions within and outside of the system. The N2 chart gives a different view of the subsystems interrelations. The horizontal rows have the outputs of a yellow block while the vertical columns contain the inputs for each yellow block. This diagram is considered to be quite self explanatory, however, just for some clarification about the central computer, it is worth mentioning that this would be the command center for the system, which is the command module. Nevertheless, each subsystem has their own unit controller which ensures executions of the commands given by the central computer.
The overall system has been divided into functional units which are represented by the yellow blocks. The idea is that the inputs and outputs of each functional unit are shown, such that the they can be developed in parallel, while still considering the interrelations. The N2 diagram can be seen in Figure 44.

N2 Diagram

ITS		Current attitude of the ITS	Current temperature of the ITS	Communication by the crew	Power required by ITS		Transport of payload/equipment
	Ground Station			Change in orbital trajectory, communication to crew			
Perform attitude manoeuvres		**ADCS**	Temperature of ADCS thruster	Pointing of the antenna, current attitude	Pointing of solar array		Landing attitude control
Temperature for the ITS		Thermal control for ADCS thruster	**Thermal control**		Thermal control for battery and power generator	Thermal control for propellant	Temperature for the lander
Communication to crew	Spacecraft data and crew communication	Change in attitude requirements		**Telecommunication**		Ground station commands	
Power available for the ITS		Power on valves, gyros and sensors	Power to generate/dissipate heat, battery temperature, power generator temperature	Power the system	**Power**		Power to lander
Thrust to move the ITS		Thrust off-set	Engine temperature			**Propulsion**	Landing thrust
		Current lander attitude	Current temperature of the lander	Lander status	Power required by lander		**Lander**

Figure 44: N2 diagram of the spacecraft, showing the interrelations between functional units i.e. inputs and outputs between systems.

Each subsystem has its own architecture, and these can be seen in their respective chapters. However, here a general system architecture is presented. It shows the interrelation of the various main components for both MARCO and POLO. In this case POLO crew and POLO cargo is considered to have the same system architecture, but this might change in the detailed design phase of the two landers. As can be seen in the figure below, the components are grouped within the subsystems to give a clear overview, and then a more detailed overview can be found in the subsystem chapter.
The connection between MARCO and POLO is also shown, and this is limited to the antennas which ensures communication between the two. This also shows that POLO can receive commands from mission control through MARCO but the commands are not directly send to POLO.

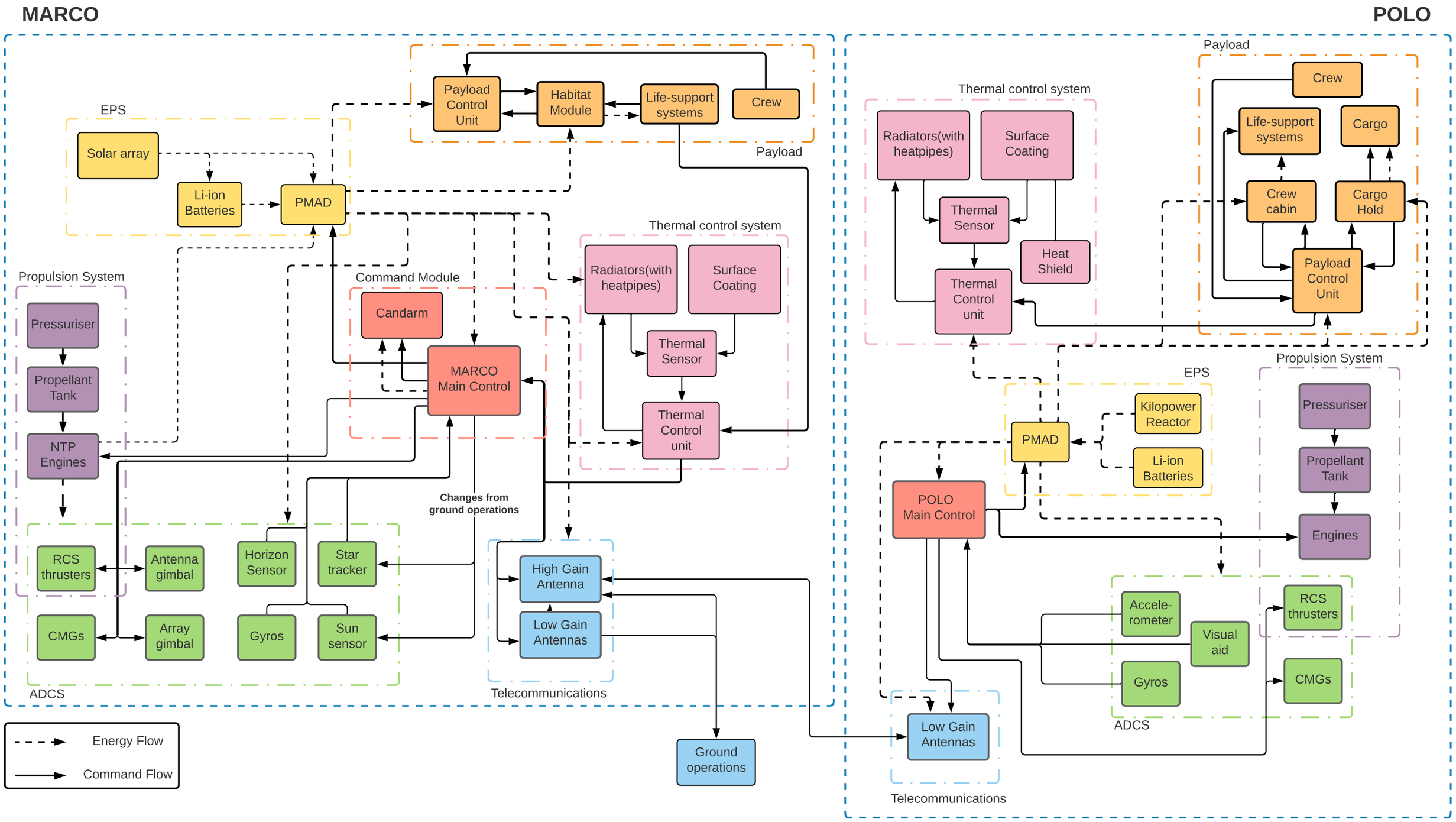
MARCO
POLO
EPS
Solar array
Li-ion Batteries
PMAD
Payload Control Unit
Habitat Module
Life-support systems
Crew
Payload
Thermal control system
Radiators(with heatpipes)
Surface Coating
Thermal Sensor
Thermal Control unit
Heat Shield
Propulsion System
Pressuriser
Propellant Tank
NTP Engines
Command Module
Candarm
MARCO Main Control
Changes from ground operations
RCS thrusters
Antenna gimbal
Horizon Sensor
Star tracker
CMGs
Array gimbal
Gyros
Sun sensor
ADCS
High Gain Antenna
Low Gain Antennas
Telecommunications
Ground operations
Energy Flow
Command Flow
Crew
Life-support systems
Cargo
Crew cabin
Cargo Hold
Payload Control Unit
Kilopower Reactor
Li-ion Batteries
POLO Main Control
Engines
Accele-rometer
Visual aid
Gyros
RCS thrusters
CMGs
Low Gain Antennas
Telecommunications

19 Budgets for MARCO

In this chapter, the budgets for MARCO will be displayed. First, the budget for MARCO will be displayed in the crew configuration and after that the budget for MARCO in the cargo configuration will be shown. These values are taken from each subsystem chapter, where further explanation can be found.

19.1 MARCO Crew

The budget breakdown for MARCO crew can be found in Table 98. Since this is the crew configuration this includes the habitat and all ten tanks. A drawing of the system is shown in Figure 45, in this drawing every subsystem drawing from throughout the report have been combined to show the full picture. In this drawing POLO is able to attach to the right of the habitat module (top view).

Table 98: Budget breakdown for the MARCO crew configuration without propellant.

Component	**Mass [t]**	**Volume [m^3]**	**Cost [M€]**
Engines	21.8	503	2680
Tanks	35.4	89.6	391
Structures	6.93	676	0.4
EPS	2.18	4.3	256
ADCS	1.89	2.13	22.8
Telecommunications	0.26	29.1	47.3
Thermal	2.36	8.59	237
Habitat	56.4	330	125
Command module	11.6	238	142
Total	139	1881	3902

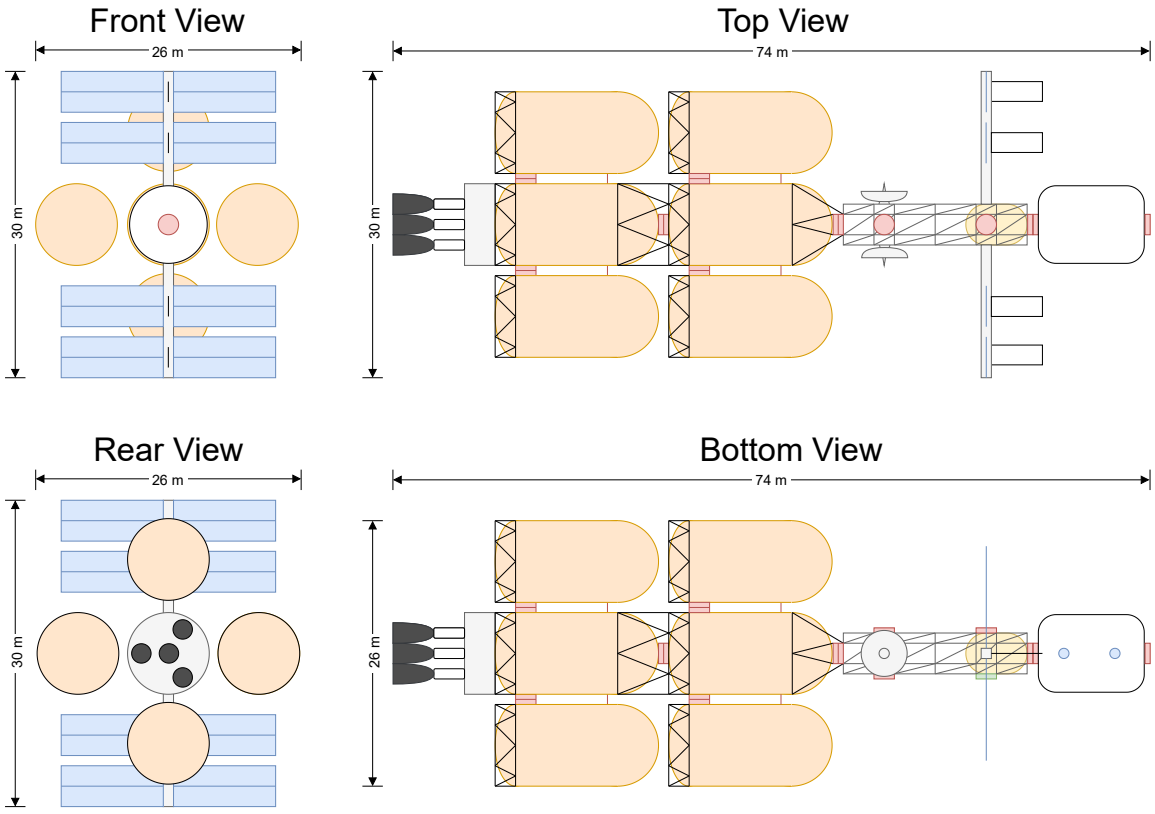

Figure 45: A schematic drawing from different sides from the MARCO-POLO crew configuration.

19.2 MARCO Cargo

The budget breakdown for MARCO cargo is shown in Table 99. This budget does not include the habitat and also has only six tanks since it does not have to bring the lander back. The schematic can be found in Figure 46. POLO can not attach to the habitat module here and will therefore attach to the right side of the control module (top view).

Table 99: Budget breakdown for the MARCO cargo configuration without propellant.

Component	**Mass [t]**	**Volume [m^3]**	**Cost [M€]**
Engines	21.8	503	2680
Tanks	22.8	55.7	312
Structures	6.93	676	0.4
EPS	2.18	4.3	256
ADCS	1.89	2.13	22.8
Telecommunications	0.26	29.1	47.3
Thermal	2.36	8.59	237
Command module	11.6	238	142
Total	69.8	1517	3698

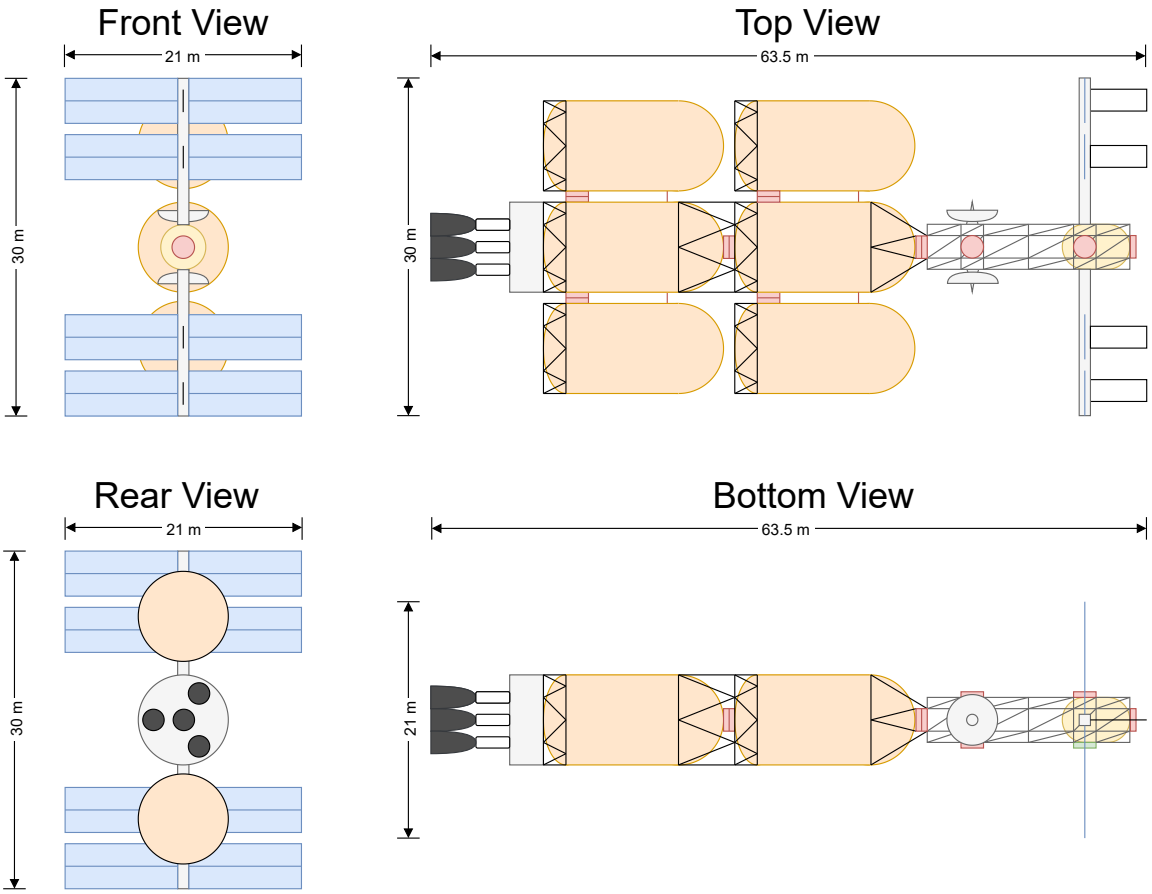

Figure 46: A schematic drawing from different sides from the MARCO-POLO cargo configuration.

19.3 Cost

In order to get the cost per launch for MARCO some explanation is needed. To start off, the maximum expected propellant mass that MARCO will need is 467 t for the crew variant and 219 t for a cargo mission. This means that

MARCO will need five tanks in the cargo variant, however, since this will give unexpected problems for the ADCS and thermal system it is better to attach six tanks for symmetry. The crew variant will need all ten tanks in order to get to Mars and back. These numbers have also been taken into account in the budget tables throughout the report.

The launch price for Starship is assumed to be 500 €kg^{-1}, or 50 M€ per launch, this is around half the price per kilogram of a launch today. Starship can fit one tank, the engines and structural adapters, the command module and trusses, or the habitat per launch. This means that MARCO can be assembled in 13 launches, or 650 M€.

The final specific payload cost for every mission can be seen in Table 100, in this table every mission has a different payload mass and cost per mission, this cost is based on the amount of refuel missions or the amount of modules that have to be sent up. The table end at the last crew mission, as it is not known what MARCO will carry after this. As can be seen the cargo missions meet **MARCH-CR-01**, the crew missions, however, do not. Although on average the requirement is met. With this pricing there is also still a budget left to perform maintenance to the system.

Table 100: Cost breakdown for every mission.

Mission	**Payload Mass [t]**	**Cost [M€]**	**Payload Cost [M€t^{-1}]**
Cargo 1	45	300	6.67
Cargo 2	45	300	6.67
Cargo 3	45	300	6.67
Crew 1	16	500	31.3
Crew 2	16	500	31.3
Crew 3	16	500	31.3
Crew 4	16	500	31.3
Total	199	3550	14.6

20 Communication and Data Handling

This chapter gives a brief overview of the communication and data flow within and outside of MARCO-POLO. The figure below is a block diagram which highlights the key elements of the communication and data handling process. In Figure 47 the flow of data and communication of all subsystems can be found. It shows how they are all connected to a central processor, which is the central part of the communication of MARCO-POLO. The communication from the ground station and to each subsystems is also depicted and depending on where MARCO is, this can either go directly through the telecommunications system on MARCO or through a relay satellite which then sends it to MARCO. Once the signals reaches MARCO, they are processed by the central processor and potential commands are given to the corresponding subsystem.

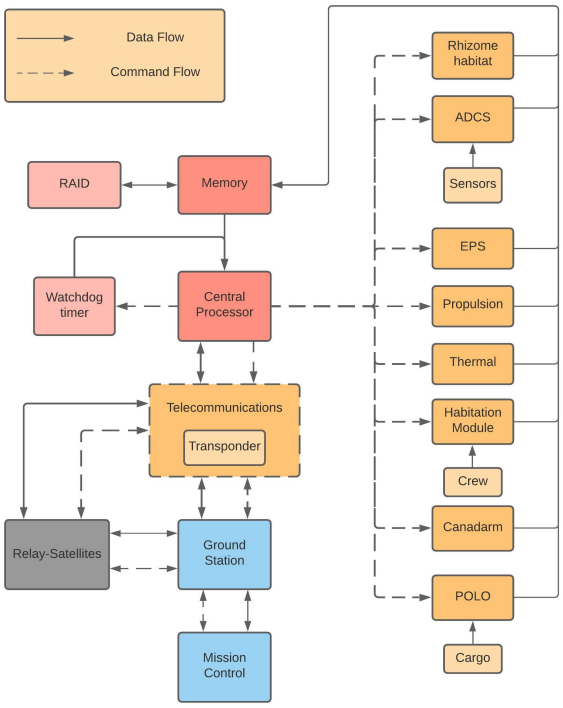

Figure 47: Communication and data handling diagram for the mission.

As seen in Figure 47, all the subsystems are connected to the main computer, which has a central processor, a memory, a redundant array of inexpensive disks (RAID) system and a watchdog timer which is used to detect and recover from computer failures. All the data is collected in the memory banks and processed in the central processor, which processes the commands for the entire MARCO-POLO system. In order to add redundancies, a RAID system is used, which is used to increase the performance and/or reliability of data storage[54], the exact speed and reliability that is achieved from the RAID depends on the type of RAID system implemented. For this specific application a RAID 10 type is used, it requires at least 4 drives and is a combination of RAID 1 (mirroring) and RAID 0 (striping). This will result in both increased speed and redundancy. In a four drive configuration, two mirrored drives hold half of the striped data and another two mirror the other half of the data. This means you can lose any single drive, and then possibly even a 2nd drive, without losing any data [55].
The watchdog timer is a hardware timer that automatically generates a system reset if the main program neglects to periodically service it. It is often used to automatically reset an embedded device that hangs because of a software or hardware fault [56].
In order to communicate with mission control on Earth, three ground stations are required such that the signal can be received and transmitted at any given time. When MARCO-POLO is in LMO, relay satellites will be engaged in order to facilitate communication between MARCO-POLO and the ground stations.

21 Operations and Logistics

In this chapter, the operations and logistics of the entire MARCO-POLO project will presented. The mission is divided into two phases, the first being the equipment and materials phase as seen in Section 21.1, followed by the crewed phase in Section 21.2.

21.1 Equipment and Materials Phase

As seen in Figure 48, the order of operations for the first phase of the mission is shown. This first phase will consist of assembling MARCO-POLO and delivering all the necessary equipment and systems to Mars in order to set up the Rhizome habitat. The first phase of the mission is entirely autonomous as no human crew members will take part in it, mission control will however follow this phase from the Earth and react if needed.

[54] https://www.prepressure.com/library/technology/raid *[cited 16 June 2021]*
[55] https://www.steadfast.net/blog/almost-everything-you-need-know-about-raid *[cited 16 June 2021]*
[56] https://os.mbed.com/cookbook/WatchDog-Timer *[cited 16 June 2021]*

The first step consists of launching the subsystems of MARCO into LEO, and here assemble these subsystems in orbit. As the habitation module is not yet required, MARCO will for the first phase consist only of the propulsion system and control module. Afterwards, a loaded POLO cargo will be launched and dock to MARCO. When the assembly of MARCO is done, and the docking of POLO cargo are complete, the first trip will commence in 2028 (as per Table 12), containing the power system for the Rhizome habitat, and the first shipment of the required robots and material for setting it up.

After performing the trans-Mars injection, MARCO-POLO will take 6-7 months to reach martian orbit. Upon reaching LMO at 500 km height, POLO cargo will separate, and land at the specified landing site, which is dependent on the Rhizome habitat. After having deployed the cargo, POLO cargo will provide the necessary power for the rovers until the power system of the Rhizome habitat is up and running. As mentioned in Section 8.1 POLO cargo is designed to carry the payload that is required to set up the Rhizome habitat. This was done at the expense of being able to rendezvous back to MARCO in LMO and return to Earth to be reused. To carry all the payload required, to have the Rhizome habitat up and running within a 10-year time frame from the maiden flight (as per user requirement: **MARCH-H-01**), POLO cargo will be left on the surface of Mars and a new POLO cargo will be manufactured and launched for the following cargo mission.

MARCO will now perform a trans-Earth injection, for its return journey to Earth. Upon reaching Earth, MARCO will perform an orbital insertion and go into a LEO with a height of 2000 km. Before beginning a new trip to Mars, several refuelling launches need to be performed to refuel MARCO, and a new POLO cargo will be launched and docked to MARCO. During this phase of the mission, all the necessary rovers (including scouting, mining and 3D-printing rovers) and some construction material/equipment will be transported in order to construct the habitat autonomously, over three trips within a 10 year time frame.

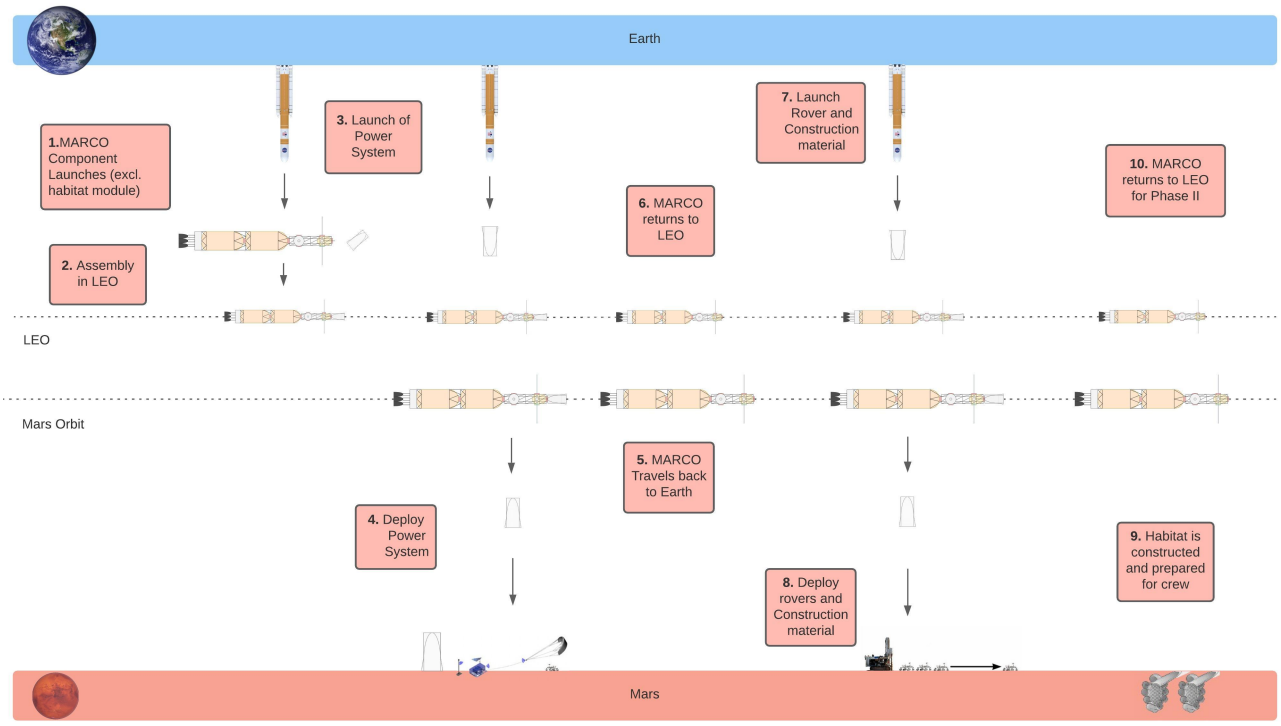

Figure 48: Phase I: Equipment and materials phase of the MARCO-POLO missions.

21.2 Crewed Phase

The second phase of the mission consists of transporting the crew members along with some supplies to the Rhizome habitat. The first crewed launch will be in 2041, and will consist of 5 people and the required supplies. As seen in Figure 49, before sending the crew members to MARCO, a habitation module needs to be launched and docked to MARCO (step 12). Upon successful docking of the habitation module and the crew capsule, the first crewed trip to Mars will commence following the same steps as mentioned in Section 21.1, with the minor alteration being that upon reaching LMO, the crew capsule will be merged with POLO crew and POLO crew will land at the landing site.

For the rest of the mission life of MARCO-POLO (total of at least 10 round-trips to Mars), it will be used to ferry

crew members from Earth to Mars and back, carrying additional supplies during each trip. Following the return of MARCO-POLO to LEO, the crew members will disembark MARCO, using the crew capsule for Earth re-entry. In case of an uncrewed mission, the habitation module and some of the propellant tanks will be detached and left in LEO, in order to reduce the mass of MARCO, and thereby also the propellant needed to bring the MARCO-POLO to LMO.

During its 40 years, or 10 round-trips to Mars, mission certain systems need to be replaced as their service life is shorter than the service life of MARCO-POLO. After 20 years of use, the solar arrays and the habitation module needs to be replaced as seen in Chapters 12 and 16, respectively. Other than the major system replacements, minor ones will be conducted during the maintenance procedures in LEO.

Upon completing its mission life and safely returning the remaining crew members from the habitat back to Earth, MARCO-POLO will need to be decommissioned. As an element of the spacecraft disposal, part of the system will be returned to Earth while the remainder will be sent out into outer space including the nuclear waste. Thus completing the MARCO-POLO mission successfully.

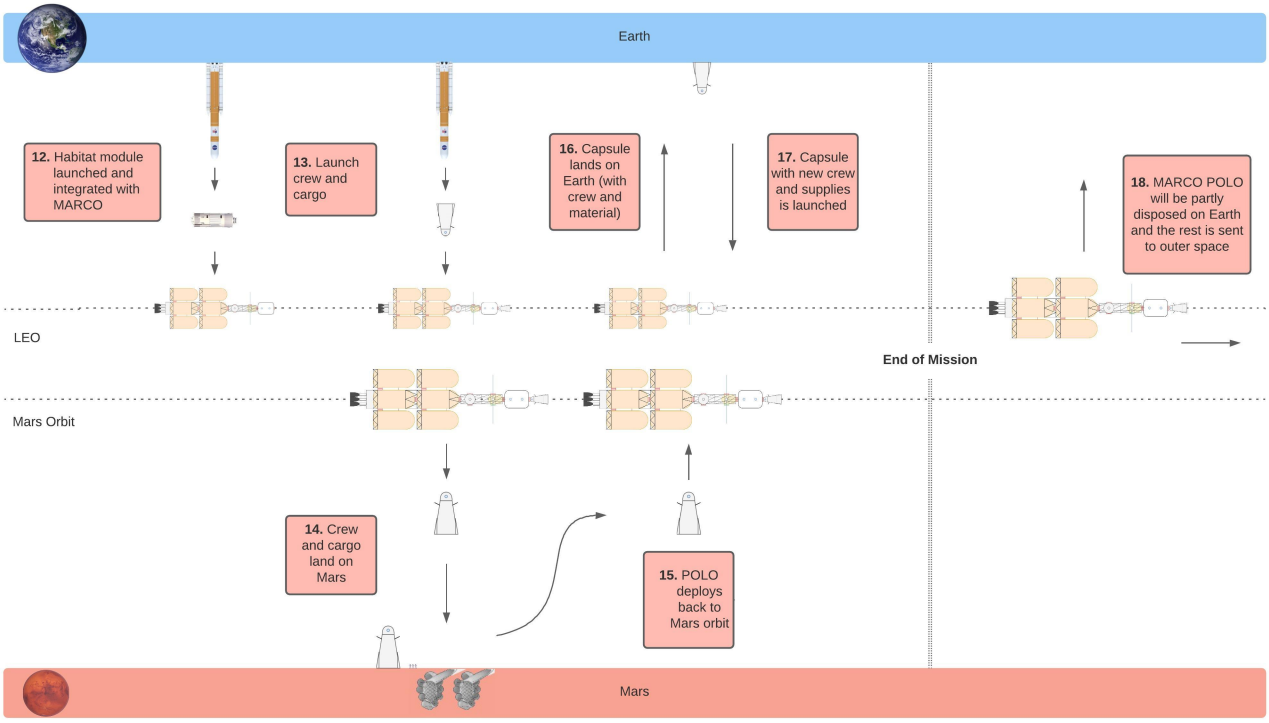

Figure 49: Phase II: Crewed phase of the MARCO-POLO missions.

22 Reliability, Availability, Maintainability and Safety

For guaranteeing the success of the mission and the safety of all crew during manned missions, it is crucial to have sufficient reliability and safety for the design. This section details the approach towards reliability, availability, maintainability, and safety, also abbreviated as RAMS. These aspects of the design are also discussed in that order.

22.1 Reliability and Availability

Guaranteeing reliability for a spacecraft is a tough task, as maintainability is very difficult, and can only be performed when the ITS is in Earth orbit. Generally, reliability of spacecraft over their operational lifetime ranges from 0.5 to 0.9 (50 to 90 %) [5]. The reliability study for this mission has been split into the subsystems of the mission. They are evaluated separately for all four RAMS factors.

The user requirement for safety and reliability states that the ITS shall be 95% reliable over its total lifespan, where reliability is the probability of not experiencing failure.

22.1.1 Control Module

The control module is the nervous system of MARCO, it consists of several crucial subsystems relating to communications and control, such as the telecommunications, thermal control and ADCS. It is therefore paramount for the functioning of the ITS that this module is reliable.

For all these subsystems, the reliability must be such that they can at the very least complete one mission with a reliability that is as high as possible, as maintenance cannot be performed before the ITS is back in Earth orbit. Complete failure of one of these subsystems is critical, as it is likely that this will lead to complete loss of the spacecraft and thus, failure of the mission.

Electrical Power System The power system uses the bi-modal nuclear thermal engine as its main power source, with solar arrays as back-up power generators. The solar arrays also provide power during the first phase of the mission, when the ITS is being assembled. The power system as a whole must have a reliability of at least 95%. The reliability of the nuclear thermal engine is discussed in subsubsection 22.1.2. For the solar arrays, extensive research has been done into the reliability of these power generators. For satellites, it is found by an unofficial survey that 40% of all failures are due to solar array failures[57]. Solar arrays also tend to have a high infant mortality rate, meaning it is crucial to have the arrays installed properly such that they survive their first life stage [15]. The reliability of solar arrays can be further illustrated by the fact that the ISS has been functional on solely solar energy as well[58]. It is therefore important to have reliable and maintainable solar arrays, which can be a back-up source of power for the entire mission. The solar arrays will be replaced halfway through the mission: after 21 years. The degradation of the solar arrays is 0.5%, meaning the maximum degradation will be 10.5%. This has been designed for, so this degradation is acceptable. The solar array is mostly there for redundancy, however it is important it is reliable for the entire mission duration. The batteries, commercial LG-MJ1 batteries, have the benefit of safety and reliability over custom large-format cells [4].

ADCS The ADCS system uses mono-propellant thrusters, control moment gyroscopes, and horizon sensors. The mono-propellant thrusters are a high reliability option, due to their simplicity. Control moment gyroscopes can also be designed for high reliability [14]. Lastly, horizon sensors were the most reliable option during the trade-off, as they utilise the same principle for orbit attitude determination in both Mars and Earth orbit. All of the components of the ADCS system have redundancy, for example by utilising a pyramid configuration for the CMG's, or by having multiple horizon sensors on board.

Telecommunications The telecommunications is another system that falls under the command module. It is crucial that this system works at all times, as no communication means that there is no way of knowing what the spacecraft is doing at a point in time, and no commands can be given to the ITS. Therefore, telecommunications must be up at all times. Firstly, the telecommunications system uses radio frequency instead of optical communication. This is a more reliable way of communication, as radio frequency has been used for way more missions than optical communication, and is deemed a very reliable way of communication for space missions. Secondly, the ITS has 2 high-gain and 2 low-gain antennas. This allows for a high level of redundancy, as only the 2 high-gain antennas are strictly needed for functioning of the telecommunications, and the low-gain antennas serve purely as back-up. The main way of ensuring the reliability of the telecommunications system is by means of redundancy, as this is implemented in the antennas, transponders and amplifiers.

Thermal control For thermal control, the reliability is mostly on the active thermal control, as this actually has to perform actions. Of course, however, it is also important that the passive control does not fail. Redundancy is added to this system by using multiple loops for the pipes, multiple radiator arms and multiple heat exchangers. For the layer of paint acting as passive control, it must be ensured that this is a resistant layer that is not easily damaged or removed by, for example, debris or radiation, for example by applying a thicker layer of paint.

22.1.2 Propulsion System

For the propulsion system, four bi-modal nuclear thermal engines are used. The reliability requirement for this subsystem states that it must be 95% reliable. Redundancy has also been implemented by using four engines, so that an engine failure is not critical.

Research was done into the reliability of nuclear thermal propulsion, where it was found that it can be a significant

[57] https://www.nts.com/services/education/articles/testing-the-reliability-of-satellite-power-systems/ *[cited 17 June 2021]*

[58] https://www.nasa.gov/mission_pages/station/structure/elements/solar_arrays-about.html *[cited 18 June 2021]*

challenge to obtain a high reliability, as nuclear systems are complex and are subject to many environmental threats and reactor radiation, increasing the difficulty of ensuring reliability [13].

Demonstrated reliability from other NTP systems had a relatively broad range, ranging from 0.69 to 0.995, which further demonstrates the need for proper robustness and redundancy of the propulsion subsystem in order to reach the reliability requirement of 95% [16].

22.1.3 Habitation Module

As discussed in Section 16, a modified Bigelow BA330 was selected for the habitation module for the mission. The BA330 is one of six ground-based demonstration projects funded as part of NASA's NextSTEP-2 program. Bigelow started out with two uncrewed modules that were delivered to orbit by Russian rockets in 2006 and 2007 and are still flying today. In 2016, an expandable test module was successfully installed onto one of the International Space Station's ports. The BA330 habitation module was tested for two weeks in 2019 at the company's facility in Nevada, which was conducted incorporation with NASA [59].

Despite never having been used in space, by the time the BA330 becomes commercially available, the reliability of the habitation module would be sufficient to be used in an interplanetary mission, such as the one that MARCO-POLO will embark on.

Bigelow Aerospace is on track to launch its first two B330 modules in 2021. And in October of 2020, the company announced that it's working with United Launch Alliance to get a B330 into orbit around the moon by 2022 [60]. Based on the information provided by the manufacturer (Bigelow Aerospace), the BA330 will be ready in time for the crewed-phase, which is set to begin in 2040. The BA330 will be built 42 months after the go-ahead for construction is given [61]., which in the case of MARCO-POLO will be in the year 2036.

22.1.4 Structures

It is crucial for any spacecraft that the structures stay intact: failure means complete loss of, at the very least, one component of the ITS, and this causes mission failure. Reliability for the structure of the ITS is ensured by performing a structural analysis and including safety margins for redundancy, such that, even under the most stressing of circumstances, the structure of the ITS does not fail as this would be utterly catastrophic, especially for a crewed mission.

22.2 Maintainability

Having good maintainability for spacecraft is a very difficult task, and for most moments during this mission nigh impossible. The only moment when it is realistic to perform any maintenance on the spacecraft is when the ITS is in Earth orbit, as the necessary resources and tools are simply not available while in transfer or martian orbit. This makes for a very short time frame for maintainability, as the ITS will only be back in Earth orbit 1000 days after launching to Mars. Even then, options for maintainability are still limited in Earth orbit. In this subsection, the maintainability for the different parts of the ITS are explained.

22.2.1 Control Module

Due to the nature of this mission, options for maintenance are very limited. It therefore needs to be as close to certain as feasible that systems will last for the full mission duration, as no maintenance can be performed after departing Earth orbit.

The solar arrays will be replaced halfway through the mission duration, after 21 years. The design is made for a degradation of 10.5%, as this is the degradation after this timespan. It is possible that the solar arrays have to be maintained or replaced, which is possible as the solar arrays are a very external part of the spacecraft.

More internal maintenance will be harder, due to accessibility issues. In case of failure, however, the possibility for maintenance *should* exist, as otherwise the mission can be compromised. Any maintenance will cost precious time and money.

[59] https://www.geekwire.com/2019/bigelow-aerospace-nasa-test-earthbound-mockup-interplanetary-space-station/ *[cited 17 June 2021]*

[60] https://www.space.com/39752-bigelow-space-operations-private-space-stations.html *[cited 17 June 2021]*

[61] https://www.geekwire.com/2019/bigelow-aerospace-nasa-test-earthbound-mockup-interplanetary-space-station/ *[cited 17 June 2021]*

A check of all the subsystems must be performed every time the ITS is in LEO, as this is only once every 1000 days.

22.2.2 Propulsion

The propulsion system is a system that is difficult to repair due to the complexity of the engines. Due to the complexity, however, it cannot be ruled out that there will be some kind of failure. Therefore checks to this system are crucial and must be performed everytime the ITS is in LEO, and maintenance must also be possible.

22.2.3 Habitation Module

MARCO has a mission life of 10 round-trips (40 years), and since the habitation module will be in service after the first ten years (during which the cargo phase will take place), the habitation module will be needed for at least 30 years. The BA330 habitation module has a service-life of 20 years [2], thus after 15 years it would be ideal to decommission the first habitation module (when MARCO is in LEO) and make use of a second one. Other than the replacement of the habitation module, after every round-trip, general maintenance needs to be conducted on the module. This includes a wide range of tasks, from swapping the filters in the ECLSS to replacing broken components in the module. In case the habitation module encounters any malfunctions during the trip to Mars or back, the crew has the ability to perform EVA's through the control module and using the spare parts which are transported in the habitat, up to a certain degree of maintenance can be performed during the journey.

22.2.4 Structures

The structures of the ITS must be designed to withstand the loads experienced during the entire mission duration, including fatigue. It is always possible, however, that the structural integrity of the structure is compromised. When this is the case, action must be taken as soon as possible, before the fault becomes incorrigible. Checks must therefore be performed as regularly as possible: every time the ITS returns to LEO.

22.3 Safety

Transporting human beings to another planet involves many risks, and to even colonise this planet and have regular transport travelling the many million kilometres back and forth will give rise to even greater risks when it comes to the aspect of human safety. Therefore, safety is in the limelight of this project, and even the smallest variations in variables can mean the difference between life and death for the crew involved. If the mission does not contain enough safety aspects, it is likely that it will be cancelled as a result thereof.

Safety Aspects

Not only is it important to keep human lives safe but also public property and the environment are aspects to consider. For doing this, ESA has set up a list of facets of safety that are involved in the development of a project like MARCO-POLO. These are safety management, safety engineering, safety assessment and safety assurance[62].

Following up on this, ESA defines safety management as the continuous and iterative process over a project's lifespan in which safety risks of the project is minimised. Using safety management in the MARCO-POLO missions should ensure that all safety risks are identified, assessed, mitigated, and finally accepted and monitored as a part of the risk management. It is important that as many unknowns as possible can be identified and dealt with before the missions start, such that there are as few unknown safety compromising risks as possible.

The term safety engineering covers the implementation of processes and techniques in both the technical and organisational aspects of MARCO-POLO.

Safety assessment is based on the entire system as a whole and involves hardware, software and human factors. Based on these aspects, analyses are conducted in which the identification, control and verification of hazards and critical failure scenarios are being done.

Safety assurance is the aspect of monitoring the activities of safety management, engineering and assessment. It is used to add credibility to the outcome of the safety assessment.

Safety throughout the MARCO-POLO life cycle can be shown when considering three main phases; production, integration and operation.

[62] https://www.esa.int/Enabling_Support/Space_Engineering_Technology/Flight_Safety *[cited 17 June 2021]*

Production of MARCO-POLO

For the production of MARCO-POLO it is important to show the importance of safety by proper guidelines, such that the workers understand the importance of their safety, and the importance that their work has on the crew's safety. In the workplace several points can be made from the safety point of view.

- Elimination of hazardous materials in the work process. This minimises the risk of the workers to gain unrecoverable health issues do to their work on MARCO-POLO.
- Set limits on the exposure of certain work environments. This could limit the time employees are in an enclosed work environment or in an environment with limited ventilation, just to mention a two.
- Hire qualified workers. Doing this hinders that mistakes are made due to inadequate qualifications of workers.
- Include administrative protocols. This could for example be a protocol for decision making, such that any employee does not make a decision that he/she is not qualified to make.
- Use of protective equipment. This ensures the employees have the necessary equipment at their disposal and that it is enough to protect them from any harmful work environment.
- Implement adequate training. This could be in specific machinery as well as in common first aid in case an injury should occur.

Integration of MARCO-POLO

Integration is a critical point for this project. Therefore, some safety aspects are also mentioned concerning this.

- Only when MARCO-POLO has been proven fit for humans, will the crew be brought into LEO. This ensures that the crew will not arrive at a non-working spacecraft. Before the crew arrives, several tests have been performed on the crew functionalities. These tests are either carried out after the delivery of the cargo at Mars or at the moment when the habitation module has been attached.
- All life support systems will have redundancy. This ensures that the crew is not at risk even though one life support system fails.
- All components shall have passed the verification and validation phases. This ensures that all components will work as intended.
- All components shall be controllable from the mission control. This ensures that the control of MARCO-POLO can be upheld during uncrewed missions, and in case anything happens to the crew, mission control can seize control with MARCO-POLO.
- The crew shall have received adequate training. MARCO-POLO will consist of many different systems and it is important that the crew can navigate in each one of them.

Operation of MARCO-POLO

Finally is the operation of MARCO-POLO. Making it to this stage, MARCO-POLO has already proven to be capable of human space flight. This however does not mean that there are no safety issues during operations of MARCO-POLO. Spending around 1000 days in an unfriendly environment with limited volume, microgravity and large amounts of radiation will pose a safety thread for the crew involved. For the operational aspect the following points have been made.

- Radiation shielding will provide the required protection of the crew members. Based on **MARCO-MD-07** the crew has a maximum dose of radiation that they can expect to be exposed to throughout the mission cycle.
- MARCO-POLO will facilitate exercising. This will help minimise the effects microgravity has on the human body when exposed to it over a long time period.
- Both MARCO and POLO will contain an extensive first aid kit. This is included in case anything unexpected will happen to a crew member, and ensure that the crew member can receive the correct treatment.

- MARCO will have standard protocols for performing EVAs. Performing EVAs is physically and mentally exhausting and clear attaching points and procedures will keep the crew members safe while performing an EVA.
- The crew members must have the required physical abilities. The risk of having one crew member not being able to perform a certain critical task due to physical incapabilities should not be present as it can directly affect the safety of the other crew members.
- To ensure the continuous health of the people involved, these will regularly be monitored to ensure the continuous physical and mental health both throughout the mission, and after the mission has ended. Health checks are performed after the mission as well, as the human consequences of such a long mission in hostile environments are not yet known.

23 Production Plan

In this chapter, the preliminary production plan for MARCO-POLO is presented. Section 23.1 covers the production strategy adopted by the project, followed by a detailed preliminary manufacturing, assembly and integration (MAI) plan in Section 23.2. This chapter is concluded with the next activities for MARCO-POLO in a Gantt chart in Section 23.3 and in a flow diagram in Section 23.4.

23.1 Production Strategy

The following section, presents a general overview of the methods and policies implemented in the production of the reusable martian transportation system, MARCO-POLO. As stated in the baseline report [9], the lean manufacturing methodology will be applied during all production processes. The concept of lean manufacturing was developed for maximising the resource utilisation through minimisation of waste. This philosophy contains elements like cellular manufacturing, which involves grouping facilities to minimise transportation, waiting times and process time [26], and 5S, which is the practice of reducing waste and optimising workplaces. Implementing this will lead to higher productivity, safer work space, reduction of cost and better working morale [28].

For this project, lean manufacturing can be implemented when looking at the production and assembly plan. It should be made such that transportation and waiting times are minimised during production and assembly, and the facilities themselves should strive to implement the 5S practices [63] (sort, set in order, shine, standardise and sustain). Over time the 5S methodology will lead to several benefits; reduced costs. higher quality, increased productivity, greater employee satisfaction and a safer work environment.

A core principle in lean methodology is the removal of waste within an operation. As such in any business, one of the heaviest drains on profitability is waste. Lean waste can come in the form of time, material and labour. Out of the eight ways waste [64] could be produced only excess processing, waiting, inventory, and transportation are dependent on the system development team. While the remaining ways (defects, overproduction, motion, non-utilised talent) are not as intense on the lean manufacturing process of this system. First of all, this is a one time project (the system will be built once only) and no component will be produced in bulk. Secondly, third party contractors (for the launcher, habitation module and for smaller subsystems, etc.) are most likely to be responsible for executing the manufacturing processes effectively and on schedule. Nevertheless, the development team is expected to hire appropriate, credible contractors who can guarantee and deliver the expected quality within the desired time frames. Moreover, this planning is not exclusively for the manufacturing and assembling process; it also involves acquiring and delivering of all the necessary raw materials at the needed times and places. With this planning, the total transportation and production delays and waste must be minimised for the sake of the sustainable execution of this mission. Nevertheless, before all the raw materials are purchased and the actual part manufacturing is started, the compatibility of components must be verified, and it most be shown that the integrity of the design is as expected. For this reason a production process plan needs to be adopted as seen in Figure 50.

[63] https://www.5stoday.com/what-is-5s/ *[cited 16 June 2021]*
[64] https://www.machinemetrics.com/blog/8-wastes-of-lean-manufacturing *[cited 16 June 2021]*

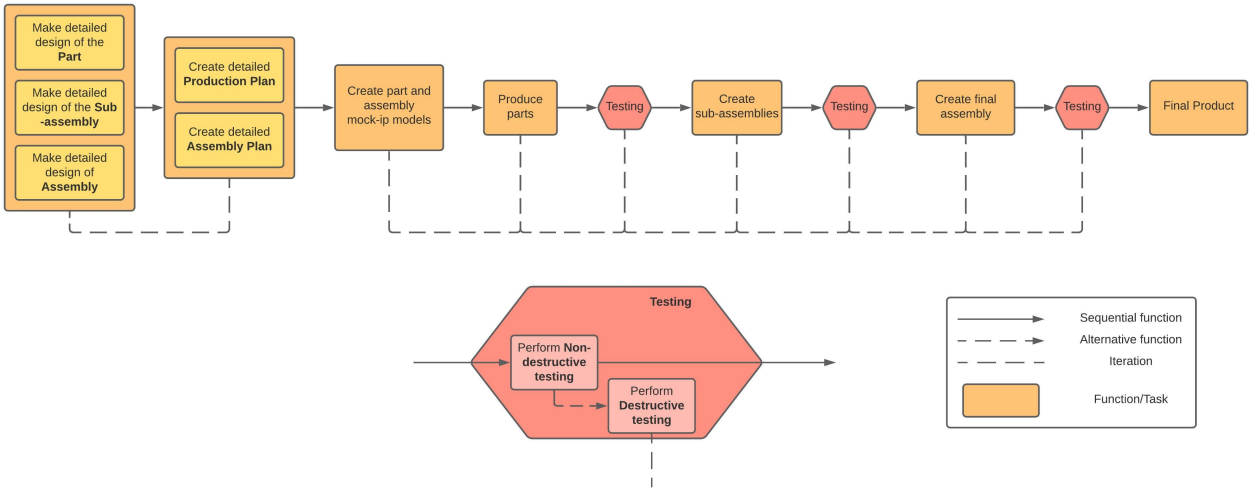

Figure 50: Production process plan.

23.2 Manufacturing, Assembly and Integration Plan

The MAI plan/flow diagram (as seen in Figure 51) gives a timely overview of the activities that are needed to produce MARCO-POLO. It starts with manufacturing all the parts/components of each subsystem of MARCO and POLO cargo, and then the subsystems are assembled and launched into LEO, where they will be integrated to form MARCO-POLO. It all starts with the control module, that forms the basis and then the propellant tanks are added along with the engines. Finally POLO cargo is launched and integrated with MARCO, and the uncrewed missions can begin.

Later in the mission crewed missions are needed and by that time the habitation module and POLO crew will have been manufactured in all its components. Once they are assembled, the habitation module will be launched into LEO, where it will dock with the control module and then POLO crew will dock to the habitation module, and the crewed mission phase can commence.

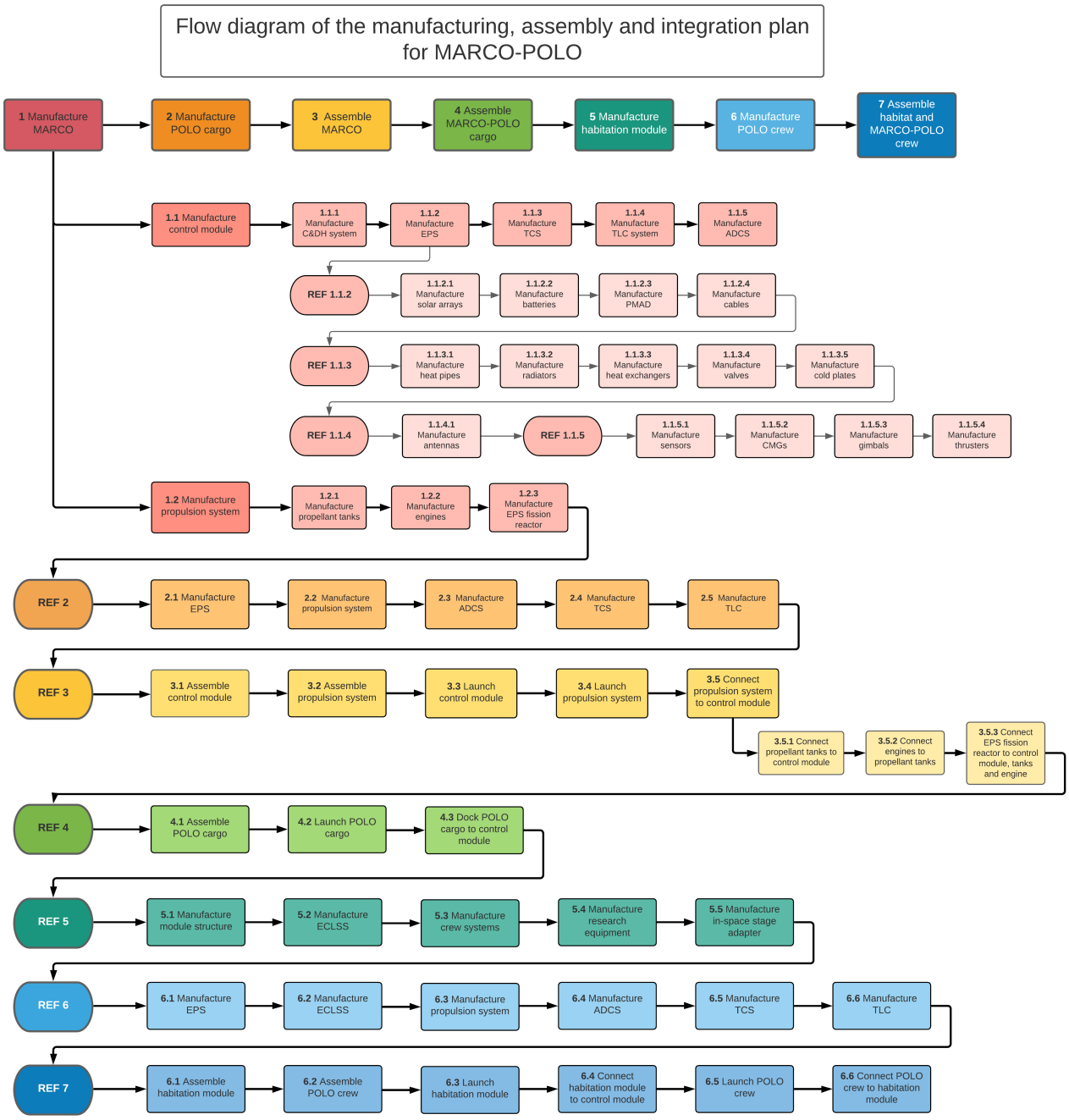

Figure 51: Flow diagram showing the steps of the MAI plan for MARCO-POLO.

23.3 Gantt chart

Bellow, all tasks to be done once this part of the project finished are shown. The first chart shows the overall whole process. The second chart shows an example of a mission, specifically the first cargo mission. The last chart shows all pre-operations tasks to be completed. More information on how these are organised is seen in subsection 23.4.

2021 2022 2023 2024 2025 2026 2027 2028 2029 2030 2031 2032 2033 2034 2035 2036 2037 2038 2039 2040 2041 2042 2043 2044 2045 2046 2047 2048 2049 2050 2051 2052 2053 2054 2055 2056 2057 2058 2059 2060 2061 2062 2063 2064 2065 2066 2067 2068 2069 2070 2071

Pre-Operations
Cargo 1
Cargo 2
Cargo 3
Crew 1
Crew 2
Crew 3
Crew 4
Extra 1
Extra 2
Extra 3
End of Life

2028	2029	2030	2031

11 12 01 02 03 04 05 06 07 08 09 10 11 12 01 02 03 04 05 06 07 08 09 10 11 12 01 02 03 04 05 06 07 08

Cargo 1
ΔV Burn from Earth
Orbit Maintenance
ΔV Burn to Mars
Orbit Maintenance
POLO lander Mars operations
POLO surface landing
Cargo unloaded from POLO
Cargo operations and power supply set-up
POLO launch to orbit
ΔV Burn from Mars
Orbit Maintenance
ΔV Burn to Earth

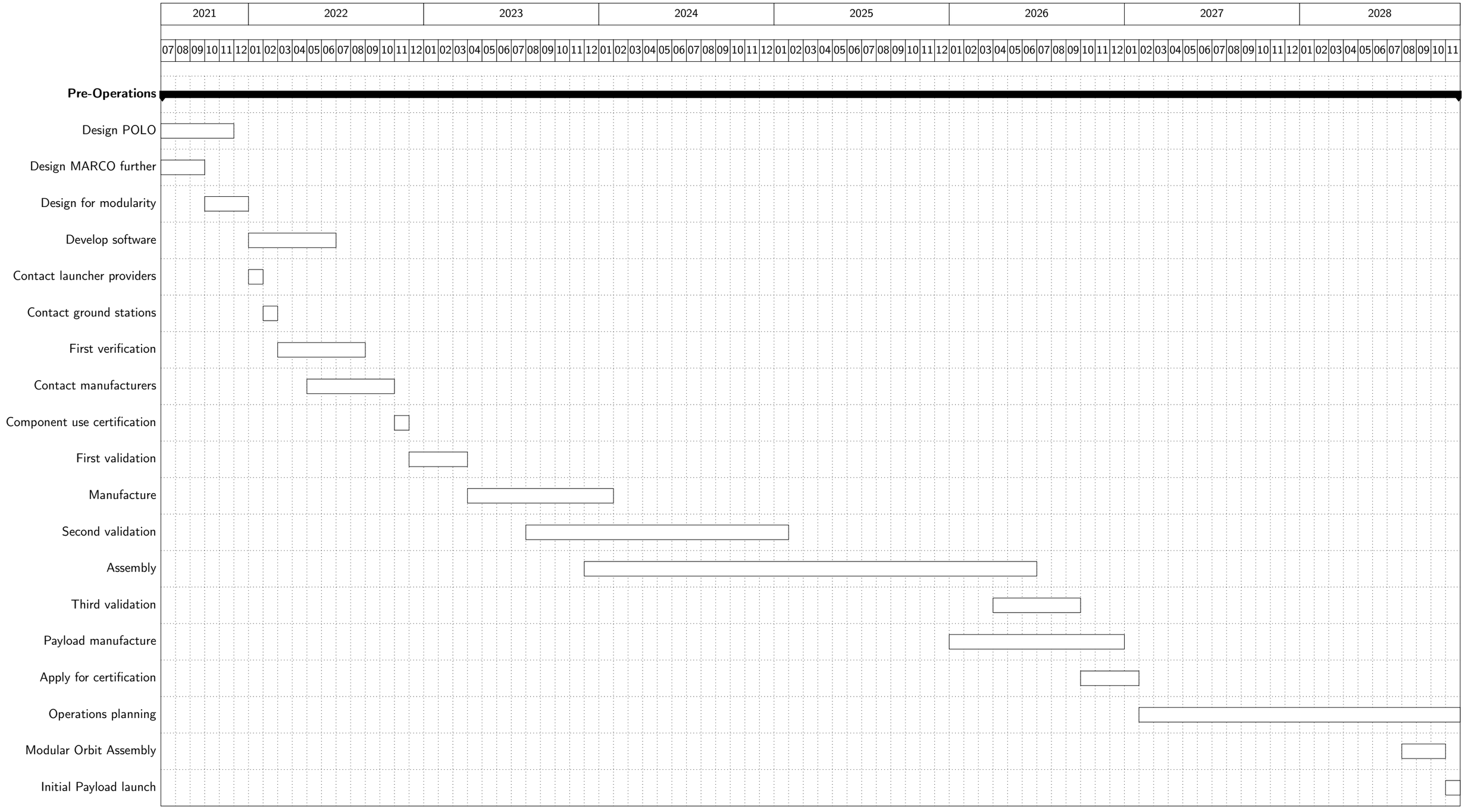
2021
2022
2023
2024
2025
2026
2027
2028
07 08 09 10 11 12 01 02 03 04 05 06 07 08 09 10 11 12 01 02 03 04 05 06 07 08 09 10 11 12 01 02 03 04 05 06 07 08 09 10 11 12 01 02 03 04 05 06 07 08 09 10 11 12 01 02 03 04 05 06 07 08 09 10 11 12 01 02 03 04 05 06 07 08 09 10 11 12 01 02 03 04 05 06 07 08 09 10 11
Pre-Operations
Design POLO
Design MARCO further
Design for modularity
Develop software
Contact launcher providers
Contact ground stations
First verification
Contact manufacturers
Component use certification
First validation
Manufacture
Second validation
Assembly
Third validation
Payload manufacture
Apply for certification
Operations planning
Modular Orbit Assembly
Initial Payload launch

23.4 Design and Development Logic

To give a logical overview of the activities that should be executed in the upcoming phases, a project design and development (PD&D) logic diagram has been made. The PD&D diagram shows the flow of the development of the project from the design phase to nominal operation, and is shown in Figure 52. As can be seen in the diagram, the project has been divided into several phases. Firstly, the engineering model is made and the components are certified. At this phase, development testing is being done on mock-ups and prototypes of the subsystems or components. In this phase new design concepts can be verified or verified concepts can be applied in a new configuration. Testing is integrated in the verification and validation steps.
Parallel to the engineering model phase is the planning phase. In this the practical planning regarding launchers and manufacturers is considered.

The next phase is the qualification model. Here a model with the same design, materials and tooling methods as the flight model will be made and verified at ultimate design conditions after which the model is discarded. That is the reason these tests can be expensive if they have to be run multiple times, hence it should only be done once the final design is considered ready. In case the tests are not passed, an iteration will take place.
Passing of the qualification model leads to the flight model, which needs to be verified in operational conditions. Once this is done, the system is ready for flight.

The final two phases includes pre-flight and in flight manufacturing and assembling. In the in flight phase, all the critical systems for the human crew will also be tested and validated to ensure they function when the crew docks. Several tests will be performed in flight and these are not limited to only the life support systems but cover all aspects of MARCO-POLO.

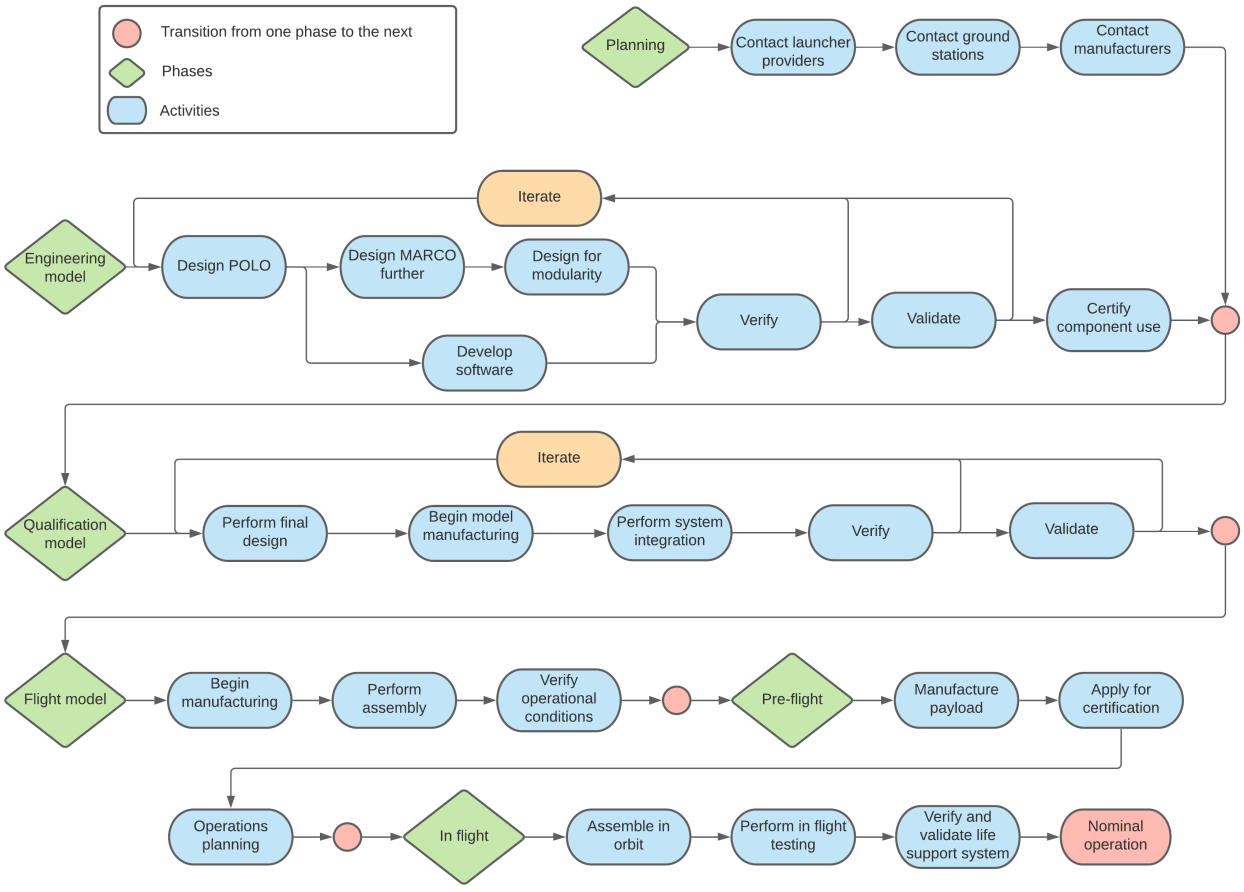

Figure 52: Project design and development logic diagram.

23.5 Cost Breakdown Structure

A final piece of information that is essential for potential investing agencies is a breakdown of the cost. In this section, the total cost of the entire 40-year project, as well as 7 years of development and manufacturing, and the disposal of the spacecraft are broken down.

In Figure 53, the cost breakdown structure is given in euros. Important to note is that the values given are based on rough estimates and therefore subject to change. The estimation method used is based on a paper by NASA that tried estimating the total cost of a future Mars mission, based on the Apollo program and ISS costs [58]. This paper determined that the development and manufacturing costs are 0.224 B$ per tonne. With a rounded up spacecraft dry mass of 150 tonnes, this results in 33.6 B$. This was set at 33.6 B€, in order to have a contingency of about 20%. As was determined in Chapter 19, the total estimated cost of the vehicle is around 5 B€. Subtracting this from 33.6 results in a development cost of 28.6 B€. The subdivision for the development cost was made assuming an equal distribution for management, planning, and systems engineering. Most resources will go towards research, verification, and validation of new technologies.

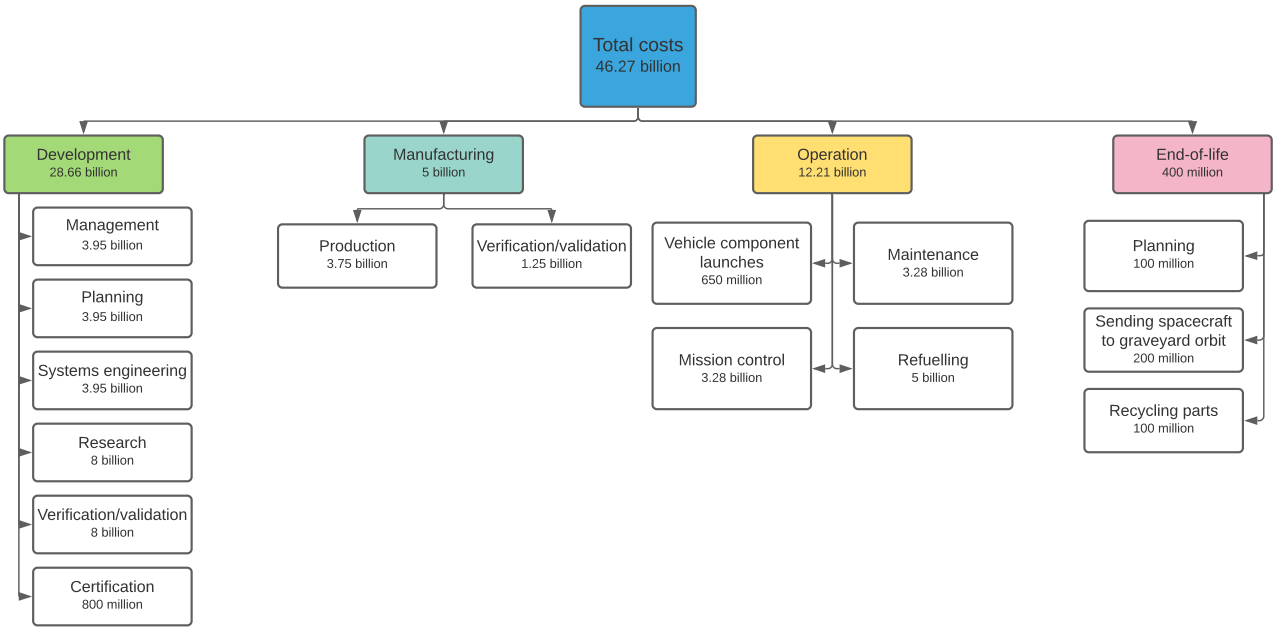

Figure 53: Cost breakdown structure.

24 Compliance Matrix

When designing a product based on certain requirements, it is important to ensure that the product actually meets these requirements. This is what the compliance matrix is for. In this chapter the three compliance matrices for the general requirements of the mission, MARCO and POLO, as stated in Section 6.2, are given. The requirement compliance matrix is a table containing all user requirements, and it is indicated whether the requirement is met or not, followed by the section in the report where the requirement is justified in. In case a requirement is not met, a justification for why the design does not meet the requirement, or which modifications would be required in order to meet the requirement needs to be stated.

For each the sub-system specific requirements, a compliance matrix is generated in their respective chapters.

Table 101: General requirements compliance.

ID	Compliance	Rationale
MARCH-H-06	✓	The MARCO-POLO missions does not interfere nor preclude any other missions to Mars.[65]
MARCH-H-10	-	The TU Delft Architecture team needs to ensure that the habitat stays within the budget.
MARCH-STS-04	✓	Section 9.4
MARCH-CR-01	✓	Section 19.
MARCH-LEG-01	✓	Section 23 and 21
MARCH-LEG-02	✓	Section 23 and 21

Table 102: MARCO requirements compliance.

ID	Compliance	Rationale
MARCO-PAY-01	X	Section 8.1.1
MARCO-CWS-01	✓	Section 16
MARCO-CWS-02	✓	Section 16
MARCO-CWS-03	✓	Section 16
MARCO-CWS-04	✓	Section 16
MARCO-CWS-05	-	Section 16
MARCO-SCH-01	✓	Section 9.3
MARCO-SCH-02	✓	Section 9.2
MARCO-SCH-03	-	The details of this requirement should be worked out by the TU Delft Architecture faculty. There will be two cargo missions to Mars in the 10-year time frame, and more than 100 t of payload will be brought to the surface by POLO cargo as seen in Section 8.1, which is enough based on the estimates given from the Rhizome habitat.
MARCO-MD-03	✓	Section 16 and 8.1
MARCO-MD-04	✓	Section 6.1
MARCO-MD-05	✓	Section 10.4.4 and 17
MARCO-MD-06	✓	Section 16
MARCO-MD-07	✓	Section 16
MARCO-MD-08	✓	Section 16
MARCO-SUS-01	✓	Section 9.4.
MARCO-SUS-02	✓	Section 4.1.
MARCO-SR-01	✓	Section 22.1.

Table 103: POLO requirements compliance.

ID	Compliance	Rationale
POLO-PAY-01	-	This relies on the design of the rovers and will be addressed in a separate report regarding the Rhizome habitat.
POLO-PAY-02	-	This relies on the design of the rovers and will be addressed in a separate report regarding the Rhizome habitat.
POLO-PAY-03	-	This relies on the design of the rovers and will be addressed in a separate report regarding the Rhizome habitat.
POLO-PAY-04	-	This relies on the design of the rovers and will be addressed in a separate report regarding the Rhizome habitat.
POLO-PAY-05	-	This relies on the design of the rovers and will be addressed in a separate report regarding the Rhizome habitat.
POLO-PAY-06	-	This relies on the design of the rovers and will be addressed in a separate report regarding the Rhizome habitat.
POLO-PAY-07	✓	Section 8.1
POLO-PAY-08	✓	Section 8.1
POLO-CWS-01	✓	Section 8.1.
POLO-CWS-02	✓	Section 8.1.
POLO-CWS-03	✓	Section 8.1.
POLO-CWS-04	✓	Section 8.1.
POLO-CWS-05	✓	Section 8.1.
POLO-SCH-01	✓	Section 8.1
POLO-SUS-01	✓	Section 4.1

25 Conclusion

10 students were given the task of designing a reusable, sustainable and easily re-configurable space transportation segment, which purpose was to serve a research and colonisation habitat on Mars. This was a part of the final bachelor project at the Aerospace faculty at TU Delft, and is related to the Rhizome project, that the university is currently conducting. The Design Synthesis Exercise (DSE) had a time frame of 11 weeks, and this report shows the finalised design of the space transportation segment called MARCO-POLO. The conclusion is divided into three aspects; the design, the execution of the DSE, and recommendations.

The Design

The design of MARCO-POLO was based on some preliminary user requirements, that were due to change throughout the project, as it was a part of a larger project being conducted. These user requirements stated that the maiden flight should be before 2030, the transportation segment should be reusable for 10 return trips to Mars, and that the habitat should be up and running within 10 years of the maiden flight. Based on these requirements, the number of launches for each phase, as well as the dates, were found. These include three cargo missions, four manned missions and three extra missions, with the maiden launch commencing in 2028 and the end-of-life being reached in 2070. This gives a total lifetime of 42 years for MARCO-POLO. However, the Rhizome habitat is only planned to be operable for 20 years. Hence, there are the three extra missions, which can support the Rhizome habitat beyond the 20 years or other unmanned or manned missions to Mars.

MARCO-POLO will consist of a main interplanetary segment called MARCO, and a lander called POLO. Furthermore, there will be two different types of POLO; namely one for the cargo missions and one for the crewed missions. POLO cargo can take significantly more payload with it and will remain on the surface of Mars to initially provide power to the rovers that will set up the habitat and keep the equipment safe from the martian environment.
MARCO will consist of 10 removable propellant tanks, a command module, a habitat for crewed missions and then POLO. The design embraces modularity, and it is possible to remove and add the propellant tanks and the habitat as wanted based on the mission needs.

Together with the design of MARCO-POLO, considerations regarding the market, sustainability, and safety have been incorporated. This includes aspects that the project would adhere to if it were to be executed. Elements that can be mentioned are that all the systems will have been tested before the human crew will dock, and almost no space debris will be generated. The only part of MARCO-POLO that will have to be disposed in outer space is the toxic nuclear waste, as it should not be brought back to Earth. The rest of MARCO-POLO will be brought back to Earth to be recycled.

Execution of the DSE

Taking it back to the beginning, the first thing to do was to get organised as a team. Each team member was given an organisational role as well as a main technical area of responsibility. This worked well and it was clear to all which team member had the final responsibility for each subsystem. A little flexibility was included into the roles, as it was decided that the detailed design would only include the interplanetary segment and not the landers, which made some subsystems redundant. Not all team members had the opportunity to meet up physically at the provided time slots and most of this design exercise was performed online, including communication with the tutor and coaches and the presentations. Overall, it worked out very well, and the quick response time from the tutor and coaches meant that the team was not stuck at any point during the design phase.
During some phases, online activities were also performed to unite the team and increase the morale of the team, which led to more efficient communication between team members and the feeling of a safer environment for the individual member.

Recommendations

This project was still affected by the outbreak of the corona virus, and this meant that a majority of the project was online. For future projects where such an integrated design process needs to be performed, it is recommended that the team members can meet up physically. This makes communication much clearer and changes in one part can easily be communicated and adapted to the other parts.

It is recommended to dedicate a complete detailed design phase for each lander. The two types of landers presented in this report are still at a very preliminary stage as the main focus was on MARCO. This means that for each of the

two types of landers, extensive designing still needs to be done before the project can move on to the next phases. Based on the outcome of these two design phases, MARCO will possibly receive small changes and needs to be reiterated alongside the two landers to secure a fully functional design.

Another important aspect that can be improved, involves how the trade-off was done. In this project, it was made on a subsystems basis, where each subsystem did its own trade-off, and then the results were combined into the concepts. Another approach, which is recommended to follow, would be to define the concepts first, and then for each concept do a trade-off of all the systems combined. This ensures that the coherence between subsystems are considered and that the design is indeed the optimal design and not just a design with optimal subsystems.

Verifying and validating a conceptual design of a spacecraft transporting humans to and from Mars cannot be done in great detail at this stage. The project is too large and too complex to develop appropriate tools to verify and validate the overall design within the given time frame. This is of course something that should be performed in greater detail at later stages of the project. The team included limited pieces on verification and validation for the subsystems in agreement with the tutor and coaches, but for work beyond the DSE, it is recommended that also these are worked out in greater detail and that dedicated tools are developed for verifying and validating the design of the subsystems.

Following the recommendations on the design, there are also some points to be made on executing the DSE. For the team performance and the relations between team members, it is recommended to perform team activities when no stressful deadline is near. Performing these activities benefited the internal communication and understanding of one another. Especially in an online environment, where you cannot see each other, communication can easily become destructive and cause tensions between team members.
The next point is to have understanding for the special circumstances. Most of the project is being done from home and this environment is unlike usual working environments, and therefore some flexibility should be shown from all the group members. In this design team, some members had long transportation times for the physical sessions, which caused them to be inactive outside the dedicated break times, while others had to leave a little earlier for training. Having the understanding for each other and the situation at hand, and allowing for a little flexibility on when the active working hours are actually being done, improves the team performance and the relation between team members.

References

[1] A. Cervone, 'AE2230-II Propulsion and Power'.

[2] D. Smitherman and A. Schnell, 'Gateway Lunar Habitat Modules as the Basis for a Modular Mars Transit Habitat', in *2020 IEEE Aerospace Conference*, 2020, pp. 1–12.

[3] A. H. Dida, 'Design and Modeling of useful Tool for Satellite Solar Array Preliminary Sizing and Power System Analysis', in *2019 European Space Power Conference (ESPC)*, 2019, pp. 1–4. DOI: 10.1109/ESPC.2019.8932060.

[4] F. Krause *et al.*, 'Performance of Commercial Li-Ion Cells for Future NASA Missions and Aerospace Applications', Apr. 2021.

[5] B. Zandbergen, *AE1222-II: Aerospace Design & Systems Engineering Elements I - Part: Spacecraft (bus/ platform) design and sizing*, 6th ed. Delft, Netherlands: TU Delft, 2021.

[6] A. Cervone and B. Zandbergen, *AE2230-II: Propulsion & Power Electrical Power Systems for Aerospace Vehicles*. Delft, Netherlands: TU Delft, 2017.

[7] A. Cervone, 'Project Guide - Design Synthesis Exercise Space Transportation Segment for a Martian Autarkic Research and Colonization Habitat', TU Delft, ESA, Project Guide, 2021.

[8] L. Bruun *et al.*, 'Mid-term Report - MARCO-POLO Space Transportation System - DSE Group 7', TU Delft, May 2021.

[9] ——, 'Baseline Report - Space Transportation Segment for a M.A.R.C.H. - DSE Group 7', TU Delft, May 2021.

[10] H. R. Zweig and R. Hundal, 'NERVA-Derived Nuclear Thermal Propulsion Dual Mode Operation', Rockwell International, 1994.

[11] Boeing, 'Active Thermal Control System (ATCS) Overview'. [Online]. Available: `https://www.nasa.gov/pdf/473486main_iss_atcs_overview.pdf`.

[12] F. C. Vargas *et al.*, 'Final Report - Arcadian Renewable Energy System', TU Delft, May 2020.

[13] E. Zampino and R. Cataldo, 'The challenge of space nuclear propulsion and power systems reliability', NASA Glenn Research Center, Feb. 2004.

[14] L. Gang *et al.*, 'Research on high accuracy, long life, and high reliability technique of control moment gyroscope', Aug. 2016.

[15] H. Brandhorst Jr. and J. Rodiek, 'Space solar array reliability: A study and recommendations', Space Research Institute, Auburn University, Dec. 2005.

[16] P. Sforza and M. Shooman, 'A Safety and Reliability Analysis for Space Nuclear Thermal Propulsion Systems', Polytechnic University Brooklyn, 1993.

[17] R. Oliveira, 'Numerical study of Earth-Mars trajectories with lunar gravity assist manoeuvres', Universidade da Beira Interior, Tech. Rep., Dec. 2017.

[18] J. Kawaguchi, 'On The Lunar and Heliocentric Gravity Assist Experienced in The PLANET-B ("Nozomi")', Tech. Rep.

[19] J. Clough *et al.*, 'Tie Tube Heat Transfer Modeling for Bimodal Nuclear Thermal Rockets', Department of Aerospace Engineering, University of Maryland, Tech. Rep., 2007.

[20] B. G. Schnitzler, 'Small Reactor Designs Suitable for Direct Nuclear Thermal Propulsion: Interim Report', Idaho National Laboratory, Tech. Rep., Jan. 2012.

[21] R. Martin, J. A. Caffrey and M. G. Houts, 'Modeling Gamma and Neutron Heating to a Liquid Hydrogen Tank for Nuclear Thermal Propulsion with RELAP5-3Dt', NASA Marshall Space Flight Center, Tech. Rep., Aug. 2019.

[22] J. Caffrey, 'Radiation Shielding for Space Nuclear Propulsion', Tech. Rep., Aug. 2017.

[23] D. Poeth, 'Summary of Lithium Hydride Material Performance and Issues in a Space Nuclear Reactor Shield', Tech. Rep., 2005.

[24] R. Woolley and C. Whetsel, 'On The Nature of Earth-Mars Porkchop Plots', NASA, Tech. Rep.

[25] A. Concini and J. Toth, 'The future of the European space sector', European Investment Bank, publication, May 2019.

[26] R. Sundar, A. Balaji and R. S. Kumar, 'A Review on Lean Manufacturing Implementation Techniques', *Procedia Engineering*, vol. 97, pp. 1875–1885, 2014.

[27] H. Bakker, *Management of Engineering Projects - People Are Key*. Nijkerk: NAP, 2014.

[28] S. Jain, G. Chaudhry, M. Talha and R. Sharma, *"5 s Housekeeping"-A Lean Tool: A Case Study*, ser. Lecture Notes in Mechanical Engineering. 2021, pp. 285–295.

[29] D. Byford, J. Goppert and T. Gangale, 'Optimal Location of Relay Satellites for Continuous Communication with Mars', 2007.

[30] T. Pham and J. Liao, 'Performance Analysis of Operational Ka-band Link with Kepler', 2016.

[31] F. Davarian, S. Shambayati and S. Slobin, 'Deep space Ka-band link management and Mars Reconnaissance Orbiter: long-term weather statistics versus forecasting', *Proceedings of the IEEE*, Dec. 2004.

[32] C. Berrou, A. Glavieux and P. Thitimajshima, 'Near Shannon limit error-correcting coding and decoding: Turbo-codes.', in *Proceedings of ICC '93 - IEEE International Conference on Communications*, May 1993.

[33] F. J. Arias, 'On the Use of a Pulsed Nuclear Thermal Rocket for Interplanetary Travel', Publication, 2016.

[34] R. Werka, R. Clark, R. Sheldon and T. Percy, 'Final Report: Concept Assessment of a Fission Fragment Rocket Engine (FFRE) Propelled Spacecraft', Publication, Sep. 2012.

[35] J. L. Finseth, 'Rover nuclear rocket engine program: Overview of rover engine tests', NASA, Feb. 1991.

[36] United Nations Office for Outer Space Affairs, *United Nations Treaties and Principles on Outer Space and Related General Assembly Resolutions*. New York: United Nations, 2008.

[37] S. K. Borowski, D. R. McCurdy and T. W. Packard, 'Conventional and Bimodal Nuclear Thermal Rocket (NTR) Artificial Gravity Mars Transfer Vehicle Concepts', in *50th AIAA/ASME/SAE/ASEE Joint Propulsion Conference*. DOI: 10.2514/6.2014-3623.

[38] J. Taylor, D. K. Lee and S. Shambayati, 'Mars Reconnaissance Orbiter Telecommunications', Sep. 2006.

[39] N. Chahat, B. Cook, H. Lim and P. Estabrook, 'All-Metal Dual-Frequency RHCP High-Gain Antenna for a Potential Europa Lander', Oct. 2018.

[40] J. H. Yuen, 'Deep Space Communications: An Introduction', Oct. 2014.

[41] C. Ho, S. Slobin, M. Sue and E. Njoku, 'Mars Background Noise Temperatures Received by Spacecraft Antennas', *Interplanetary Network Progress Report*, Jan. 2002.

[42] T. Cornish, T. T. Pham and C. Chang, '34-m and 70-m Command', Dec. 2014.

[43] A. Dinardi, 'High Performance Green Propulsion (HPGP)', Mar. 2013.

[44] D. R. Williams, 'Mars Fact Sheet', NASA, Nov. 2020.

[45] S. Surampudi, 'Overview of the Space Power Conversion and Energy Storage Technologies', NASA, Jan. 2011.

[46] E. Schwanbeck and P. Dalton, 'International Space Station Lithium-ion Batteries for Primary Electric Power System', in *2019 European Space Power Conference (ESPC)*, 2019, pp. 1–1.

[47] P. Dalton, E. Bowens, T. North and S. Balcer, 'International Space Station Lithium-Ion Battery Status', NASA, Nov. 2019.

[48] F. C. Krause, J. P. Ruiz, S. C. Jones, E. J. Brandon, E. C. Darcy, C. J. Iannello and R. V. Bugga, 'Performance of Commercial Li-Ion Cells for Future NASA Missions and Aerospace Applications', *Journal of The Electrochemical Society*, vol. 168, no. 4, p. 040 504, Apr. 2021.

[49] B. Kenny, R. Cull and M. Kankam, 'An analysis of space power system masses', Feb. 1990.

[50] R. Dempsey, 'The International Space Station; Operating an Outpost in the New Frontier', NASA, 2017.

[51] J. Chapel, T. Bevacqua, D. Stancliffe, G. Ramsey, T. Rood, D. Freesland, J. Fiorello and A. Krimchansky, 'GOES-R Spacecraft Verification and Validation compared with Flight Results', Lockheed Martin Corporation, 2019.

[52] C. B. F. Ensworth, 'Thrust Vector Control For Nuclear Thermal Rockets', NASA Glenn Research Center, Oct. 2013.

[53] M. L. Belair, C. S. Sarmiento and T. M. Lavelle, 'Nuclear Thermal Rocket Simulation in NPSS', NASA Glenn Research Center, Jul. 2013.

[54] C. Gurrisi, R. Seidel, S. Dickerson and S. Didziulis, 'Space Station Control Moment Gyroscope Lessons Learned', May 2010.

[55] T. Balint, 'Nuclear Systems for Mars Exploration', 2004.

[56] S. K. Borowski *et al.*, 'Affordable Development and Demonstration of a Small Nuclear Thermal Rocket (NTR) Engine and Stage: How Small Is Big Enough?', Dec. 2016.

[57] R. Webb, 'Propulsion Cost Model (PCM)', Mar. 2019.

[58] H. W. Jones, 'Humans to Mars Will Cost About "Half a Trillion Dollars" and Life Support Roughly Two Billion Dollars', Jul. 2016.

[59] NASA, 'On-Orbit Assembly, Modeling, and Mass Properties Data Book', Jan. 2008.

[60] Airbus, 'CMG 75-75 S. A compact, cost-effective, high performance Control Momentum Gyroscope solution for large satellites', 2020.

[61] NASA, 'FY 2022 Budget Estimates', 2021.

[62] J. R. Wertz, D. F. Everett and J. J. Puschell, *Space Mission Engineering: The New SMAD*. Hawthorne, CA: Microcosm Press, 2011.

[63] K. Nagai, T. Yuri, T. Ogata, O. Umezawa, K. Ishikawa, T. Nishimura, T. Mizoguchi and Y. Ito, 'Cryogenic Mechanical Properties of Ti-6Al-4V Alloys with Three Levels of Oxygen Content', *ISIJ International*, vol. 31, no. 8, pp. 882–889, 1991. DOI: 10.2355/isijinternational.31.882.

[64] B. Zandbergen, *AE1222-II: Aerospace Design & Systems Engineering Elements I - Part: Launch Vehicle design and sizing*, 6th ed. Delft, Netherlands: TU Delft, Nov. 2019.

[65] D. A. Smith, 'Space Launch System (SLS) Mission Planner's Guide', 19th Dec. 2018.

[66] C. McLean, G. Mills, M. Riesco, D. Plachta, M. Meyer and E. Hurlbert, 'Long Term Space Storage and Delivery of Cryogenic Propellants for Exploration', in *44th AIAA/ASME/SAE/ASEE Joint Propulsion Conference & Exhibit*. DOI: 10.2514/6.2008-4853.

[67] H. ter Brake and G. Wiegerinck, 'Low-power cryocooler survey', *Cryogenics*, vol. 42, no. 11, pp. 705–718, 2002, ISSN: 0011-2275.

[68] NASA, 'NASA Docking System (NDS) Interface Definitions Document (IDD)', 2018.

[69] ASME, *Appendix 13, Vessels of Noncircular Cross Section*, ASME, 2001, ch. 13.

[70] T. J. Rudman and K. L. Austad, 'The Centaur Upper Stage Vehicle', Dec. 2002.

[71] D. Smitherman and A. Schnell, 'Gateway Lunar Habitat Modules as the Basis for a Modular Mars Transit Habitat', in *2020 IEEE Aerospace Conference*, 2020, pp. 1–12.

[72] H. M. Van Rensburg, 'An Infrared Earth Horizon Sensor for a LEO Satellite', Mar. 2008.

[73] E. Seedhouse, *Bigelow Aerospace; Colonizing Space One Module at a Time*, 1st ed. Switzerland: Springer, 2015.

[74] E. W. Schmidt, G. T. Brewster and G. E. Cain, 'Mars Lander Retro Propulsion.', Publication, Oct. 1999.

[75] N. S. Bedrossian, S. Bhatt, W. Kang and I. M. Ross, 'Zero-propellant maneuver guidance.', publication, Nov. 2009.

[76] C. Buchner, R. H. Pawelke, T. Schlauf, A. Reissner and A. Makaya, 'A new planetary structure fabrication process using phosphoric acid', *Acta Astronautica*, vol. 143, pp. 272–284, 2018, ISSN: 0094-5765.

[77] A. M. Korzun and R. D. Braun, 'Performance Characterization of Supersonic Retropropulsion for High-Mass Mars Entry Systems', *Journal of Spacecraft and Rockets*, vol. 47, no. 5, pp. 836–848, 2010. DOI: 10.2514/1.49803.

[78] C. G. Lorenz and Z. R. Putnam, 'Entry Trajectory Options for High Ballistic Coefficient Vehicles at Mars', *Journal of Spacecraft and Rockets*, vol. 56, no. 3, pp. 811–822, 2019. DOI: 10.2514/1.A34262.

[79] T. P. Polsgrove, M. A. Simon, J. Waggoner, D. V. Smitherman, R. L. Howard and T. K. Percy, 'Transit Habitat Design for Mars Exploration', publication, Sep. 2018.

[80] G. Swinerd, *How Spacecraft Fly*. New York: Springer, 20th Oct. 2008.

Appendices

A Astrodynamics

A.1 Second Cargo Mission

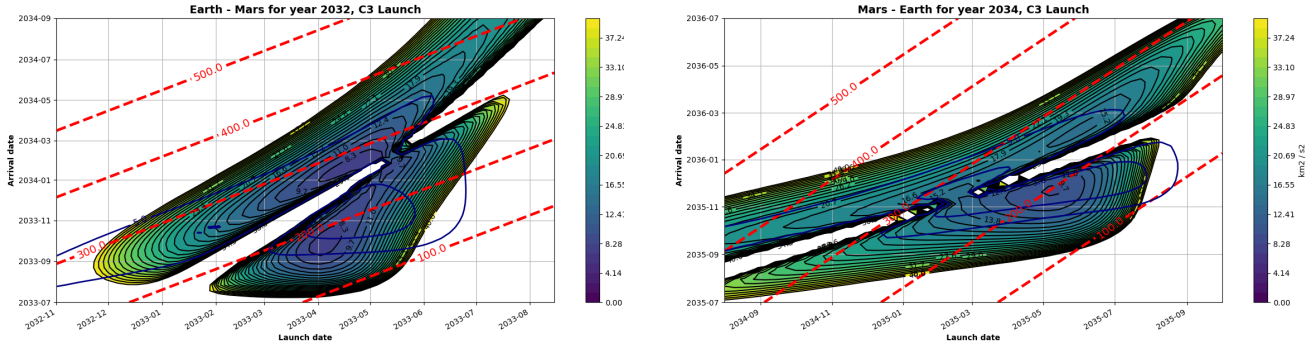

(a) Porkchop plot for the launch window in 2033.

(b) Porkchop plot for the launch window in 2035.

Figure 54: The porkchop plots for the second cargo mission.

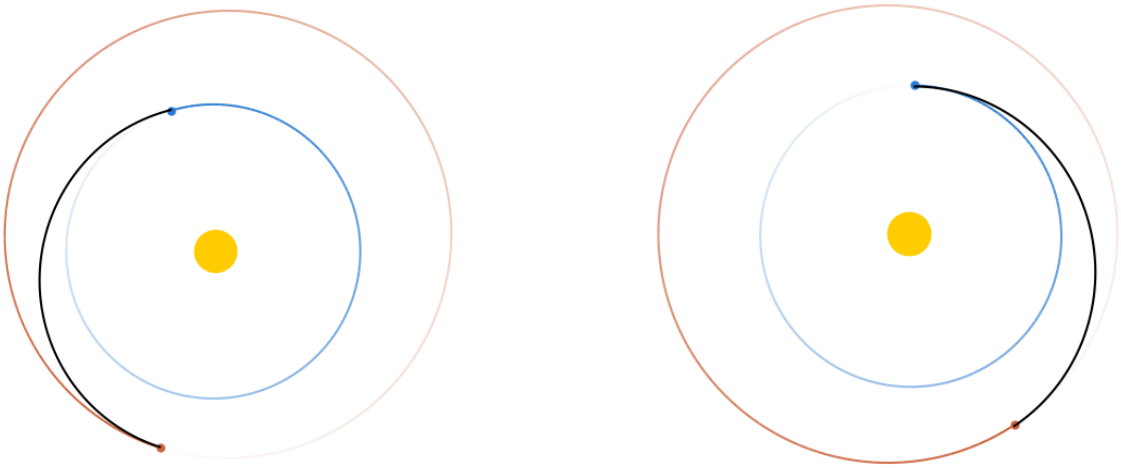

(a) Mapping of the trajectory to Mars.

(b) Mapping of the trajectory to Earth.

Figure 55: The trajectories of the second cargo mission.

Table 104: Mission values for the second mission.

Destination	ΔV [km s^{-1}]	**Launch Date**	**Arrival Date**	**Duration [days]**
Mars	5.656	20-04-2033	04-11-2033	198
Earth	5.669	14-05-2035	27-11-2035	197
Total	11.325	20-04-2033	27-11-2035	951

A.2 Third Cargo Mission

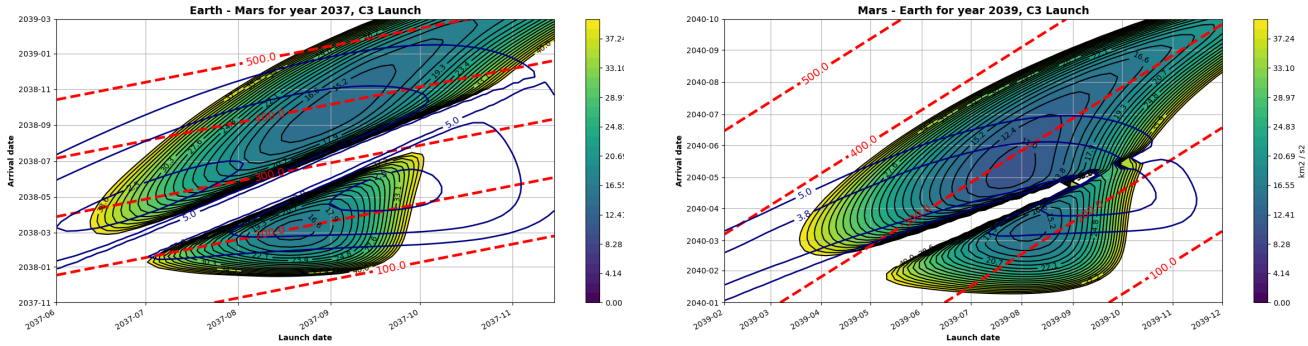

(a) Porkchop plot for the launch window in 2037.

(b) Porkchop plot for the launch window in 2039.

Figure 56: The porkchop plots for the third cargo mission.

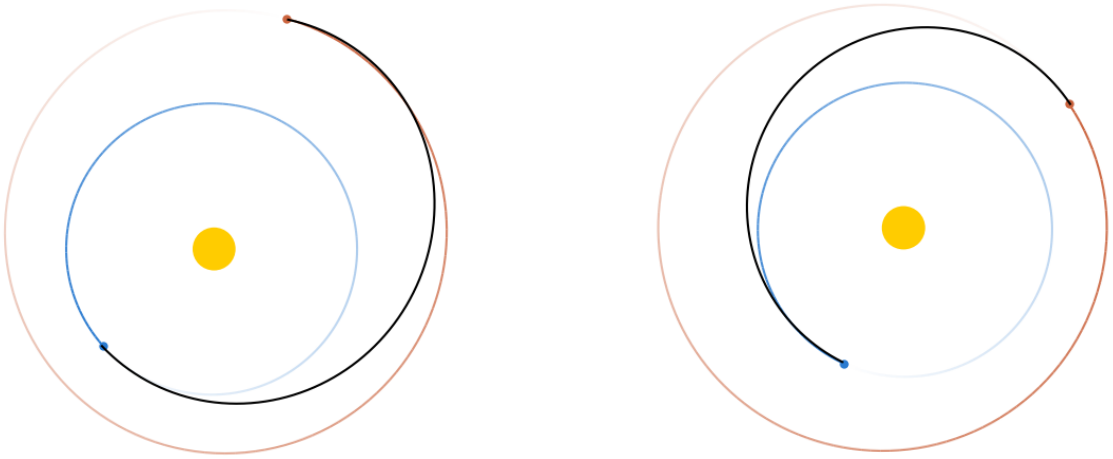

(a) Mapping of the trajectory to Mars.

(b) Mapping of the trajectory to Earth.

Figure 57: The trajectories of the third cargo mission.

Table 105: Mission values for the third mission.

Destination	ΔV [km s^{-1}]	**Launch Date**	**Arrival Date**	**Duration [days]**
Mars	5.701	14-08-2037	26-07-2038	345
Earth	5.667	24-07-2039	03-05-2040	284
Total	11.368	14-08-2037	03-05-2040	993

A.3 First Manned Mission

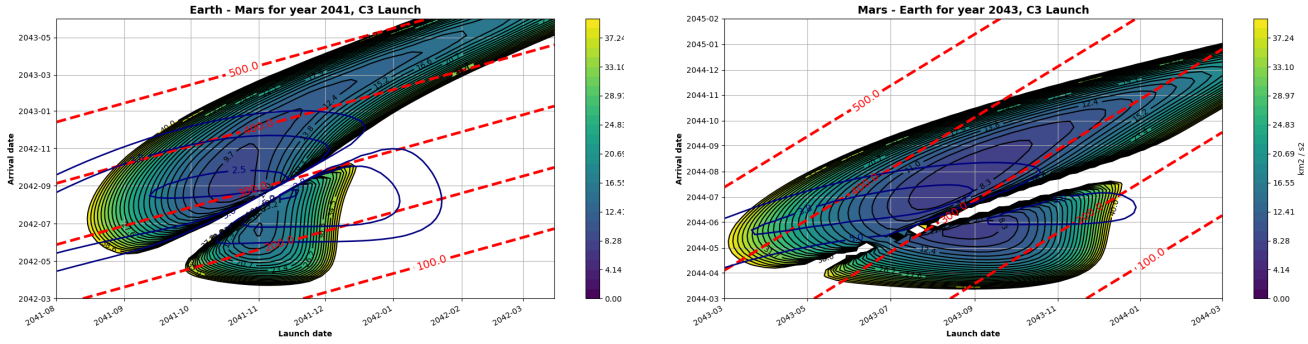

(a) Porkchop plot for the launch window in 2041.

(b) Porkchop plot for the launch window in 2043.

Figure 58: The porkchop plots for the first manned mission.

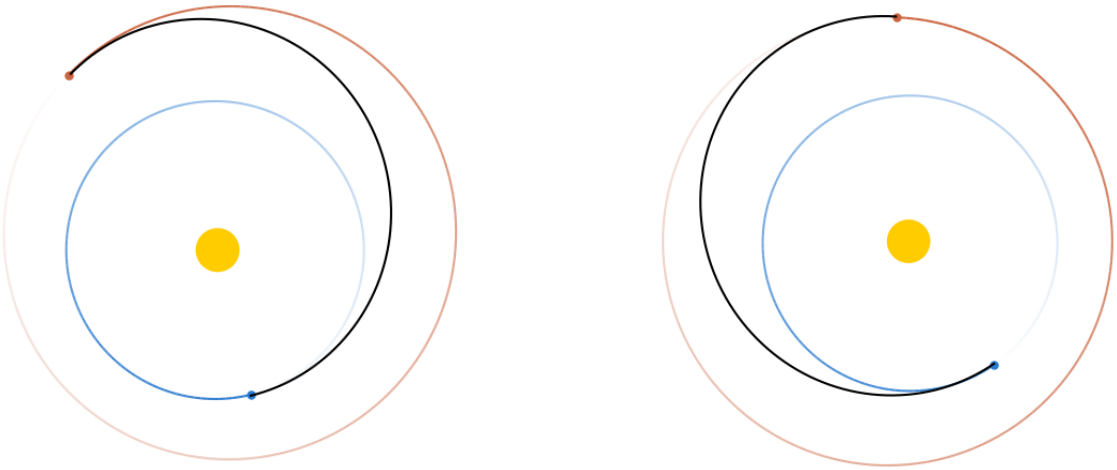

(a) Mapping of the trajectory to Mars.

(b) Mapping of the trajectory to Earth.

Figure 59: The trajectories of the first manned mission.

Table 106: Mission values for the first manned mission.

Destination	ΔV [km s^{-1}]	**Launch Date**	**Arrival Date**	**Duration [days]**
Mars	5.228	18-10-2041	03-09-2042	320
Earth	5.560	04-08-2043	02-07-2044	333
Total	10.788	18-10-2041	02-07-2044	988

A.4 Second Manned Mission

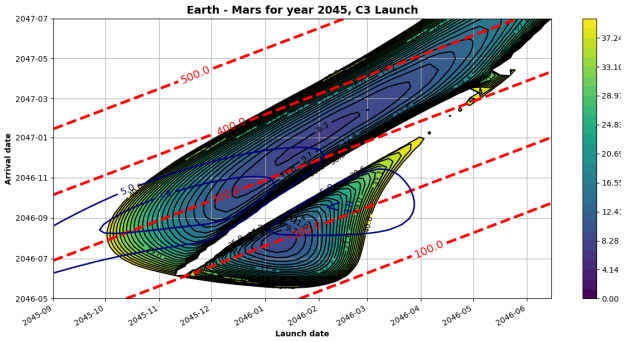

(a) Porkchop plot for the launch window in 2045.

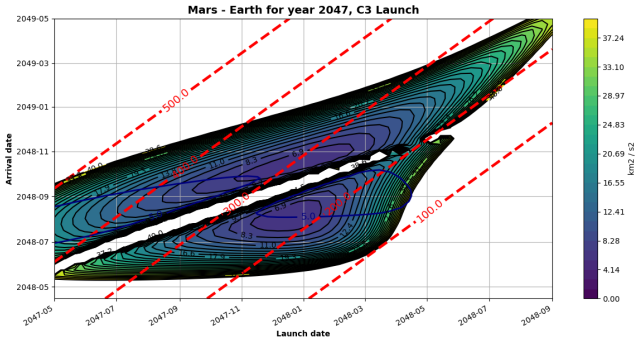

(b) Porkchop plot for the launch window in 2047.

Figure 60: The porkchop plots for the second manned mission.

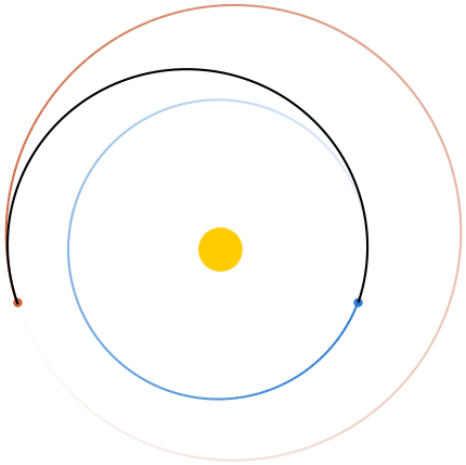

(a) Mapping of the trajectory to Mars.

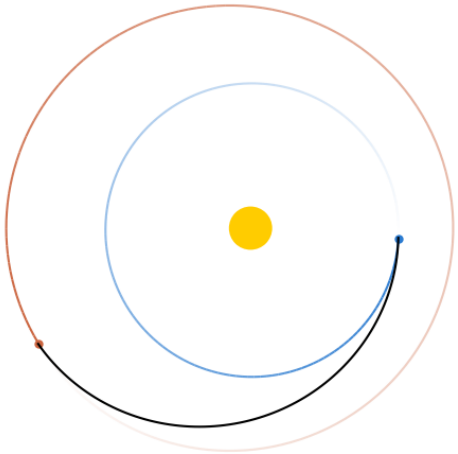

(b) Mapping of the trajectory to Earth.

Figure 61: The trajectories of the second manned mission.

Table 107: Mission values for the the second manned mission.

Destination	ΔV [km s^{-1}]	**Launch Date**	**Arrival Date**	**Duration [days]**
Mars	5.728	09-12-2045	25-09-2046	290
Earth	5.696	15-01-2048	25-08-2048	223
Total	11.424	09-12-2045	25-08-2048	990

A.5 Third Manned Mission

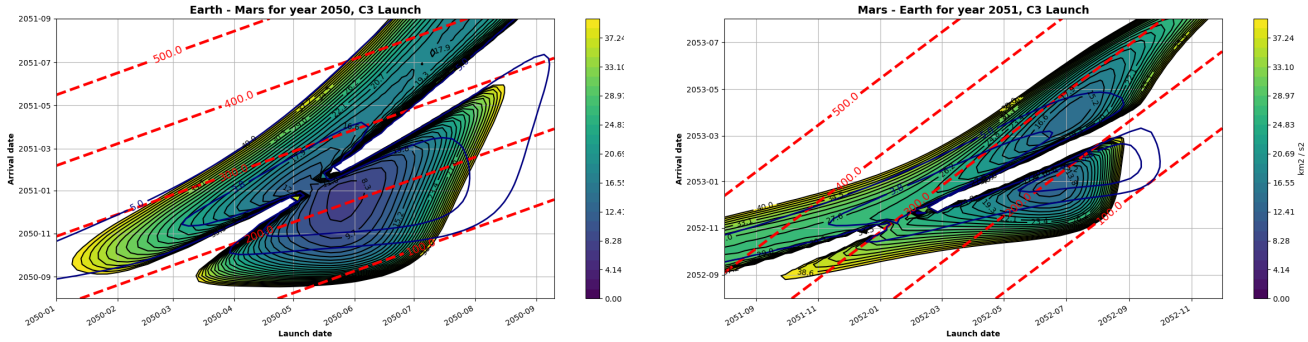

(a) Porkchop plot for the launch window in 2050.

(b) Porkchop plot for the launch window in 2051.

Figure 62: The porkchop plots for the third manned mission.

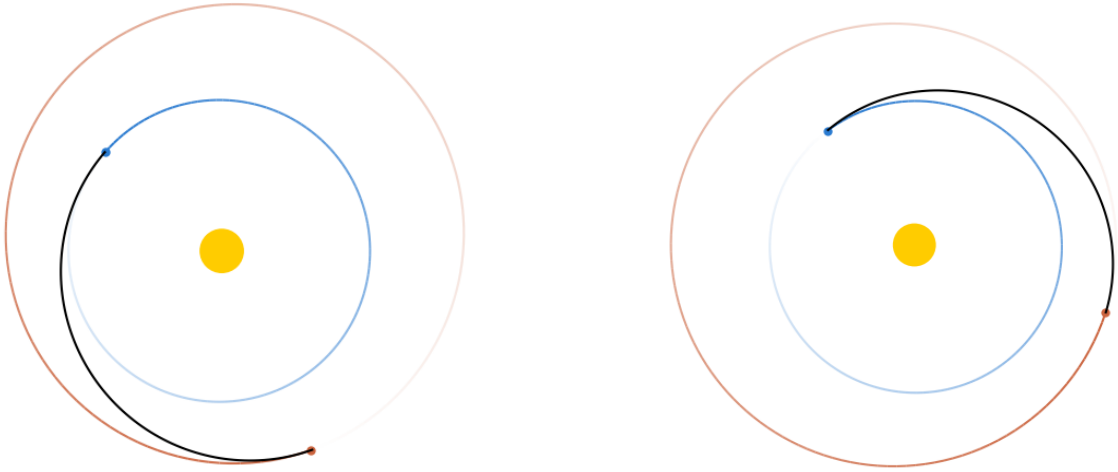

(a) Mapping of the trajectory to Mars.

(b) Mapping of the trajectory to Earth.

Figure 63: The trajectories of the third manned mission.

Table 108: Mission values for the third manned mission.

Destination	ΔV [km s^{-1}]	**Launch Date**	**Arrival Date**	**Duration [days]**
Mars	5.390	25-05-2050	16-12-2050	205
Earth	6.004	24-06-2052	04-01-2053	194
Total	11.394	25-05-2050	04-01-2053	955

A.6 Fourth Manned Mission

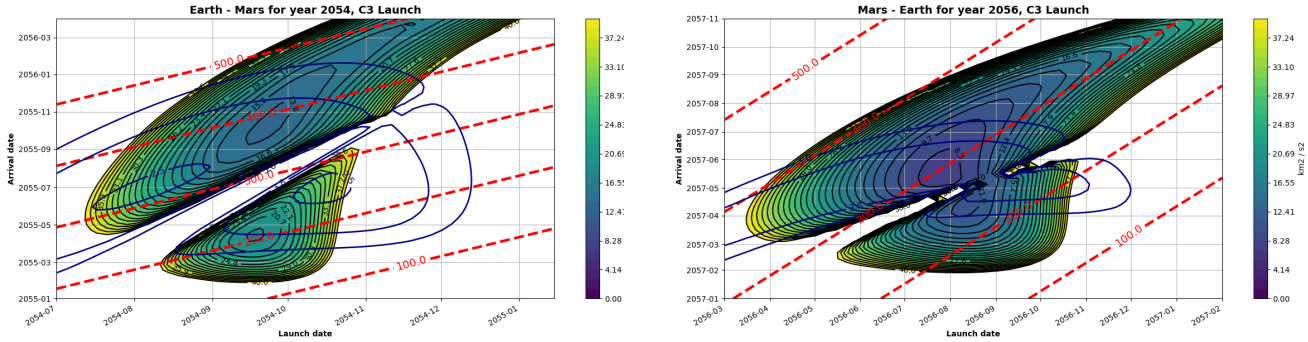

(a) Porkchop plot for the launch window in 2054.

(b) Porkchop plot for the launch window in 2056.

Figure 64: The porkchop plots for the fourth manned mission.

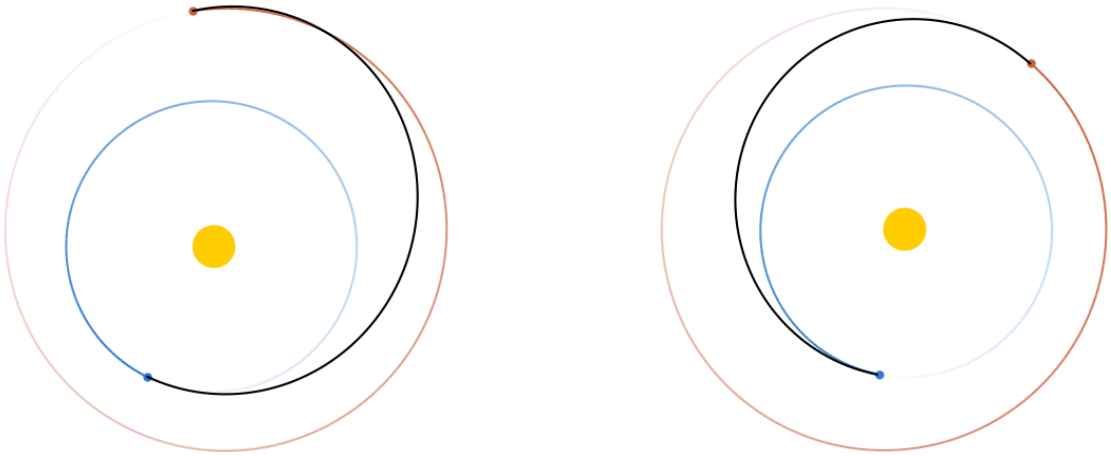

(a) Mapping of the trajectory to Mars.

(b) Mapping of the trajectory to Earth.

Figure 65: The trajectories of the fourth manned mission.

Table 109: Mission values for the fourth manned mission.

Destination	ΔV [km s^{-1}]	**Launch Date**	**Arrival Date**	**Duration [days]**
Mars	5.607	07-09-2054	21-08-2055	348
Earth	5.369	23-07-2056	17-05-2057	298
Total	10.977	07-09-2054	17-05-2057	993

A.7 First Extra Mission

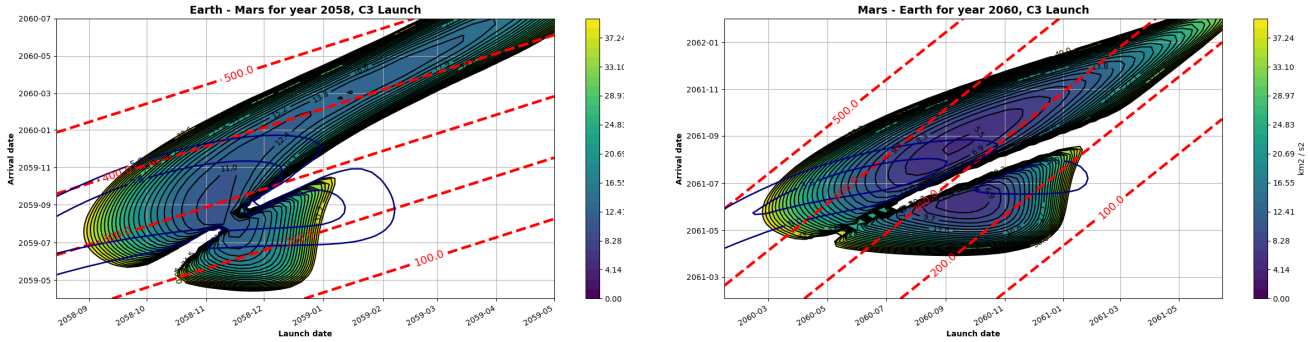

(a) Porkchop plot for the launch window in 2058.

(b) Porkchop plot for the launch window in 2060.

Figure 66: The porkchop plots for the first extra mission.

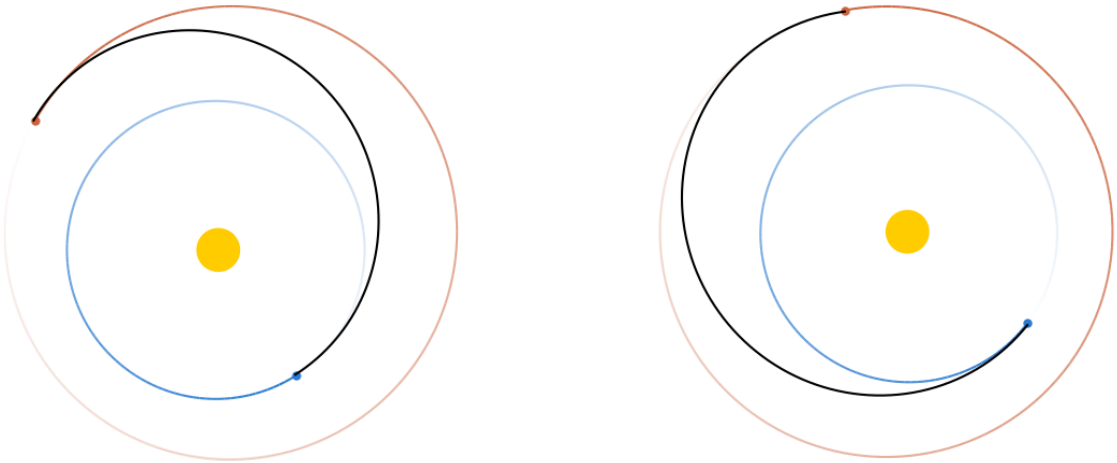

(a) Mapping of the trajectory to Mars.

(b) Mapping of the trajectory to Earth.

Figure 67: The trajectories of the first extra mission.

Table 110: Mission values for the first extra mission

Destination	ΔV [km s^{-1}]	**Launch Date**	**Arrival Date**	**Duration [days]**
Mars	5.523	07-11-2058	06-09-2059	303
Earth	5.433	02-08-2060	22-07-2061	354
Total	10.956	07-11-2058	22-07-2061	988

A.8 Second Extra Mission

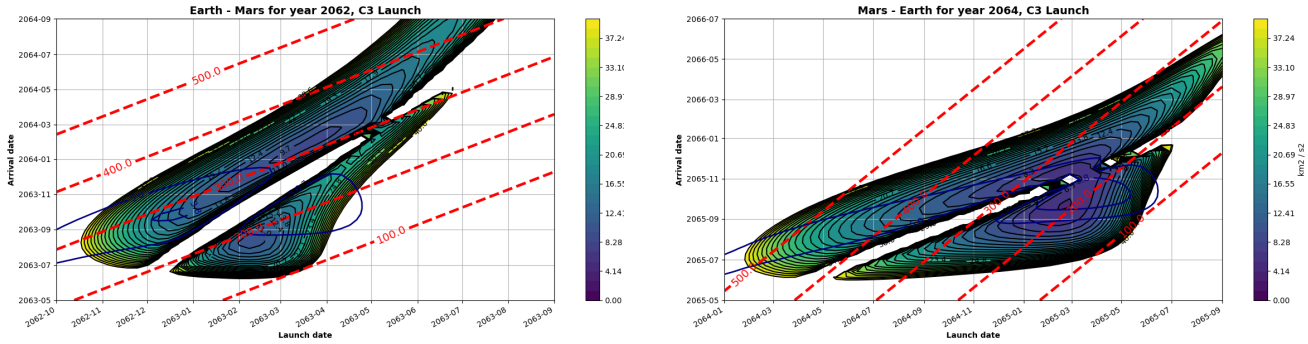

(a) Porkchop plot for the launch window in 2062.

(b) Porkchop plot for the launch window in 2064.

Figure 68: The porkchop plots for the second extra mission.

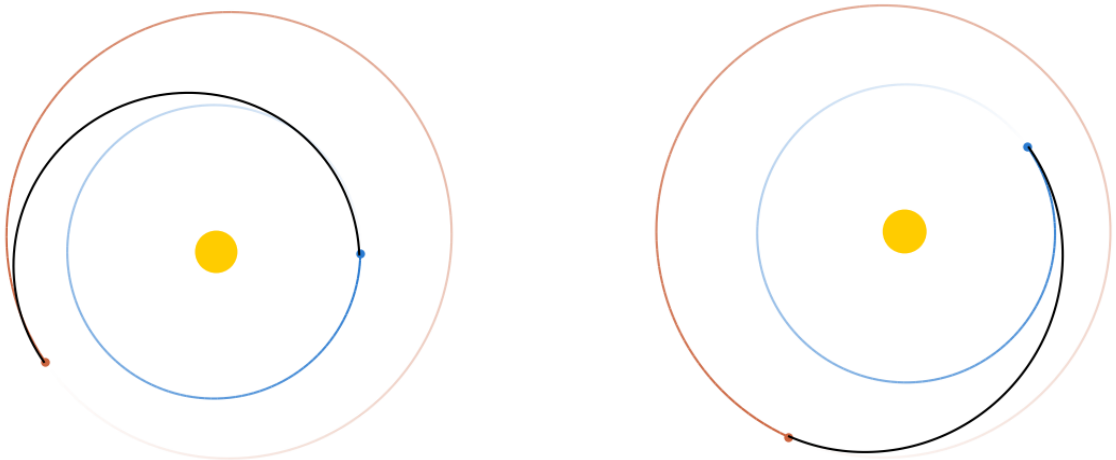

(a) Mapping of the trajectory to Mars.

(b) Mapping of the trajectory to Earth.

Figure 69: The trajectories of the second extra mission.

Table 111: Mission values for the second extra mission.

Destination	ΔV [km s^{-1}]	**Launch Date**	**Arrival Date**	**Duration [days]**
Mars	6.158	04-01-2063	07-10-2063	276
Earth	5.293	26-02-2065	04-10-2065	220
Total	11.450	04-01-2063	04-10-2065	1004

A.9 Third Extra Mission

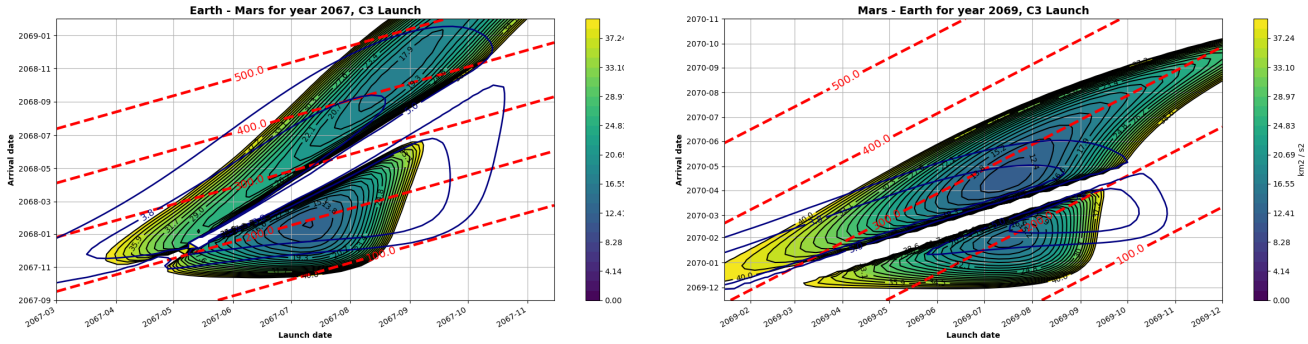

(a) Porkchop plot for the launch window in 2066

(b) Porkchop plot for the launch window in 2069

Figure 70: The porkchop plots for the third extra mission

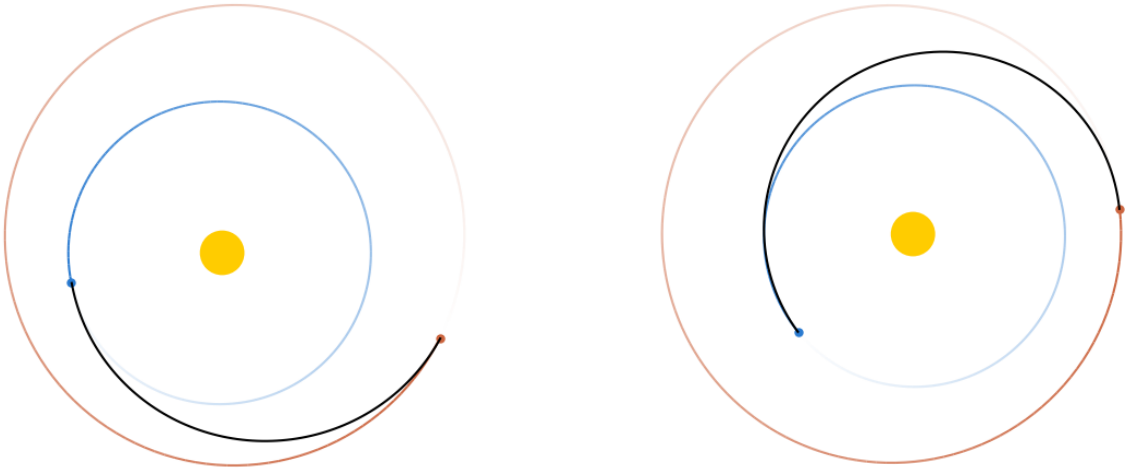

(a) Mapping of the trajectory to Mars.

(b) Mapping of the trajectory to Earth.

Figure 71: The trajectories of the third extra mission.

Table 112: Mission values for the third extra mission.

Destination	ΔV [km s^{-1}]	**Launch Date**	**Arrival Date**	**Duration [days]**
Mars	5.557	16-07-2067	06-02-2068	205
Earth	5.844	10-07-2069	07-04-2070	271
Total	11.401	16-07-2067	07-04-2070	996

B Telecommunications Link Budgets

Table 113: Link budget from Earth ground stations to Gangale relay satellites.

	Units	Value
Transmitted Power (Earth DSN)	dBW	43.01
Frequency	Hz	3.45E+10
Wavelength	m	0.00870
Diameter (Relay Antenna)	m	7.00
Diameter (Earth Antenna)	m	34.00
Relay Antenna Efficiency	-	0.80
Earth Antenna Efficiency	-	0.94
Gain (Earth Antenna)	dBi	81.52
Gain (Relay Antenna)	dBi	67.09
Noise Temperature (blackbody)	K	15
Noise Temperature (Relay)	K	30
Max Distance	m	4.01E+11
Loss (propagation loss)	dB	-2.95E+02
Bandwidth	Hz	1.70E+07
Design Margin	dB	3
Efficiency Bitrate	-	0.90
Bitrate	Mbps	168.3
Signal Power Received	dBW	-106.6
Noise Power at Relay	dBW	-139.8
SNR	dB	33.1
Required SNR	dB	15.0
Extra SNR Margin	dB	18.11

Table 114: Link budget from Gangale relay satellites to Earth ground stations.

	Units	Value
Transmitted Power	W	500.00
Transmitted Power	dBW	26.99
Frequency	Hz	3.20E+10
Wavelength	m	0.00938
Diameter (Relay Antenna)	m	7.00
Diameter (Earth Antenna)	m	34.00
Relay Antenna Efficiency	-	0.80
Earth Antenna Efficiency	-	0.85
Gain (Earth Antenna)	dBi	80.86
Gain (Relay Antenna)	dBi	66.44
Earth Antenna Noise Temp.	K	20
Max Distance	m	4.01E+11
Loss (propagation loss)	dB	-294.61
Bandwidth	Hz	2.00E+07
Design Margin	dB	3
Efficiency Bitrate	-	0.90
Bitrate	Mbps	115
Signal Power Received	dBW	-123.32
Noise Power at Earth	dBW	-142.58
SNR	dB	19.26
Required SNR	dB	15
Extra SNR Margin	dB	4.26

Table 115: Link budget from Earth ground stations to Mars stationary relay satellites.

	Units	Value
Transmitted Power (Earth DSN)	dBW	43.01
Frequency	Hz	3.45E+10
Wavelength	m	0.00870
Diameter (Relay Antenna)	m	4.50
Diameter (Earth Antenna)	m	34.00
Relay Antenna Efficiency	-	0.80
Earth Antenna Efficiency	-	0.94
Gain (Earth Antenna)	dBi	81.52
Gain (Relay Antenna)	dBi	63.25
Noise Temperature (blackbody)	K	15
Noise Temperature (Relay)	K	30
Max Distance	m	4.01E+11
Loss (propagation loss)	dB	-2.95E+02
Bandwidth	Hz	1.75E+07
Design Margin	dB	3
Efficiency Bitrate	-	0.90
Bitrate	Mbps	153
Signal Power Received	dBW	-110.49
Noise Power at Relay	dBW	-139.64
SNR	dB	29.15
Required SNR	dB	15
Extra SNR Margin	dB	14.15

Table 116: Link budget from Mars stationary relay satellites to Earth ground stations.

	Units	Value
Transmitted Power	W	1000.00
Transmitted Power	dBW	30.00
Frequency	Hz	3.20E+10
Wavelength	m	0.00938
Diameter (Relay Antenna)	m	4.50
Diameter (Earth Antenna)	m	34.00
Relay Antenna Efficiency	-	0.80
Earth Antenna Efficiency	-	0.85
Gain (Earth Antenna)	dBi	80.86
Gain (Relay Antenna)	dBi	62.60
Earth Antenna Noise Temp.	K	20
Max Distance	m	4.01E+11
Loss (propagation loss)	dB	-294.61
Bandwidth	Hz	2.00E+07
Design Margin	dB	3
Efficiency Bitrate	-	0.90
Bitrate	Mbps	111
Signal Power Received	dBW	-124.15
Noise Power at Earth	dBW	-142.58
SNR	dB	18.43
Required SNR	dB	15
Extra SNR Margin	dB	3.43

Table 117: Link budget from Mars stationary relay satellites to POLO.

	Units	Value
Transmitted Power	W	100.00
Transmitted Power	dBW	20.00
Frequency	Hz	7.00E+09
Wavelength	m	0.04286
Gain (POLO Antenna)	dBi	8.00
Diameter (Relay Antenna)	m	4.50
Satellite Antenna Efficiency	-	0.80
Gain (Relay Antenna)	dBi	49.40
Noise Temperature (blackbody)	K	450
Noise Temperature (POLO)	K	185
Max Distance	m	1.90E+07
Loss (propagation loss)	dB	-194.92
Bandwidth	Hz	2.00E+06
Design Margin	dB	3
Efficiency Bitrate	-	0.90
Bitrate	Mbit/s	10.2
Signal Power Received	dBW	-120.52
Noise Power	dBW	-137.56
SNR	dB	17.04
Required SNR	dB	15
Extra SNR Margin	dB	2.04

Table 118: Link budget from POLO to Mars stationary relay satellites.

	Units	Value
Transmitted Power	W	60.00
Transmitted Power	dBW	17.78
Frequency	Hz	7.00E+09
Wavelength	m	0.04286
Gain (POLO Antenna)	dBi	8.00
Gain (Relay Antenna)	dBi	49.40
Noise Temperature (blackbody)	K	80
Noise Temperature (POLO)	K	450
Max Distance	m	1.90E+07
Loss (propagation loss)	dB	-194.92
Bandwidth	Hz	2.20E+06
Design Margin	dB	3
Efficiency Bitrate	-	0.90
Bitrate	Mbit/s	10.1
Signal Power Received	dBW	-122.74
Noise Power	dBW	-137.93
SNR	dB	15.19
Required SNR	dB	15
Extra SNR Margin	dB	0.19

Table 119: Link budget from Earth ground stations to MARCO.

	Units	Value
Transmitted Power	W	20000.00
Transmitted Power	dBW	43.01
Frequency	Hz	3.45E+10
Wavelength	m	0.00870
Gain (MARCO Antenna)	dBi	63.25
Gain (Earth Antenna)	dBi	81.52
Noise Temperature (blackbody)	K	15
Noise Temperature (MARCO)	K	290
Max Distance	m	4.01E+11
Loss (propagation loss)	dB	-295.27
Bandwidth	Hz	1.11E+06
Design Margin	dB	3
Efficiency Bitrate	-	0.90
Bitrate	Mbit/s	10.85
Signal Power Received	dBW	-110.49
Noise Power	dBW	-143.32
SNR	dB	32.84
Required SNR	dB	15
Extra SNR Margin	dB	17.84

Table 120: Link budget from MARCO to Earth ground stations.

	Units	Value
Transmitted Power	W	330.00
Transmitted Power	dBW	25.19
Frequency	Hz	3.20E+10
Wavelength	m	0.00937
Gain (MARCO Antenna)	dBi	62.60
Gain (Earth Antenna)	dBi	81.52
Noise Temperature (blackbody)	K	15
Noise Temperature (MARCO)	K	290
Max Distance	m	4.01E+11
Loss (propagation loss)	dB	-294.62
Bandwidth	Hz	1.11E+06
Design Margin	dB	3
Efficiency Bitrate	-	0.90
Bitrate	Mbit/s	5.00
Signal Power Received	dBW	-128.31
Noise Power	dBW	-143.32
SNR	dB	15.01
Required SNR	dB	15
Extra SNR Margin	dB	0.01

Table 121: Link budget from Gangale relay satellites to Mars stationary relay satellites and vice versa.

	Units	Value
Transmitted Power	W	750.00
Transmitted Power	dBW	28.75
Frequency	Hz	2.50E+10
Wavelength	m	0.01200
Diameter (Gangale Antenna)	m	7.00
Diameter (Stationary Antenna)	m	4.50
Satellite Antenna Efficiency	-	0.80
Gain (Gangale Antenna)	dBi	64.29
Gain (Stationary Antenna)	dBi	60.45
Noise Temperature (blackbody)	K	15
Noise Temperature (Relay)	K	30
Max Distance	m	3.49E+10
Loss (propagation loss)	dB	-271.26
Bandwidth	Hz	2.00E+07
Possible Alignment Error	dB	3
Design Margin	dB	3
Efficiency Bitrate	-	0.90
Bit rate	Mbps	92
Signal Power Received	dBW	-123.76
Noise Power	dBW	-139.06
SNR	dB	15.30
Required SNR	dB	15
Extra SNR Margin	dB	0.30

Table 122: Link budget from Gangale relay satellites to MARCO and vice versa.

	Units	Value
Transmitted Power	W	330.00
Transmitted Power	dBW	25.19
Frequency	Hz	2.50E+10
Wavelength	m	0.01200
Diameter (MARCO Antenna)	m	4.50
Diameter (Gangale Antenna)	m	7.00
Satellite Antenna Efficiency	-	0.80
Gain (Gangale Antenna)	dBi	60.45
Gain (Stationary Antenna)	dBi	64.29
Noise Temperature (blackbody)	K	15
Noise Temperature (Relay)	K	30
Max Distance	m	3.49E+10
Loss (propagation loss)	dB	-271.26
Bandwidth	Hz	8.50E+06
Possible Alignment Error	dB	3
Design Margin	dB	3
Efficiency Bitrate	-	0.90
Bit rate	Mbps	40
Signal Power Received	dBW	-127.33
Noise Power	dBW	-142.77
SNR	dB	15.45
Required SNR	dB	15
Extra SNR Margin	dB	0.45